



LHC phenomenology and higher order electroweak corrections in supersymmetric models with and without R -parity

Dissertation zur Erlangung des naturwissenschaftlichen Doktorgrades
der Bayerischen Julius-Maximilians-Universität Würzburg

vorgelegt von
Stefan Rainer Liebler
aus Bayreuth

September 2011

Eingereicht am:_____

bei der Fakultät für Physik und Astronomie.

1. Gutachter:_____

2. Gutachter:_____

3. Gutachter:_____

der Dissertation.

1. Prüfer:_____

2. Prüfer:_____

3. Prüfer:_____

im Promotionskolloquium.

Tag des Promotionskolloquiums:_____

Doktorurkunde ausgehändigt am:_____

Ihre Theorie ist verrückt, aber nicht
verrückt genug um wahr zu sein.
Niels Bohr

Zusammenfassung

Das heutige Standardmodell der Teilchenphysik ist eine der präzisesten Theorien der Physik, welche die Eigenschaften der bekannten Elementarteilchen und deren Wechselwirkungen in zahlreichen Experimenten mit hoher Genauigkeit beschreibt. Gleichwohl zeigt es Schwachpunkte auf experimenteller wie theoretischer Seite: Zwar gibt es mit dem Higgs-Mechanismus einen theoretischen Ansatz für die Erzeugung von Massen der Elementarteilchen im Standardmodell, jedoch ist dieser experimentell (noch) nicht nachgewiesen. Insbesondere benötigt das Standardmodell für die Erklärung der leichten Massen der Neutrinos noch eine Erweiterung. Darüber hinaus liefert das Standardmodell keinen Kandidaten für dunkle Materie, welche den dominanten Anteil der Materie im Universum ausmacht. Antworten auf viele dieser Fragestellungen liefern supersymmetrische Modelle, auf denen auch diese Arbeit fußt. Statt der einfachsten supersymmetrischen Realisierung des Standardmodells beschäftigen wir uns mit Erweiterungen, darunter das nächstminimale supersymmetrische Standardmodell (NMSSM), welches ein zusätzliches Singletfeld enthält, sowie R -Paritätsverletzende Modelle. R -Parität ist eine diskrete Symmetrie, die die Stabilität des Protons in supersymmetrischen Erweiterungen garantiert. Die Nutzung von leptonzahlverletzenden Termen im Kontext von bilinearer R -Paritätsverletzung und dem $\mu\nu$ SSM erlaubt die Erklärung von Neutrinodaten, da besagte Terme eine Mischung der Neutralinos mit den Neutrinos bewirken.

Seit 2009 stößt der “Large Hadron Collider” (Großer Hadronenbeschleuniger, LHC) am CERN in Genf in den Energiebereich von Teraelektronenvolt vor und erlaubt so die Produktion von schweren, noch unbekanntem Teilchen. Somit könnte die nahe Zukunft die Frage nach der Massenerzeugung im Standardmodell beantworten und Hinweise auf neue Physik liefern. Daher arbeiten wir die Phänomenologie der oben erwähnten supersymmetrischen Modelle an Beschleunigerexperimenten heraus und diskutieren die Unterschiede zur einfachsten supersymmetrischen Realisierung des Standardmodells. Im Falle von R -Paritätsverletzung können die Zerfälle des leichtesten Neutralinos Vertices mit Abstand zum Wechselwirkungspunkt erzeugen. In Kombination mit leichten singletartigen Teilchen können diese Zerfälle eine reiche Phänomenologie bereithalten wie beispielsweise Higgszerfälle in leichte singletartige Neutralinos, welche vor ihrem Zerfall eine messbare Strecke im Detektor zurücklegen.

In dieser Arbeit präsentieren wir auch Rechnungen in der nächsthöheren Ordnung Störungstheorie, da Einschleifenbeiträge große Korrekturen zu den Massen und Zerfallsbreiten auf Baumgraphenniveau liefern können. Wir berechnen die Massen von Neutralinos und Charginos, welche im Falle der R -Paritätsverletzung Neutrinos und Leptonen beinhalten, in nächsthöherer Ordnung und heben die Gemeinsamkeiten und Unterschiede zu existierenden Rechnungen in anderen Renormierungsschemata hervor. Darüberhinaus betrachten wir Zweikörperzerfälle der Form $\tilde{\chi}_j^0 \rightarrow \tilde{\chi}_l^\pm W^\mp$ auf Einschleifenniveau. Im Falle von verschwindenden Zerfallsbreiten auf Baumgraphenniveau können die Korrekturen groß werden, genauso auch für die R -Paritätsverletzenden Zerfälle des leichtesten Neutralinos $\tilde{\chi}_1^0 \rightarrow l^\pm W^\mp$. Ein Charakteristikum von Modellen basierend auf bilinearer R -Paritätsverletzung ist die Korrelation zwischen den Verzweigungsverhältnissen der leichtesten Neutralinozerfälle und den Neutrinomischungswinkeln. Wir zeigen diese Beziehungen auf Baumgraphenniveau und für die Zweikörperzerfälle $\tilde{\chi}_1^0 \rightarrow l^\pm W^\mp$ auch in nächsthöherer Ordnung, da nur die volle Einschleifenkorrektur das erwartete Ergebnis liefert. Im Anhang werden die zwei für diese Arbeit erzeugten Programme **MaCoR** und **CNNDecays** vorgestellt. Während **MaCoR** die Berechnung von Massenmatrizen und Kopplungen in den besagten Modellen erlaubt, wurde mit **CNNDecays** die numerische Auswertung der Einschleifenrechnungen vorgenommen.

During the last decades the standard model of particle physics has evolved to one of the most precise theories in physics, describing the properties and interactions of fundamental particles in various experiments with a high accuracy. However it lacks on some shortcomings from experimental as well as from theoretical point of view: There is no approved mechanism for the generation of masses of the fundamental particles, in particular also not for the light, but massive neutrinos. In addition the standard model does not provide an explanation for the observance of dark matter in the universe. Moreover the gauge couplings of the three forces in the standard model do not unify, implying that a fundamental theory combining all forces can not be formulated. Within this thesis we address supersymmetric models as answers to these various questions, but instead of focusing on the most simple supersymmetrization of the standard model, we consider basic extensions, namely the next-to-minimal supersymmetric standard model (NMSSM), which contains an additional singlet field, and R -parity violating models. R -parity is a discrete symmetry introduced to guarantee the stability of the proton. Using lepton number violating terms in the context of bilinear R -parity violation and the $\mu\nu$ SSM we are able to explain neutrino physics intrinsically supersymmetric, since those terms induce a mixing between the neutralinos and the neutrinos.

Since 2009 the Large Hadron Collider (LHC) at CERN explores the new energy regime of Tera-electronvolt, allowing the production of potentially existing heavy particles by the collision of protons. Thus the near future might provide answers to the open questions of mass generation in the standard model and show hints towards physics beyond the standard model. Therefore this thesis works out the phenomenology of the supersymmetric models under consideration and tries to point out differences to the well-known features of the simplest supersymmetric realization of the standard model. In case of the R -parity violating models the decays of the light neutralinos can result in displaced vertices. In combination with a light singlet state these displaced vertices might offer a rich phenomenology like non-standard Higgs decays into a pair of singlinos decaying with displaced vertices.

Within this thesis we present some calculations at next order of perturbation theory, since one-loop corrections provide possibly large contributions to the tree-level masses and decay widths. We are using an on-shell renormalization scheme to calculate the masses of neutralinos and charginos including the neutrinos and leptons in case of the R -parity violating models at one-loop level. The discussion shows the similarities and differences to existing calculations in another renormalization scheme, namely the $\overline{\text{DR}}$ scheme. Moreover we consider two-body decays of the form $\tilde{\chi}_j^0 \rightarrow \tilde{\chi}_l^\pm W^\mp$ involving a heavy gauge boson in the final state at one-loop level. Corrections are found to be large in case of small or vanishing tree-level decay widths and also for the R -parity violating decay of the lightest neutralino $\tilde{\chi}_1^0 \rightarrow l^\pm W^\mp$. An interesting feature of the models based on bilinear R -parity violation is the correlation between the branching ratios of the lightest neutralino decays and the neutrino mixing angles. We discuss these relations at tree-level and for two-body decays $\tilde{\chi}_1^0 \rightarrow l^\pm W^\mp$ also at one-loop level, since only the full one-loop corrections result in the tree-level expected behavior. The appendix describes the two programs `MaCoR` and `CNNDecays` being developed for the analysis carried out in this thesis. `MaCoR` allows for the calculation of mass matrices and couplings in the models under consideration and `CNNDecays` is used for the one-loop calculations of neutralino and chargino mass matrices and the two-body decay widths.

Contents

Glossary	xv
1. Vectors, spinors and helicities	xv
2. More nomenclature	xvii
1. Introduction	1
2. Basic principles	5
2.1. Particle physics - The standard model	5
2.2. Electroweak symmetry breaking	6
2.3. Neutrino physics	8
2.3.1. Neutrino experiments and data	8
2.3.2. Neutrino mass models within the standard model of particle physics . . .	12
3. Supersymmetry - MSSM	15
3.1. Motivation	15
3.2. Supersymmetric algebra	16
3.3. Supermultiplets in the MSSM	17
3.4. Supersymmetric Lagrangian density	18
3.5. Superfield notation	20
3.6. Superpotential of the MSSM	20
3.7. Supersymmetry breaking	21
3.8. Mass eigenstates in the MSSM	23
3.9. R -parity	25
4. Extensions of the MSSM	27
4.1. Next-to-minimal supersymmetric standard model - NMSSM	27
4.2. Supersymmetric seesaw mechanisms	28
4.3. Models with broken R -parity	29
4.3.1. Bilinear R -parity violation - BRpV	30
4.3.2. $\mu\nu$ SSM	31
5. Supersymmetric models at tree-level	33
5.1. Scalar sectors, tadpole equations and parameters	33
5.1.1. MSSM and BRpV	34
5.1.2. NMSSM and $\mu\nu$ SSM	38
5.1.3. LEP bounds on light neutral scalar/pseudoscalar states	43
5.2. Gauge fixing and unphysical states	46
5.3. Masses of neutralinos and charginos	48
5.3.1. MSSM and NMSSM	49
5.3.2. BRpV and $\mu\nu$ SSM	50

5.3.3.	Approximate diagonalization	52
5.3.4.	Neutrino masses	53
5.4.	Decays $\tilde{\chi}_j^0 \rightarrow \tilde{\chi}_l^\pm W^\mp$ and $\tilde{\chi}_l^\pm \rightarrow \tilde{\chi}_j^0 W^\pm$	55
5.5.	Coupling $\tilde{\chi}_i^0 - \tilde{\chi}_j^\pm - W^\mp$ - Approximate formulas	56
6.	One-loop calculations - Theory	59
6.1.	Regularization and renormalization - The basics	59
6.1.1.	Regularization	59
6.1.2.	Passarino-Veltman integrals	61
6.1.3.	Renormalization schemes	62
6.2.	On-shell renormalization	65
6.2.1.	Renormalization of the gauge sector in R_ξ -gauge	65
6.2.2.	Renormalization of Dirac fermions with mixing	69
6.2.3.	On-shell masses of neutralinos and charginos	76
6.3.	Neutrino physics	83
6.4.	Decays $\tilde{\chi}_j^0 \rightarrow \tilde{\chi}_l^\pm W^\mp$ and $\tilde{\chi}_l^\pm \rightarrow \tilde{\chi}_j^0 W^\pm$	85
6.4.1.	Vertex corrections	85
6.4.2.	Counterterm corrections	86
6.4.3.	Real corrections	87
7.	Parameter choice for the models under consideration	91
8.	LHC phenomenology of the $\mu\nu$SSM	95
8.1.	Phenomenology of the 1 $\hat{\nu}^c$ -model	95
8.1.1.	Decays of a gaugino-like lightest neutralino	97
8.1.2.	Decays of a singlino-like lightest neutralino	99
8.2.	Phenomenology of the n $\hat{\nu}^c$ -model	101
8.2.1.	$\tilde{\chi}_1^0$ decay length and type of fit	102
8.2.2.	Several light singlets	103
9.	One-loop calculations - Masses and total decay widths	105
9.1.	One-loop masses of neutralinos and charginos	105
9.1.1.	Heavy neutralinos and charginos	105
9.1.2.	Neutrino and lepton masses, neutrino mixing angles	105
9.1.3.	Relation between $\vec{\Lambda}$, $\vec{\epsilon}$ and the neutrino mass differences/mixing angles	109
9.2.	Corrections to neutralino and chargino decays	111
9.2.1.	Two-body decays $\tilde{\chi}_j^0 \rightarrow \tilde{\chi}_i^- W^+$ and $\tilde{\chi}_i^+ \rightarrow \tilde{\chi}_j^0 W^+$ in the (N)MSSM	111
9.2.2.	Two-body decays $\tilde{\chi}_1^0 \rightarrow l^+ W^-$ in R -parity violating models	118
10.	Neutrino mixing angles and leptonic branching ratios	121
10.1.	Tree-level correlations in the $\mu\nu$ SSM with 1 $\hat{\nu}^c$	121
10.2.	One-loop correlations in the $\mu\nu$ SSM with 1 $\hat{\nu}^c$ and BRpV	123
10.3.	Tree-level correlations in the $\mu\nu$ SSM with 2 $\hat{\nu}^c$	126
11.	Conclusion	129
A.	Tadpole equations and mass matrices in the $\mu\nu$SSM	131
A.1.	Tadpole equations	131

A.2. Scalar matrices	132
A.2.1. Charged Scalars	132
A.2.2. Neutral Scalars	133
A.2.3. Pseudoscalars	135
A.2.4. Squarks	137
B. Expansion matrices in BRpV and the $\mu\nu$SSM	139
C. Passarino-Veltman integrals	141
C.1. Notation and basic integral	141
C.2. Scalar integrals	142
C.3. Tensor integrals	144
C.4. Special cases for B functions	145
C.5. Derivatives of the B functions	146
D. Vertex corrections for the decays $F_i \rightarrow F_o W^\pm$	149
E. Technical aspects of one-loop calculations	153
E.1. Masses	153
E.2. Decay widths	154
F. Programs	157
F.1. The Mathematica package MaCoR	157
F.2. The program CNNDecays	158
F.3. Used commercial programs/public codes	163
List of Figures	165
Bibliography	167
Acknowledgments	183

Glossary

In this section we present our nomenclature, which is used throughout the following thesis.

1. Vectors, spinors and helicities

Despite of α and β greek indices in this work refer to the space-time components and are running from $\mu, \nu, \rho, \dots = 0, 1, 2, 3$ with the possibility of real numbers in case of dimensional regularization. Space-time coordinates and the four momentum are defined as follows

$$x^\mu = (t, \vec{x}) \quad \text{and} \quad p^\mu = (E, \vec{p}) \quad , \quad (1)$$

where we have used the metric $g_{\mu\nu} = g^{\mu\nu} = \text{diag}(-1, +1, +1, +1)$. The well-known Dirac spinors u and v presenting particles and anti-particles as defined in [1] are used in the notation u and u^ζ , where ζ implies charge conjugation in accordance to

$$u^\zeta = v = C\bar{u}^T = C\gamma_0 u^* \quad \text{with} \quad \bar{u} = u^\dagger \gamma_0 \quad (2)$$

and the charge conjugation matrix C . The helicity states with helicity $\frac{1}{2}$ and $-\frac{1}{2}$ can then be written in the form

$$u_{R/L} = \frac{1}{2}(1 \pm \gamma_5) u \quad \text{and} \quad u_{R/L}^\zeta = \frac{1}{2}(1 \mp \gamma_5) u^\zeta \quad , \quad (3)$$

so that the projection operators are given by

$$P_L = \frac{1}{2}(1 - \gamma_5) \quad \text{und} \quad P_R = \frac{1}{2}(1 + \gamma_5) \quad . \quad (4)$$

Supersymmetric theories are very often expressed in terms of two-component Weyl spinors, which carry dotted and undotted indices. However we will suppress this notation in the following and will just use them to point out the construction of the Weyl spinor and its relation to the Dirac spinor u

$$u = \begin{pmatrix} \rho_\alpha \\ \eta^{\dagger\dot{\alpha}} \end{pmatrix} \quad \text{with the Weyl spinors} \quad \rho_\alpha \quad \text{and} \quad \eta^{\dagger\dot{\alpha}} \quad . \quad (5)$$

In this notation yields $(\eta)^{\dagger\dot{\alpha}} = \epsilon^{\dot{\alpha}\beta} (\eta)^\dagger_\beta$, where the antisymmetric ϵ contracts the $SU(2)$ indices $\alpha, \dot{\alpha} = 1, 2$. The first Weyl spinor ρ is equivalent to the left-handed part of the Dirac spinor u and the second Weyl spinor η^\dagger is equivalent to the charge conjugation of the left-handed part of the Dirac spinor representing the anti-particle u^ζ similar to [2], which transforms as a right-handed particle. This implies that our notation is only based on left-handed Weyl spinors ρ and η , which can be transformed into right-handed Weyl spinors by hermitian conjugation. Without

the dotted and undotted indices the following relations hold

$$u = \begin{pmatrix} \rho \\ \eta^\dagger \end{pmatrix} \quad \text{implying} \quad \bar{u} = \begin{pmatrix} \eta \\ \rho^\dagger \end{pmatrix}^T . \quad (6)$$

Acting with the projection operators on the Dirac spinor u necessarily results in

$$P_L u = \begin{pmatrix} \rho \\ 0 \end{pmatrix} \quad \text{and} \quad P_R u = \begin{pmatrix} 0 \\ \eta^\dagger \end{pmatrix} . \quad (7)$$

In addition this notation allows to write

$$\bar{u}_i P_L u_j = \rho_i \eta_j, \quad \bar{u}_i P_R u_j = \rho_i^\dagger \eta_j^\dagger \quad (8)$$

$$\bar{u}_i \gamma^\mu P_L u_j = \rho_i^\dagger \bar{\sigma}^\mu \rho_j, \quad \bar{u}_i \gamma^\mu P_R u_j = \eta_i \sigma^\mu \rho_j^\dagger \quad (9)$$

in accordance to [2] with the γ matrices split into (2×2) -blocks shown in the following Section 2. In this notation the upper two indices of the Dirac spinor are separated from the two lower ones, such that projection operators are no longer necessary, the Weyl spinors are by definition in different representations of the Lorentz group. Later supersymmetry will make use of chiral supermultiplets, which contain only left-handed Weyl fermions. We consider another example focusing on the mass eigenstates of the charged fermions, which are called F_i^\pm in Weyl notation and the neutral fermions being called F_i^0 and which transform via

$$\tilde{\chi}_i^- = \begin{pmatrix} F_i^- \\ (F_i^+)^\dagger \end{pmatrix} \quad \text{and} \quad \tilde{\chi}_i^0 = \begin{pmatrix} F_i^0 \\ (F_i^0)^\dagger \end{pmatrix} \quad (10)$$

to the Dirac spinors $\tilde{\chi}_i^-$ and $\tilde{\chi}_i^0$ of the charged and neutral fermions. Using this definition the neutral fermions are Majorana particles. Taking the example of the superfield \tilde{e}^c , the scalar component $\tilde{e}^c = \tilde{e}_R^*$ is the supersymmetric partner of the Weyl spinor $e^c = e_R^\dagger$. The notation c appears in the context of Weyl spinors and should not be confused with the ζ representing the charge conjugation in case of Dirac spinors.

The thesis contains Weyl- as well as Dirac spinors depending on the discussed subject: Mass matrices and the Lagrangian density in terms of the superpotential are presented in Weyl notation partially using superfields, whereas the one-loop calculations are expressed in Dirac notation.

2. More nomenclature

The following table should clarify the notation and summarizes important abbreviations:

Used symbols - spinor notation	
σ^μ	$\sigma^0 = \begin{pmatrix} 1 & 0 \\ 0 & 1 \end{pmatrix} = \bar{\sigma}^0, \sigma^1 = \begin{pmatrix} 0 & 1 \\ 1 & 0 \end{pmatrix} = -\bar{\sigma}^1, \sigma^2 = \begin{pmatrix} 0 & -i \\ i & 0 \end{pmatrix} = -\bar{\sigma}^2$ and $\sigma^3 = \begin{pmatrix} 1 & 0 \\ 0 & -1 \end{pmatrix} = -\bar{\sigma}^3$ Not to be confused with the scalars σ_d^0 and σ_u^0 appearing in several chapters together with the matrix σ^0 .
ϵ^{ab}	$\epsilon^{11} = \epsilon^{22} = 0, \epsilon^{12} = +1, \epsilon^{21} = -1$
ϕ	scalar field
ψ	chiral field (Weyl spinor)
$\hat{\Phi}$	chiral superfield, in the form $\hat{\Phi}(\theta) = \phi + \sqrt{2}\theta \cdot \psi + \theta \cdot \theta F$ (see Section 3.5)
θ	Grassmann variable in superfield notation
Used symbols - particle physics	
T^a	generator of $SU(N)$, either $\frac{\lambda^a}{2}$ with $a = 1, \dots, 8$ of $SU(3)$ or $\frac{\sigma^a}{2}$ with $a = 1, \dots, 3$ of $SU(2)$
g, g'	gauge couplings of $SU(2)_L$ or $U(1)_Y$
θ_W	weak mixing angle, Weinberg angle
G_F	Fermi constant $\frac{G_F}{\sqrt{2}} = \frac{g^2}{8m_W^2}$
m_Z, m_W	masses of the heavy gauge bosons Z and W
v_d, v_u	vacuum expectation values of H_d and H_u
$\tan \beta$	Ratio of vacuum expectation values $\tan \beta = v_u/v_d$
v_e, v_S	vacuum expectation values of the right-handed sneutrinos $\tilde{\nu}^c$ or the scalar singlet S
v_i	vacuum expectation values of the left-handed sneutrinos $\tilde{\nu}_i, i = 1, 2, 3$
s	Mandelstam variable, center of mass system energy \sqrt{s}
$\hbar = c = 1$	Planck's constant and the speed of light are set to 1.
Abbreviations	
BRpV	Bilinear R -parity violation
MSSM	Minimal supersymmetric standard model
NMSSM	Next-to-minimal supersymmetric standard model
$\mu\nu$ SMS	μ via ν supersymmetric standard model
VEV	Vacuum Expectation Value
(N)LO	(Next-to-)leading order
SPS	Snowmass Points and Slopes, see [3]
GUT	Grand Unified Theory
h.c.	Hermitian conjugate (\dagger)
LEP	Large Electron-Positron Collider at CERN, 1989-2000
LHC	Large Hadron Collider at CERN, since 2009
ILC	International Linear Collider, design stage
CLIC	Compact Linear Collider, design stage

Introduction

During the last century particle physics evolved to one of the most precise theories in physics with the standard model of particle physics describing fundamental particles to a high accuracy. The observation of the smallest scales in nature corresponds to the study of high energetic particles. Those high energies explain the need of collider experiments for the terrestrial investigation of fundamental physics. However also the universe offers high energies at its early stage and in massive galaxies. Thus also the observation of high energetic particles resulting from astrophysical sources allows conclusions about the fundamental particles and their formation. Although the standard model of particle physics precisely describes experiments performed in the last decades, it poses some open theoretical but also experimental questions. The most important shortcoming is the generation of masses for the standard model particles. The Higgs mechanism provides an explanation, but is not (yet) approved by experiments. Astrophysical observations indicate the existence of dark matter, for which the standard model does not offer a reasonable candidate. In addition theoretical questions like instabilities under quantum corrections or the desire for a fundamental theory explaining all forces by a unification of couplings ask for physics beyond the standard model of particle physics. The list of open questions could be extended, however we focus on possible explanations: Supersymmetry is able to answer several of these open questions as we will see later. Therefore the work presented in this thesis is based on the supersymmetrization of the standard model. Apart from the simplest realization, the minimal supersymmetric standard model (MSSM) we consider the next-to-minimal supersymmetric standard model, which contains an additional singlet field and allows for a solution of the μ -problem, the question why a certain parameter has the dimension of the electroweak scale. In addition we consider models violating R -parity, a discrete symmetry, which was originally introduced for experimental reasons. Using only lepton number violating terms we present two models, namely bilinear R -parity violation and the $\mu\nu$ S SM, which both allow for an intrinsically supersymmetric generation of neutrino masses induced by the mixing between neutralino states and the neutrinos. The Higgs mechanism a priori does not give an explanation for the lightness of the neutrino masses.

To test physics beyond the standard model the smallest scales have to be observed: Apart from the measurements of high energetic particles at colliders or from the universe, also precision observables at low energies being influenced by heavy particles allow for the search of physics beyond the standard model. The Large Hadron Collider (LHC) at CERN in Geneva, which explores the energy regime of Tera-electronvolt since 2009, can produce still unknown heavy particles detectable with the experiments ATLAS and CMS and also focuses on precision observables in the B hadrons sector using LHCb. In addition various measurements of neutrino data and dark matter strengthen the need for models beyond the standard model.

Thus current times in particle physics are very exciting, since within the next years the origin of masses in the standard model might be explained and the first hints for physics beyond the

standard model can account for the various open questions. To be able to make predictions about how and what experiments might see theorists have to provide accurate predictions about possible signals. In this thesis we therefore work out higher order corrections to the supersymmetric models under consideration. These higher order corrections are carried out in an on-shell scheme first sticking to the one-loop corrected masses of neutralinos and charginos including neutrinos and leptons in case of R -parity violation and then to two-body decays of the form $\tilde{\chi}_j^0 \rightarrow \tilde{\chi}_l^\pm W^\mp$, which are important for SUSY cascade decays in the (N)MSSM, but also for R -parity violating decays of the lightest neutralino. Special emphasis is put on the gauge invariance of our calculations. Moreover we provide the LHC phenomenology for the $\mu\nu$ SSM predicting measurable effects like displaced vertices, which differ from the well-known phenomenology of the MSSM. In addition we show relations between collider experiments and measurements at neutrino detectors in the presented models of R -parity violation.

This thesis is organized as follows: We start with an introduction to the basic principles of particle physics in Chapter 2. This introduction covers the symmetries of the standard model describing the today known fundamental particles. The concept of spontaneous symmetry breaking provides a mechanism to explain the observance of masses for those particles. We close the chapter by a discussion of neutrino experiments, which emphasize the existence of neutrino masses and present the seesaw mechanism to allow for an explanation of those.

In the subsequent Chapter 3 we motivate supersymmetry and explain the basic concepts covering the introduction of supersymmetric partners to existing particles, the superfield formalism and its usage in model building. We present the minimal supersymmetric standard model (MSSM) and show the particle content after the discussion of possible soft SUSY breaking mechanisms. Since some lepton and baryon number violating terms in the superpotential, which are allowed by gauge and SUSY symmetries, induce proton decay, we finally define R -parity, a discrete symmetry introduced to circumvent these experimental constraints. It forbids the presence of the mentioned terms.

After the introduction of supersymmetry we focus on the solution of the μ -problem and the generation of neutrino masses in supersymmetric models in Chapter 4. Therein we present the next-to-MSSM (NMSSM) and illustrate the supersymmetrization of the seesaw mechanisms. Afterwards we list arguments for R -parity violation. One major advantage of lepton number violating terms is the explanation of neutrino masses, which motivates bilinear R -parity violation and the so-called $\mu\nu$ SSM, two models being introduced within this chapter.

Chapter 5 describes the models of interest at tree-level. This discussion covers the scalar sectors with focus on the masses of the supersymmetric Higgs bosons and the role of the singlet Higgs in the NMSSM and $\mu\nu$ SSM. Moreover we summarize the procedure of gauge fixing using R_ξ -gauge, which we use to show the gauge invariance of our calculations. Thereafter the neutralino and chargino sectors are illustrated including the mixture with neutrinos and leptons in case of R -parity violation. Lastly two-body decays of the form $\tilde{\chi}_j^0 \rightarrow \tilde{\chi}_l^\pm W^\mp$ with a heavy gauge boson in the final state are discussed, since they are of great importance in SUSY cascade decays. In case of R -parity violation similar decays $\tilde{\chi}_1^0 \rightarrow l^\pm W^\mp$ are dominant compared to different final states. For those scenarios we present some approximations at tree-level, which illustrate the connection of those decay modes to the neutrino mixing angles in models based on bilinear R -parity violation.

The following Chapter 6 presents neutralino and chargino masses and two-body decay widths of the form $\tilde{\chi}_j^0 \rightarrow \tilde{\chi}_l^\pm W^\mp$ at one-loop level using an on-shell renormalization scheme. Therefore we start with a detailed discussion of renormalization schemes, then stick to the usage of the on-shell scheme for heavy gauge bosons and neutralinos as well as charginos, before we show the one-loop contributions to the decay widths of $\tilde{\chi}_j^0 \rightarrow \tilde{\chi}_l^\pm W^\mp$ analytically. The discussion includes

the real emission of a photon to obtain infrared finite results. In addition we focus on the gauge invariance of the calculations, which requires a certain treatment of the renormalization of mixing matrices.

In Chapter 7 benchmark scenarios for the various models under consideration are presented. We make use of them in Chapter 8 presenting the LHC phenomenology of the $\mu\nu$ SSM in detail including the discussion of the decay widths for the lightest supersymmetric particle being the lightest neutralino. Light singlet states in combination with the R -parity violating decays of the lightest neutralino result in a phenomenology, which clearly differs from the one of the MSSM, since displaced vertices and final states with several leptons or quarks uncommon in the MSSM can show up. The discussion covers the $\mu\nu$ SSM with one- but also with two right-handed neutrino superfields.

The subsequent Chapter 9 presents the one-loop corrections for masses of neutralinos and charginos including the generation of neutrino masses using the on-shell renormalization scheme described in Chapter 6. It follows the discussion of the one-loop corrections for the decays of the form $\tilde{\chi}_j^0 \rightarrow \tilde{\chi}_l^\pm W^\mp$ in the (N)MSSM. Since the tree-level decay width can vanish the corrections at one-loop level can be very important. Afterwards we show the size of corrections for the R -parity violating decays using an example spectrum in the $\mu\nu$ SSM.

Thereafter we discuss the correlations between the neutrino mixing angles and ratios of branching ratios of R -parity violating decays in bilinear R -parity violation and the $\mu\nu$ SSM in Chapter 10 for two- and three-body decays. For the two-body decays we present the correlations at one-loop level emphasizing that naive tree-level expectations turn out to be correct at full next-to-leading order.

Finally Chapter 11 summarizes the main results of this thesis. In Appendix A-F we present various formulas, namely mass matrices and tadpole equations for the $\mu\nu$ SSM and vertex corrections for $\tilde{\chi}_j^0 \rightarrow \tilde{\chi}_l^\pm W^\mp$. We address Passarino-Veltman integrals and the technical details of our calculations in more detail and finally describe the programs `MaCoR` and `CNNDecays`, which were developed for the analysis presented in this thesis. Whereas `MaCoR` is a Mathematica package to calculate the mass matrices and couplings, `CNNDecays` is a Fortran code to evaluate the one-loop corrections.

Basic principles

In this chapter we discuss the basic principles of particle physics starting with an introduction to the standard model of particle physics, which is followed by the detailed explanation of electroweak symmetry breaking. Moreover we show the current knowledge of neutrino physics, which includes a discussion of the various experiments. Before passing to the introduction of supersymmetry, we complete the chapter by a possible explanation of neutrino physics in the context of the standard model.

2.1. Particle physics - The standard model

Today particle physics is based on the mathematical formalism of relativistic quantum field theory in combination with group theory, which can be used to express the well-known standard model of particle physics. Although this work is based on these basic principles, we will not give a detailed introduction, but refer to the literature [1, 4, 5, 6]. However, symmetries are of such an importance in particle physics, that some comments are helpful for the understanding of supersymmetry: Quantum field theory, based on special relativity, includes the symmetries of space-time, which are given by the Poincaré group. Within this group structure coordinate transformations are of the form

$$x^\mu \rightarrow x'^\mu = \Lambda_\nu^\mu x^\nu + a^\mu \quad (2.1)$$

with the Lorentz transformation Λ_ν^μ and the space-time translation a^μ . Those transformations are induced by the generators of the four translations P_μ and the generators of the homogeneous Lorentz transformations $M_{\mu\nu}$, which include rotations and boosts. They follow the Poincaré algebra:

$$\begin{aligned} [P_\mu, P_\nu] &= 0 \\ [M_{\mu\nu}, P_\rho] &= i(g_{\nu\rho}P_\mu - g_{\mu\rho}P_\nu) \\ [M_{\mu\nu}, M_{\rho\sigma}] &= -i(g_{\mu\rho}M_{\nu\sigma} - g_{\mu\sigma}M_{\nu\rho} + g_{\nu\sigma}M_{\mu\rho} - g_{\nu\rho}M_{\mu\sigma}) \end{aligned} \quad (2.2)$$

In order to identify a “particle” we have to construct the irreducible representations of the Poincaré group, thus we need the Casimir operators, which commute with the generators of the Poincaré algebra. They are given by

$$C_1 = P^\mu P_\mu = P^2, \quad C_2 = \mathcal{W}^\mu \mathcal{W}_\mu = \mathcal{W}^2 \quad (2.3)$$

with the Pauli-Lubanski-vector $\mathcal{W}^\mu = \frac{1}{2}\epsilon^{\mu\nu\rho\sigma}P_\nu M_{\rho\sigma}$. Whereas C_1 identifies the mass of a particle, the eigenvalues of C_2 are related to the spin or to the helicity in case of a massless particle.

Beside these Poincaré group the standard model of particle physics is based on the internal symmetry groups $SU(3)_C \times SU(2)_L \times U(1)_Y$, which have to be combined with the Poincaré group by a direct product. Internal symmetries act on internal properties of the particles and have Lorentz scalars as generators. The question, whether it is possible to find additional symmetry groups, which can be unified with the Poincaré group, will be addressed in the section of supersymmetry.

In brevity we will sketch the particle content of the standard model based on the combination of the internal symmetry groups $SU(3)_C \times SU(2)_L \times U(1)_Y$: The combination of the three symmetry groups represent the three fundamental interactions, namely the strong, the weak and the electromagnetic interaction. They come together with the gauge bosons as elements of the gauge groups, which are spin-1 particles and mediate the interactions. In detail there are eight gluons g_μ^α as elements of $SU(3)_C$, three gauge bosons W_μ^i as elements of $SU(2)_L$ and one gauge boson B_μ as element of $U(1)_Y$. The indices C, L and Y are the quantum numbers, which describe the behavior of a particle under each group, and represent the color charge with respect to the strong interaction, the weak isospin and the hypercharge of a particle. Beside the gauge bosons the fermionic leptons and quarks appear in three families. This includes the electron e , myon μ and tau τ and their antiparticles, the neutrinos ν with left-handed helicity and their antiparticles with right-handed helicity. Note that the standard model does not include a right-handed neutrino in its original definition. The standard model is completed by the three families of quarks, which are up- and down-quark, charm- and strange-quark and top- and bottom-quark and their antiparticles. For a list of all particles we refer to the tables of the minimal supersymmetric standard model in Section 3, which contain the standard model particles together with their quantum numbers under the shown gauge groups.

However we did not mention yet the non-existence of masses for the fundamental fermions as well as for the heavy gauge bosons. The most famous mechanism to account for this problem is the Higgs mechanism based on spontaneous symmetry breaking [7, 8]. The interactions between the proposed Higgs particle and the fermions are then given by the Yukawa couplings [9], whose exact values can not be determined from the theory of the standard model, but flavor symmetries have to account for those.

The practical use of the mathematical concepts and methods of quantum field theory and the standard model can later be seen in the usage for decays and one-loop contributions. In particular the method of regularization and renormalization will be discussed in some more detail.

Since the process of electroweak symmetry breaking plays an important role in this thesis, we will give a more detailed introduction in the following section.

2.2. Electroweak symmetry breaking

In this section we want to explain the basic principles of electroweak symmetry breaking by discussing a very simple example. Given a complex, scalar field $\phi(x) = \frac{1}{\sqrt{2}}(\phi_1(x) + i\phi_2(x))$ with the Lagrangian density

$$\mathcal{L} = \partial^\nu \phi(x) (\partial_\nu \phi(x))^\dagger - V(\phi) \quad \text{with the potential} \quad V(\phi) = \mu^2 |\phi(x)|^2 + \lambda |\phi(x)|^4 \quad (2.4)$$

the system is invariant under a global $U(1)$ phase transformation $\phi'(x) = e^{i\alpha} \phi(x)$. Asking for the minimal energy, the ground state, one has to distinguish the following cases: If $\mu^2 > 0$, the minimum of $V(\phi)$ is obviously given by $\phi(x) = 0$, thus $\phi(x)$ describes a massive scalar boson.

However in case of $\mu^2 < 0$ the minimum of $V(\phi)$ is given for

$$|\phi(x)| = \sqrt{\frac{-\mu^2}{2\lambda}} =: \frac{1}{\sqrt{2}}v > 0 \quad , \quad (2.5)$$

which can also be seen from Figure 2.1.

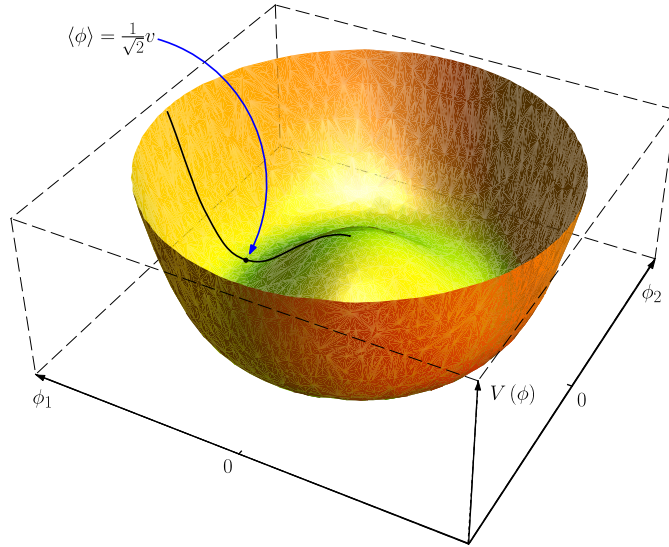


Figure 2.1.: Illustration of the potential $V(\phi)$.

Expanding the fields around a vacuum expectation value (VEV) v breaks the original symmetry of the Lagrangian density. This procedure is called spontaneous symmetry breaking. In detail the transformation yields $\phi_1(x) = v + \sigma(x)$ and $\phi_2(x) = \eta(x)$ with two real fields $\sigma(x)$ and $\eta(x)$, so that the quadratic terms in the Lagrangian density can be written in the form

$$\mathcal{L} \supset \frac{1}{2}\partial^\nu\sigma(x)\partial_\nu\sigma(x) - \frac{1}{2}(2\lambda v^2)\sigma^2(x) + \frac{1}{2}\partial^\nu\eta(x)\partial_\nu\eta(x) \quad . \quad (2.6)$$

The fields obviously describe a massive σ -boson with mass $\sqrt{2\lambda v^2}$ and a massless η -boson, which is called Goldstone boson [10]. In case of the standard model of particle physics the introduced procedure is used for a local $SU(2) \times U(1)$ transformation instead of a global $U(1)$ transformation. Then the breaking $SU(2)_L \times U(1)_Y \rightarrow U(1)_{EW}$, also called electroweak symmetry breaking (EWSB), induces the following mixing between the three gauge bosons W_μ^i and the gauge boson B_μ , which partially acquire a mass:

$$\begin{aligned} W_\mu^{(\pm)} &= \frac{1}{\sqrt{2}} (W_\mu^1 \mp W_\mu^2) \quad \text{with mass} \quad m_W = \frac{1}{2}gv \quad , \\ Z_\mu &= \frac{1}{\sqrt{g^2 + g'^2}} (gW_\mu^3 - g'B_\mu) \quad \text{with mass} \quad m_Z = \frac{1}{2}\sqrt{g^2 + g'^2}v \quad , \\ A_\mu &= \frac{1}{\sqrt{g^2 + g'^2}} (g'W_\mu^3 + gB_\mu) \quad \text{with mass} \quad m_\gamma = 0 \quad . \end{aligned} \quad (2.7)$$

Whereas the photon γ represented by the photon field A_μ remains massless, the W and Z bosons become massive particles in accordance to experimental data. The masses are given as

combinations of the vacuum expectation value v of the Higgs field σ' and the gauge couplings g of $SU(2)_L$ and g' of $U(1)_Y$. The Lagrangian density without the interaction terms in σ' can be written in the form

$$\begin{aligned} \mathcal{L} \supset & -\frac{1}{4}F_{\mu\nu}F^{\mu\nu} - \frac{1}{2}F_{W,\mu\nu}^\dagger F_W^{\mu\nu} + m_W^2 W_\mu^\dagger W^\mu \\ & - \frac{1}{4}F_{Z,\mu\nu}F_Z^{\mu\nu} + \frac{1}{2}m_Z^2 Z_\mu Z^\mu + \frac{1}{2}(\partial^\mu \sigma')(\partial_\mu \sigma') - \frac{1}{2}m_H^2 \sigma'^2 \quad , \end{aligned} \quad (2.8)$$

where the field strength tensor $F_{\mu\nu}^a = \partial_\mu A_\nu^a - \partial_\nu A_\mu^a + gf^{abc}A_\mu^b A_\nu^c$ is used, the structure constants only being relevant in case of non-abelian gauge groups. Since we will later use the weak mixing angle or Weinberg angle θ_W and the fine-structure constant α_{EM} and the electric charge e , we define in addition:

$$\cos \theta_W = \frac{g}{\sqrt{g^2 + g'^2}}, \quad e = \frac{gg'}{\sqrt{g^2 + g'^2}}, \quad \alpha_{EM} = \frac{e^2}{4\pi}. \quad (2.9)$$

The non-presence of the massless and unphysical Goldstone boson η in Equation (2.8) is only possible in case of the unitary gauge, whereas in arbitrary gauges like the R_ξ -gauges the Goldstone bosons of the theory have to be taken into account. We will discuss this issue later in Section 5.2, since we put a particular focus on the gauge invariance of our calculations.

Although the Higgs mechanism can account for the masses for the W and Z gauge bosons and the fermions via the introduction of Yukawa couplings [9], we pointed out already that neutrinos remain massless, since there is a priori no right-handed neutrino present.

2.3. Neutrino physics

Since the late 1990s it has become clear that neutrinos are not massless, but massive particles, since measurements of solar and atmospheric neutrinos pointed out that neutrinos oscillate. With the current standard solar model the rate of electron neutrinos ν_e , which is measurable on earth, can be calculated precisely. The first results of Homestake, SAGE, GALLEX, Kamiokande and SNO [11] however showed that the actual measured rate is much smaller and oscillations to other flavors seem to be reasonable. Similar questions arose in case of atmospheric neutrinos, which are produced in hadronic showers in the atmosphere, where oscillations were first observed in [12]. Before presenting the newest results in neutrino physics, we first explain the relation between neutrino oscillations and the neutrino masses and mixing angles following [13] and [14] in the next subsection.

2.3.1. Neutrino experiments and data

Having three active (meaning weakly interacting) neutrinos the relation between between flavor ν_α and mass eigenstates ν_k can be written in the form

$$|\nu_\alpha\rangle = \mathcal{U}_{\alpha k}^* |\nu_k\rangle \quad , \quad (2.10)$$

where \mathcal{U} is a unitary mixing matrix with $\mathcal{U}^\dagger \mathcal{U} = 1$ and is called Pontecorvo-Maki-Nakagawa-Sakata (PMNS) matrix [15]. Choosing the charged lepton Yukawa couplings to be diagonal, the

PMNS matrix can be parameterized in the following form

$$\mathcal{U} = \begin{pmatrix} c_{12}c_{13} & s_{12}c_{13} & s_{13}e^{-i\delta} \\ -s_{12}c_{23} - c_{12}s_{23}s_{13}e^{i\delta} & c_{12}c_{23} - s_{12}s_{23}s_{13}e^{i\delta} & s_{23}c_{13} \\ s_{12}c_{23} - c_{12}s_{23}s_{13}e^{i\delta} & -c_{12}c_{23} - s_{12}s_{23}s_{13}e^{i\delta} & c_{23}c_{13} \end{pmatrix} \cdot \begin{pmatrix} e^{i\alpha_1/2} & 0 & 0 \\ 0 & e^{i\alpha_2/2} & 0 \\ 0 & 0 & 1 \end{pmatrix} \quad (2.11)$$

using the abbreviations $c_{ij} = \cos \theta_{ij}$ and $s_{ij} = \sin \theta_{ij}$ with the three neutrino mixing angles θ_{ij} . δ , α_1 and α_2 are CP violating phases, from which α_1 and α_2 can only be present in case of neutrinos being Majorana particles. Majorana phases are irrelevant in case of neutrino oscillations, but can be tested by the observation of neutrinoless double beta decay and similar processes [16]. Using Schrödinger's equation in flavor space allows to calculate the time evolution of a single

parameter	best-fit	2σ	3σ
$\Delta m_{21}^2 [10^{-5} \text{ eV}^2]$	$7.59^{+0.20}_{-0.18}$	$7.24 - 7.99$	$7.09 - 8.19$
$\Delta m_{31}^2 [10^{-3} \text{ eV}^2]$	$2.45^{+0.09}_{-0.09}$ $-(2.34^{+0.10}_{-0.09})$	$2.28 - 2.64$ $-(2.17 - 2.54)$	$2.18 - 2.73$ $-(2.08 - 2.64)$
$\tan^2 \theta_{12}$	$0.453^{+0.037}_{-0.031}$	$0.39 - 0.54$	$0.37 - 0.56$
$\tan^2 \theta_{23}$	$1.04^{+0.29}_{-0.22}$ $1.08^{+0.30}_{-0.23}$	$0.69 - 1.56$ $0.72 - 1.56$	$0.64 - 1.78$ $0.64 - 1.78$
$\tan^2 \theta_{13}$	$0.010^{+0.009}_{-0.006}$ $0.013^{+0.009}_{-0.006}$	≤ 0.028 ≤ 0.032	≤ 0.036 ≤ 0.041

Table 2.1.: Current bounds on neutrino data taken from [17], the errors given together with the best-fit values are the 1σ bounds; the upper rows correspond to the normal, the lower rows to the inverted hierarchy.

flavor state, so that the transition or survival probability $P_{\alpha\beta}$ between the flavors α and β can be deduced

$$P_{\alpha\beta} = \sum_{k,j=1}^3 J_{jk}^{\alpha\beta} \exp\left(-i \frac{\Delta m_{kj}^2 L}{2E}\right) \quad (2.12)$$

$$= \delta_{\alpha\beta} - 4 \sum_{j=1}^2 \sum_{k=j+1}^3 \text{Re} J_{kj}^{\alpha\beta} \sin^2\left(\frac{\Delta m_{kj}^2 L}{4E}\right) + 2 \sum_{j=1}^2 \sum_{k=j+1}^3 \text{Im} J_{kj}^{\alpha\beta} \sin\left(\frac{\Delta m_{kj}^2 L}{2E}\right),$$

where $J_{jk}^{\alpha\beta} = \mathcal{U}_{\alpha k}^* \mathcal{U}_{\beta k} \mathcal{U}_{\alpha j} \mathcal{U}_{\beta j}^*$ and $\Delta m_{kj}^2 = m_k^2 - m_j^2$, E denotes the neutrino energy and L the length of the baseline, meaning the distance from the source to the detector. The imaginary part of this equation accounts for CP violating effects due to the different behavior of antineutrinos compared to neutrinos. The transition/survival probabilities already disclose that the absolute measurement of neutrino masses is not possible by the consideration of neutrino oscillations, only the differences of the squared masses Δm_{ij}^2 can be measured. Assuming a hierarchy of the mass splitting in the form $\Delta m_{21}^2 \ll |\Delta m_{31}^2|$ in combination with large mixing angles θ_{12} and θ_{23} and a small angle θ_{13} and no CP violating phases, the transition/survival probability between

different flavors can be approximated by:

$$P_{\alpha\beta} = \delta_{\alpha\beta} - 4 \left(J_{31}^{\alpha\beta} + J_{32}^{\alpha\beta} \right) \sin^2(\Delta_{31}) - 4 J_{21}^{\alpha\beta} \sin^2(\Delta_{21}) \quad \text{with} \quad \Delta_{ij} = \frac{\Delta m_{ij}^2 L}{4E} \quad (2.13)$$

By inserting the simplified PMNS matrix \mathcal{U} from Equation (2.11) with $\theta_{13} = \delta = \alpha_1 = \alpha_2 = 0$ the transition/survival probability can be used to explain the different measurements of neutrino data at detectors:

- ▷ Atmospheric experiments: Within hadronic showers in the atmosphere the decay of the charged pion according to $\pi^+ \rightarrow \mu^+ \nu_\mu \rightarrow e^+ \nu_e \nu_\mu \bar{\nu}_\mu$ (similar for π^-) generates a large number of ν_e and ν_μ and their antiparticles. If one chooses the baseline L (~ 1000 km) and the energy E (\sim GeV) such that $\Delta_{31} \approx \frac{\pi}{2}$ and $\Delta_{21} \approx 0$, the transition/survival probabilities are given by:

$$P_{ee} \approx 1, \quad P_{e\mu} = P_{\mu e} \approx 0, \quad P_{\mu\mu} \approx 1 - \sin^2(2\theta_{23}) \sin^2(\Delta_{31}) \quad (2.14)$$

The survival probability $P_{\mu\mu}$ is smaller than one, since ν_μ oscillate into ν_τ , which escape the detector. Experiments like Superkamiokande [18] therefore measure the atmospheric angle θ_{23} and the difference of the squared masses Δm_{31}^2 by the consideration of the survival probabilities $P_{\mu\mu}$.

- ▷ Solar experiments: The easiest way to measure the solar mixing angle is to use electron antineutrinos $\bar{\nu}_e$ from terrestrial nuclear power plants with a baseline L (~ 100 km) and the energy E (\sim MeV) resulting in $\Delta_{21} \approx \frac{\pi}{2}$ and $\Delta_{31} \rightarrow \frac{1}{2}$ (averaged). In this case the survival probability $P_{\bar{e}\bar{e}}$ can be approximated by

$$P_{\bar{e}\bar{e}} \approx 1 - \sin^2(2\theta_{12}) \sin^2(\Delta_{21}) \quad . \quad (2.15)$$

Thus, detectors like KamLAND [19] deduce the solar difference of the squared masses Δm_{21}^2 and the solar mixing angle θ_{12} from the $\bar{\nu}_e$ rates. The precise measurements of those data from solar neutrinos is more complicated, implying that terrestrial experiments are preferred.

- ▷ Reactor experiments: Choosing a short baseline L of a few kilometers gives a survival rate of $P_{\bar{e}\bar{e}} \approx 1$ for $\theta_{13} \rightarrow 0$. Necessarily deviations can be interpreted as nonvanishing θ_{13} .

Three different measurements, namely tritium beta decay, neutrinoless double beta decay and the observation of cosmological effects, allow an estimation for the absolute scale of neutrino masses. However note that these measurements often involve elements of the PMNS matrix or assumptions of an underlying model, so that their comparison has to be done advisedly:

- ▷ Tritium beta decay experiments: The decay ${}^3\text{H} \rightarrow {}^3\text{He} e^- \bar{\nu}_e$ of a tritium nucleus was used in several experiments like Mainz [20] or Troitsk [21] to obtain an upper bound for the effective electron neutrino mass given by

$$m_\beta^2 = \sum_{i=1}^3 |\mathcal{U}_{1i}|^2 m_i^2 \quad (2.16)$$

with a current value of $m_\beta < 2.2$ eV at 95%CL [22]. In Karlsruhe KATRIN [23] will improve these bounds within the next years.

- ▷ Neutrinoless double beta decay: Neutrinoless double beta decay ($0\nu 2\beta$) is only possible in case of neutrinos to be Majorana particles [24]. In particular decays within the nucleus ^{76}Ge were used to set an upper bound for the quantity

$$m_{\beta\beta} = \sum_{i=1}^3 \mathcal{U}_{1i}^2 m_i \quad (2.17)$$

to be $m_{\beta\beta} \leq 0.3 - 0.6$ eV [14] by the Heidelberg-Moscow collaboration [25]. $m_{\beta\beta}$ can vanish, although the individual neutrino masses m_i are nonzero. Many experiments like GERDA [26], CUORE [27] and EXO [28] focus on $0\nu 2\beta$, in particular to test the fundamental question, if neutrinos are Majorana particles.

- ▷ Cosmology: Bounds from cosmology to neutrino masses arise from the fact, that neutrinos with a large mass would serve as hot dark matter, suppressing the formation of small scale structures in the universe. In particular the consideration of the cosmic microwave background (CMB) therefore results in a bound of $\sum_i m_i \leq 0.3 - 1.0$ eV [29] depending on the underlying model of the early stages of the universe.

All these experiments give an upper value for the absolute neutrino mass of ~ 1 eV. Let us comment on some additional facts: CP violation in the neutrino sector is obviously proportional to θ_{13} using the above parameterization of the PMNS matrix. Choosing $\Delta m_{21}^2 > 0$ the sign of Δm_{31}^2 is not known, but might be deduced in future from neutrino oscillations in matter [30] via the Mikheyev-Smirnov-Wolfenstein effect [31]. The different hierarchies are called normal hierarchy (NH) in case of $\Delta m_{31}^2 > 0$, which implies $m_1 < m_2 < m_3$, and inverted hierarchy (IH) for $\Delta m_{31}^2 < 0$ coming together with $m_3 < m_1 < m_2$. Within this work we will mainly generate normal hierarchies, since inverted hierarchies need finetuning of parameters in the models under consideration.

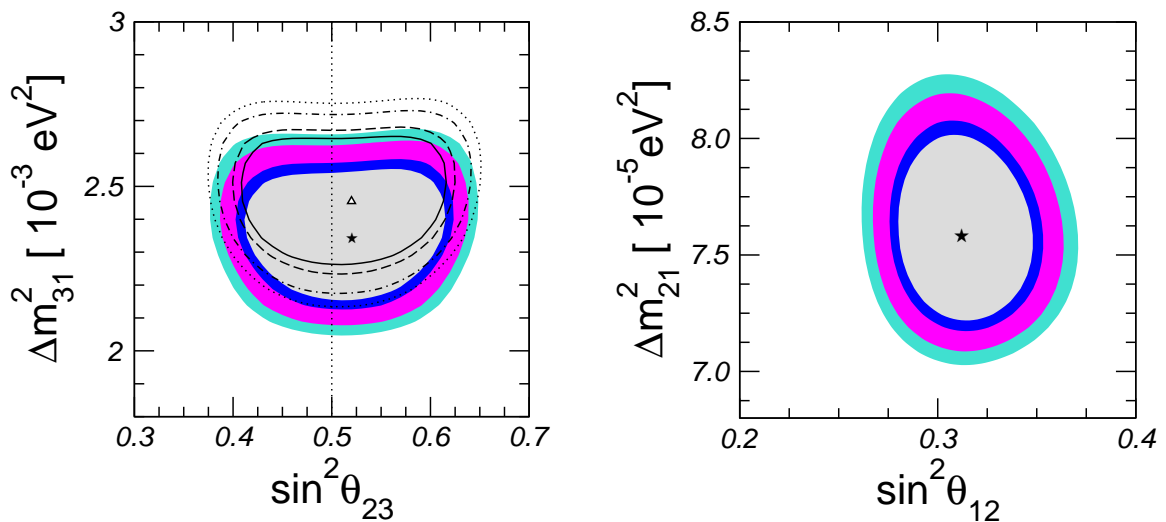


Figure 2.2.: **a)** (left) Allowed regions in the $\sin^2 \theta_{23}$ - Δm_{31}^2 -plane for normal (black curves) and inverted hierarchy (colored regions) at 90%, 95%, 99% and 99.73% CL; **b)** (right) Allowed regions in the $\sin^2 \theta_{12}$ - Δm_{21}^2 -plane at 90%, 95%, 99%, 99.73% CL; for details see [17], taken from [17].

The newest results from neutrino experiments by KamLAND [19], Super-Kamiokande [18], SAGE [32], SNO [33] and MINOS [34] were summarized and combined in [17], from which we show the newest results in the Figures 2.2 and 2.3. In contrast to [17] we present the best-fit

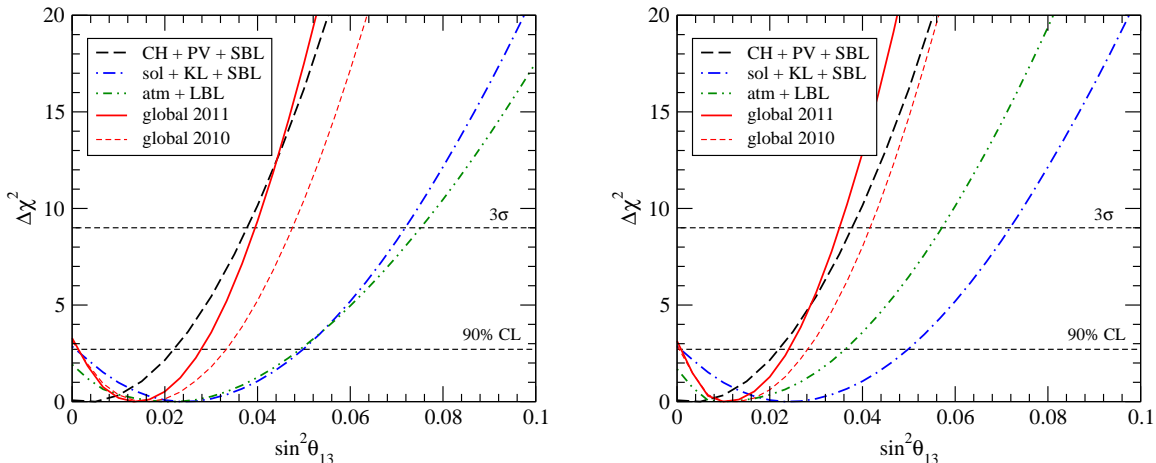


Figure 2.3.: Constraints on $\sin^2 \theta_{13}$ from different data sets for inverse hierarchy on the left and normal hierarchy on the right; for details see [17], taken from [17].

values, the 2σ and 3σ bounds of $\tan^2 \theta_{ij}$ instead of $\sin^2 \theta_{ij}$ in Table 2.1. Not included in this data is the indication of a nonvanishing value of $\theta_{13} > 0$ by T2K [35], however the best-fit value in Figure 2.3 already points to a positive value for θ_{13} .

Due to the naming of neutrino oscillations we use the differences of the squared masses and mixing angles within this thesis also in the following form

$$\theta_{sol} = \theta_{12}, \quad \theta_{atm} = \theta_{23}, \quad \theta_R = \theta_{13}, \quad \Delta m_{sol}^2 = \Delta m_{21}^2, \quad \Delta m_{atm}^2 = \Delta m_{31}^2 \quad . \quad (2.18)$$

2.3.2. Neutrino mass models within the standard model of particle physics

We pointed out in Section 2.1 that the standard model does not provide an explanation for neutrino masses and mixings in its original form. Before presenting a solution to this question within supersymmetric models via the breaking of R -parity, we want to mention possible explanations of neutrino masses within the standard model.

If neutrinos are Majorana particles, neutrino masses can be induced via the seesaw mechanism resulting in a unique dimension 5 operator (Weinberg operator) [36] of the generic form

$$G_5 = \frac{f_{\alpha\beta}}{\Lambda} (L_\alpha H) (H L_\beta) \quad , \quad (2.19)$$

where H denotes the Higgs $SU(2)_L$ doublet and L is the $SU(2)_L$ doublet, which contains the left-handed neutrinos and the left-handed leptons. It violates lepton number by two units, resulting in a Majorana mass term for the neutrinos. If f is a coupling of $\mathcal{O}(1)$, then Λ has to be at a very high scale $\geq 10^{15}$ GeV to allow for neutrino masses, which are in agreement with experimental data. A large Λ , implying a successful suppression, calls for a heavy intermediate particle, which is integrated out in the formulation of an effective theory. On tree-level exist only three possible realizations of this mechanism [37], since the dimension 5 operator couples four $SU(2)_L$ doublets, which can only be done via a singlet fermion or a triplet fermion or a triplet scalar state as intermediate particles. Whereas in the seesaw II the particle is a scalar $SU(2)_L$ triplet with hypercharge [38], a fermionic $SU(2)_L$ triplet generates the dimension 5 operator in the seesaw III model [39]. The simplest realization is given in the seesaw I model [40], which is working with a gauge singlet fermion.

Instead of presenting the details of seesaw mechanisms, we want to give a motivation for the naming “seesaw” itself by considering the neutrino mass generation for one left-handed neutrino ν_L via a right-handed neutrino ν_R , which is comparable to the seesaw I scenario. Since ν_R is neutral and a gauge singlet, it does not interact with the gauge bosons of the standard model. However it allows to write down a Dirac mass term $\propto \bar{\nu}_L \nu_R$ for neutrinos mixing the right-handed ν_R with the left-handed neutrino ν_L . In addition, the neutral charge of the neutrino allows a Majorana mass term $\propto \nu_R \nu_R$ for the the right-handed neutrinos or $\propto \nu_L \nu_L$ for the left-handed ones, provided the neutrino is its own antiparticle. The latter term is only possible after electroweak symmetry breaking not to affect the charged leptons. In the previous section we mentioned experiments on neutrinoless double beta decay $0\nu 2\beta$, which try to clarify this open question of particle physics, namely if the neutrino is a Majorana particle or not. If we allow for Majorana and Dirac mass terms of left- and right-handed neutrinos the Lagrangian density is of the form

$$\mathcal{L}_{\text{seesaw}} = -\frac{1}{2} (\bar{\nu}_L, \bar{\nu}_R^c) M \begin{pmatrix} \nu_L^c \\ \nu_R \end{pmatrix} + \text{h.c.} \quad \text{with} \quad M = \begin{pmatrix} m_M^L & m_D \\ m_D & m_M^R \end{pmatrix} . \quad (2.20)$$

In this notation yields $\nu^c = C \bar{\nu}^T = C \gamma_0 \nu^*$ with the charge conjugation matrix C for Dirac spinors. The eigenvalues of the matrix M are given by

$$m_{1,2} = \frac{1}{2} \left(m_M^L + m_M^R \pm \sqrt{(m_M^L - m_M^R)^2 + 4m_D^2} \right) , \quad (2.21)$$

which in case of $m_M^R \gg m_D$ and $m_M^L = 0$ can be approximated by:

$$m_1 \approx m_M^R \quad \text{and} \quad m_2 \approx \frac{m_D^2}{m_M^R} \quad (2.22)$$

Whereas m_1 corresponds to the mass of the heavy right-handed neutrino ν_R , the eigenvalue m_2 describes the generation of a small neutrino mass for the left-handed neutrino ν_L , which is suppressed by the heavy mass scale m_M^R . In this sense the naming “seesaw” has to be understood, since m_M^R on the one hand describes the mass of a heavy particle, but on the other hand allows for a small mass of the left-handed neutrino. The larger $m_1 \approx m_M^R$ gets, the smaller m_2 will be. Another possibility for neutrino masses are radiative models, most important the Zee model [41] and the Babu model [42], where the scalar sector is modified in combination with the introduction of lepton number violating interactions. Both mentioned models add charged bosons being singlets under $SU(2)_L$, in case of the Babu model supplemented by a double charged singlet.

Supersymmetry - MSSM

3.1. Motivation

After the short introduction to the standard model of particle physics, electroweak symmetry breaking and modern aspects of neutrino physics, we proceed with the concepts of supersymmetry (SUSY) in combination with R -parity violation. Although the standard model of particle physics together with possible explanations of neutrino physics is a highly accurate theory, in particular theoretical questions remain open motivating supersymmetry. Our discussion of SUSY in the following is based on [2]. Advantages of supersymmetry and open theoretical questions, to which SUSY can give an answer, are:

- ▷ Spinorial symmetry and connection to general relativity:

It is known from the Haag-Lopuszanski-Sohnius-theorem [43] in combination with the Coleman-Mandula-theorem [44] that apart from the generators of the Poincaré group P_μ and $M_{\mu\nu}$ as given in Section 2.1 no additional vectorial or tensorial conserved charges are possible. As we have argued in Section 2.1 the internal symmetries of a particle are independent of the Poincaré group and can be combined by a direct product. However, there is the possibility to add a spinorial charge Q_α , which transform fermions into bosons and vice versa. For a particle with spin J it yields

$$Q_\alpha^{(\dagger)} |J\rangle = |J \pm \frac{1}{2}\rangle \quad , \quad (3.1)$$

where $\alpha = 1, 2$ denotes the spinor components. This spinorial charge is an anticommuting generator and can be combined with the Poincaré group as we will see in Section 3.2, resulting in the Super-Poincaré group. Thus supersymmetry contains a complete realization of all possible symmetries.

In addition the formulation as local supersymmetry allows a formulation of a quantum theory for gravity. This connection is the source of supergravity theories [45].

- ▷ Gauge coupling unification and prediction of the weak mixing angle:

Renormalization group equations allow for the calculation of the couplings of strong, weak and electromagnetic interaction at arbitrary scales. Starting at the electroweak scale in the standard model, it turns out that those three couplings do not unify at a high scale, implying that a grand unified theory (GUT) cannot be formulated. However in supersymmetry the additional particle content allows for a different running and within the minimal supersymmetric standard model the three couplings unify at $m_{GUT} \sim 10^{16}$ GeV [46]. Moreover the weak mixing angle θ_W , which can be predicted in GUTs, is within the experimental bounds at the electroweak scale using supersymmetry [47].

▷ Hierarchy problem:

In grand unified theories the considered models are valid up to a large scale of $m_{GUT} \sim 10^{16}$ GeV, where the strong, the weak and the electromagnetic force are supposed to unify. However we know that $SU(2)_L \times U(1)_Y$ is broken at the electroweak scale according to Section 2.2. Knowing the mass of the charged gauge boson $m_W = \frac{1}{2}gv$ and the gauge coupling g of $SU(2)_L$, the vacuum expectation value is $v \approx 246$ GeV, implying that also the Higgs boson with $m_H = \sqrt{2\lambda v^2}$ should have a mass of the same order. Quantum corrections to the Higgs mass can be estimated by

$$\Delta m_H^2 = m_W^2 \mathcal{O} \left(\frac{m_{GUT}^2}{m_W^2} \right) \quad , \quad (3.2)$$

implying that the standard model needs large finetuning over $\sim 10^{26}$ orders of magnitude to allow for a Higgs mass at the electroweak scale.

In unbroken supersymmetry this problem is solved by adding supersymmetric partners to the standard model particles, which give the same contribution as in Equation (3.2), but with the opposite sign resulting in a stable Higgs mass [48].

▷ Spontaneous symmetry breaking:

Symmetry breaking $SU(2)_L \times U(1)_Y \rightarrow U(1)_{EW}$ via the Higgs mechanism as explained in Section 2.2 needs a negative parameter μ^2 , which has to be set negative within the standard model (neglecting the possibility of radiative corrections [49] as origin of spontaneous symmetry breaking). In supersymmetric theories the degeneration of SUSY masses at m_{GUT} with positive squared masses results in a negative μ^2 at the electroweak scale using the renormalization group equations due to the large top mass. In this sense electroweak symmetry breaking is given automatically in supersymmetry [50, 51].

▷ Dark matter:

From measurements of rotation curves of galaxies and the cosmic microwave background (CMB) it became certain that the largest part of matter in the universe stems from dark matter, for which the standard model does not provide a candidate. For recent data from the WMAP satellite we refer to [52]. Supersymmetry offers such a candidate: In case of R -parity conservation the lightest supersymmetric particle (LSP) is stable and serves as a dark matter candidate, if it is neutral. Also in R -parity violating scenarios a light gravitino [53] as superpartner of the graviton (gauge boson of the gravitational force) or an axion [54] (solving the strong CP problem) as well as its superpartner, the axino [55], offer this solution.

3.2. Supersymmetric algebra

After motivating supersymmetry we will start with a more detailed discussion of the symmetry itself and the construction of supermultiplets therein. We have presented the Poincaré group and its generators P_μ and $M_{\mu\nu}$ in Section 2.1 and introduced the spinorial charge Q_α in Section 3.1 using the indices $\alpha = 1, 2$ in Weyl notation. Their combination leads to the following (anti-)

commutation relations [2] in addition to the Poincaré algebra in Equation (2.2)

$$\begin{aligned}
\{Q_\alpha, Q_\beta^\dagger\} &= 2(\sigma^\mu)_{\alpha\beta} P_\mu \\
\{Q_\alpha, Q_\beta\} &= \{Q_\alpha^\dagger, Q_\beta^\dagger\} = 0 \\
[P_\mu, Q_\alpha] &= [P_\mu, Q_\beta^\dagger] = 0 \\
[Q_\alpha, M_{\mu\nu}] &= \frac{1}{2}(\sigma_{\mu\nu})_\alpha^\beta Q_\beta \\
[Q_\alpha^\dagger, M_{\mu\nu}] &= -\frac{1}{2}Q_\beta (\bar{\sigma}_{\mu\nu})^\beta_\alpha
\end{aligned} \tag{3.3}$$

with $\sigma_{\mu\nu} = \frac{1}{4}(\sigma_\mu\bar{\sigma}_\nu - \sigma_\nu\bar{\sigma}_\mu)$ and σ^μ being defined in the glossary. These relations imply in particular $[P^2, Q_\alpha] = 0$. Together with $P^2 = P_\mu P^\mu = m^2$ we can deduce that all particles of the same supermultiplet, which are obtained by acting with Q_α on a particle state, have the same masses in SUSY theories. Since this is experimentally excluded, SUSY has to be a broken symmetry, what will be discussed in more detail in Section 3.7.

To calculate the number of bosonic and fermionic degrees of freedom in a supermultiplet, we introduce the operator $(-1)^{2s}$ with the spin s of the particle, which anticommutes with the spinorial charge Q_α , since Q_α changes the fermion or boson number by one unit. Starting with Equation (3.3) shows in accordance to [2] that all particles $|i\rangle$ of a supermultiplet with the completeness relation $\sum_i |i\rangle\langle i| = 1$ and the same eigenvalue p^μ of the four-momentum operator P^μ fulfill:

$$\begin{aligned}
p^\mu \text{tr} [(-1)^{2s}] &= \sum_i \langle i| (-1)^{2s} P^\mu |i\rangle \propto \sum_i \langle i| (-1)^{2s} Q Q^\dagger |i\rangle + \sum_i \langle i| (-1)^{2s} Q^\dagger Q |i\rangle \\
&= \sum_i \langle i| (-1)^{2s} Q Q^\dagger |i\rangle - \sum_j \langle j| (-1)^{2s} Q Q^\dagger |j\rangle = 0
\end{aligned} \tag{3.4}$$

Therein we used the anticommutation of $(-1)^{2s}$ with the spinorial charge Q . The first expression is proportional to the number of bosonic n_B minus the number of fermionic degrees n_F of freedom, so that they have to be equal in a supermultiplet with $p^\mu \neq 0$.

3.3. Supermultiplets in the MSSM

Knowing about the bosonic and fermionic degrees of freedom, we can now construct chiral and gauge supermultiplets. For each Weyl fermion ψ represented by a two-component Weyl spinor and for each gauge boson A_μ of the standard model we introduce a supersymmetric partner resulting in the minimal supersymmetric standard model (MSSM). To have also “off-shell” equal fermionic and bosonic degrees of freedom a complex scalar field F in case of the chiral supermultiplet and a real scalar field D in case of the gauge supermultiplet have to be added, who enter the Lagrangian density in the form $\mathcal{L} = F^*F + \frac{1}{2}DD$. The kinetic terms both vanish “on-shell”, where the number of degrees of freedom coincide. Although those particles are only auxiliary fields and not real particles, they induce new interactions, which are called F - and D -terms and are shown when constructing the full Lagrangian density of the MSSM. The resulting particle content of the MSSM is presented in Table 3.1.

As it can be seen from Table 3.1 the MSSM contains two Higgs doublets. The need of an additional Higgs doublet can be motivated by different arguments: The second Higgs doublet

chiral supermultiplets	superfield notation	spin 0	spin $\frac{1}{2}$	$SU(3)_C, SU(2)_L, U(1)_Y$
squarks, quarks ($\times 3$ generations)	\widehat{Q}	$(\tilde{u}_L, \tilde{d}_L)$	(u_L, d_L)	$(\mathbf{3}, \mathbf{2}, \frac{1}{6})$
	\widehat{u}^c	\tilde{u}_R^*	u_R^\dagger	$(\bar{\mathbf{3}}, \mathbf{1}, -\frac{2}{3})$
	\widehat{d}^c	\tilde{d}_R^*	d_R^\dagger	$(\bar{\mathbf{3}}, \mathbf{1}, \frac{1}{3})$
sleptons, leptons ($\times 3$ generations)	\widehat{L}	$(\tilde{\nu}_e, \tilde{e}_L)$	(ν_e, e_L)	$(\mathbf{1}, \mathbf{2}, -\frac{1}{2})$
	\widehat{e}^c	\tilde{e}_R^*	e_R^\dagger	$(\mathbf{1}, \mathbf{1}, 1)$
Higgs, Higgsinos	\widehat{H}_u	(H_u^+, H_u^0)	$(\tilde{H}_u^+, \tilde{H}_u^0)$	$(\mathbf{1}, \mathbf{2}, \frac{1}{2})$
	\widehat{H}_d	(H_d^0, H_d^-)	$(\tilde{H}_d^0, \tilde{H}_d^-)$	$(\mathbf{1}, \mathbf{2}, -\frac{1}{2})$

gauge supermultiplets	spin $\frac{1}{2}$	spin 1	$SU(3)_C, SU(2)_L, U(1)_Y$
gluinos, gluons	\tilde{g}	g	$(\mathbf{8}, \mathbf{1}, 0)$
winos, W-bosons	$\tilde{W}^\pm, \tilde{W}_3^0$	W^\pm, W_3^0	$(\mathbf{1}, \mathbf{3}, 0)$
bino, B-boson	\tilde{B}	B	$(\mathbf{1}, \mathbf{1}, 0)$

Table 3.1.: Particle content of the minimal supersymmetric standard model (MSSM) including their behavior under $SU(3)_C \times SU(2)_L \times U(1)_Y$.

allows for the absence of gauge anomalies induced by the fermionic superpartners of the Higgs, the Higgsinos, since its hypercharge is opposite to those of the first Higgs doublet, so that the requirements $\text{tr}[T_3^2 Y] = \text{tr}[Y^3] = 0$ are fulfilled, where T_3 and Y are the third component of weak isospin and the weak hypercharge respectively. Second the structure of SUSY needs two Higgs doublets, one for the coupling to the u-squarks/quarks and a second for the couplings to the d-quarks/squarks to allow for an analytic form of the superpotential, which is introduced later in Section 3.6. Moreover the superpotential has to be a holomorphic function, which does not allow terms like $H_u^* H_u$ violating the Cauchy-Riemann differential equations.

3.4. Supersymmetric Lagrangian density

The Lagrangian density of a free propagating, noninteracting, chiral supermultiplet in Weyl notation without the use of the superfield notation is given by:

$$\mathcal{L}_{\text{free}} = \partial^\mu \phi^{*i} \partial_\mu \phi_i + i \psi^{\dagger i} \bar{\sigma}^\mu \partial_\mu \psi_i + F^{*i} F_i \quad (3.5)$$

Possible interactions and mass terms can be expressed in terms of the so called superpotential W , which will be introduced in the following section using the superfield notation. Here, we explain how to construct the Lagrangian density with all the interactions from the scalar analog of the superpotential:

$$W = \frac{1}{2} M^{ij} \phi_i \phi_j + \frac{1}{6} Y^{ijk} \phi_i \phi_j \phi_k \quad (3.6)$$

Note that we omit linear terms of the form $L^i \phi_i$, since they are only allowed for gauge singlets and only contribute to the scalar potential. Four-point couplings would lead to nonrenormalizable terms and are therefore not shown. The couplings M^{ij} and Y^{ijk} are totally symmetric in their indices. In this definition the interactions can then be expressed in the form

$$\mathcal{L}_I = \left(-\frac{1}{2} W^{ij} \psi_i \psi_j + W^i F_i \right) + \text{h.c.} \quad \text{with} \quad W^i = \frac{\partial W}{\partial \phi_i}, \quad W^{ij} = \frac{\partial W}{\partial \phi_i \partial \phi_j} \quad . \quad (3.7)$$

The equations of motion for the auxiliary fields F are given by

$$\mathcal{L}_{\text{free}}|_F + \mathcal{L}_I|_F = F^{*i} F_i + W^i F_i + W^{*i} F_i^* \quad \Longrightarrow \quad F_i = -W_i^*, \quad F^{*i} = -W^i. \quad (3.8)$$

In this sense the auxiliary fields F , originally introduced to allow equal bosonic and fermionic degrees of freedom within the chiral supermultiplet, lead to a new form of interaction, which can be written in the form:

$$\mathcal{L} = \partial^\mu \phi^{*i} \partial_\mu \phi_i + i \psi^{\dagger i} \bar{\sigma}^\mu \partial_\mu \psi_i - \frac{1}{2} \left(W^{ij} \psi_i \psi_j + W^{*ij} \psi_i^\dagger \psi_j^\dagger \right) - W^i W_i^*. \quad (3.9)$$

Adding the gauge supermultiplets the Lagrangian density in total is given by

$$\begin{aligned} \mathcal{L} = & - (D^\mu \phi^i)^\dagger D_\mu \phi_i - i \psi^{\dagger i} \bar{\sigma}^\mu D_\mu \psi_i - \frac{1}{2} \left(W^{ij} \psi_i \psi_j + W^{*ij} \psi_i^\dagger \psi_j^\dagger \right) - W^i W_i^* \\ & - \frac{1}{4} F_{\mu\nu}^a F_a^{\mu\nu} - i \lambda^{\dagger a} \bar{\sigma}^\mu D_\mu \lambda_a + \frac{1}{2} D^a D_a \\ & - \sqrt{2} g_a (\phi^{*i} T^a \psi_i) \lambda_a - \sqrt{2} g_a \lambda_a^\dagger (\psi^{\dagger i} T^a \phi_i) + g_a (\phi^{*i} T^a \phi_i) D_a \quad . \end{aligned} \quad (3.10)$$

The equations of motions for the D -terms yield

$$D^a = -g_a (\phi^{*i} T^a \phi_i) \quad . \quad (3.11)$$

The covariant derivatives in the Lagrangian density are

$$\begin{aligned} D_\mu \phi_i &= \partial_\mu \phi_i - i g_a A_\mu^a (T^a \phi)_i \\ D_\mu \psi_i &= \partial_\mu \psi_i - i g_a A_\mu^a (T^a \psi)_i \\ D_\mu \lambda^a &= \partial_\mu \lambda^a + g f^{abc} A_\mu^b \lambda^c \quad . \end{aligned} \quad (3.12)$$

In non-abelian gauge groups the field strength tensor has the general form

$$F_{\mu\nu}^a = \partial_\mu A_\nu^a - \partial_\nu A_\mu^a + g f^{abc} A_\mu^b A_\nu^c \quad . \quad (3.13)$$

Finally the Lagrangian density results in the following scalar potential

$$V(\phi_i, \phi_i^*) = W^i W_i^* + \frac{1}{2} \left| \sum_{a,i} g_a (\phi^{*i} T^a \phi_i) \right|^2 \geq 0 \quad , \quad (3.14)$$

which is positive by definition. This simplest model of supersymmetry working with chiral and gauge supermultiplets was introduced by Wess and Zumino and is therefore known as Wess-Zumino-model [56].

3.5. Superfield notation

To discuss the superpotential of the MSSM in its most convenient form, we give a short introduction to the superfield notation. More details about the superspace and the advantages of the superfield notation can be found in [57] or [58]. The basis of the superfield notation are Grassmann variables, which obey the relation:

$$\{\theta_i, \theta_j\} = 0 \quad \text{and in particular} \quad \theta_i^2 = 0 \quad . \quad (3.15)$$

Moreover the Grassmann variables commute with arbitrary complex numbers. For left-handed superfields we need spinorial Grassmann variables, which fulfill $\theta_1^2 = \theta_2^2 = 0$ and allow for terms independent of θ , proportional to θ and proportional to $\theta_1\theta_2$. Having the scalar product $\theta_a\theta_b = -\frac{1}{2}\epsilon_{ab}\theta \cdot \theta$ in mind, a chiral superfield can be written in the form

$$\widehat{\Phi}(\theta) = \phi + \sqrt{2}\theta \cdot \psi + \theta \cdot \theta F \quad . \quad (3.16)$$

Together with the relation [59]

$$\theta \cdot \psi_i \theta \cdot \psi_j = -\frac{1}{2}\theta \cdot \theta \psi_i \psi_j \quad (3.17)$$

we can write for products of superfields:

$$\widehat{\Phi}_i(\theta) \widehat{\Phi}_j(\theta) = \phi_i \phi_j + \sqrt{2}\theta \cdot (\psi_i \phi_j + \psi_j \phi_i) + \theta \cdot \theta (\phi_i F_j + \phi_j F_i - \psi_i \psi_j) \quad (3.18)$$

$$\begin{aligned} \widehat{\Phi}_i(\theta) \widehat{\Phi}_j(\theta) \widehat{\Phi}_k(\theta) &= \phi_i \phi_j \phi_k + \sqrt{2}\theta \cdot (\psi_i \phi_j \phi_k + \psi_j \phi_i \phi_k + \psi_k \phi_i \phi_j) \\ &+ \theta \cdot \theta (\phi_i \phi_k F_j + \phi_j \phi_k F_i + \phi_i \phi_j F_k \\ &- \phi_k \psi_i \psi_j - \phi_i \psi_j \psi_k - \phi_j \psi_i \psi_k) \end{aligned} \quad (3.19)$$

Taking the F -terms only, which are the terms proportional to $\theta \cdot \theta$ and are denoted by $\left[\widehat{\Phi}_i \widehat{\Phi}_j\right]_F$ and $\left[\widehat{\Phi}_i \widehat{\Phi}_j \widehat{\Phi}_k\right]_F$, the interaction part of the Lagrangian density induced by the superpotential

$$W(\widehat{\Phi}) = \frac{1}{2} M^{ij} \widehat{\Phi}_i \widehat{\Phi}_j + \frac{1}{6} Y^{ijk} \widehat{\Phi}_i \widehat{\Phi}_j \widehat{\Phi}_k \quad (3.20)$$

is given by

$$\mathcal{L}_{WW} = \left(\left[W(\widehat{\Phi}) \right]_F + \text{h.c.} \right) \quad . \quad (3.21)$$

Again the auxiliary fields F_i can be replaced using the equations of motions resulting in

$$F_i = -W_i^* = -M^{ij} \phi_j - \frac{1}{2} Y^{ijk} \phi_j \phi_k \quad . \quad (3.22)$$

3.6. Superpotential of the MSSM

The superpotential of the MSSM in superfield notation is given by

$$W_{\text{MSSM}} = \epsilon_{ab} \left(Y_u^{ij} \widehat{H}_u^b \widehat{Q}_i^a \widehat{u}_j^c + Y_d^{ij} \widehat{H}_d^a \widehat{Q}_i^b \widehat{d}_j^c + Y_e^{ij} \widehat{H}_d^a \widehat{L}_i^b \widehat{e}_j^c - \mu \widehat{H}_d^a \widehat{H}_u^b \right) \quad , \quad (3.23)$$

so that the full Lagrangian density of the MSSM can be constructed with the knowledge of the sections before. It includes $SU(2)_L$ -superfields, which have to be contracted using ϵ_{ab} from the

glossary. The scalar and fermionic components of the superfields can be taken from Table 3.1. The indices i, j have to be summed over the three generations, whereas color indices are omitted in the notation above. As already indicated the superpotential is at most trilinear in the superfields, so that nonrenormalizable terms are not generated. The μ -term is equivalent to the Higgs boson mass in the standard model and has a dimension of mass.

Just to point out an example for interactions within the MSSM we present the ones arising from the first term in the superpotential in Equation (3.23) between top-squarks/quarks and the Higgs/Higgsino in Figure 3.1.

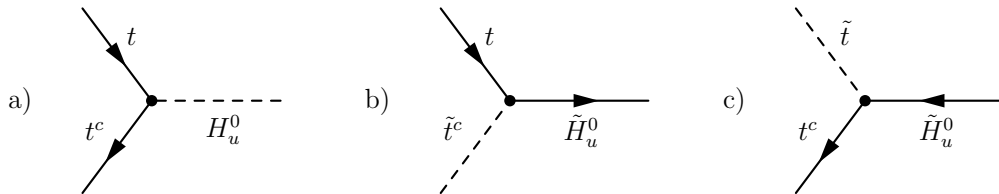


Figure 3.1.: Illustration of the interactions arising from the first term of the superpotential in Equation (3.23), t and t^c can be understood as t_L and t_R^\dagger according to the glossary.

Whereas the first graph from Figure 3.1 a) exists also in the standard model, the other two are additional contributions arising in supersymmetry. They can be obtained by replacing two particles with their supersymmetric partners. Please note that supersymmetry also allows interactions between four scalar particles and additional interactions between fermions, scalars and the fermionic partners of the gauge bosons, the gauginos, which can all be obtained using the Lagrangian density of Equation (3.10) together with the superpotential in Equation (3.23). The Lagrangian density of the MSSM in superfield notation can for example be found in [60], whereas all the Feynman rules can be taken from [61].

3.7. Supersymmetry breaking

As we have argued in Section 3.2 supermultiplets in exact SUSY require the same mass for particles and their superpartners. Since this is experimentally excluded, SUSY has to be a broken symmetry. However the breaking should respect the “nonrenormalizable theorem” [62] to allow for a simple calculation of the renormalization group equations describing the running of the parameters in a supersymmetric theory, since according to the theorem they do not have to be renormalized. There are two ways to break SUSY:

▷ Global spontaneous breaking: The energy of the vacuum state in SUSY is

$$E_{vac} = \langle 0 | H | 0 \rangle \geq 0 \quad , \quad (3.24)$$

where the spinorial charge has to fulfill:

$$Q_\alpha |0\rangle = 0 \quad \text{and} \quad Q_\alpha^\dagger |0\rangle = 0 \quad (3.25)$$

The corresponding Hamilton operator can be constructed in the following form:

$$H = \sum_{\alpha=1}^2 \left\{ Q_{\alpha}, Q_{\alpha}^{\dagger} \right\} = 2\text{tr} [\sigma^{\mu} P_{\mu}] = P_0 \quad (3.26)$$

However, if the vacuum is not a supersymmetric state

$$Q_{\alpha} |0\rangle = |\psi_{\alpha}\rangle \neq 0 \quad \text{and/or} \quad Q_{\alpha}^{\dagger} |0\rangle = |\psi_{\alpha}\rangle \neq 0 \quad (3.27)$$

and $E_{vac} > 0$, SUSY is a spontaneously broken theory and the Goldstone theorem necessarily predicts a state $|\psi_{\alpha}\rangle$, which has an odd fermion number. It describes a massless fermion, named Goldstone fermion or Goldstino. Neglecting space-time dependent effects and fermion condensates, it yields $\langle 0|H|0\rangle = \langle 0|V|0\rangle$ with the scalar potential V given in Equation (3.14). The vacuum state $|\psi_{\alpha}\rangle$ can be induced via two different mechanisms: If the F -terms (first term in V) generate such a vacuum state, the mechanism is called O’Raifeartaigh- [63] and in case of the D -terms (second term in V with an additional term like $-\kappa D$) Fayet-Iliopoulos-mechanism [64]. Also mixtures of these two mechanisms are possible. In both cases the broken operator Q_{α} and thus the Goldstino is a spin- $\frac{1}{2}$ fermion. The Goldstino is “eaten” by the Gravitino in case of supergravity, where supersymmetry is formulated as local supersymmetry [65]. The Gravitino is a spin- $\frac{3}{2}$ fermion, which is the superpartner of the spin-2 graviton and acquires a mass once supersymmetry is spontaneously broken (super-Higgs mechanism).

- ▷ Explicit breaking: By adding explicit terms to the Lagrangian density only resulting in logarithmic divergences in case of higher loop calculations, SUSY can be broken softly. Therefore, the hierarchy problem is still solved. All the possible terms were first presented in [66]. In case of the MSSM they consist of masses for the Higgs bosons, the scalar particles and the gauginos. Moreover additional trilinear couplings T and the term B_{μ} in the scalar sector are possible:

$$\begin{aligned} -\mathcal{L}_{\text{SB,all}} = & \left(m_{\tilde{Q}}^2\right)_{ij} \tilde{Q}_i^{a*} \tilde{Q}_j^a + \left(m_{\tilde{u}^c}^2\right)_{ij} \tilde{u}_i^{c*} \tilde{u}_j^c + \left(m_{\tilde{d}^c}^2\right)_{ij} \tilde{d}_i^{c*} \tilde{d}_j^c + \left(m_{\tilde{L}}^2\right)_{ij} \tilde{L}_i^{a*} \tilde{L}_j^a \\ & + \left(m_{\tilde{e}^c}^2\right)_{ij} \tilde{e}_i^{c*} \tilde{e}_j^c + m_{H_d}^2 H_d^{a*} H_d^a + m_{H_u}^2 H_u^{a*} H_u^a \\ & + \epsilon_{ab} \left[T_u^{ij} H_u^b \tilde{Q}_i^a \tilde{u}_j^c + T_d^{ij} H_d^a \tilde{Q}_i^b \tilde{d}_j^c + T_e^{ij} H_d^a \tilde{L}_i^b \tilde{e}_j^c + \text{h.c.} \right] \\ & + \frac{1}{2} \left(M_1 \tilde{B}^0 \tilde{B}^0 + M_2 \tilde{W}^x \tilde{W}^x + M_3 \tilde{g}^z \tilde{g}^z + \text{h.c.} \right) \end{aligned} \quad (3.28)$$

$$-\mathcal{L}_{\text{SB,MSSM}} = -\mathcal{L}_{\text{SB,all}} - \epsilon_{ab} \left[B_{\mu} H_d^a H_u^b + \text{h.c.} \right] \quad (3.29)$$

We split the soft breaking terms, such that the common part for all models, which are discussed later, is separated from the MSSM specific part. Within these terms the indices x and z represent the three and eight gauge bosons of $SU(2)_L$ and $SU(3)_C$. In addition the shown (3×3) -couplings T and B_{μ} can be chosen complex and the (3×3) -matrices of the masses hermitian, resulting in a real Lagrangian density. In total this explicit breaking introduces 105 arbitrary masses, phases and angles [67], which cannot be rotated away by redefinitions of fields. Therefore such a supersymmetric model comes together with a large parameter space. However this is contrary to the idea of unification. In addition the terms in Equation (3.29) induce flavor mixing and CP violating processes, which are constrained by experiments. Those effects can be avoided by choosing the couplings T proportional to

the corresponding Yukawa couplings Y and the (3×3) -matrices of the masses diagonal as it can be seen from [2].

Although we have now presented two methods how to break supersymmetry, this is not the full story: Explicit breaking introduces a huge number of unknown parameters and the origin of the vacuum expectation values for F - and D -terms in case of spontaneous breaking induces several questions [2]. We will just point out one example: Taking only the MSSM particle content spontaneous breaking at tree-level comes together with sum rules for masses, which are experimentally excluded. An example is

$$m_{\tilde{e}_1}^2 + m_{\tilde{e}_2}^2 = 2m_e^2 \quad , \quad (3.30)$$

which relates the mass eigenstates \tilde{e}_1 and \tilde{e}_2 of the two gauge eigenstates \tilde{e}_L and \tilde{e}_R of the selectron with the electron mass [2]. Equation (3.30) necessarily results in a very light scalar particle not consistent with experiments.

Therefore the breaking of SUSY is often transferred into a “hidden sector”, which is connected to the “visible sector”, the MSSM, via (very) weak mostly flavor blind interactions. The breaking is done spontaneously, resulting in terms similar to the explicit breaking terms presented in Equation (3.29), but induces several relations between the parameters therein, so that the parameter space is drastically reduced. The most popular of such interactions are: minimal supergravity (mSUGRA) [68], gauge-mediated SUSY breaking (GMSB) [69] and anomaly-mediated SUSY breaking (AMSB) [70].

To point out an example, we will have a glimpse at mSUGRA inspired scenarios, where the spontaneous breaking connects to the MSSM via gravitational-strength interactions. The breaking mechanism results in the following relations between the parameters given in Equation (3.29)

$$\begin{aligned} M_3 &= M_2 = M_1 = m_{1/2} \\ m_{\tilde{Q}}^2 &= m_{\tilde{u}^c}^2 = m_{\tilde{d}^c}^2 = m_{\tilde{L}}^2 = m_{\tilde{e}^c}^2 = m_0^2 \cdot I_3, \quad m_{H_d}^2 = m_{H_u}^2 = m_0^2 \\ T_u &= A_0 Y_u, \quad T_d = A_0 Y_d, \quad T_e = A_0 Y_e \\ B_\mu &= B_0 \mu \end{aligned} \quad (3.31)$$

with the scalar parameters $m_{1/2}$, m_0^2 , A_0 and B_0 and the (3×3) -identity matrix I_3 set at the GUT scale. Using the renormalization group equations the soft breaking parameters at the electroweak scale can be calculated by programs like **SPheno** [71]. Within this work we will use these low-energy parameters sets of mSUGRA, GMSB or AMSB motivated scenarios. For the MSSM such parameter sets were defined in the “Snowmass Points and Slopes” [3], resulting in comparable results within different works on SUSY. We present those benchmark scenarios in Chapter 7.

3.8. Mass eigenstates in the MSSM

We illustrated the particle content of the MSSM already in Table 3.1. However, the gauge eigenstates presented within this table are different from the mass eigenstates after electroweak symmetry breaking. Moreover the soft SUSY breaking mass terms modulate several masses. The mixing of gauge eigenstates to mass eigenstates is shown in Table 3.2. Whereas the case of neutralinos, charginos and the scalars will be extensively discussed later, we will comment on the mixing in the slepton and squark sector in more detail in this section:

Gauge eigenstates	Mass eigenstates
$H_u^0, H_d^0, H_u^+, H_d^-$	h, H, A^0, H^\pm
$\tilde{t}_L, \tilde{t}_R, \tilde{b}_L, \tilde{b}_R$	$\tilde{t}_1, \tilde{t}_2, \tilde{b}_1, \tilde{b}_2$
$\tilde{B}, \tilde{W}^0, \tilde{H}_u^0, \tilde{H}_d^0$ $\tilde{W}^\pm, \tilde{H}_u^\pm, \tilde{H}_d^\pm$	$\tilde{\chi}_1^0, \tilde{\chi}_2^0, \tilde{\chi}_3^0, \tilde{\chi}_4^0$ $\tilde{\chi}_1^\pm, \tilde{\chi}_2^\pm$
\tilde{g}	(no mixing)

Table 3.2.: Gauge and mass eigenstates after electroweak symmetry breaking in the MSSM. Since it is commonly used, the fermions to the left are Weyl spinors, the fermions to the right Dirac spinors. The masses eigenstates representing the Goldstone bosons G^0 and G^\pm are not shown.

▷ Neutralinos and charginos:

The neutral components of the Higgsinos together with the bino and the neutral wino mix to four neutral mass eigenstates, the neutralinos $\tilde{\chi}_1^0, \dots, \tilde{\chi}_4^0$. Similarly the charged winos and the charged Higgsinos form the charginos, named $\tilde{\chi}_1^\pm, \tilde{\chi}_2^\pm$. The mass matrices in gauge eigenstates will be presented later, where we will also focus on the on-shell renormalization of those. Similar to the neutrino in case of the seesaw mechanism neutralinos are Majorana particles.

▷ Sleptons and squarks:

Sleptons and squarks are mixing in pairs, if flavor violating effects are neglected. This implies a mixing of the left-handed particles with the right-handed particles to two mass eigenstates. In general the part in the Lagrangian density, which contains the masses of the fermion \tilde{f} at tree-level, can be written in the form

$$\mathcal{L}_{\tilde{f}} = -\frac{1}{2} \begin{pmatrix} \tilde{f}_L^\dagger & \tilde{f}_R^\dagger \end{pmatrix} M_{\tilde{f}} \begin{pmatrix} \tilde{f}_L \\ \tilde{f}_R \end{pmatrix}, \quad (3.32)$$

where the mass matrix $M_{\tilde{f}}$ supposing real parameters is given by

$$M_{\tilde{f}} = \begin{pmatrix} m_{\tilde{f}}^2 + m_Z^2 \cos(2\beta)(I_3^f - Q_f s_W^2) + m_f^2 & m_f(A_f + \mu \{\cot \beta, \tan \beta\}) \\ m_f(A_f + \mu \{\cot \beta, \tan \beta\}) & m_{\tilde{f}_R}^2 + m_Z^2 \cos(2\beta)Q_f s_W^2 + m_f^2 \end{pmatrix}. \quad (3.33)$$

Therein $\{\cot \beta, \tan \beta\}$ is valid for $\{u, d\}$ or $\{\nu, e\}$ fermions. Beside the Weinberg angle $s_W^2 = \sin^2 \theta_W$ this formula includes the mass of the fermionic superpartner m_f , the soft breaking coupling T_f , the third component of the weak isospin I_3^f , the electric charge Q_f and the following soft breaking parameters $m_{\tilde{f}} = m_{\tilde{Q}}, m_{\tilde{L}}$ for left-handed squarks, sleptons and $m_{\tilde{f}'} = m_{\tilde{u}^c}, m_{\tilde{d}^c}, m_{\tilde{e}^c}$ for right-handed u -squarks, d -squarks and sleptons.

Since m_f is large in case of the third generation, the mixing in the third generation squarks and sleptons are large, resulting in one light scalar state, typically lighter than the squarks and sleptons from the first two generations.

▷ Higgs sector:

As we have argued, supersymmetry needs two complex $SU(2)_L$ -doublets, resulting in eight degrees of freedom and thus also 8 mass eigenstates. However, after electroweak symmetry

breaking the three Goldstone bosons G^0 and G^\pm are the longitudinal components of the Z - and W^\pm -gauge bosons. Physical particles are the lightest Higgs h , the heavy Higgs H , the CP-odd Higgs A^0 and two charged Higgs H^\pm . A detailed discussion of the Higgs sector of all models under consideration will follow in Section 5.1.

3.9. R -parity

Having introduced the MSSM in all details, we did not discuss one important point: In principle neither gauge symmetries nor supersymmetry forbids the following additional terms in the superpotential

$$W = W_{\text{MSSM}} + W_{\mathcal{R}} \quad \text{with}$$

$$W_{\mathcal{R}} = \epsilon_{ab} \left(\frac{1}{2} \lambda_{ijk} \widehat{L}_i^a \widehat{L}_j^b \widehat{e}_k^c + \lambda'_{ijk} \widehat{L}_i^a \widehat{Q}_j^b \widehat{d}_k^c - \epsilon_i \widehat{L}_i^a \widehat{H}_u^b \right) + \frac{1}{2} \lambda''_{ijk} \widehat{u}_i^c \widehat{d}_j^c \widehat{d}_k^c, \quad (3.34)$$

which are bi- or trilinear in the superfields. For reasons of gauge symmetry it yields $\lambda_{ijk} = -\lambda_{jik}$ and $\lambda''_{ijk} = -\lambda''_{ikj}$. By a rotation of \widehat{H}_d and \widehat{L}_i the bilinear term ϵ_i can in principle be reabsorbed in the terms λ_{ijk} and λ'_{ijk} . However, the soft SUSY breaking terms

$$-\mathcal{L}_{\text{SB},\mathcal{R}} = -B_i \widetilde{L}_i H_u + \dots \quad (3.35)$$

do not vanish simultaneously. The baryon B and lepton numbers L for the fields involved are equal to $B = +\frac{1}{3}$ for \widehat{Q}_i . It yields $B = -\frac{1}{3}$ for $\widehat{u}_i^c, \widehat{d}_i^c$, whereas all the other particles have baryon number $B = 0$. Moreover it is $L = +1$ for \widehat{L}_i and $L = -1$ for \widehat{e}_i^c , otherwise $L = 0$. Thus the terms with $\lambda_{ijk}, \lambda'_{ijk}$ and ϵ_i violate lepton number by one unit, whereas the term with λ''_{ijk} violates baryon number by one unit. Allowing lepton and baryon number violation at the same time gives rise to a possible decay of the proton, which is experimentally not observable.

We will point out one example: In case of non-vanishing λ'_{11k} and λ''_{11k} the decay $p \rightarrow \pi^0 e^+$ has the following decay width:

$$\Gamma(p \rightarrow e^+ \pi^0) \propto \sum_{k=2,3} \frac{1}{m_{\widetilde{d}_k}^4} |\lambda'_{11k} \lambda''_{11k}|^2 \quad (3.36)$$

The contribution mediated by a \widetilde{s}_R -squark is shown in Figure 3.2. Since the lifetime of the proton is larger than 10^{32} years, this results in an upper bound for the product of these couplings:

$$\lambda'_{11k} \lambda''_{11k} \leq 2 \cdot 10^{-27} \left(\frac{m_{\widetilde{d}_k}}{100 \text{ GeV}} \right)^2 \quad (3.37)$$

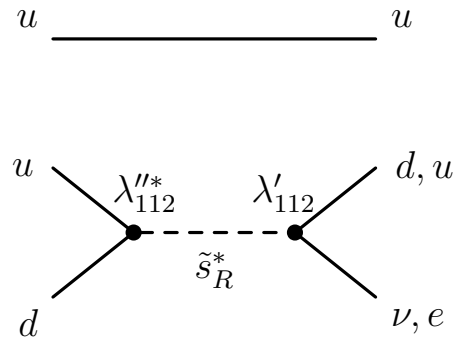


Figure 3.2.: Contribution to the proton decay via couplings λ' and λ'' in Equation (3.23).

Whereas the bilinear parameters ϵ have their strongest bounds from neutrino physics, the trilinear parameters λ, λ' and λ'' are not only constrained from proton decay and neutrino masses, but several other effects like charged current universality, neutral current interactions, anomalous magnetic dipole moments, CP violation, flavor violating processes of hadrons and leptons and

lepton and baryon number violating processes have to be considered. A nice overview is given in [72] and more recent bounds can be found in [73].

Thus a new symmetry, namely R -parity, was introduced to explain these various experimental constraints. The standard model of particle physics taking into account renormalizable terms only does not contain any term, which violates baryon or lepton number. R -parity guarantees the same feature also in supersymmetric models. It is defined in the form

$$R_p = (-1)^{3(B-L)+2s} \quad (3.38)$$

with the spin s of a particle. Its original definition can be traced back to [74] and [75]. In fact it forbids all terms given in Equation (3.34) and is a simple, discrete Z_2 -symmetry. Inserting the quantum numbers of each particle shows that all particles of the standard model and the Higgs bosons have R -parity $R_p = +1$, whereas all the squarks, sleptons, gauginos and Higgsinos have $R_p = -1$. Thus conserved R -parity has extensive phenomenological implications, since it forbids any mixing between standard model particles and their superpartners. Therefore the lightest supersymmetric particle (LSP) is stable and a dark matter candidate in case it is neutral. Moreover each supersymmetric particle necessarily decays in a final state with an odd number of $R_p = -1$ particles, so that the end of a supersymmetric cascade decay always includes the LSP. Moreover supersymmetric particles can only be produced in even numbers at colliders, starting with an initial state formed by standard model particles.

However, R -parity is not motivated theoretically, but is a result of experimental data. The discrete symmetries (charge conjugation C , parity P and time reversal T) of the standard model are no exact symmetries, thus also R -parity conservation is questionable. In fact other symmetries like Z_3 -symmetries defined in [76] or [77], called “baryon triality”, can be used to forbid other terms of Equation (3.34). Since R -parity violation is a crucial part of this thesis, we will motivate it in the next chapter about extensions of the MSSM.

Extensions of the MSSM

Although we have shown that the MSSM as simplest supersymmetric extension of the standard model solves a variety of theoretical questions and is a nice completion of all possible external symmetries, some subtle questions were not addressed yet: the μ -problem of the MSSM described in the subsequent section and the question, how neutrino masses can be explained in supersymmetric models.

In the following we will motivate the next-to-minimal supersymmetric standard model (NMSSM) giving a solution to the μ -problem. Afterwards we comment on the seesaw mechanism in supersymmetric models, before we give an introduction to models with R -parity violation. A review on simple MSSM extensions can be found in [78].

4.1. Next-to-minimal supersymmetric standard model - NMSSM

The μ -term in the superpotential of the MSSM in Equation (3.23) has a dimension of mass, which poses the question, why it is at the electroweak scale and not at a much larger scale. This question is commonly known as μ -problem. In accordance to [79] we briefly sketch the arguments, why μ has to be at the electroweak scale and cannot vanish: The μ -term gives rise to identical positive masses μ^2 for the Higgs fields $|H_u|^2$ and $|H_d|^2$, but in addition it provides a Dirac mass term μ for their fermionic superpartners. Whereas the soft SUSY breaking mass term B_μ effects the scalar sector, the masses of the fermionic superpartners at tree-level are only determined by μ itself. Thus, the non-observance of light charginos - where the charged Higgsino components \tilde{H}_u^+ and \tilde{H}_d^- enter - induces a bound of $|\mu| \gtrsim 100$ GeV. In addition a vanishing μ induces a Peccei-Quinn-symmetry [80] in the scalar sector resulting in a massless axion. Also the soft SUSY breaking term B_μ has to be nonzero to guarantee that both neutral components H_u^0 and H_d^0 are nonvanishing at the minimum of the Higgs potential. In total μ cannot vanish, but is also bounded by $|\mu| \lesssim m_{\text{SUSY}}$: If the mass contributions to H_u and H_d induced by the μ -term dominate the potentially negative soft SUSY breaking mass terms, the Higgs potential is not unstable and electroweak symmetry breaking is not generated.

A simple solution to this μ -problem can be found by replacing the bilinear μ -term in the superpotential with a trilinear term involving a new particle, namely a chiral supermultiplet \hat{S} , which is a gauge singlet. The resulting model is named next-to-minimal supersymmetric standard model (NMSSM) and is characterized by the following superpotential:

$$W_{\text{NMSSM}} = \epsilon_{ab} \left(Y_u^{ij} \hat{H}_u^b \hat{Q}_i^a \hat{u}_j^c + Y_d^{ij} \hat{H}_d^a \hat{Q}_i^b \hat{d}_j^c + Y_e^{ij} \hat{H}_d^a \hat{L}_i^b \hat{e}_j^c - \lambda \hat{S} \hat{H}_d^a \hat{H}_u^b \right) + \frac{1}{3} \kappa \hat{S} \hat{S} \hat{S} \quad (4.1)$$

The procedure is similar to the generation of fermion masses in the standard model via Yukawa couplings: As soon as the scalar component S of the new superfield \hat{S} gets a vacuum expectation

value by the soft SUSY breaking terms, an effective μ -term of the form

$$\mu = \lambda \langle S \rangle =: \frac{1}{\sqrt{2}} \lambda v_S \quad (4.2)$$

is generated. Since the SUSY breaking terms are of the order of the electroweak scale to allow for a soft breaking, also v_S and necessarily μ are naturally of this order, if λ is chosen to be of order $\mathcal{O}(1)$. In fact the first attempts to supersymmetrize the standard model contained such a singlet field [81] similar to the first globally supersymmetric GUT models [82, 50].

The soft SUSY breaking terms, which have to be added to $\mathcal{L}_{\text{SB,all}}$ in Equation (3.28), are

$$-\mathcal{L}_{\text{SB,NMSSM}} = -\mathcal{L}_{\text{SB,all}} + m_S^2 S S^* - \epsilon_{ab} \left[T_\lambda S H_d^a H_u^b + \text{h.c.} \right] + \left[\frac{1}{3} T_\kappa S S S + \text{h.c.} \right] . \quad (4.3)$$

The last term in the superpotential given in Equation (4.1) avoids the presence of a global $U(1)$ -symmetry $H_d H_u \rightarrow e^{i\alpha} H_d H_u, S \rightarrow e^{-i\alpha} S$ (Peccei-Quinn-symmetry [80]), which guarantees the bilinear μ -term in the MSSM. Since only trilinear couplings are present, it is easier to embed the NMSSM in string theories [83]. In addition the superpotential in Equation (4.1) shows a discrete Z_3 -symmetry. Transforming all superfields according to $\hat{S} \rightarrow e^{2\pi i/3} \hat{S}$, the superpotential is not changed. Electroweak symmetry breaking and the generation of the effective μ -term destroys this Z_3 -symmetry. However, this Z_3 -symmetry induces a subtle problem in the early universe: the “domain wall”-problem. During electroweak symmetry breaking causal horizons between domains with different vacua might have formed [84]. A solution to this problem is given by nonrenormalizable operators [85], which break the Z_3 -symmetry in the superpotential, but have no implications for the phenomenology of the model. For more details we refer to [86]. An alternative would be an additional $U(1)$ -symmetry, which is summarized in [87]. In particular in the Higgs and neutralino sector the particle content of the NMSSM differs clearly from the one in the MSSM, since the singlet gets involved in the formation of mass eigenstates in those sectors as we will show in the subsequent chapters. A detailed overview about the NMSSM can be found in [79].

4.2. Supersymmetric seesaw mechanisms

The second problem we want to address is the generation of neutrino masses. The seesaw mechanisms we presented in Section 2.3.2 can be easily supersymmetrized. Taking our example with the right-handed neutrino we can simply introduce a right-handed neutrino superfield $\hat{\nu}^c$ and add it to the superpotential of the MSSM:

$$W = W_{\text{MSSM}} + \epsilon_{ab} Y_\nu^i \hat{H}_u^b \hat{L}_i^a \hat{\nu}^c + m_M \hat{\nu}^c \hat{\nu}^c \quad (4.4)$$

Note that instead of ν_L and ν_R denoting Dirac spinors as originally used for the introduction to the seesaw mechanism, we are working with Weyl spinors ν and ν^c in the context of supersymmetry. The Yukawa couplings Y_ν induce Dirac masses $m_D = Y_\nu v_u$ after electroweak symmetry breaking. In addition one can add explicit Majorana masses m_M , so that the seesaw mechanism is equivalent to the one we presented for the standard model [78]. In principle, the Yukawa couplings Y_ν are already sufficient to generate neutrino masses. However the seesaw mechanism allows to explain the suppression of the neutrino masses $m_i \leq 1$ eV compared to the other fermion masses without the need of choosing the Yukawa couplings unnaturally small $Y_\nu < 10^{-10}$.

The only difference between the supersymmetric extension of the seesaw mechanism and its original definition is the additional right-handed sneutrino $\tilde{\nu}^c$, which is in general mixed with the left-handed sneutrino $\tilde{\nu}$ by the soft SUSY breaking coupling T_ν . There exist seesaw extensions, which allow for a small mixing $T_\nu = A_\nu Y_\nu$ and a light $\tilde{\nu}^c$, so that the right-handed sneutrino couples very weak to all the other particles and can serve as a dark matter candidate [88]. Moreover such models might offer a collider phenomenology, which is not known from the MSSM. In case $\tilde{\nu}^c$ is the LSP, the decay of the next-to-LSP (NLSP) is suppressed and might show a long, measurable decay length [89].

The seesaw mechanisms based on the three different realizations of the Weinberg operator were also supersymmetrized at an early stage [90]. The additional intermediate particles can be embedded in $SU(5)$ and are therefore compatible with GUTs. Supersymmetric versions of the seesaw mechanisms can either be tested at colliders [91] through the masses of the superpartners or via their effect on lepton flavor violating decays, which is practically unavoidable even in case of flavor blind SUSY breaking [92].

4.3. Models with broken R -parity

As argued in Section 3.9 R -parity was introduced for experimental reasons resulting in a stable proton and respecting the various experimental constraints given in [72]. However we will formulate two arguments against the conservation of R -parity:

- ▷ Whereas in the standard model baryon B and lepton L number conservation at tree-level are given “accidentally”, since terms violating B or L number are not gauge invariant, supersymmetry makes use of R -parity not to allow for L and B number violating processes. However, there’s a priori no theoretical motivation for such a symmetry. With regard to the proton decay, L or B number conservation is sufficient. Thus, also other discrete symmetries can account for this problem like the already mentioned “baryon triality”, which is defined in the form

$$Z_3^B = \exp\left(\frac{2\pi i}{3}(B - 2Y)\right) \quad (4.5)$$

and forbids only the B number violating term in the superpotential in Equation (3.34).

- ▷ In addition R -parity does not forbid dimension 5 operators, which induce proton decay as shown in [75] or [76]. In particular in SUSY grand unified theories operators like $G_5 = (f/\Lambda)QQQL$ are generated. They conserve R -parity, but allow for the decay of the proton, so that strong bounds on the coupling $f < 10^{-7}$ for $\Lambda \sim m_{GUT}$ arise [93].

We now listed some arguments, which show that R -parity does not have to be the correct discrete symmetry to be consistent with experimental data. In fact, R -parity violation does not only pose open questions, but can also give an answer to unsolved problems within the MSSM, the most important being the explanation of neutrino masses, if one allows for lepton number violating terms. This issue will be discussed in more detail in later sections. In addition it provides a rich phenomenology at colliders and might moreover give a connection between collider phenomenology and neutrino physics.

Before discussing the simplest models of R -parity violation, which will also be part of this thesis, we want to address the explanation of dark matter once again: If R -parity is broken, the LSP is not a stable particle any more, but can decay into standard model particles. Therefore, the lightest neutralino is lost as dark matter candidate. However, non-standard explanations of dark

matter are still accessible in R -parity violating SUSY, namely light gravitinos [53], the axion [54] or its superpartner, the axino [55].

We presented all R -parity violating terms in Equation (3.34). Supposing for example baryon triality as underlying symmetry, we consider only the lepton number violating terms. The trilinear terms provide a huge number of free parameters, where different attempts tried to reduce them, see [77] or [94]. We will focus on the more predictive bilinear terms $\epsilon_i \widehat{L}_i \widehat{H}_u$, which are mainly constrained by neutrino physics [72]. Other bounds are automatically fulfilled, when neutrino physics is described by the bilinear terms. The R -parity violating models under consideration contain either an explicit ϵ_i -term or generate this term effectively.

In the following we start with a discussion of the minimal realization of bilinear R -parity violation, which can also be generated in a model with spontaneously broken R -parity. Afterwards we will give an introduction to the $\mu\nu$ SMSM, which combines the advantages of bilinear R -parity violation together with a solution of the μ -problem similar to the NMSSM.

4.3.1. Bilinear R -parity violation - BRpV

The superpotential of bilinear R -parity violation, which we call BRpV, is given by

$$W_{\text{BRpV}} = \epsilon_{ab} \left(Y_u^{ij} \widehat{H}_u^b \widehat{Q}_i^a \widehat{u}_j^c + Y_d^{ij} \widehat{H}_d^a \widehat{Q}_i^b \widehat{d}_j^c + Y_e^{ij} \widehat{H}_d^a \widehat{L}_i^b \widehat{e}_j^c - \mu \widehat{H}_d^a \widehat{H}_u^b + \epsilon_i \widehat{L}_i^a \widehat{H}_u^b \right) \quad , \quad (4.6)$$

where ϵ_{ab} is again the complete antisymmetric $SU(2)$ tensor with $\epsilon_{12} = 1$. The ansatz of this model is based on work done in [95]. The last term in Equation (4.6) explicitly breaks lepton number, so that no Goldstone boson is associated with the breaking itself. The soft SUSY breaking terms are despite from the terms of $\mathcal{L}_{\text{SB,all}}$ in Equation (3.28):

$$-\mathcal{L}_{\text{SB,BRpV}} = -\mathcal{L}_{\text{SB,all}} + \epsilon_{ab} \left[B_i \tilde{L}_i^a H_u^b - B_\mu H_d^a H_u^b + \text{h.c.} \right] \quad (4.7)$$

The ϵ_i -terms induce a mixing between the well-known gauge eigenstates of the neutralinos $\tilde{B}, \tilde{W}_3^0, \tilde{H}_d^0$ and \tilde{H}_u^0 and the three left-handed neutrinos ν_i at tree-level, resulting in an effective Majorana mass term for one of the neutrinos at tree-level as we will point out later. For an explanation of the full neutrino spectrum one-loop corrections have to be taken into account, which was done in [96, 97] using $\overline{\text{DR}}$ neutralino-neutrino masses. In fact the generation of the single neutrino mass at tree-level is comparable to the seesaw mechanism, since the neutrino masses are suppressed by the determinant of the heavy neutralino mass matrix. However the accessibility of those particles at colliders in contrast to naturally heavier particles in the seesaw mechanisms generates a collider phenomenology correlated with neutrino data. Additionally also the charginos mix with the leptons and the scalar, pseudoscalar and charged scalar states have to be combined with the sneutrinos and sleptons.

The neutrino parameters are determined by six R -parity violating parameters, namely the three parameters ϵ_i and the three soft SUSY breaking parameters B_i . However we derive the latter ones from the tadpole equations and take the vacuum expectation values of the left-handed sneutrinos v_i as additional input to ϵ_i . Similar to the μ -problem in the MSSM it is a priori unclear, why the parameters ϵ_i should be near the electroweak scale. Thus we introduce spontaneous R -parity violation or the $\mu\nu$ SMSM, which both offer a solution to this problem in the manner of the NMSSM. Finally we want to comment on the renormalization group running of the bilinear and trilinear parameters: If trilinear couplings λ, λ' are present at a fundamental scale, they will induce bilinear R -parity violation at a different scale. However bilinear terms ϵ_i can exist in the absence of trilinear parameters, since massive terms ϵ_i do not generate massless parameters

λ or λ' . This can also be seen from spontaneous bilinear R -parity violation, where R -parity is conserved at high energies:

Spontaneous R -parity violation can be understood as a violation of lepton number by the vacuum expectation value of some singlet field [98]. Thus the bilinear term can be interpreted as the low-energy limit of some spontaneous R -parity violating model, where the new singlet fields are all decoupled. This includes a solution to the question, why the bilinear terms ϵ_i have to be chosen at $\mathcal{O}(0.1 \text{ GeV})$, since they are generated similar to the μ -term in the NMSSM. An example of such a model of spontaneous R -parity violation using only trilinear terms [98] can be constructed from the superpotential of the NMSSM in the following form

$$W_{\text{spRpV}} = W_{\text{NMSSM}} + \epsilon_{ab} \left(Y_{\nu}^{ij} \widehat{H}_u^b \widehat{L}_i^a \widehat{\nu}_j^c \right) + h \widehat{S} \widehat{\nu}^c \widehat{\Phi} \quad . \quad (4.8)$$

In addition to the singlet superfield \widehat{S} from the NMSSM, right-handed neutrino superfields $\widehat{\nu}_j^c$ and a singlet superfield $\widehat{\Phi}$ with the lepton numbers $L = 0, -1, 1$ are added. Obviously all terms conserve lepton number, so that also R -parity is not broken. However, as soon as the vacuum expectation values of the scalar components of the superfields and the sneutrinos arise R -parity is broken spontaneously and effective bilinear terms $\epsilon_i = \frac{1}{\sqrt{2}} Y_{\nu}^i v_c$ with the VEV of the right-handed sneutrino $\langle \widehat{\nu}^c \rangle = \frac{1}{\sqrt{2}} v_c$ are induced. Spontaneous breaking results in a Goldstone boson, which is called Majoron J and has phenomenological implications: The lightest neutralino can decay in the form $\widetilde{\chi}_1^0 \rightarrow J \nu_i$ with branching ratios up to 100% [99, 100]. Moreover measurements to lepton flavor violating decays like $\mu \rightarrow e \gamma$ have to account for the additional decays $\mu \rightarrow e J$ or $\mu \rightarrow e J \gamma$, so that bounds on spontaneous R -parity violating couplings can be deduced [101]. However spontaneous R -parity violation includes several new singlet superfields and we show in the following section that using a right-handed neutrino superfield is sufficient to avoid bilinear terms in the superpotential.

4.3.2. $\mu\nu$ SSM

The $\mu\nu$ SSM, which was first proposed in [102], uses the same right-handed neutrino superfield(s) $\widehat{\nu}_k^c$ not only to generate Dirac mass terms for the left-handed neutrinos but in addition the μ -term. The superpotential is given by:

$$W_{\mu\nu\text{SSM}} = \epsilon_{ab} \left(Y_u^{ij} \widehat{H}_u^b \widehat{Q}_i^a \widehat{u}_j^c + Y_d^{ij} \widehat{H}_d^a \widehat{Q}_i^b \widehat{d}_j^c + Y_e^{ij} \widehat{H}_d^a \widehat{L}_i^b \widehat{e}_j^c + Y_{\nu}^{ik} \widehat{H}_u^b \widehat{L}_i^a \widehat{\nu}_k^c \right) - \epsilon_{ab} \lambda_k \widehat{\nu}_k^c \widehat{H}_d^a \widehat{H}_u^b + \frac{1}{3} \kappa_{klm} \widehat{\nu}_k^c \widehat{\nu}_l^c \widehat{\nu}_m^c \quad . \quad (4.9)$$

Similar to the NMSSM the presence of dimensionless trilinear couplings only can be motivated from string theory limits. The last two terms in Equation (4.9) explicitly break lepton number and R -parity if we assign lepton number to $\widehat{\nu}_k^c$. In addition the last term in Equation (4.9) avoids a Goldstone boson associated to a global $U(1)$ -symmetry (Peccei-Quinn-symmetry) as in the NMSSM. It generates effective Majorana neutrino masses for the right-handed neutrinos at the electroweak scale. As soon as the right-handed sneutrinos obtain a VEV $\langle \widehat{\nu}_k^c \rangle = \frac{1}{\sqrt{2}} v_{ck}$ an effective μ -term and effective bilinear terms of the form

$$\mu = \frac{1}{\sqrt{2}} \lambda_k v_{ck} \quad \text{and} \quad \epsilon_i = \frac{1}{\sqrt{2}} Y_{\nu}^{ik} v_{ck} \quad (4.10)$$

are generated. Similar to the NMSSM and spontaneous R -parity violation the $\mu\nu$ SSM only contains trilinear terms, so that the “domain wall”-problem is also present due to a discrete Z_3 -symmetry, but the solutions of the NMSSM can be adopted. We want to add that the terms $\widehat{\nu}^c \widehat{H}_d \widehat{H}_u$ and $\widehat{\nu}^c \widehat{\nu}^c \widehat{\nu}^c$ have been considered as possible sources for the baryon asymmetry of the universe [103] and for the generation of neutrino masses and bilarge mixing already in [104]. The soft SUSY breaking terms can be written in the form:

$$\begin{aligned}
 -\mathcal{L}_{\text{SB},\mu\nu\text{SSM}} = & -\mathcal{L}_{\text{SB,all}} + m_{\widehat{\nu}^c}^2 \tilde{\nu}_k^c \tilde{\nu}_l^{c*} \\
 & + \epsilon_{ab} \left[T_{\nu}^{ik} H_u^b \tilde{L}_i^a \tilde{\nu}_k^c - T_{\lambda}^k \tilde{\nu}_k^c H_d^a H_u^b + \text{h.c.} \right] + \left[\frac{1}{3} T_{\kappa}^{klm} \tilde{\nu}_k^c \tilde{\nu}_l^c \tilde{\nu}_m^c + \text{h.c.} \right] \quad (4.11)
 \end{aligned}$$

Please note that for practical purposes it is useful to write the superpotential in the basis where the right-handed neutrinos have a diagonal mass matrix. Since their masses are induced by the κ term in Equation (4.9), this is equivalent to writing this term including only diagonal couplings $\kappa_{klm} \widehat{\nu}_k^c \widehat{\nu}_l^c \widehat{\nu}_m^c \rightarrow \kappa_k (\widehat{\nu}_k^c)^3$ with $k = 1, \dots, n$ and n being the number of right-handed neutrino superfields $\widehat{\nu}^c$. However, the rotation made in the superpotential does not necessarily diagonalize the soft trilinear terms T_{κ}^{klm} in Equation (4.11) and the soft mass terms $m_{\widehat{\nu}^c}^2$ implying in general additional mixing between the right-handed sneutrinos.

Concerning the generation of neutrino masses the $\mu\nu$ SSM is very similar to BRpV. If we take the $\mu\nu$ SSM with one-right handed neutrino superfield as example, we count six new parameters compared to the NMSSM. This can be seen in the following: If no lepton number is assigned to $\widehat{\nu}^c$ the fourth term in Equation (4.9) explicitly breaks lepton number. Thus both models end up with the same number of R -parity violating parameters. Note that for the phenomenology it does not matter if $\widehat{\nu}^c$ carries lepton number as it is broken explicitly by a least one interaction of this field. Therefore the R -parity violating parameters are the Yukawa couplings Y_{ν}^i and the soft SUSY breaking couplings T_{ν}^i . As in the case of BRpV we can choose the VEVs of the left-handed sneutrinos v_i as input and calculate the parameters T_{ν}^i from the tadpole equations. In fact it turns out that in the $\mu\nu$ SSM with one right-handed neutrino superfield only one neutrino acquires a mass, so that loop contributions have to be taken into account as in BRpV. In contrast more than one right-handed neutrino superfield allow an explanation of neutrino data at pure tree-level as we will point out in the subsequent chapters.

Very similar to the $\mu\nu$ SSM are models with the well-known NMSSM singlet together with (right-handed) singlet neutrino superfields. This induces explicit bilinear terms and was discussed in [105], in combination with tri-bi maximal mixing in [106]. In [107] the authors propose a model similar to the $\mu\nu$ SSM with only one singlet.

Supersymmetric models at tree-level

In this chapter we will discuss the basic features of the MSSM, NMSSM, bilinear R -parity violation and the $\mu\nu$ SSM at tree-level, whereas considerations on one-loop level will be part of the next chapter. We start with a detailed discussion of the scalar sectors including tadpole equations and unphysical states. In addition we summarize the bounds on light scalar and pseudoscalar states given by LEP within this section. Thereafter we present the procedure of gauge fixing and unphysical states, namely Goldstone bosons and Faddeev-Popov ghosts in more detail, since we will put special emphasis on the gauge invariance of our calculation. Then we present the formation of mass eigenstates in the neutralino and chargino sector in the various models under consideration including the generation of neutrino masses at tree-level. In the last section we focus on the two-body decays $\tilde{\chi}_j^0 \rightarrow \tilde{\chi}_l^\pm W^\mp$ and $\tilde{\chi}_l^\pm \rightarrow \tilde{\chi}_j^0 W^\pm$, which are of particular interest for SUSY cascade decays and with regard to the R -parity violating final state $\tilde{\chi}_1^0 \rightarrow l^\pm W^\mp$.

5.1. Scalar sectors, tadpole equations and parameters

In this section we will focus on the determination of parameters from the scalar and pseudoscalar sectors of the various models under consideration. This discussion includes the minimization conditions of the scalar potential V with respect to the different vacuum expectation values, resulting in the so called tadpole equations. The scalar potential V can be obtained from Equation (3.14) together with the soft SUSY breaking terms we gave in the previous chapter and is of the form

$$V = W_i W_i^* + \frac{1}{2} g_a^2 (\phi_i^* T_a \phi_i) (\phi_j^* T_a \phi_j) - \mathcal{L}_{\text{SB}} \quad . \quad (5.1)$$

In addition we will define several new angles and abbreviations, which are helpful for the discussion of neutrino physics and on-shell masses later.

All the results we show in the following subsections can be reproduced by the program **MaCoR**, which we present in Appendix F.1. It allows to calculate the electroweak Lagrangian of all considered models including the scalar potential, from which the tadpole equations and mass matrices of the scalar, pseudoscalars and charged scalars can be deduced.

Before presenting the individual models we will point out our general notation for the scalars, pseudoscalars and charged scalars. We denote the gauge eigenstates by $S^{0'}$, $P^{0'}$ and $S^{\pm'}$, which are vectors with 2 to 10 components depending on the model, so that the quadratic form of the scalar potential is given by

$$V_{S^0, P^0, S^\pm} = \frac{1}{2} S^{0'T} M_{S^0}^2 S^{0'} + \frac{1}{2} P^{0'T} M_{P^0}^2 P^{0'} + S^{-'T} M_{S^\pm}^2 S^{+'} \quad (5.2)$$

with the mass matrices of the scalars $M_{S^0}^2$, the pseudoscalars $M_{P^0}^2$ and the charged scalars $M_{S^\pm}^2$. The mixing matrices, which rotate these gauge into mass eigenstates, are defined as follows:

$$S_i^\pm = R_{ij}^{S^\pm} S_j^{\pm'}, \quad S_i^0 = R_{ij}^{S^0} S_j^{0'}, \quad P_i^0 = R_{ij}^{P^0} P_j^{0'} \quad (5.3)$$

Since $M_{S^\pm}^2$ is a hermitian matrix, R^{S^\pm} is a unitary rotation matrix, $M_{S^0}^2$ and $M_{P^0}^2$ are real symmetric matrices, so that the corresponding rotation matrices R^{S^0} and R^{P^0} are orthogonal. They diagonalize the mass matrices in the form:

$$M_{S^\pm, \text{dia.}}^2 = R^{S^\pm} M_{S^\pm}^2 \left(R^{S^\pm}\right)^\dagger \quad (5.4)$$

$$M_{S^0, \text{dia.}}^2 = R^{S^0} M_{S^0}^2 \left(R^{S^0}\right)^T \quad (5.5)$$

$$M_{P^0, \text{dia.}}^2 = R^{P^0} M_{P^0}^2 \left(R^{P^0}\right)^T \quad (5.6)$$

For the sfermion sector we showed the general form of the mass matrices already in Section 3.8 for the MSSM. They have the same form also in the NMSSM. However R -parity violation results in additional contributions for the squarks and in case of sneutrinos and sleptons it induces a mixing with the scalars, pseudoscalars and charged scalars presented above. Thus the latter case is included in the discussion below. The squark mass matrices for BRpV can be found in [97], for the $\mu\nu$ SMS they are shown in the Appendix A. We present our results for the Landau gauge resulting in massless Goldstone bosons, whereas the additional contributions in R_ξ -gauge are shown in the following section.

5.1.1. MSSM and BRpV

MSSM

We sketched the scalar and pseudoscalar sector of the MSSM already in Section 3.8. However, the scalars and pseudoscalars are of such an importance, that we want to present the Higgs sector in combination with the gauge boson sector once again for the MSSM. We follow [58] and start with the neutral sector, where the fields H_d^0 and H_u^0 can be expanded in the following way

$$H_d^0 = \frac{1}{\sqrt{2}} (\sigma_d^0 + v_d + i\phi_d^0), \quad H_u^0 = \frac{1}{\sqrt{2}} (\sigma_u^0 + v_u + i\phi_u^0), \quad (5.7)$$

where σ^0 indicates the scalar and ϕ^0 the pseudoscalar component. The angle $\tan \beta$ is defined as the ratio of the VEVs v_u and v_d in the following form

$$\tan \beta = \frac{v_u}{v_d} \quad . \quad (5.8)$$

The mass matrices can be deduced as second derivatives with respect to the fields from the scalar potential in Equation (5.1), resulting in:

$$V_{S^0} = \frac{1}{2} (\sigma_d^0, \sigma_u^0) M_{S^0}^2 \begin{pmatrix} \sigma_d^0 \\ \sigma_u^0 \end{pmatrix} \quad \text{and} \quad V_{P^0} = \frac{1}{2} (\phi_d^0, \phi_u^0) M_{P^0}^2 \begin{pmatrix} \phi_d^0 \\ \phi_u^0 \end{pmatrix} \quad \text{with} \quad (5.9)$$

$$M_{S^0}^2 = \frac{1}{2} \begin{pmatrix} 2m_{H_d}^2 + \frac{1}{4}(g'^2 + g^2)(3v_d^2 - v_u^2) & -(B_\mu + B_\mu^*) - \frac{1}{2}v_d v_u (g'^2 + g^2) \\ -(B_\mu + B_\mu^*) - \frac{1}{2}v_d v_u (g'^2 + g^2) & 2m_{H_u}^2 + \frac{1}{4}(g'^2 + g^2)(3v_u^2 - v_d^2) \end{pmatrix} \quad (5.10)$$

$$M_{P^0}^2 = \frac{1}{2} \begin{pmatrix} 2m_{H_d}^2 + \frac{1}{4}(g'^2 + g^2)(v_d^2 - v_u^2) & B_\mu + B_\mu^* \\ B_\mu + B_\mu^* & 2m_{H_u}^2 - \frac{1}{4}(g'^2 + g^2)(v_d^2 - v_u^2) \end{pmatrix} \quad (5.11)$$

Taking the scalar potential V the minimization conditions can be calculated

$$t_d^0 = \frac{\partial V}{\partial v_d} = -\frac{1}{2}(B_\mu + B_\mu^*)v_u + (m_{H_d}^2 + \mu\mu^*)v_d + v_d D = 0 \quad (5.12)$$

$$t_u^0 = \frac{\partial V}{\partial v_u} = -\frac{1}{2}(B_\mu + B_\mu^*)v_d + (m_{H_u}^2 + \mu\mu^*)v_u - v_u D = 0 \quad (5.13)$$

with the abbreviation $D = \frac{1}{8}(g^2 + g'^2)(v_d^2 - v_u^2)$. Note that a redefinition of the fields H_u and H_d allows to choose B_μ real and positive in the MSSM. In the following we calculate the soft SUSY breaking masses $m_{H_d}^2$ and $m_{H_u}^2$ from the tadpole equations. Choosing real VEVs and a real and positive B_μ we can insert $m_{H_d}^2$ and $m_{H_u}^2$ in $M_{P^0}^2$ in Equation (5.11):

$$M_{P^0}^2 = B_\mu \begin{pmatrix} v_u/v_d & 1 \\ 1 & v_d/v_u \end{pmatrix} \quad (5.14)$$

The eigenvalues of this matrix are:

$$m_{P_1}^2 = m_{G^0}^2 = 0, \quad m_{P_2}^2 = m_A^2 = \frac{B_\mu}{v_d v_u} (v_d^2 + v_u^2) = \frac{2B_\mu}{\sin(2\beta)} \quad (5.15)$$

The first eigenvalue corresponds to the Goldstone boson G^0 , which is eaten up by the Z boson. Knowing these two equations we can present our input parameters in the Higgs and gauge boson sector, which we will use if not stated otherwise:

$$\tan \theta_W, \quad \alpha_{EM}, \quad m_Z \quad \text{and} \quad \tan \beta, \quad \mu, \quad m_A^2 \quad (5.16)$$

The Weinberg angle θ_W and the fine-structure constant α_{EM} were defined in Equation (2.9). Together with the mass of the Z boson m_Z they are known from various experiments, in particular LEP. $\tan \beta, \mu$ and the mass of the pseudoscalar Higgs m_A^2 are free parameters in supersymmetry. From these quantities we can deduce the gauge couplings g' and g in accordance to Equation (2.9) and the vacuum expectation values v_d and v_u using the formulas for the heavy gauge boson masses in combination with $\tan \beta$:

$$m_Z^2 = \frac{1}{2}(g^2 + g'^2)(v_d^2 + v_u^2), \quad m_W^2 = \frac{1}{2}g^2(v_d^2 + v_u^2) = m_Z^2 \cos^2 \theta_W, \quad m_\gamma = 0 \quad (5.17)$$

Using this input we can also reexpress the matrix of the scalars $M_{S^0}^2$ in Equation (5.10) and we get

$$M_{S^0}^2 = \begin{pmatrix} m_A^2 \sin^2 \beta + m_Z^2 \cos^2 \beta & -(m_A^2 + m_Z^2) \sin \beta \cos \beta \\ -(m_A^2 + m_Z^2) \sin \beta \cos \beta & m_A^2 \cos^2 \beta + m_Z^2 \sin^2 \beta \end{pmatrix} \quad (5.18)$$

with the eigenvalues:

$$m_{S_{1,S_2}}^2 = m_{h,H}^2 = \frac{1}{2} \left[m_A^2 + m_Z^2 \pm \sqrt{(m_A^2 + m_Z^2)^2 - 4m_Z^2 m_A^2 \cos^2(2\beta)} \right] \quad (5.19)$$

Similarly we can rewrite the mass matrix of the charged scalars:

$$V_{S^\pm} = (H_d^-, H_u^-) M_{S^\pm}^2 \begin{pmatrix} H_d^+ \\ H_u^+ \end{pmatrix} \quad \text{with} \quad (5.20)$$

$$M_{S^\pm}^2 = \begin{pmatrix} m_{H_d}^2 + \frac{1}{8}(g'^2 + g^2)(v_d^2 - v_u^2) + \frac{1}{4}g^2v_u^2 & B_\mu + \frac{1}{4}g^2v_dv_u \\ B_\mu + \frac{1}{4}g^2v_dv_u & m_{H_u}^2 - \frac{1}{8}(g'^2 + g^2)(v_d^2 - v_u^2) + \frac{1}{4}g^2v_d^2 \end{pmatrix} \quad (5.21)$$

$$= \left(\frac{B_\mu}{v_dv_u} + \frac{1}{4}g^2 \right) \begin{pmatrix} v_u^2 & v_dv_u \\ v_dv_u & v_d^2 \end{pmatrix} \quad , \quad (5.22)$$

where again B_μ is chosen to be real in the last equality. This results in the following eigenvalues

$$m_{S^\pm}^2 = m_{G^\pm}^2 = 0, \quad m_{S^\pm}^2 = m_A^2 + m_W^2 \quad . \quad (5.23)$$

The first eigenvalue represents the massless Goldstone bosons G^\pm . Last we want to comment on the mass of the lightest Higgs h in the MSSM: From Equation (5.19) follows $m_h^2 = m_Z^2 \cos^2(2\beta)$ in the limit $m_A^2 \gg m_Z^2$. This imposes the bound $m_h < m_Z \approx 91.2$ GeV at tree-level, which is experimentally already excluded. However, taking into account loop contributions allows for a light Higgs h with masses up to 135 GeV [108].

BRpV

Apart from the neutral components of the Higgs fields in Equation (5.7) also the left-handed sneutrinos have to be expanded after electroweak symmetry breaking according to:

$$\tilde{\nu}_i = \frac{1}{\sqrt{2}} (\tilde{\nu}_i^R + v_i + i\tilde{\nu}_i^I) \quad (5.24)$$

The minimization conditions in case of BRpV take the form

$$t_d^0 = \frac{\partial V}{\partial v_d} = -\frac{1}{2} (B_\mu + B_\mu^*) v_u + (m_{H_d}^2 + \mu\mu^*) v_d + v_d D - v_j \frac{1}{2} (\mu^* \epsilon_j + \mu \epsilon_j^*) = 0 \quad (5.25)$$

$$t_u^0 = \frac{\partial V}{\partial v_u} = -\frac{1}{2} (B_\mu + B_\mu^*) v_d + (m_{H_u}^2 + \mu\mu^*) v_u - v_u D + \frac{1}{2} (B_j + B_j^*) v_j + v_u \epsilon_j \epsilon_j^* = 0 \quad (5.26)$$

$$t_i^0 = \frac{\partial V}{\partial v_i} = v_i D + v_j \frac{1}{2} (\epsilon_i^* \epsilon_j + \epsilon_i \epsilon_j^*) - v_d (\mu^* \epsilon_i + \mu \epsilon_i^*) \\ + \frac{1}{2} (B_i + B_i^*) v_u + \frac{1}{2} \left(v_j (m_{\tilde{L}}^2)_{ji} + (m_{\tilde{L}}^2)_{ij} v_j \right) = 0 \quad , \quad (5.27)$$

where a summation over j has to be performed, whereas $i = 1, 2, 3$ is fixed. In case of VEVs of the left-handed sneutrinos D is given by $D = \frac{1}{8}(g^2 + g'^2)(v_d^2 - v_u^2 + \sum_i v_i^2)$. The mass matrices have to be extended, since the R -parity violating terms induce a mixing between the sneutrinos and the neutral scalars/pseudoscalars and a mixing between the sleptons and the charged scalars. Therefore the particle content entering the potential in Equation (5.2) is given by:

$$S^{0'T} = (\sigma_d^0, \sigma_u^0, \tilde{\nu}_i^R), \quad P^{0'T} = (\phi_d^0, \phi_u^0, \tilde{\nu}_i^I) \quad (5.28)$$

$$S^{+T} = ((H_d^-)^*, H_u^+, \tilde{e}^*, \tilde{\mu}^*, \tilde{\tau}^*, \tilde{e}^c, \tilde{\mu}^c, \tilde{\tau}^c) \quad (5.29)$$

$$S^{-T} = (H_d^-, (H_u^+)^*, \tilde{e}, \tilde{\mu}, \tilde{\tau}, (\tilde{e}^c)^*, (\tilde{\mu}^c)^*, (\tilde{\tau}^c)^*) \quad (5.30)$$

We will not give the detailed matrices here, but refer to [97]. However we will point out, what parameters are input values in case of BRpV and what is deduced from the tadpole equations. Despite from $m_{H_d}^2$ and $m_{H_u}^2$ we calculate $B_i = B_i^\epsilon \epsilon_i$ from the tadpole equations, so that BRpV has the additional parameters v_i, ϵ_i compared to the MSSM:

$$\tan \theta_W, \quad \alpha_{EM}, \quad m_Z \quad \text{and} \quad \tan \beta, \quad \mu, \quad m_A^2, \quad \epsilon_i, \quad v_i \quad (5.31)$$

Of course also the soft SUSY breaking masses $m_{\tilde{L}_{ij}}^2$ and $m_{\tilde{e}c_{ij}}^2$, which entered the slepton and sneutrino mass matrix in the MSSM, are now present in the scalar mass matrices. Note that we use m_A^2 to calculate B_μ according to Equation (5.15), although the resulting pseudoscalar mass suffers corrections from the R -parity violating parameters. It agrees to a good accuracy with m_A^2 , but is not exactly equal to it. In the calculation of gauge boson masses we have to take into account the VEVs of the left-handed sneutrinos, resulting in:

$$m_Z^2 = \frac{1}{4}(g^2 + g'^2)(v_d^2 + v_u^2 + \sum_i v_i^2), \quad m_W^2 = \frac{1}{4}g^2(v_d^2 + v_u^2 + \sum_i v_i^2) = m_Z^2 \cos^2 \theta_W \quad (5.32)$$

In particular, when fitting v_i to the neutrino data, these relations have to be kept in mind. They imply an adoption of v_d and v_u each time the VEVs v_i are changed. In addition to $\tan \beta$ we define

$$\tan \beta_i = \frac{v_i}{v_d} \quad , \quad (5.33)$$

which will be used in our discussions later.

The elements mixing the MSSM scalar sector with the sneutrinos or sleptons are proportional to v_i, ϵ_i and $B_i \propto (v_i, \epsilon_i)$. To explain neutrino data correct, they have to be chosen small compared to the electroweak scale, so that the MSSM scalar sector is only slightly influenced by the lepton number violating terms. Thus, in particular the lightest Higgs h in BRpV has identical theoretical upper bounds as in the MSSM.

CP violation in BRpV

An interesting question in R -parity violating supersymmetry via (effective) bilinear terms is, whether complex couplings ϵ_i can account for the observed baryogenesis via leptogenesis in the universe and to which extent they wash out existing asymmetries. Thus we consider the charge conjugate final states in the LSP decays $\tilde{\chi}_1^0 \rightarrow l^+ W^-$ and $l^- W^+$, which are the most important LSP decays in many parameter points under consideration. Although we do not present any results, but leave them open for future work, we want to comment on the treatment of the scalar sector in case of complex couplings for BRpV as we have implemented it in `CNNDecays`: The tadpole equations and mass matrices for BRpV and the MSSM we presented so far were formulated supposing to have complex parameters. However we have to take into account the additional mixing between scalar and pseudoscalar states in case of complex parameters. If we choose the following additional phases

$$H_d = e^{i\theta} \begin{pmatrix} \frac{1}{\sqrt{2}}(\sigma_d^0 + v_d + i\phi_d^0) \\ H_d^- \end{pmatrix}, \quad H_u = \begin{pmatrix} H_u^+ \\ \frac{1}{\sqrt{2}}(\sigma_u^0 + v_u + i\phi_u^0) \end{pmatrix} \quad (5.34)$$

$$\tilde{L}_i = e^{i\eta_i} \begin{pmatrix} \frac{1}{\sqrt{2}}(\tilde{\nu}_i^R + v_i + i\tilde{\nu}_i^I) \\ \tilde{l}_i \end{pmatrix} \quad , \quad (5.35)$$

where a phase of H_u is absorbed into the other two phases, and complex parameters

$$\epsilon_i = \epsilon_i^R + i\epsilon_i^I, \quad B_i = B_i^R + iB_i^I, \quad \mu = \mu^R + i\mu^I, \quad B_\mu = B_\mu^R + iB_\mu^I \quad (5.36)$$

we get in addition to the tadpole equations for the real components of the VEVs t_d, t_u and t_i in the last subsection:

$$t_d^I = \frac{\partial V}{\partial \theta} = B_\mu^I v_d v_u + \mu^I v_d v_j \epsilon_j^R - \mu^R v_d v_j \epsilon_j^I = 0 \quad (5.37)$$

$$t_i^I = \frac{\partial V}{\partial \eta_i} = v_i v_u B_i^I - v_d v_i (\mu^R \epsilon_i^I - \mu^I \epsilon_i^R) + v_i v_j (\mu_i^R \mu_j^I - \epsilon_i^I \epsilon_j^R) = 0 \quad (5.38)$$

where we sum over j and fix i . The equations allow us to choose real vacuum expectation values, implying $\theta = \eta_i = 0$. However, if we choose ϵ_i to be complex, we have to allow for complex values of B_μ^I and B_i^I , which can be determined from the latter tadpole equations. In addition the scalar and pseudoscalar states are mixed, so that we get

$$V_{S^0} = \frac{1}{2} S^{0'T} M_{SP}^2 S^{0'} \quad \text{with} \quad M_{SP}^2 = \begin{pmatrix} M_{S^0}^2 & (M_{SPmix}^2)^T \\ M_{SPmix}^2 & M_{P^0}^2 \end{pmatrix} \quad (5.39)$$

based on the following particle content:

$$S^{0'T} = (\sigma_d^0, \sigma_u^0, \tilde{\nu}_i^R, \phi_d^0, \phi_u^0, \tilde{\nu}_i^I) \quad (5.40)$$

Whereas the diagonal parts $M_{S^0}^2$ and $M_{P^0}^2$ can be taken from [97] the new nondiagonal entries are in accordance to [109]:

$$M_{SPmix}^2 = \begin{pmatrix} 0 & B_\mu^I & \mu^I \epsilon_1^R - \mu^R \epsilon_1^I & \mu^I \epsilon_2^R - \mu^R \epsilon_2^I & \mu^I \epsilon_3^R - \mu^R \epsilon_3^I \\ B_\mu^I & 0 & -B_1^I & B_2^I & B_3^I \\ \mu^R \epsilon_1^I - \mu^I \epsilon_1^R & -B_1^I & 0 & -\epsilon_2^R \epsilon_1^I + \epsilon_1^R \epsilon_2^I & -\epsilon_3^R \epsilon_1^I + \epsilon_1^R \epsilon_3^I \\ \mu^R \epsilon_2^I - \mu^I \epsilon_2^R & -B_2^I & \epsilon_2^R \epsilon_1^I - \epsilon_1^R \epsilon_2^I & 0 & -\epsilon_3^R \epsilon_2^I + \epsilon_2^R \epsilon_3^I \\ \mu^R \epsilon_3^I - \mu^I \epsilon_3^R & -B_3^I & \epsilon_3^R \epsilon_1^I - \epsilon_1^R \epsilon_3^I & \epsilon_3^R \epsilon_2^I - \epsilon_2^R \epsilon_3^I & 0 \end{pmatrix} \quad (5.41)$$

A simple numerical check of the correctness of these formulas is the presence of the Goldstone boson $m_{S^0}^2 = m_{G^0}^2 = 0$, when $m_{H_d}^2$, $m_{H_u}^2$, B_i^R , B_i^I and B_μ^I from the tadpole equations are inserted. The complex variant of BRpV is also included in **CNNDecays**. However in the following subsection we will come back to the case of having real parameters, although most formulas are presented in the general form of complex parameters, so that the generalization to the additional tadpole equations and mixing matrices is straight forward.

5.1.2. NMSSM and $\mu\nu$ SSM

NMSSM

The scalar and pseudoscalar sector of the NMSSM differ from those of the MSSM, since the additional singlet S has to be taken into account. Similar to H_d^0 and H_u^0 the singlet S is expanded:

$$S = \frac{1}{\sqrt{2}} (\sigma_S^0 + v_d + i\phi_S^0) \quad (5.42)$$

The minimization conditions in case of the NMSSM are given by:

$$t_d^0 = \frac{\partial V}{\partial v_d} = -\frac{1}{2\sqrt{2}}v_S v_u (T_\lambda + T_\lambda^*) + \frac{1}{2}v_d(v_u^2 + v_S^2)\lambda\lambda^* - \frac{1}{4}v_S^2 v_u (\lambda\kappa^* + \kappa\lambda^*) + \frac{1}{8}(g^2 + g'^2)v_d(v_d^2 - v_u^2) + m_{H_d}^2 v_d = 0 \quad (5.43)$$

$$t_u^0 = \frac{\partial V}{\partial v_u} = -\frac{1}{2\sqrt{2}}v_d v_S (T_\lambda + T_\lambda^*) + \frac{1}{2}v_u(v_d^2 + v_S^2)\lambda\lambda^* - \frac{1}{4}v_d v_S^2 (\lambda\kappa^* + \kappa\lambda^*) + \frac{1}{8}(g^2 + g'^2)v_u(v_u^2 - v_d^2) + m_{H_u}^2 v_u = 0 \quad (5.44)$$

$$t_S^0 = \frac{\partial V}{\partial v_S} = \frac{1}{2\sqrt{2}}v_S^2 (T_\kappa + T_\kappa^*) - \frac{1}{2\sqrt{2}}v_d v_u (T_\lambda + T_\lambda^*) + \frac{1}{2}v_S(v_d^2 + v_u^2)\lambda\lambda^* - \frac{1}{2}v_d v_S v_u (\lambda\kappa^* + \kappa\lambda^*) + v_S^3 \kappa\kappa^* + m_S^2 v_S = 0 \quad (5.45)$$

Apart from $m_{H_d}^2$ and $m_{H_u}^2$ we also calculate m_S^2 from the tadpole equations. The mass matrix of the charged scalar sector is based on the same particle content as in the MSSM, but includes additional entries

$$V_{S^\pm} = (H_d^-, H_u^-) M_{S^\pm}^2 \begin{pmatrix} H_d^+ \\ H_u^+ \end{pmatrix} \quad \text{with} \quad (5.46)$$

$$M_{S^\pm}^2 = \begin{pmatrix} \left[\begin{array}{c} m_{H_d}^2 + \frac{1}{8}(g'^2 + g^2)(v_d^2 - v_u^2) \\ + \frac{1}{4}g^2 v_u^2 + \frac{1}{2}\lambda\lambda^* v_S^2 \end{array} \right] & \left[\begin{array}{c} \frac{1}{4}g^2 v_d v_u - \frac{1}{2}\lambda\lambda^* v_d v_u \\ + \frac{1}{2}\lambda\kappa^* v_S^2 + \frac{1}{\sqrt{2}}T_\lambda v_S \end{array} \right] \\ \left[\begin{array}{c} \frac{1}{4}g^2 v_d v_u - \frac{1}{2}\lambda\lambda^* v_d v_u \\ + \frac{1}{2}\lambda^* \kappa v_S^2 + \frac{1}{\sqrt{2}}T_\lambda^* v_S \end{array} \right] & \left[\begin{array}{c} m_{H_u}^2 - \frac{1}{8}(g'^2 + g^2)(v_d^2 - v_u^2) \\ + \frac{1}{4}g^2 v_d^2 + \frac{1}{2}\lambda\lambda^* v_S^2 \end{array} \right] \end{pmatrix} \quad (5.47)$$

$$= \left(\frac{1}{4}g^2 - \frac{1}{2}\lambda^2 + \frac{\kappa\lambda v_S^2}{2v_d v_u} + \frac{T_\lambda v_S}{\sqrt{2}v_d v_u} \right) \begin{pmatrix} v_u^2 & v_d v_u \\ v_d v_u & v_d^2 \end{pmatrix}, \quad (5.48)$$

where the latter formula made use of the tadpole equations and is only valid in case of real parameters λ, κ and T_λ . This results in the two eigenvalues:

$$m_{S_1^\pm}^2 = m_{G^\pm}^2 = 0, \quad m_{S_2^\pm}^2 = \left(\frac{1}{4}g^2 - \frac{1}{2}\lambda^2 + \frac{\kappa\lambda v_S^2}{2v_d v_u} + \frac{T_\lambda v_S}{\sqrt{2}v_d v_u} \right) (v_d^2 + v_u^2) \quad (5.49)$$

Our input parameters of the scalar and gauge sectors of the NMSSM are

$$\tan\theta_W, \quad \alpha_{EM}, \quad m_Z \quad \text{and} \quad \tan\beta, \quad \mu, \quad \lambda, \quad \kappa, \quad T_\lambda, \quad T_\kappa. \quad (5.50)$$

From μ and λ we can derive the VEV v_S of the singlet S using Equation (4.2). Later we will replace λ by the VEV v_S , the latter one being expressed by the new angle β_S , and κ by the singlino mass $m_{\tilde{S}}$, both defined by:

$$\tan\beta_S = \frac{v_S}{v_u} \quad \text{and} \quad m_{\tilde{S}} = \sqrt{2}\kappa v_S \quad (5.51)$$

In order to allow for positive squared masses in the scalar and pseudoscalar sector we will work out a strategy in the following how T_λ and T_κ have to be chosen in principle to avoid tachyonic states.

The scalar potential of the scalar and pseudoscalar sector is of the form

$$V_{S^0, P^0, S^\pm} = \frac{1}{2} S^{0'T} M_{S^0}^2 S^{0'} + \frac{1}{2} P^{0'T} M_{P^0}^2 P^{0'} \quad (5.52)$$

with the following particle content:

$$S^{0'T} = (\sigma_d^0, \sigma_u^0, \sigma_S^0), \quad P^{0'T} = (\phi_d^0, \phi_u^0, \phi_S^0) \quad (5.53)$$

Solving the tadpole equations for $m_{H_d}^2, m_{H_u}^2$ and m_S^2 the mass matrix of the pseudoscalar states yields:

$$M_{P^0}^2 = \begin{pmatrix} M_{HH}^2 & M_{HS}^2 \\ (M_{HS}^2)^T & M_{SS}^2 \end{pmatrix} \quad (5.54)$$

with

$$\begin{aligned} M_{HH}^2 &= \begin{pmatrix} (\Omega_1 + \Omega_2) \frac{v_u}{v_d} & \Omega_1 + \Omega_2 \\ \Omega_1 + \Omega_2 & (\Omega_1 + \Omega_2) \frac{v_d}{v_u} \end{pmatrix}, & M_{HS}^2 &= \begin{pmatrix} (-2\Omega_1 + \Omega_2) \frac{v_u}{v_S} \\ (-2\Omega_1 + \Omega_2) \frac{v_d}{v_S} \end{pmatrix} \\ M_{SS}^2 &= (4\Omega_1 + \Omega_2) \frac{v_d v_u}{v_S^2} - 3\Omega_3 \end{aligned} \quad (5.55)$$

where we have introduced the following abbreviations Ω_i :

$$\Omega_1 = \frac{1}{4} (\lambda \kappa^* + \lambda^* \kappa) v_S^2, \quad \Omega_2 = \frac{1}{2\sqrt{2}} (T_\lambda + T_\lambda^*) v_S, \quad \Omega_3 = \frac{1}{2\sqrt{2}} (T_\kappa + T_\kappa^*) v_S \quad (5.56)$$

Diagonalizing $M_{P^0}^2$ results in the Goldstone boson G^0 and two pseudoscalar states A_1 and A_2 :

$$\begin{aligned} m_{P^0}^2 &= m_{G^0}^2 = 0 \\ m_{P^0}^2 &= m_{A_1}^2 = \frac{1}{2} (\Omega_1 + \Omega_2) \left(\frac{v_d}{v_u} + \frac{v_u}{v_d} + \frac{v_d v_u}{v_S^2} \right) - \frac{3}{2} \Omega_3 - \sqrt{\Gamma} \\ m_{P^0}^2 &= m_{A_2}^2 = \frac{1}{2} (\Omega_1 + \Omega_2) \left(\frac{v_d}{v_u} + \frac{v_u}{v_d} + \frac{v_d v_u}{v_S^2} \right) - \frac{3}{2} \Omega_3 + \sqrt{\Gamma} \\ \text{with } \Gamma &= \left(\frac{1}{2} (\Omega_1 + \Omega_2) \left(\frac{v_d}{v_u} + \frac{v_u}{v_d} + \frac{v_d v_u}{v_S^2} \right) - \frac{3}{2} \Omega_3 \right)^2 \\ &\quad + 3 (\Omega_1 + \Omega_2) \Omega_3 \left(\frac{v_d}{v_u} + \frac{v_u}{v_d} \right) - 9 \Omega_1 \Omega_2 \left(\frac{v_S^2}{v_d^2} + \frac{v_S^2}{v_u^2} \right) \end{aligned} \quad (5.57)$$

To get only positive eigenvalues for the physical mass eigenstates, the inequality

$$\Omega_3 < \frac{v_d v_u}{v_S^2} \frac{3\Omega_1 \Omega_2}{\Omega_1 + \Omega_2} =: f_1(\Omega_2) \quad (5.58)$$

has to be fulfilled. The mass matrix of the neutral scalars is given by

$$M_{S^0}^2 = \begin{pmatrix} M_{HH}^2 & M_{HS}^2 \\ (M_{HS}^2)^T & M_{SS}^2 \end{pmatrix} \quad (5.59)$$

with

$$\begin{aligned}
M_{HH}^2 &= \begin{pmatrix} (\Omega_1 + \Omega_2) \frac{v_u}{v_d} + \Omega_6 \frac{v_d}{v_u} & -\Omega_1 - \Omega_2 - \Omega_6 + \Omega_4 \\ -\Omega_1 - \Omega_2 - \Omega_6 + \Omega_4 & (\Omega_1 + \Omega_2) \frac{v_d}{v_u} + \Omega_6 \frac{v_u}{v_d} \end{pmatrix} \\
M_{HS}^2 &= \begin{pmatrix} (-2\Omega_1 - \Omega_2) \frac{v_u}{v_S} + \Omega_4 \frac{v_S}{v_u} \\ (-2\Omega_1 - \Omega_2) \frac{v_d}{v_S} + \Omega_4 \frac{v_S}{v_d} \end{pmatrix}, \quad M_{SS}^2 = \Omega_2 \frac{v_d v_u}{v_S^2} + \Omega_3 + \Omega_5
\end{aligned} \tag{5.60}$$

using the additional parameters

$$\Omega_4 = \lambda \lambda^* v_d v_u > 0, \quad \Omega_5 = 2\kappa \kappa^* v_S^2 > 0, \quad \Omega_6 = \frac{1}{4} (g^2 + g'^2) v_d v_u > 0 \quad . \tag{5.61}$$

In principle the eigenvalues $m_{S_{1,2,3}}^2$ can be determined analytically, but the lengthy result is not very illuminating. Though we make use of the following theorem: A symmetric matrix is positive definite, meaning all eigenvalues are positive, if all principal minors are positive (Sylvester criterion). Thus we get three conditions

$$\begin{aligned}
0 &< (\Omega_1 + \Omega_2) \frac{v_u}{v_d} + \Omega_6 \frac{v_d}{v_u} \\
0 &< (\Omega_1 + \Omega_2) \left(\Omega_6 \left(\frac{v_d^2}{v_u^2} + \frac{v_u^2}{v_d^2} \right) - 2\Omega_6 + 2\Omega_4 \right) + 2\Omega_4 \Omega_6 - \Omega_4^2 \\
0 &< \Omega_3 - f_2(\Omega_2) \quad ,
\end{aligned} \tag{5.62}$$

where $f_2(\Omega_2)$ is given by:

$$f_2(\Omega_2) = \frac{\Sigma_1}{\Sigma_2} \quad \text{with} \tag{5.63}$$

$$\begin{aligned}
\Sigma_1 &= (\Omega_1 + \Omega_2) \Omega_5 (-2\Omega_4 + 2\Omega_6) + (\Omega_4^2 - 2\Omega_4 \Omega_6) \Omega_5 \\
&+ (\Omega_1 + \Omega_2) \Omega_4^2 v_S^2 \left(\frac{v_d}{v_u^3} + \frac{v_u}{v_d^3} \right) + (4\Omega_1^2 + 3\Omega_1 \Omega_2) \Omega_6 \frac{1}{v_S^2} \left(\frac{v_d^3}{v_u} + \frac{v_u^3}{v_d} \right) \\
&- (\Omega_1 + \Omega_2) \Omega_5 \Omega_6 \left(\frac{v_d^2}{v_u^2} + \frac{v_u^2}{v_d^2} \right) + 2(\Omega_1 + \Omega_2 - \Omega_4 + 2\Omega_6) \Omega_4^2 \frac{v_S^2}{v_d v_u} \\
&- 2(2\Omega_1 + \Omega_2) (2\Omega_1 + 2\Omega_2 - \Omega_4 + 2\Omega_6) \Omega_4 \left(\frac{v_d}{v_u} + \frac{v_u}{v_d} \right) \\
&+ [16\Omega_1^3 + 8(4\Omega_2 - \Omega_4 + \Omega_6) \Omega_1^2 + 10\Omega_1 \Omega_2 (2\Omega_2 - \Omega_4 + \Omega_6) \\
&+ \Omega_2 (2\Omega_2 - \Omega_4) (2\Omega_2 - \Omega_4 + 2\Omega_6)] \frac{v_d v_u}{v_S^2}
\end{aligned} \tag{5.64}$$

$$\begin{aligned}
\Sigma_2 &= (\Omega_1 + \Omega_2) \Omega_6 \left(\frac{v_d^2}{v_u^2} + \frac{v_u^2}{v_d^2} \right) + 2(\Omega_1 + \Omega_2) (\Omega_4 - \Omega_6) \\
&+ 2\Omega_4 \Omega_6 - \Omega_4^2
\end{aligned} \tag{5.65}$$

Except for special values of $\tan \beta$ and λ the first two conditions are fulfilled in general. Therefore combining our knowledge from the scalar and pseudoscalar sector results in the following conditions:

$$f_2(\Omega_2) < \Omega_3 < f_1(\Omega_2) \tag{5.66}$$

Taking a negative value of Ω_3 ($\propto T_\kappa$) near $f_2(\Omega_2)$ results in a very light singlet scalar, whereas for a value of Ω_3 near $f_1(\Omega_2)$ a very light singlet pseudoscalar is present. Thus we find a value of Ω_3 in between, where both particles have the same mass. A similar discussion of the singlet scalar and pseudoscalar mass can be found in [110] formula (37). We want to add that a light scalar and/or pseudoscalar always comes together with a light mass of the singlet fermion.

Before proceeding to the $\mu\nu$ SSM, we comment on the theoretical upper bound of the lightest scalar S_1^0 at tree-level: The smallest eigenvalue of $M_{S_0}^2$ has to be less than the lower eigenvalue of any (2×2) -submatrix. Taking the submatrix M_{HH}^2 the maximized value of the lower eigenvalue at tree-level is given by [58]:

$$m_{S_1}^2 \leq m_Z^2 \left[\cos^2(2\beta) + \frac{2\lambda^2}{g^2 + g'^2} \sin^2(2\beta) \right] \quad (5.67)$$

In contrast to MSSM this expression imposes a priori no upper bound, as long as the Higgs self-coupling λ is not limited. However, supposing perturbativity up to the GUT scale in combination with loop corrections results in an upper bound of $m_{S_1}^2 \lesssim 145$ GeV. In fact, also in models with a more complicated particle content together with additional gauge groups as internal symmetries the upper bound of the lightest Higgs is at a maximum 200 GeV, if the considered model should be perturbatively treatable up to the GUT scale and contain a weak scale supersymmetry [58].

$\mu\nu$ SSM

We are left with the discussion of the scalar sector of the $\mu\nu$ SSM with in general n right-handed neutrino superfields. Apart from H_d^0 and H_u^0 and the left-handed sneutrinos $\tilde{\nu}_i$ also the right-handed sneutrinos $\tilde{\nu}_k^c$ with $k = 1, \dots, n$ can be expanded similarly:

$$\tilde{\nu}_k^c = \frac{1}{\sqrt{2}} (\tilde{\nu}_k^{cR} + v_{ck} + i\tilde{\nu}_k^{cI}) \quad (5.68)$$

Calculating the scalar potential in accordance to Equation (5.1) results in rather lengthy minimization conditions, which we will not present here, but in Appendix A. Similar to BRpV the mass matrices have to be extended. Therefore the particle content entering the potential in Equation (5.2) is given by:

$$S^{0'T} = (\sigma_d^0, \sigma_u^0, \tilde{\nu}_k^{cR}, \tilde{\nu}_i^R), \quad P^{0'T} = (\phi_d^0, \phi_u^0, \tilde{\nu}_k^{cI}, \tilde{\nu}_i^I) \quad (5.69)$$

$$S^{+'T} = ((H_d^-)^*, H_u^+, \tilde{e}^*, \tilde{\mu}^*, \tilde{\tau}^*, \tilde{e}^c, \tilde{\mu}^c, \tilde{\tau}^c) \quad (5.70)$$

$$S^{-'T} = (H_d^-, (H_u^+)^*, \tilde{e}, \tilde{\mu}, \tilde{\tau}, (\tilde{e}^c)^*, (\tilde{\mu}^c)^*, (\tilde{\tau}^c)^*) \quad (5.71)$$

Again i denotes the index of the 3 left-handed sneutrinos and k numbers the n right-handed ones. The mass matrices of the $\mu\nu$ SSM for the general case of n right-handed neutrino superfields can also be found in Appendix A. From the tadpole equations we calculate the soft SUSY breaking masses $m_{H_d}^2, m_{H_u}^2, m_{\tilde{\nu}^c}^2$ and the couplings T_ν . Thus the input parameters of the scalar and gauge boson sector in the $\mu\nu$ SSM are given by:

$$\tan \theta_W, \quad \alpha_{EM}, \quad m_Z, \quad \tan \beta, \quad \mu, \quad \lambda_k, \quad \kappa_k, \quad T_\lambda^k, \quad T_\kappa^{klm}, \quad Y_\nu^{ik}, \quad v_i \quad (5.72)$$

Moreover the soft SUSY breaking parameters of the slepton and sneutrino sector are input parameters in case of the $\mu\nu$ SSM, namely $m_{\tilde{L}_{ij}}^2$ and $m_{\tilde{e}^c_{ij}}^2$. In case of the $\mu\nu$ SSM with one right-handed neutrino superfield, now also called 1 $\tilde{\nu}^c$ case, we will replace $\lambda_1 = \lambda$ later by v_c ,

$\kappa_1 = \kappa$ by the singlino mass m_c and $Y_\nu^{i1} = Y_\nu^i$ by ϵ_i using Equation (4.10) and define similar to the NMSSM and BRpV:

$$\tan \beta_i = \frac{v_i}{v_d}, \quad \tan \beta_c = \frac{v_c}{v_u} \quad \text{and} \quad m_c = \sqrt{2}\kappa v_c \quad (5.73)$$

The masses of the heavy gauge bosons are influenced by the VEVs of the left-handed sneutrinos in the same way as in BRpV, see Equation (5.32). Considering the case of just one right-handed neutrino superfield and neglecting the R -parity violating couplings, the scalar sector of the $\mu\nu$ SSM is identical to the one of the NMSSM. Thus the statements about the masses of the scalars $S_{1,2,3}^0$ and the pseudoscalars $P_{1,2}^0$ also hold for the $\mu\nu$ SSM, so that a reasonable choice of T_λ and T_κ allows to avoid tachyonic states. Also the upper bound for the lightest Higgs S_1^0 is not changed compared to the NMSSM [111].

In the n generation case ($n \hat{\nu}^c$ case) a similar result holds as long as T_κ and $m_{\hat{\nu}^c}^2$ do not have off-diagonal entries compared to κ . Inspecting Equations (A.20) and (A.29) it is possible to show that the singlet scalars and pseudoscalars can be heavy by appropriately chosen values for the off-diagonal entries of T_κ while keeping at the same time the singlet fermions relatively light. We illustrate this feature in the chapter about the phenomenology of the $\mu\nu$ SSM.

5.1.3. LEP bounds on light neutral scalar/pseudoscalar states

In this thesis we are partly working with parameter points, which provide a light mass spectrum of supersymmetric particles and scalars. If the singlino-like neutralino \tilde{S} in the NMSSM or ν_k^c in the $\mu\nu$ SSM are light, namely below 100 GeV, they often show up together with a light scalar or pseudoscalar. However, the ‘‘Large Electron-Positron Collider (LEP)’’ operating from 1989 to 2000 at CERN set strong bounds on the masses of light scalar or pseudoscalar particles. The various experiments, namely ALEPH, DELPHI, L3 and OPAL [112], have combined their results in [113], to which we refer for our used bounds within this thesis. Therein one can find the lower bound for the standard model Higgs being 114.4 GeV. Relevant production processes for a neutral scalar particle S_i^0 at LEP are the ‘‘Bjorken process’’ $e^+e^- \rightarrow Z^0 S_i^0$ and for scalars S_i^0 in company with pseudoscalars P_j^0 in addition the associated production mechanism $e^+e^- \rightarrow S_i^0 P_j^0$. Other processes are subdominant. Thus, the mass exclusion bounds on $m_{S_i^0}$ and $m_{P_j^0}$ are strongly dependent on the production rates of the two mentioned processes. In case of small couplings due to the singlet character as possible in the NMSSM or $\mu\nu$ SSM, the mass bounds are weaker than the one for the standard model Higgs. Our discussion follows [114], where the results of both processes for spontaneous R -parity violating models were discussed. Given n scalars S_i^0 and m pseudoscalars P_j^0 the relevant couplings for the production processes are contained in the Lagrangian density

$$\mathcal{L} \supset \sum_{i=1}^n \left(\sqrt{2} G_F \right)^{1/2} m_Z^2 \eta_B^i S_i^0 Z_\mu^0 Z^{0\mu} + \sum_{i=1}^n \sum_{j=1}^m \left(\sqrt{2} G_F \right)^{1/2} m_Z \eta_A^{ij} \left(Z^{0\mu} S_i^0 \overleftrightarrow{\partial}_\mu P_j^0 \right) \quad (5.74)$$

with the Fermi constant given by $G_F = \frac{\sqrt{2}g^2}{8m_W^2}$. The parameters η are defined as follows

$$\eta_B^i = \frac{1}{v} \left(v_d R_{i1}^{S^0} + v_u R_{i2}^{S^0} + \sum_{j=1}^3 v_j R_{i,j+l}^{S^0} \right) \quad (5.75)$$

$$\eta_A^{ij} = R_{i1}^{S^0} R_{j1}^{P^0} - R_{i2}^{S^0} R_{j2}^{P^0} + \sum_{k=1}^3 R_{i,k+l}^{S^0} R_{j,k+l}^{P^0} \quad , \quad (5.76)$$

where the rotation matrices of the scalars R^{S^0} and pseudoscalars R^{P^0} appear and l has to be chosen such that the rotation matrices point on the sneutrino gauge eigenstates ($l = 2$ in BRpV and $l = 3$ in the $\mu\nu$ SSM with one right-handed neutrino superfield). Within this notation B refers to the “Bjorken process” and A to the associated production mechanism. The MSSM results given in [115] can be easily transferred to our case using the couplings η , which results for the “Bjorken process” [114] in

$$\begin{aligned} \sigma(e^+e^- \rightarrow Z^0 S_i^0) &= (\eta_B^i)^2 \frac{G_F^2 m_Z^4}{96\pi s} (v_e^2 + a_e^2) \beta \frac{\beta^2 + 12m_Z^2/s}{(1 - m_Z^2/s)^2 + (\Gamma_Z m_Z/s)^2} \\ \text{with} \quad v_e &= -1 + 4 \sin^2 \theta_W^2, \quad a_e = -1, \quad \beta = \frac{1}{s} \sqrt{\kappa(s, m_Z^2, m_i^2)} \quad , \end{aligned} \quad (5.77)$$

where κ is the well-known Kaellen function $\kappa(x, y, z) = x^2 + y^2 + z^2 - 2xy - 2yz - 2xz$ and \sqrt{s} denotes the center-of-mass energy. For the associated production mechanism yields

$$\begin{aligned} \sigma(e^+e^- \rightarrow S_i^0 P_j^0) &= (\eta_A^{ij})^2 \frac{G_F^2 m_Z^4}{96\pi s} (v_e^2 + a_e^2) \frac{\beta^3}{(1 - m_Z^2/s)^2 + (\Gamma_Z m_Z/s)^2} \\ \text{with} \quad \beta &= \frac{1}{s} \sqrt{\kappa(s, m_j^2, m_i^2)} \quad . \end{aligned} \quad (5.78)$$

We abbreviated the masses of the scalar and pseudoscalar by $m_i = m(S_i^0)$ and $m_j = m(P_j^0)$ in both formulas. The results of the experiments at LEP [113] make use of a scale factor S_{95} , which is defined in the following form

$$S_{95} = \frac{\sigma_{\max}}{\sigma_{\text{ref}}} \quad , \quad (5.79)$$

where σ_{\max} refers to the maximal production cross section, which is still compatible with the measurements at 95% confidence level and σ_{ref} is the reference production cross section. Thus, S_{95} gives the maximal production cross sections as a function of the mass of the scalar or pseudoscalar in a certain model, which justifies the non-observance. The reference production cross section for the “Bjorken process” is the standard model Higgs production $\sigma_{HZ}^{SM} = \sigma(e^+e^- \rightarrow Z^0 H)$, for the associated production mechanism it is given by

$$\sigma_{\text{ref}} = \bar{\beta} \sigma_{HZ}^{SM} \quad \text{with} \quad \bar{\beta} = \frac{\sqrt{\kappa^3(s, m_j^2, m_i^2)/s^3}}{\left(\sqrt{\kappa(s, m_Z^2, m_i^2)}/s\right) (\kappa(s, m_Z^2, m_i^2)/s^2 + 12m_Z^2/s)} \quad . \quad (5.80)$$

This results in $S_{95} = (\eta_B^i)^2$ and $S_{95} = (\eta_A^{ij})^2$, implying that no kinematics is involved in the comparison of a certain model with the bounds given by LEP. Figure 5.1 is taken from [113] and shows the maximal value of S_{95} as a function of the scalar or the sum of the scalar and pseudoscalar mass. The regions above the shown graphs are excluded. The branching ratios of the scalars S_i^0 and pseudoscalars P_i^0 are supposed to be standard model like, implying a dominant decay into $b\bar{b}$ and $\tau^+\tau^-$. Despite from some special cases, where a decay into a pair of neutralinos $\tilde{\chi}_1^0 \tilde{\chi}_1^0$ can be dominant, this is also true in the considered models. We used the corresponding tables in [113] (Table 14 and Table 17) to implement the bounds in **CNNDecays**

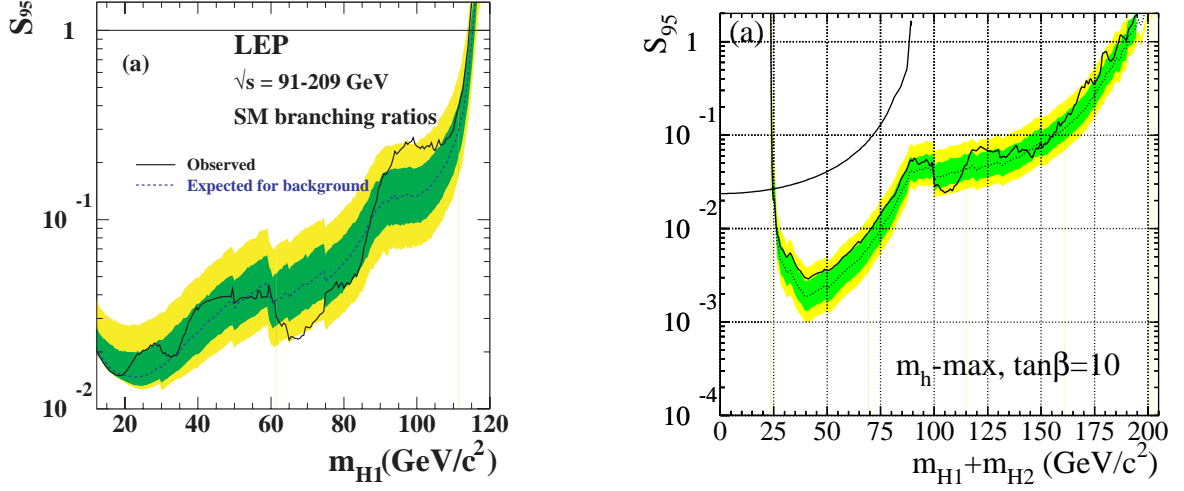


Figure 5.1.: **a)** (left) Maximum value of S_{95} at 95% confidence level for the “Bjorken process” $e^+e^- \rightarrow Z^0 S_i^0$ as a function of the scalar mass $m_{H1} = m_{S_i^0}$, Assumption: Branching ratios of S_i^0 are similar to the ones of the standard model Higgs H ; **b)** (right) Maximum value of S_{95} at 95% confidence level for the associated production mechanism $e^+e^- \rightarrow S_i^0 P_j^0$ as a function of the scalar $m_{H1} = m_{S_i^0}$ and pseudoscalar mass $m_{H2} = m_{P_j^0}$, Assumption: Branching ratios of S_i^0 and P_j^0 are similar to the ones of the standard model Higgs H ; In both cases the solid line is the observed limit. The green and yellow bands around the dashed median denote the 68% and 95% probability. Both figures are taken from [113].

and modified versions of **SPheno**.

Since the Higgs mass h in the MSSM at tree-level has a theoretical upper bound of m_Z , which is experimentally excluded by the shown LEP data, we include the dominant one-loop correction to all the (2, 2)-elements of the scalar mass matrices

$$(M_{S^0})_{22}^{1L} = (M_{S^0})_{22} + \frac{3}{4\pi^2 v_u^2 C_v} m_t^2 \log \left(\frac{m_{\tilde{t}_1} m_{\tilde{t}_2}}{m_t^2} \right)$$

$$\text{with } C_v = 1 - \frac{v_1^2 + v_2^2 + v_3^2}{v_d^2 + v_u^2 + v_1^2 + v_2^2 + v_3^2} \quad (5.81)$$

Here m_t denotes the top mass and $m_{\tilde{t}_{1,2}}$ the stop masses. Note that the correction is only added for the comparison with LEP data, but not for the proper calculation of one-loop diagrams, not to mix different orders of perturbation theory.

5.2. Gauge fixing and unphysical states

In this section we describe the procedure of gauge fixing followed by the discussion of unphysical modes, which include Faddeev-Popov ghosts and the already mentioned Goldstone bosons. More details can be found in [6]. Using the path-integral formulation for a non-abelian gauge theory results in the following ansatz for the generating functional of Green functions:

$$T\{J\} = \frac{Z\{J\}}{Z\{0\}} \quad \text{with} \quad (5.82)$$

$$Z\{J\} = \int \mathcal{D}[A] \exp\left(iS\{A\} + i \int d^4x J^{\mu,a}(x) A_\mu^a(x)\right) \quad (5.83)$$

$$S\{A\} = \int d^4x \left(-\frac{1}{4} F_{\mu\nu}^a(x) F^{a,\mu\nu}(x)\right) \quad (5.84)$$

In this notation the gauge fields $A = (A_\mu^a)$ and the sources $J = (J_\mu^a)$ appear. Moreover $F_{\mu\nu}^a$ denotes the field strength tensor as defined in Section 2.2 and the measure $\mathcal{D}[A] = \prod_{x,\mu,a} dA_\mu^a(x)$ involves a product over all group and vector components of the field $A_\mu^a(x)$ at each space-time point. Performing this integration results in a divergence, the reason being the gauge invariance of the theory. To fix the gauge locally in order not to integrate over states, which are related by a gauge transformation, one can use a δ -functional with conditions of the form $C^a\{A; x\} - c^a(x) = 0$. For their exact definition we refer to [6]. The integration can be rewritten by a variable transformation using two anticommuting scalar fields $u^a(x)$ and $\bar{u}^a(x)$, which are just auxiliary fields and are called Faddeev-Popov ghost fields. This procedure results in the Lagrangian

$$\mathcal{L} = -\frac{1}{4} F_{\mu\nu}^a(x) F^{a,\mu\nu}(x) - \frac{1}{2\xi} C^a\{A; x\} C^a\{A; x\} - \int d^4z \bar{u}^a(x) \frac{\delta C^a\{A; x\}}{\delta A_\nu^c(z)} D_\nu^{cb} u^b(z) \quad , \quad (5.85)$$

where ξ stems from a Gaussian weight function, so it can be chosen arbitrary, and D_ν^{cb} denotes the covariant derivative in the notation of infinitesimal gauge transformations $D_\nu^{ab} \delta\theta^b(x) = \partial_\nu \delta\theta^a(x) + g f^{abc} A_\nu^b(x) \delta\theta^c(x)$. Thus, this procedure of gauge fixing generates mass contributions for the unphysical states and interactions parametrized by the gauge-fixing Lagrangian, the second term in Equation (5.85). In addition the masses and interactions of the unphysical Faddeev-Popov ghosts are contained in the last term of the Lagrangian given in Equation (5.85).

In the following we want to discuss the gauge fixing, which will be used throughout this thesis. In the standard model and in supersymmetric theories spontaneous breaking of a gauge theory as shown in Section 2.2 induces mixing terms between the gauge boson fields A_μ and the Goldstone bosons G of the form $A_\mu \partial^\mu G$. However there exists a class of renormalizable gauge, where these terms are absent. It is given by the gauge fixing conditions

$$\begin{aligned} C^\pm &= \partial^\mu W_\mu^\pm \mp im_W \xi'_W G^\pm \\ C^Z &= \partial^\mu Z_\mu - m_Z \xi'_Z G^0 \\ C^\gamma &= \partial^\mu A_\mu \end{aligned} \quad (5.86)$$

in combination with the gauge-fixing terms

$$\mathcal{L} = -\frac{1}{2\xi_A} (C^A)^2 - \frac{1}{2\xi_Z} (C^Z)^2 - \frac{1}{\xi_W} C^+ C^- \quad . \quad (5.87)$$

Choosing $\xi' = \xi$ cancels the mentioned mixing terms up to irrelevant total derivatives. This is the class of 't Hooft-Feynman gauge or R_ξ -gauge, which we partially use in our later calculations. By a variation of ξ_A , ξ_Z and ξ_W a simple check of the correctness of our calculations is possible, since physical observables should not be dependent on these unphysical gauge fixing conditions.

In a last step of this section we want to present the propagators of the gauge bosons and the unphysical modes, namely the Faddeev-Popov ghosts and the Goldstone bosons. For a massive gauge boson the procedure above results in a propagator of the form:

$$iG_V^{\mu\nu}(k^2) = \frac{g^{\mu\nu}}{k^2 - m_V^2} - (1 - \xi_V) \frac{k^\mu k^\nu}{(k^2 - m_V^2)(k^2 - \xi_V m_V^2)} \quad (5.88)$$

The one of the massless photon is:

$$iG_\gamma^{\mu\nu}(k^2) = \frac{g^{\mu\nu}}{k^2} - (1 - \xi_A) \frac{k^\mu k^\nu}{k^4} \quad (5.89)$$

The propagator of the scalar Goldstone bosons and the scalar Faddeev-Popov ghosts is given by

$$iG(k^2) = \frac{-1}{k^2 - \xi_V m_V^2} \quad , \quad (5.90)$$

implying that both have a mass of $m_{G_V}^2 = m_{u_V}^2 = \xi_V m_V^2$ in R_ξ -gauge. Be aware that the photon does not have a Goldstone boson, but a ghost. The masses of the Goldstone bosons in supersymmetric models stem from the following additional contributions to the pseudoscalar and charged scalar mass matrices

$$M_{P^0}^2 \longrightarrow M_{P^0}^2 + \xi_Z m_Z^2 M_{G^{P^0}}^2 \quad (5.91)$$

$$M_{S^\pm}^2 \longrightarrow M_{S^\pm}^2 + \xi_W m_W^2 M_{G^{S^\pm}}^2 \quad . \quad (5.92)$$

In case of the MSSM the matrices are given by

$$M_{G^{P^0}}^2 = M_{G^{S^\pm}}^2 = \frac{1}{v_d^2 + v_u^2} \begin{pmatrix} v_d^2 & -v_u v_d \\ -v_u v_d & v_u^2 \end{pmatrix} \quad . \quad (5.93)$$

In case of the NMSSM the matrix in Equation (5.93) is the upper (2×2) -block of the pseudoscalar (3×3) -matrix, since the singlet does not contribute. However in BRpV the VEVs of the left-handed sneutrinos have to be taken into account, resulting in

$$M_{G^{P^0}}^2 = \frac{1}{v_d^2 + v_u^2 + \sum_i v_i^2} \begin{pmatrix} v_d^2 & -v_u v_d & v_1 v_d & v_2 v_d & v_3 v_d \\ -v_u v_d & v_u^2 & -v_1 v_u & -v_2 v_u & -v_3 v_u \\ v_1 v_d & -v_1 v_u & v_1^2 & v_1 v_2 & v_1 v_3 \\ v_2 v_d & -v_2 v_u & v_1 v_2 & v_2^2 & v_2 v_3 \\ v_3 v_d & -v_3 v_u & v_1 v_3 & v_2 v_3 & v_3^2 \end{pmatrix} \quad (5.94)$$

$$M_{G^{S^\pm}}^2 = \begin{pmatrix} M_{G^{P^0}}^2 & 0 \\ 0 & 0 \end{pmatrix} \quad , \quad (5.95)$$

where in the latter case the zeros are the elements in rows and columns with right-handed sleptons. In case of the $\mu\nu$ SSM rows and columns with zeros for each right-handed sneutrino in $M_{G^{P^0}}^2$ have to be added. All these contributions result in the unphysical mass eigenstate describing the Goldstone boson with mass $\sqrt{\xi_Z} m_Z$ in case of the pseudoscalars and $\sqrt{\xi_W} m_W$

in case of the charged scalars. Apart from the propagator and the masses the gauge-fixing parameters ξ_V also appear in the couplings of a scalar to two ghost fields, which can be calculated from the Lagrangian defined in Equation (5.85). We just point out one example, namely the coupling of a scalar S_k^0 to the Faddeev-Popov fields of the Z boson in BRpV, where R^{S^0} denotes the mixing matrix of the neutral scalars:

$$C_{S_k^0 u_Z \bar{u}_Z} = -\frac{i}{4} \xi_Z (g \cos \theta_W + g' \sin \theta_W) \left(v_d R_{k1}^{S^0} + v_u R_{k2}^{S^0} + \sum_l v_l R_{kl+2}^{S^0} \right) \quad (5.96)$$

In case of the $\mu\nu$ S SM $R_{kl+2}^{S^0}$ has to be shifted to $R_{kl+2+m}^{S^0}$ with m being the number of right-handed neutrino superfields. All the other couplings can be found within the program `CNNDecays` in the files `couplings/model/ready/callcouplings.f90` for the various models under consideration.

5.3. Masses of neutralinos and charginos

An important part of this thesis is the discussion of the masses of neutralinos and charginos at tree- and one-loop level for the various models under consideration. In case of R -parity violating models the mass matrices have to be extended by the neutrinos and leptons, which allows an entirely supersymmetric explanation of neutrino masses. Denoting the neutralinos and charginos with the vectors ψ^0 and ψ^\pm , which contain the Weyl spinors mixing after electroweak symmetry breaking, the relevant part of the Lagrangian density can be written in the form

$$\mathcal{L} \supset -\frac{1}{2} (\psi^0)^T \mathcal{M}_n \psi^0 - \frac{1}{2} \left((\psi^-)^T \mathcal{M}_c \psi^+ + (\psi^+)^T \mathcal{M}_c^T \psi^- \right) + \text{h.c.} \quad (5.97)$$

The gauge eigenstates are rotated into mass eigenstates using the rotation matrices \mathcal{N} , V and U according to

$$F_i^0 = \mathcal{N}_{is} \psi_s^0, \quad F_i^+ = V_{it} \psi_t^+ \quad \text{and} \quad F_i^- = U_{it} \psi_t^- \quad , \quad (5.98)$$

so the rotation matrices U and V diagonalize the mass matrix \mathcal{M}_c of the charginos in the form:

$$\mathcal{M}_{c,\text{dia.}} = U^* \mathcal{M}_c V^{-1} \quad (5.99)$$

The rotation matrices can be obtained by the relations:

$$\mathcal{M}_{c,\text{dia.}}^2 = V \mathcal{M}_c^\dagger \mathcal{M}_c V^{-1} = U^* \mathcal{M}_c \mathcal{M}_c^\dagger (U^*)^{-1} \quad (5.100)$$

The neutralino mass matrix \mathcal{M}_n is a complex, but symmetric matrix. According to [116] a complex and symmetric matrices A can be diagonalized in the form $SAS^T = A_{\text{dia.}}$ with a unitary matrix $SS^\dagger = 1$. Thus, using the unitary matrix \mathcal{N} the neutralino mass matrix is diagonalized by

$$\mathcal{N}^* \mathcal{M}_n \mathcal{N}^\dagger = \mathcal{M}_{n,\text{dia.}} \quad . \quad (5.101)$$

For our later calculations of decays and loop corrections we work with Dirac spinors, which can be constructed from the Weyl spinors describing the mass eigenstates by:

$$\begin{aligned}\tilde{\chi}_i^0 &= \begin{pmatrix} F_i^0 \\ (F_i^0)^\dagger \end{pmatrix}, & \tilde{\chi}_i^+ &= \begin{pmatrix} F_i^+ \\ (F_i^-)^\dagger \end{pmatrix}, & \tilde{\chi}_i^- &= \begin{pmatrix} F_i^- \\ (F_i^+)^\dagger \end{pmatrix} \\ \overline{\tilde{\chi}}_i^0 &= \left(F_i^0, (F_i^0)^\dagger \right), & \overline{\tilde{\chi}}_i^+ &= \left(F_i^-, (F_i^+)^\dagger \right), & \overline{\tilde{\chi}}_i^- &= \left(F_i^+, (F_i^-)^\dagger \right)\end{aligned}\quad (5.102)$$

We will start with the MSSM and NMSSM, before explaining the generation of neutrino masses in BRpV and the $\mu\nu$ SSM. All the results in the following can be reproduced by MaCoR presented in Appendix F.1.

5.3.1. MSSM and NMSSM

In case of the MSSM and NMSSM the neutrinos remain massless particles, whereas the leptons obtain masses via the VEV v_d of the Higgs field H_d^0 as in the standard model. The gauge eigenstates of the neutral gauginos \tilde{B} and \tilde{W}_3 mix with the neutral Higgsinos \tilde{H}_d^0 and \tilde{H}_u^0 to four neutralinos $\tilde{\chi}_i$ in the MSSM, in case of the NMSSM the singlino \tilde{S} has to be added. In the charged sector the charged gauginos \tilde{W}^\pm , which are mixed according to

$$\tilde{W}^\pm = \frac{1}{\sqrt{2}} \left(\tilde{W}_1 \mp i\tilde{W}_2 \right) \quad , \quad (5.103)$$

form together with the charged Higgsinos \tilde{H}_d^\pm and \tilde{H}_u^\pm two charginos $\tilde{\chi}_i^\pm$. In the basis

$$(\psi^-)^T = \left(\tilde{W}^-, \tilde{H}_d^- \right), \quad (\psi^+)^T = \left(\tilde{W}^+, \tilde{H}_u^+ \right) \quad ,$$

the (2×2) mass matrix of the charged fermions is given by

$$\mathcal{M}_c = \begin{pmatrix} M_2 & \frac{1}{\sqrt{2}}g v_u \\ \frac{1}{\sqrt{2}}g v_d & \mu \end{pmatrix} = \begin{pmatrix} M_2 & \sqrt{2}m_W \sin \beta \\ \sqrt{2}m_W \cos \beta & \mu \end{pmatrix} \quad , \quad (5.104)$$

where μ can be obtained from Equation (4.2) in the NMSSM. For the neutralinos we use the basis

$$(\psi^0)^T = \left(\tilde{B}^0, \tilde{W}_3^0, \tilde{H}_d^0, \tilde{H}_u^0, \tilde{S} \right) \quad , \quad (5.105)$$

where the singlino \tilde{S} is of course only present in the NMSSM. The symmetric (4×4) - respectively (5×5) -matrix of the neutralinos have the form:

$$\begin{aligned}\mathcal{M}_n^{\text{MSSM}} &= \begin{pmatrix} M_1 & 0 & -\frac{1}{2}g'v_d & \frac{1}{2}g'v_u \\ 0 & M_2 & \frac{1}{2}g v_d & -\frac{1}{2}g v_u \\ -\frac{1}{2}g'v_d & \frac{1}{2}g v_d & 0 & -\mu \\ \frac{1}{2}g'v_u & -\frac{1}{2}g v_u & -\mu & 0 \end{pmatrix} \\ &= \begin{pmatrix} M_1 & 0 & -m_Z \sin \theta_W \cos \beta & m_Z \sin \theta_W \sin \beta \\ & M_2 & m_Z \cos \theta_W \cos \beta & -m_Z \cos \theta_W \sin \beta \\ & & 0 & -\mu \\ \text{sym.} & & & 0 \end{pmatrix}\end{aligned}\quad (5.106)$$

$$\begin{aligned}
\mathcal{M}_n^{\text{NMSSM}} &= \begin{pmatrix} M_1 & 0 & -\frac{1}{2}g'v_d & \frac{1}{2}g'v_u & 0 \\ 0 & M_2 & \frac{1}{2}gv_d & -\frac{1}{2}gv_u & 0 \\ -\frac{1}{2}g'v_d & \frac{1}{2}gv_d & 0 & -\frac{1}{\sqrt{2}}\lambda v_S & -\frac{1}{\sqrt{2}}\lambda v_u \\ \frac{1}{2}g'v_u & -\frac{1}{2}gv_u & -\frac{1}{\sqrt{2}}\lambda v_S & 0 & -\frac{1}{\sqrt{2}}\lambda v_d \\ 0 & 0 & -\frac{1}{\sqrt{2}}\lambda v_u & -\frac{1}{\sqrt{2}}\lambda v_d & \sqrt{2}\kappa v_S \end{pmatrix} \\
&= \begin{pmatrix} M_1 & 0 & -m_Z \sin \theta_W \cos \beta & m_Z \sin \theta_W \sin \beta & 0 \\ & M_2 & m_Z \cos \theta_W \cos \beta & -m_Z \cos \theta_W \sin \beta & 0 \\ & & 0 & -\mu & -\frac{\mu}{\tan \beta_S} \\ \text{sym.} & & & 0 & \frac{-\mu}{\tan \beta \tan \beta_S} \\ & & & & m_{\tilde{\zeta}} \end{pmatrix} \quad (5.107)
\end{aligned}$$

In case of the NMSSM μ , $\tan \beta_S$ and $m_{\tilde{\zeta}}$ were defined in Equation (4.2) and Equation (5.51). According to the equations at the beginning of this section this allows to calculate the mass eigenstates F_i^0 and F_j^\pm and from those the Dirac spinors $\tilde{\chi}_i^0$ and $\tilde{\chi}_j^\pm$, which we will use for our later calculations. Note that the chargino mass matrix could be diagonalized analytically. However, since it has to be combined with the lepton mass matrix in the R -parity violating case, the complete diagonalization procedure will be done numerically.

5.3.2. BRpV and $\mu\nu$ SSM

In case of R -parity violating models we have to add the neutrinos to the neutralinos and the leptons to the charginos. In all R -parity violating models under consideration the (5×5) -mass matrix of the charginos \mathcal{M}_c using the basis

$$\begin{aligned}
(\psi^-)^T &= (\tilde{W}^-, \tilde{H}_d^-, e, \mu, \tau) \\
(\psi^+)^T &= (\tilde{W}^+, \tilde{H}_u^+, e^c, \mu^c, \tau^c), \quad (5.108)
\end{aligned}$$

has the same form, namely

$$\begin{aligned}
\mathcal{M}_c &= \begin{pmatrix} M_2 & \frac{1}{\sqrt{2}}gv_u & 0 & 0 & 0 \\ \frac{1}{\sqrt{2}}gv_d & \mu & -\frac{1}{\sqrt{2}}Y_e^{i1}v_i & -\frac{1}{\sqrt{2}}Y_e^{i2}v_i & -\frac{1}{\sqrt{2}}Y_e^{i3}v_i \\ \frac{1}{\sqrt{2}}gv_1 & -\epsilon_1 & \frac{1}{\sqrt{2}}Y_e^{11}v_d & \frac{1}{\sqrt{2}}Y_e^{12}v_d & \frac{1}{\sqrt{2}}Y_e^{13}v_d \\ \frac{1}{\sqrt{2}}gv_2 & -\epsilon_2 & \frac{1}{\sqrt{2}}Y_e^{21}v_d & \frac{1}{\sqrt{2}}Y_e^{22}v_d & \frac{1}{\sqrt{2}}Y_e^{23}v_d \\ \frac{1}{\sqrt{2}}gv_3 & -\epsilon_3 & \frac{1}{\sqrt{2}}Y_e^{31}v_d & \frac{1}{\sqrt{2}}Y_e^{32}v_d & \frac{1}{\sqrt{2}}Y_e^{33}v_d \end{pmatrix} \\
&= \begin{pmatrix} M_2 & \sqrt{2}m_W \sin \beta \Theta & 0 & 0 & 0 \\ \sqrt{2}m_W \cos \beta \Theta & \mu & -\tan \beta_i m_e^{i1} & -\tan \beta_i m_e^{i2} & -\tan \beta_i m_e^{i3} \\ \sqrt{2}m_W \cos \beta \tan \beta_1 \Theta & -\epsilon_1 & m_e^{11} & m_e^{12} & m_e^{13} \\ \sqrt{2}m_W \cos \beta \tan \beta_2 \Theta & -\epsilon_2 & m_e^{21} & m_e^{22} & m_e^{23} \\ \sqrt{2}m_W \cos \beta \tan \beta_3 \Theta & -\epsilon_3 & m_e^{31} & m_e^{32} & m_e^{33} \end{pmatrix}, \quad (5.109)
\end{aligned}$$

where μ and ϵ_i have to be taken from Equation (4.10) in case of the $\mu\nu$ SSM. Apart from $\tan \beta_i = v_i/v_d$ we define $m_e^{ij} = \frac{1}{\sqrt{2}}Y_e^{ij}v_d$. Note that we allow for nondiagonal lepton masses m_e^{ij} , since the counterterms δm_e^{ij} are needed to cancel nondiagonal contributions in the lepton mass matrix at one-loop level. However the lepton Yukawa couplings Y_e and thus m_e^{ij} can be chosen

diagonal at tree-level. The quantity Θ is a function of $\tan \beta$ and $\tan \beta_i$:

$$\Theta = \Theta(\beta, \beta_i) = \sqrt{\frac{1}{1 + \cos^2 \beta \sum_i \tan^2 \beta_i}} \xrightarrow{v_i \rightarrow 0} 1 \quad (5.110)$$

It allows to express the elements of the chargino and later also the neutralino mass matrix in terms of the physical observables m_Z or m_W defined in the gauge boson sector, whereas the small contributions from R -parity violation are encoded in $\tan \beta_i$, ϵ_i or Θ , the latter one being approximately 1 for reasonable small VEVs v_i of the left-handed sneutrinos.

The R -parity violating elements, which induce the mixing between the lepton sector and the ordinary charginos, have of course an impact on the lepton masses after diagonalization. Therefore we use a fit adopting the diagonal Yukawa couplings Y_e^{ii} such that the experimental values for the lepton masses are obtained at tree-level.

The neutralino mass matrix however should be discussed for BRpV and the $\mu\nu$ SSM independently. We start with BRpV, where we get in the basis

$$(\psi^0)^T = (\tilde{B}^0, \tilde{W}_3^0, \tilde{H}_d^0, \tilde{H}_u^0, \nu_1, \nu_2, \nu_3) \quad (5.111)$$

the following mass matrix for the neutralinos:

$$\mathcal{M}_n = \begin{pmatrix} M_n & \hat{m} \\ \hat{m}^T & 0 \end{pmatrix} \quad (5.112)$$

$$M_n = \begin{pmatrix} M_1 & 0 & -\frac{1}{2}g'v_d & \frac{1}{2}g'v_u \\ 0 & M_2 & \frac{1}{2}g'v_d & -\frac{1}{2}g'v_u \\ -\frac{1}{2}g'v_d & \frac{1}{2}g'v_d & 0 & -\mu \\ \frac{1}{2}g'v_u & -\frac{1}{2}g'v_u & -\mu & 0 \end{pmatrix} \quad (5.113)$$

$$= \begin{pmatrix} M_1 & 0 & -m_Z \sin \theta_W \cos \beta \Theta & m_Z \sin \theta_W \sin \beta \Theta \\ & M_2 & m_Z \cos \theta_W \cos \beta \Theta & -m_Z \cos \theta_W \sin \beta \Theta \\ & & 0 & -\mu \\ \text{sym.} & & & 0 \end{pmatrix} \quad (5.114)$$

$$(\hat{m}^T)_i = \left(-\frac{1}{2}g'v_i \quad \frac{1}{2}gv_i \quad 0 \quad \epsilon_i\right) \quad (5.115)$$

$$= \left(-m_Z \sin \theta_W \cos \beta \tan \beta_i \Theta \quad m_Z \cos \theta_W \cos \beta \tan \beta_i \Theta \quad 0 \quad \epsilon_i\right) \quad (5.116)$$

Again we rewrote the matrix to adopt our notation for the renormalization procedure later. Thus the R -parity violating parameters ϵ_i and v_i are encoded in ϵ_i , $\tan \beta_i$ and Θ as defined in Equation (5.110). The generation of neutrino masses at tree-level similar to the procedure in the seesaw mechanism will be explained in the next section. A priori there is no Majorana mass term for the left-handed neutrinos.

In the $\mu\nu$ SSM the gauge eigenstates of the neutralinos are ordered in the form

$$(\psi^0)^T = (\tilde{B}^0, \tilde{W}_3^0, \tilde{H}_d^0, \tilde{H}_u^0, \nu_k^c, \nu_1, \nu_2, \nu_3) \quad (5.117)$$

with $k = 1, \dots, n$ and n being the number of right-handed neutrino superfields. For the general case the $((7+n) \times (7+n))$ -mass matrix \mathcal{M}_n can be written as follows

$$\mathcal{M}_n = \begin{pmatrix} M_n & \hat{m} \\ \hat{m}^T & 0 \end{pmatrix} \quad (5.118)$$

$$M_n = \begin{pmatrix} M_1 & 0 & -\frac{1}{2}g'v_d & \frac{1}{2}g'v_u & 0 \\ 0 & M_2 & \frac{1}{2}gv_d & -\frac{1}{2}gv_u & 0 \\ -\frac{1}{2}g'v_d & \frac{1}{2}gv_d & 0 & -\frac{1}{\sqrt{2}}\lambda_l v_{cl} & -\frac{1}{\sqrt{2}}\lambda_k v_u \\ \frac{1}{2}g'v_u & -\frac{1}{2}gv_u & -\frac{1}{\sqrt{2}}\lambda_l v_{cl} & 0 & \frac{1}{\sqrt{2}}(Y_\nu^{ik}v_i - \lambda_k v_d) \\ 0 & 0 & -\frac{1}{\sqrt{2}}\lambda_k v_u & \frac{1}{\sqrt{2}}(Y_\nu^{ik}v_i - \lambda_k v_d) & \frac{1}{\sqrt{2}}\kappa_k v_{ck} \end{pmatrix}, \quad (5.119)$$

where the last row and column of M_n have to be copied n -times using $k = 1, \dots, n$, whereas it has to be summed over i and l . The part of the mass matrix containing the right-handed neutrinos is diagonal with the elements $\frac{1}{\sqrt{2}}\kappa_k v_{ck}$. The $(3 \times (4 + n))$ -mass matrix \hat{m} yields

$$(\hat{m}^T)_i = \left(-\frac{1}{2}g'v_i \quad \frac{1}{2}gv_i \quad 0 \quad \frac{1}{\sqrt{2}}Y_\nu^{il}v_{cl} \quad \frac{1}{\sqrt{2}}Y_\nu^{ik}v_u \right), \quad (5.120)$$

again with the last element being copied n -times with indices $k = 1, \dots, n$.

In the special case of only one right-handed neutrino superfield the mass matrix \mathcal{M}_n can be rewritten in the following way

$$\mathcal{M}_n = \begin{pmatrix} M_n & \hat{m} \\ \hat{m}^T & 0 \end{pmatrix} \quad (5.121)$$

$$M_n = \begin{pmatrix} M_1 & 0 & -m_Z \sin \theta_W \cos \beta \Theta & m_Z \sin \theta_W \sin \beta \Theta & 0 \\ & M_2 & m_Z \cos \theta_W \cos \beta \Theta & -m_Z \cos \theta_W \sin \beta \Theta & 0 \\ & & 0 & -\mu & -\frac{\mu}{\tan \beta_c} \\ \text{sym.} & & & 0 & \frac{\tan \beta_i \epsilon_i - \mu}{\tan \beta \tan \beta_c} \\ & & & & m_c \end{pmatrix} \quad (5.122)$$

$$(\hat{m}^T)_i = \left(-m_Z \sin \theta_W \cos \beta \Theta \tan \beta_i \quad m_Z \cos \theta_W \cos \beta \Theta \tan \beta_i \quad 0 \quad \epsilon_i \quad \frac{\epsilon_i}{\tan \beta_c} \right), \quad (5.123)$$

where the effective μ and effective bilinear terms ϵ_i are defined in accordance to Equation (4.10). Moreover the definitions for $\tan \beta_c$, $\tan \beta_i$ and m_c , which we presented in the discussion of the scalar sector in Equation (5.73), are used.

5.3.3. Approximate diagonalization

In order to gain insight into the generation of neutrino masses in BRpV and the $\mu\nu$ SSM we will present an approximate diagonalization of the neutralino mass matrices \mathcal{M}_n , which we showed in the last section. The diagonalization of the neutralino mass matrix can be approximated according to [117] as follows:

$$\mathcal{N}^* \mathcal{M}_n \mathcal{N}^\dagger = \mathcal{M}_{n,\text{dia.}} \quad \text{with} \quad \mathcal{N}^* = \begin{pmatrix} N^* & 0 \\ 0 & \mathcal{V}^T \end{pmatrix} \begin{pmatrix} 1 - \frac{1}{2}\xi^\dagger \xi & \xi^\dagger \\ -\xi & 1 - \frac{1}{2}\xi \xi^\dagger \end{pmatrix} \quad (5.124)$$

For small values of the (3×4) - respectively $(3 \times (5 + n))$ -matrix ξ , namely $\xi_{ij} \ll 1$, \mathcal{N}^* is approximately a unitary matrix, since N^* and \mathcal{V}^T are chosen to be unitary. Setting $\xi = \hat{m}^T M_n^{-1}$ allows the following transformation

$$\mathcal{N}^* \mathcal{M}_n \mathcal{N}^\dagger \approx \begin{pmatrix} N^* & 0 \\ 0 & \mathcal{V}^T \end{pmatrix} \begin{pmatrix} M_n & 0 \\ 0 & -\hat{m}^T M_n^{-1} \hat{m} \end{pmatrix} \begin{pmatrix} N^\dagger & 0 \\ 0 & \mathcal{V} \end{pmatrix}, \quad (5.125)$$

if higher orders in ξ are neglected. Thus, using the definition of an effective neutrino mass matrix $m_{\nu\nu}^{\text{eff.}} = -\hat{m}^T M_n^{-1} \hat{m}$ we define N^* and \mathcal{V}^T to diagonalize

$$N^* M_n N^\dagger = M_{n,\text{dia.}} \quad \text{and} \quad \mathcal{V}^T m_{\nu\nu}^{\text{eff.}} \mathcal{V} = m_{\nu\nu}^{\text{eff.,dia.}} \quad . \quad (5.126)$$

The advantage of this procedure is a possible analytic approximation of the neutrino masses very similar to the seesaw mechanism, whereas in case of the full neutralino mass matrix \mathcal{M}_n only a numerical determination of the eigenvalues is possible. The matrices ξ are also important for approximate couplings later, therefore they can be found in Appendix B.

Similarly an approximate diagonalization in case of the charginos is possible, which is not important for the calculation of masses, but for the approximation of couplings. If we split the chargino mass matrix in the form

$$\mathcal{M}_c = \begin{pmatrix} M_c & E' \\ E & m_e \end{pmatrix} \quad , \quad (5.127)$$

where we have used the (3×3) -mass matrix of the leptons m_e and the (2×2) -mass matrix of the charginos M_c , one can do the following approximation for small values of $E' \approx 0$, i.e. small VEVs of the left-handed sneutrinos v_i

$$U = \begin{pmatrix} U_c & U_c \xi_L^T \\ -\xi_L & I_3 \end{pmatrix}, \quad V = \begin{pmatrix} V_c & V_c \xi_R^T \\ -\xi_R & I_3 \end{pmatrix} \quad , \quad (5.128)$$

where the matrices ξ_L and ξ_R can be deduced from

$$\begin{aligned} \xi_L^* &= E M_c^{-1} \\ \xi_R^* &= m_e^\dagger E M_c^{-1} (M_c^{-1})^T = m_e^\dagger \xi_L^* (M_c^{-1})^T \quad . \end{aligned} \quad (5.129)$$

and the identity matrix I_3 implies a diagonal form of the lepton Yukawa couplings. U_c and V_c diagonalize the (2×2) -mass matrix of the charginos. Finally in the next section we can calculate the neutrino masses using the approximations presented here.

5.3.4. Neutrino masses

As we have seen in the last section, we can calculate approximate neutrino masses in R -parity violating models by using the effective neutrino mass matrix $m_{\nu\nu}^{\text{eff.}} = -\hat{m}^T M_n^{-1} \hat{m}$. In case of BRpV and the $\mu\nu$ SSM with one right-handed neutrino superfield and assuming real parameters this results in

$$(m_{\nu\nu}^{\text{eff.}})_{ij} = a \Lambda_i \Lambda_j \quad (5.130)$$

with a being

$$a^{\text{BRpV}} = \frac{m_\gamma}{4\text{Det}_0^{\text{BRpV}}}, \quad a^{1\mu\nu\text{SSM}} = \frac{m_\gamma(\lambda^2 v_d v_u + \mu m_c)}{4\mu\text{Det}_0^{1\mu\nu\text{SSM}}} \quad , \quad (5.131)$$

where we have introduced the alignment parameter

$$\Lambda_i = \mu v_i + v_d \epsilon_i \quad (5.132)$$

with μ given by Equation (4.10) in the $\mu\nu$ S SM and the abbreviation

$$m_\gamma = g^2 M_1 + g'^2 M_2 \quad . \quad (5.133)$$

The determinants of M_n are given by

$$\text{Det}_0^{\text{BRpV}} = \frac{1}{2} m_\gamma \mu v_d v_u - M_1 M_2 \mu^2 \quad (5.134)$$

$$\text{Det}_0^{1\mu\nu\text{SSM}} = \frac{1}{8} m_\gamma (\lambda^2 (v_d^2 + v_u^2)^2 + 4m_c \mu v_d v_u) - M_1 M_2 \mu (v_d v_u \lambda^2 + m_c \mu) \quad . \quad (5.135)$$

A matrix of the type $\propto \Lambda_i \Lambda_j$ only has one nonzero eigenvalue, so that only one neutrino can acquire a mass in BRpV and the $\mu\nu$ S SM with one right-handed neutrino superfield at tree-level. The mass of the neutrino can be easily approximated by the formula

$$m(\nu_3) = a |\vec{\Lambda}| \quad , \quad (5.136)$$

allowing an estimation for the correct magnitude of $\vec{\Lambda}$. The fact that only one neutrino acquires a mass is not owed to the used approximation: Calculating the characteristic polynomial for the full neutralino mass matrix \mathcal{M}_n yields

$$\det(\mathcal{M}_n - \rho I) = \rho^2 P(\rho) \quad , \quad (5.137)$$

where $P(\rho)$ is a polynomial in ρ . It shows that in both models two zero eigenvalues corresponding to two massless neutrinos are present. Since one massive neutrino cannot explain the full neutrino spectrum, we have to go to the one-loop level to explain the full neutrino data, which will be done in the next chapter. Also in case of complex parameters in BRpV only one neutrino acquires a mass at tree-level. Then the exact diagonalization of the mass matrix of the neutralinos has to be done using the squared mass matrix, so that a precise numerical calculation has to be guaranteed.

In case of more than one right-handed neutrino superfields in the $\mu\nu$ S SM one can explain the neutrino data using the tree-level neutrino mass matrix only. For the sake of simplicity we will only consider two generations of right-handed neutrinos, since more right-handed neutrino superfields do not provide new features. Despite from Λ_i as defined in Equation (5.132) we have a new alignment parameter

$$\alpha_i = v_u (\lambda_2 Y_\nu^{i1} - \lambda_1 Y_\nu^{i2}) \quad . \quad (5.138)$$

Based on these parameters we define the expansion matrices ξ in the Appendix B for the $\mu\nu$ S SM with two right-handed neutrino superfields. The effective neutrino mass matrix reads as

$$(m_{\nu\nu}^{\text{eff.}})_{ij} = a \Lambda_i \Lambda_j + b (\Lambda_i \alpha_j + \Lambda_j \alpha_i) + c \alpha_i \alpha_j \quad (5.139)$$

with

$$\begin{aligned} a &= \frac{m_\gamma}{4\mu \text{Det}_0^{2\mu\nu\text{SSM}}} (m_{c1} \lambda_2^2 v_u v_d + m_{c2} \lambda_1^2 v_u v_d + m_{c1} m_{c2} \mu) \\ b &= \frac{m_\gamma}{8\sqrt{2}\mu \text{Det}_0^{2\mu\nu\text{SSM}}} (v_u^2 - v_d^2) (m_{c1} v_{c1} \lambda_2 - m_{c2} v_{c2} \lambda_1) \\ c &= - \frac{1}{16\mu^2 \text{Det}_0^{2\mu\nu\text{SSM}}} \left[\mu^2 (m_\gamma (v_d^2 + v_u^2)^2 - 8M_1 M_2 \mu v_u v_d) \right. \\ &\quad \left. + 4\text{Det}_0^{\text{BRpV}} (m_{c1} v_{c1}^2 + m_{c2} v_{c2}^2) \right] \end{aligned} \quad (5.140)$$

using $m_{ck} = \sqrt{2}\kappa_k v_{ck}$ and the determinant of the (6×6) -mass matrix of the heavy states

$$\text{Det}_0^{2\mu\nu\text{SSM}} = \frac{1}{8} \left[(m_{c2}\lambda_1^2 + m_{c1}\lambda_2^2)(m_\gamma(v_d^2 + v_u^2)^2 - 8M_1M_2\mu v_u v_d) + 8m_{c1}m_{c2}\text{Det}_0^{\text{BRpV}} \right] . \quad (5.141)$$

The mass matrix in Equation (5.139) has two nonzero eigenvalues in contrast to BRpV and the $\mu\nu\text{SSM}$ with only one right-handed neutrino superfield. Therefore loop corrections for the explanation of the full spectrum of neutrino data are not needed.

We address the fit to neutrino data in all R -parity violating models under consideration after the discussion of one-loop corrections in the next chapter.

5.4. Decays $\tilde{\chi}_j^0 \rightarrow \tilde{\chi}_l^\pm W^\mp$ and $\tilde{\chi}_l^\pm \rightarrow \tilde{\chi}_j^0 W^\pm$

As we have argued in the introduction two-body decays of neutralinos and charginos involving a heavy gauge boson in the final state are of great importance in SUSY cascade decays. Moreover they include the R -parity violating decays $\tilde{\chi}_1^0 \rightarrow l^\pm W^\mp$, which play an important role within this thesis. Thus, it is reasonable to discuss the decays $\tilde{\chi}_l^\pm \rightarrow \tilde{\chi}_j^0 W^\pm$ and the couplings $\tilde{\chi}_i^0 - \tilde{\chi}_j^\pm - W^\mp$ in more detail within this and the next section. For all the other two- and three body decays, we have used the decay routines of **SPheno** or implemented them in **CNNDecays**.

The partial widths for the decays under consideration are obtained from the following interaction Lagrangian:

$$\mathcal{L} = \overline{\tilde{\chi}_l} \gamma^\mu (P_L O_{Ll} + P_R O_{Rl}) \tilde{\chi}_j^0 W_\mu^- + \text{h.c.} . \quad (5.142)$$

The couplings are given by

$$O_{Ll} = -g\mathcal{N}_{j2}^* U_{l1} - \frac{1}{\sqrt{2}}g \left(\mathcal{N}_{j3}^* U_{l2} + \sum_{k=1}^3 U_{l,2+k} \mathcal{N}_{j,4(4+n)+k}^* \right) \quad (5.143)$$

$$O_{Rl} = -gV_{l1}^* \mathcal{N}_{j2} + \frac{1}{\sqrt{2}}gV_{l2}^* \mathcal{N}_{j4} , \quad (5.144)$$

where in Equation (5.143) $4(4+n)$ stands for BRpV ($\mu\nu\text{SSM}$ with n right-handed neutrino superfields). Of course the last term in O_{Ll} is only present in case of R -parity violating models. The widths have the form

$$\Gamma^0 = \frac{1}{16\pi m_i^3} \sqrt{\kappa(m_i^2, m_o^2, m_W^2)} \frac{1}{2} \sum_{pol} |M_T|^2 , \quad (5.145)$$

where m_i (m_o) is the mass of the mother (daughter) particle and M_T is the tree-level matrix element. Explicitly they are

$$\Gamma^0 (\tilde{\chi}_j^0 \rightarrow \tilde{\chi}_l^+ W^-) = \frac{1}{16\pi m_j^3} \sqrt{\kappa(m_j^2, m_l^2, m_W^2)} \times \left((|O_{Llj}|^2 + |O_{Rlj}|^2) f(m_j^2, m_l^2, m_W^2) - 6\text{Re}(O_{Llj} O_{Rlj}^*) m_j m_l \right) \quad (5.146)$$

$$\Gamma^0 (\tilde{\chi}_i^+ \rightarrow \tilde{\chi}_k^0 W^+) = \frac{1}{16\pi m_i^3} \sqrt{\kappa(m_i^2, m_k^2, m_W^2)} \times \left((|O_{Lik}|^2 + |O_{Rik}|^2) f(m_i^2, m_k^2, m_W^2) - 6\text{Re}(O_{Lik} O_{Rik}^*) m_i m_k \right) \quad (5.147)$$

making use of the following functions

$$f(x, y, z) = \frac{1}{2}(x + y) - z + \frac{(x - y)^2}{2z} \quad (5.148)$$

$$\kappa(x, y, z) = x^2 + y^2 + z^2 - 2xy - 2xz - 2yz \quad . \quad (5.149)$$

5.5. Coupling $\tilde{\chi}_i^0 - \tilde{\chi}_j^\pm - W^\mp$ - Approximate formulas

The tree-level couplings O_{Li1} in Equation (5.143) and O_{Ri1} in Equation (5.144) for the special case of the lightest neutralino $\tilde{\chi}_1^0$ coupling to a lepton l_i^\pm in the R -parity violating models can be approximated in terms of the alignment parameters Λ_i , ϵ_i and in case of the $\mu\nu$ SSM with two right-handed neutrino superfields also α_i , which allows to understand the correlations to the neutrino mixing angles.

As mentioned for the case of neutral fermions in Section 5.3, we define the matrices ξ , ξ_L and ξ_R being taken as expansion parameters in the mixing matrices \mathcal{N} , U and V in such a way, that one gets the leading order expressions

$$\mathcal{N} = \begin{pmatrix} N & N\xi^T \\ -\mathcal{V}^\dagger\xi^* & \mathcal{V}^\dagger \end{pmatrix}, \quad U = \begin{pmatrix} U_c & U_c\xi_L^T \\ -\xi_L & I_3 \end{pmatrix}, \quad V = \begin{pmatrix} V_c & V_c\xi_R^T \\ -\xi_R & I_3 \end{pmatrix}, \quad (5.150)$$

where I_3 is the (3×3) -identity matrix. Inserting the expressions for ξ , ξ_L and ξ_R given in Appendix B in the couplings shown in Equations (5.143) and (5.144) and assuming that all parameters are real, those can be approximated by:

$$\begin{aligned} O_{Li1} &\approx \frac{g}{\sqrt{2}} \left[\frac{gN_{12}\Lambda_i}{\text{Det}_+} - \left(\frac{\epsilon_i}{\mu} + \frac{g^2v_u\Lambda_i}{2\mu\text{Det}_+} \right) N_{13} - \sum_{k=1}^{4(4+n)} N_{1k}\xi_{ik} \right] \\ O_{Ri1} &\approx \frac{gY_e^{ii}v_d}{2\text{Det}_+} \left[\frac{gv_uN_{12} - M_2N_{14}}{\mu} \epsilon_i + \frac{g(2\mu^2 + g^2v_u^2)N_{12} - g^2(v_d\mu + M_2v_u)N_{14}}{2\mu\text{Det}_+} \Lambda_i \right] \end{aligned} \quad (5.151)$$

Whereas the approximated right-handed couplings O_{Ri1} are the same in BRpV and the $\mu\nu$ SSM and differ slightly from the ones presented in [118], inserting the expansion matrices ξ_{ij} yields for the left-handed coupling O_{Li1} in BRpV and the $\mu\nu$ SSM with one right-handed neutrino superfield the following expressions:

$$\begin{aligned} O_{Li1}^{\text{BRpV}} &\approx \frac{g\Lambda_i}{\sqrt{2}} \left[-\frac{g'M_2\mu}{2\text{Det}_0} N_{11} + \left(\frac{g}{\text{Det}_+} + \frac{gM_1\mu}{2\text{Det}_0} \right) N_{12} \right. \\ &\quad \left. - \frac{v_u}{2} \left(\frac{m_\gamma}{2\text{Det}_0} + \frac{g^2}{\mu\text{Det}_+} \right) N_{13} + \frac{v_d m_\gamma}{4\text{Det}_0} N_{14} \right] \end{aligned} \quad (5.152)$$

$$\begin{aligned} O_{Li1}^{1\mu\nu\text{SSM}} &\approx \frac{g\Lambda_i}{\sqrt{2}} \left[-\frac{g'M_2}{2\text{Det}_0} (v_d v_u \lambda^2 + m_c \mu) N_{11} + \left(\frac{g}{\text{Det}_+} + \frac{gM_1}{2\text{Det}_0} (v_d v_u \lambda^2 + m_c \mu) \right) N_{12} \right. \\ &\quad \left. - \left(\frac{g^2 v_u}{2\mu\text{Det}_+} - \frac{m_\gamma}{8\mu\text{Det}_0} (\lambda^2 v_d (v_d^2 + v_u^2) + 2m_c \mu v_u) \right) N_{13} \right. \\ &\quad \left. + \frac{m_\gamma}{8\mu\text{Det}_0} (\lambda^2 v_u (v_d^2 + v_u^2) + 2m_c \mu v_d) N_{14} - \frac{\lambda m_\gamma}{4\sqrt{2}\text{Det}_0} (v_u^2 - v_d^2) N_{15} \right] \end{aligned} \quad (5.153)$$

The couplings include the abbreviations defined in Equations (4.10), (5.132) and (5.133) and the determinants given in Equations (5.134) and (5.135). In addition the determinant of the

heavy states in the chargino mass matrix appears as presented in Equation (B.12). Neglecting the right-handed couplings, which are generally smaller than the left-handed ones due to the proportionality to the lepton Yukawa couplings Y_e , it is obvious that the lightest neutralino $\tilde{\chi}_1^0$ couples to $l_i^+ W^-$ proportional to Λ_i without any dependence on the ϵ_i parameters. This fact is in case of the considered BRpV and the $\mu\nu$ SVM with one right-handed neutrino superfield independent of the nature of the lightest neutralino $\tilde{\chi}_1^0$.

The case of the $\mu\nu$ SVM with two right-handed neutrino superfields offers a richer structure, since not only the alignment parameters Λ_i and ϵ_i , but in addition α_i is relevant. Neglecting the right-handed coupling the expression for a bino-like neutralino with $N_{11}^2 = 1$ yields

$$O_{Li1}^{2\mu\nu\text{SVM}} = - \frac{\sqrt{2}gg' M_2 \mu}{m_\gamma} (a\Lambda_i + b\alpha_i) \quad . \quad (5.154)$$

The latter formula implies that a bino-like neutralino $\tilde{\chi}_1^0$ couples to $l_i^+ W^-$ dependent on two pieces being proportional to either Λ_i or α_i . However the relative importance of those two terms can be easily estimated: If we assume that all masses are at the same scale m_{SUSY} and the couplings λ, κ are of order $\mathcal{O}(0.1)$ and the R -parity violating parameters Y_ν^i and v_i are of order $\mathcal{O}(Y_\nu)$ and $\mathcal{O}(m_{\text{SUSY}} Y_\nu)$ respectively, we get $a\Lambda_i \sim 200 b\alpha_i$. Thus the coupling is dominated by the term proportional to Λ_i .

For a pure Higgsino-like neutralino characterized by $N_{13}^2 + N_{14}^2 = 1$ we observe a dependence on Λ_i and α_i using the expansion matrices ξ , ξ_L and ξ_R from Appendix B. We add one example for a singlino-like neutralino defined by $N_{1k}^2 = 1$: The coupling of ν_1^c in the $\mu\nu$ SVM with two right-handed neutrino superfields is given by ξ_{i5} resulting in a dependence on Λ_i and α_i . The latter one gives the dominant contribution, which can be tested numerically.

However it is important to emphasize that all previous formulas are tree-level results. A priori it is not clear, what happens if one uses the mixing matrices \mathcal{N} , U and V for masses at one-loop level in BRpV or the $\mu\nu$ SVM with one right-handed neutrino superfield or performs a complete NLO calculation of the considered decay width.

One-loop calculations - Theory

Higher order corrections using perturbation theory are known to be important for masses and processes in the standard model. Since technical questions have to be addressed when performing those calculations, we present the general process of regularization and renormalization within this chapter. We put special focus on the on-shell renormalization, which was first proposed in [119] and is reasonable in case of electroweak corrections, where strong interactions are not involved and the masses of the particles can in principle be measured with high precision. This is in particular true for neutralinos and charginos in initial and final states.

After the theoretical introduction we discuss the on-shell renormalization of heavy gauge bosons and mixing fermions in all detail, since the knowledge of one-loop masses and decay widths is crucial to make reliable predictions for various experiments. Using the R_ξ -gauge presented in the last chapter we work out a gauge invariant formulation of the NLO corrections. The consideration of one-loop contributions in models of R -parity violation can be easily understood from the fact, that in BRpV and the $\mu\nu$ SSM with one right-handed neutrino superfield the full neutrino spectrum cannot be explained at tree-level, since only one neutrino acquires a mass according to Section 5.3.4. Note that the next order in perturbation theory for the masses of the neutralinos was illustrated using a $\overline{\text{DR}}$ scheme in BRpV [97, 120, 121] and in the $\mu\nu$ SSM [106, 122]. However, the more convenient on-shell scheme is first worked out for these models in the context of this thesis. We also focus on the decay width $\Gamma(\tilde{\chi}_i^0 \rightarrow \tilde{\chi}_i^\pm W^\mp)$ at one-loop level using the on-shell scheme, the reason being that in the (N)MSSM the corrections to these decays can be sizable and therefore relevant for the phenomenology of the model. In case of the R -parity violating decays of the lightest neutralino the corrections to $\Gamma(\tilde{\chi}_1^0 \rightarrow l_i^\pm W^\mp)$ turn out to be important for the relations between branching ratios and the neutrino mixing angles.

6.1. Regularization and renormalization - The basics

6.1.1. Regularization

The basis of relativistic quantum field theory is the expansion of interactions using a perturbation theory in the couplings. If we consider the example of a scalar ϕ^4 -theory with the Lagrangian density

$$\mathcal{L} = \frac{1}{2}(\partial_\mu \phi_0)(\partial^\mu \phi_0) - \frac{1}{2}m_0^2 \phi_0^2 - \frac{\lambda_0}{4!} \phi_0^4 \quad , \quad (6.1)$$

it contains a four-point interaction λ_0 , which can be represented as tree-level Feynman graph.

However using two of these interactions, also the next order in perturbation theory can be depicted:

(6.2)

Note that this is only one possibility for a Feynman graph at one-loop level. The major problem in the evaluation of those graphs is the integration over the unknown momentum k of the intermediate particle in the loop. Apart from infrared divergences for low values of k also ultraviolet divergences for very large values of k can occur. Thus, we need a procedure to parameterize the divergences and to separate them from the finite parts of the loop integrals. Afterwards the renormalization procedure has to give a prescription how to subtract those divergences and to reinterpret them in terms of finite physical observables.

Before discussing the renormalization procedure, we will first focus on the different possibilities of divergences and their regularization: We move the discussion of infrared divergences to Section 6.4.3, where we show that the combination of real and virtual corrections leads to finite results. However the discussion of ultraviolet divergences is more subtle [123]:

The easiest way is the “cut-off”-method: The integration over the four-momentum d^4k is rewritten in spherical coordinates and the radius of the 4-dimensional sphere is limited to a maximum value of Λ , which can be interpreted as the energy scale to which the considered theory should be valid. Thus, in principle every integral can be made finite, however this procedure breaks Poincaré invariance. Lattice gauge theories [124], often used in quantum chromodynamics, are working with a discretized space-time. This results in a regularization procedure, which is similar to the “cut-off”-method and therefore induces the same problems.

More elegant is the regularization making use of fictitious heavy particles. Within this method the propagators $G(p, m)$ are substituted by

$$G^{\text{reg}}(p, m) = G(p, m) + \sum_k C_k G(p, M_k) \quad (6.3)$$

with coefficients C_k , which are functions of the masses m and M_k . Using a finite number of additional terms allows to regularize arbitrary Feynman graphs. A well-known application is the Pauli-Villars regularization [125] in case of quantum electrodynamics, where the photon propagator is replaced accordingly.

The most famous method of regularization is based on the reduction of space-time dimensions. Counting the dimensions of mass in loop integrals (“power counting”) allows to assign a degree of divergence to each loop integral, which can be lowered by the reduction of space-time dimensions. Nonrenormalizable, renormalizable and super-renormalizable theories can also be distinguished by the method of “power counting” [1]. The concept of dimensional regularization was worked out by ’t Hooft and Veltman. All integrals are written in d dimensions ($d < 4$, real number), which allows to split the integrals in the UV divergent parts containing a pole with denominator $d - 4$ and finite contributions. We will present the notation of this procedure in the next section. However we will discuss the mass dimensions of fields and couplings in advance:

Having the kinetic term of a fermion written as Dirac spinor $\bar{u}\gamma^\mu\partial_\mu u$, it follows a mass dimension of $[u] = (d - 1)/2$, so that the mass dimension of the Lagrangian density is d . Similarly we obtain for scalar fields and gauge bosons $[\phi] = [A_\mu] = (d - 2)/2$. In 4 dimension the electric charge e has no mass dimension. However a glimpse at the coupling $e\bar{u}\gamma^\mu A_\mu u$ shows that in d dimensions

it should yield $[e] = (4 - d)/2$. To solve this problem a mass parameter Q is introduced

$$e \rightarrow eQ^{\frac{4-d}{2}} \quad (6.4)$$

allowing for a massless electric charge also in d dimensions. Within supersymmetric models another complication of dimensional regularization (DimReg) has to be kept in mind: The superfields we introduced in Section 3.5 contain for example the gauge bosons and their superpartner, the gauginos, which have different degrees of freedom in $d = 4 - \epsilon$ dimensions. Therefore, in supersymmetry dimensional reduction (DRED) instead of DimReg is used, where tensors and spinors stay in 4 dimensions with an index μ from 0 to 3 and only momenta and the space-time are reduced to d dimensions. To account for this problem in DimReg scalar particles, so called ϵ -scalars have to be introduced as auxiliary fields, so that the degrees of freedom of gauge bosons match with the ones of their superpartners [123]. For dimensional reduction in general we refer to the [126] and subsequent publications [127].

6.1.2. Passarino-Veltman integrals

Using dimensional regularization Passarino, Veltman and 't Hooft [128, 129] developed a simple representation of the one-loop integrals with a unique regularization of the UV divergences, which is the basis of many computer codes like the `FF` package [130] and `LoopTools` [131]. A nice review was written by Jorge Romão [132].

Starting with dimensional regularization or reduction in d dimensions the generic one-loop tensor integral is of the form

$$T_n^{\mu_1 \dots \mu_p} = \frac{(2\pi Q)^{4-d}}{i\pi^2} \int d^d k \frac{k^{\mu_1} \dots k^{\mu_p}}{D_0 D_1 \dots D_{n-1}} \quad (6.5)$$

with the denominators being defined as follows

$$D_i = (r_i + k)^2 - m_{i+1}^2 + i\epsilon \quad , \quad (6.6)$$

where r_i can be interpreted from Figure 6.1.

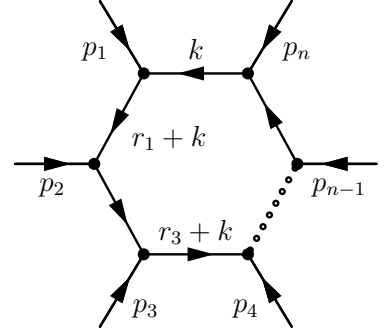


Figure 6.1.: Definition and notation of Passarino-Veltman integrals

In this notation the following relations hold:

$$r_j = \sum_{i=1}^j p_i \quad \text{with} \quad j = 1, \dots, n-1, \quad r_0 = \sum_{i=1}^n p_i = 0 \quad (6.7)$$

Using this definition one integral is in particular relevant for the following calculations, namely:

$$\begin{aligned} I_n(f^2) &:= \frac{(2\pi Q)^{4-d}}{i\pi^2} \int d^d k \frac{1}{(k^2 - f^2)^n} = \frac{(4\pi Q^2)^{2-\frac{d}{2}}}{i\pi^{d/2}} \int d^d k \frac{1}{(k^2 - f^2)^n} \\ &= (-1)^n (4\pi Q^2)^{2-\frac{d}{2}} \frac{\Gamma(n - \frac{d}{2})}{\Gamma(n)} f^{d-2n} \end{aligned} \quad (6.8)$$

The full calculation of this integral including the definition of the Γ function can be found in Appendix C. To regularize the UV divergences we set $d = 4 - 2\epsilon$ with $\epsilon > 0$. The most simple

case $n = 1$ yields

$$I_1(f^2) = -(4\pi Q^2)^\epsilon \Gamma(-1 + \epsilon) f^{2-2\epsilon} \xrightarrow{\epsilon \rightarrow 0} f^2 \left(\Delta + 1 + \ln \left(\frac{Q^2}{f^2} \right) \right) + \mathcal{O}(\epsilon) \quad , \quad (6.9)$$

where we have defined:

$$\Delta = \frac{1}{\epsilon} - \gamma_E + \ln(4\pi) \quad \text{with} \quad \gamma_E = - \int_0^\infty dt \ln t e^{-t} \approx 0.577 \quad (6.10)$$

Therein the Euler-Mascheroni constant γ_E is used. The scalar 1-point function A_0 is exactly given by $A_0(m^2) = I_1(m^2)$. Hence, the result is:

$$A_0(m^2) = \frac{(2\pi Q)^{4-d}}{i\pi^2} \int d^d k \frac{1}{k^2 - m^2} = m^2 \left[\Delta + 1 + \ln \left(\frac{Q^2}{m^2} \right) \right] \quad (6.11)$$

The UV divergence is contained in the parameter Δ together with two constant terms. Setting $\Delta = 0$ gives the finite parts of the integrals, which can be found in full detail in Appendix C. The discussion includes also the derivatives with respect to in- or outgoing momenta, since those are needed for the considered renormalization scheme in R_ξ -gauge. Next we need a reasonable description how to treat the UV divergent parts Δ of the Passarino-Veltman integrals.

6.1.3. Renormalization schemes

We have now parameterized the UV divergent parts by the use of the Passarino-Veltman notation. However, we are still left with the question how to interpret these divergences physically. Using our example of ϕ^4 -theory, which we introduced in Section 6.1.1, we want to discuss two renormalization schemes, namely the $\overline{\text{MS}}$ (DimReg) scheme and the on-shell scheme. The $\overline{\text{DR}}$ (DRED) scheme in supersymmetric models follows the same ansatz as the $\overline{\text{MS}}$ scheme. Suppose the parameters of the Lagrangian density are not the physical parameters, but bare parameters, which are related to the physical ones by a multiplicative renormalization constant in the form:

$$\phi_0 = Z^{\frac{1}{2}} \phi, \quad Z = 1 + \delta Z \quad (6.12)$$

$$m_0^2 = Z_m m^2, \quad Z_m = 1 + \delta Z_m \rightarrow m_0^2 = m^2 + \delta Z_m m^2 =: m^2 + \delta m^2 \quad (6.13)$$

$$\lambda_0 = Z_\lambda \lambda, \quad Z_\lambda = 1 + \delta Z_\lambda \quad (6.14)$$

Then we can rewrite the Lagrangian density in Equation (6.1) as follows:

$$\mathcal{L} = \frac{1}{2} Z (\partial_\mu \phi) (\partial^\mu \phi) - \frac{1}{2} Z Z_m m^2 \phi^2 - \frac{\lambda}{4!} Z_\lambda Z^2 \phi^4 \quad (6.15)$$

$$\begin{aligned} &= \frac{1}{2} (\partial_\mu \phi) (\partial^\mu \phi) - \frac{1}{2} m^2 \phi^2 - \frac{\lambda}{4!} \phi^4 \\ &\quad + \frac{1}{2} \delta Z (\partial_\mu \phi) (\partial^\mu \phi) - \frac{1}{2} (\delta Z_m + \delta Z) m^2 \phi^2 - \frac{\lambda}{4!} (\delta Z_\lambda + 2\delta Z) \phi^4 \\ &\quad + \mathcal{O}(\delta Z^2) \end{aligned} \quad (6.16)$$

Whereas the first three terms represent the physical Lagrangian, the second line of Equation (6.16) contains the counterterms, which can be interpreted as additional Feynman rules and allow to absorb divergent parts based on the considered renormalization scheme. Terms proportional to products of δZ are only important for higher-loop calculations. Thus, the Feyn-

man rules are:

$$\text{---} = \frac{i}{p^2 - m^2 + i\epsilon} \quad \text{and} \quad \text{---} \times \text{---} = i((p^2 - m^2)\delta Z - m^2\delta Z_m) \quad (6.17)$$

$$\begin{array}{c} \diagup \\ \bullet \\ \diagdown \end{array} = -i\lambda \quad \text{and} \quad \begin{array}{c} \diagup \\ \times \\ \diagdown \end{array} = -i(\delta Z_\lambda + 2\delta Z)\lambda \quad (6.18)$$

To discuss the relation between the divergent parts of the Passarino-Veltman integrals and the counterterms introduced by multiplicative renormalization, we consider the self-energy contribution and the scattering amplitude at one-loop level. The correction to the tree-level mass is given by:

$$-iM(p^2) = \text{---} \text{---} \text{---} + \text{---} \times \text{---} = \frac{\lambda}{2}I_1(m^2) + i((p^2 - m^2)\delta Z - \delta Z_m m^2)$$

It enters the propagator at one-loop level as follows:

$$\begin{aligned} \text{---} \text{---} \text{---} &= \text{---} + \text{---} \text{---} \text{---} + \text{---} \times \text{---} \\ &\sim \frac{i}{p^2 - m^2} + \frac{i}{p^2 - m^2} (-iM(p^2)) \frac{i}{p^2 - m^2} = \frac{i}{p^2 - m^2} \left(1 + \frac{M(p^2)}{p^2 - m^2}\right) \end{aligned} \quad (6.19)$$

The scattering amplitude at one-loop level can be written in the form

$$\begin{aligned} i\mathcal{M}(p_1 p_2 \rightarrow p_3 p_4) &= \begin{array}{c} \diagup \\ \bullet \\ \diagdown \end{array} + \begin{array}{c} \diagup \\ \bullet \\ \text{---} \\ \bullet \\ \diagdown \end{array} + \begin{array}{c} \diagup \\ \bullet \\ \text{---} \\ \bullet \\ \diagdown \end{array} + \begin{array}{c} \diagup \\ \bullet \\ \text{---} \\ \bullet \\ \text{---} \\ \bullet \\ \diagdown \end{array} + \begin{array}{c} \diagup \\ \times \\ \diagdown \end{array} \\ &= -i\lambda + (-i\lambda)^2 [iV(s) + iV(t) + iV(u)] - i(\delta Z_\lambda + 2\delta Z)\lambda \end{aligned} \quad (6.20)$$

with the Mandelstam variables $s = (p_1 + p_2)^2$, $t = (p_1 - p_3)^2$ and $u = (p_1 - p_4)^2$ and the integral

$$V(p^2) = \frac{i}{2} \int_0^1 dx I_2(m^2 - x(1-x)p^2) \quad . \quad (6.21)$$

The basic idea of renormalization is to absorb the divergences of $I_1(f^2)$ in the self-energy and those of $I_2(f^2)$ in the scattering amplitude into the renormalization constants δZ , δZ_m and δZ_λ . Since $I_1(m^2)$ is independent of p^2 we choose $\delta Z = 0$ in the following. However the absorption of divergent parts is not unique, since finite parts can always be shifted. Moreover we will see the role of the mass parameter Q , which originally was introduced to account for the correct mass dimensions. We address two common renormalization schemes, which impose renormalization conditions fixing the counterterms.

$\overline{\text{MS}}$ scheme

Using DimReg or DRED all integrals $I_n(f^2)$ can be split in the form

$$I_n(f^2) \propto A\Delta + B \quad \text{for} \quad \epsilon \rightarrow 0 \quad . \quad (6.22)$$

In the minimal subtraction scheme (MS) the renormalization constants are chosen such that they cancel the A_ϵ^1 -pole of the integrals, in case of the $\overline{\text{MS}}$ scheme they cancel $A\Delta$. For our example this implies in the $\overline{\text{MS}}$ scheme for the self-energy:

$$-iM(p^2) = \frac{\lambda}{2} I_1(m^2) - im^2 \delta Z_m \xrightarrow{\epsilon \rightarrow 0} i \frac{\lambda m^2}{32\pi^2} \left(\Delta + 1 - \log \left(\frac{m^2}{Q^2} \right) \right) - im^2 \delta Z_m \quad (6.23)$$

$$\implies \delta Z_m^{\overline{\text{MS}}} = \frac{\lambda}{32\pi^2} \Delta, \quad M(p^2) = -\frac{\lambda m^2}{32\pi^2} \left(1 - \log \left(\frac{m^2}{Q^2} \right) \right) \quad (6.24)$$

Obviously the mass correction $M(p^2)$ is UV finite, but dependent on the mass parameter Q . Doing the same procedure for the scattering amplitude yields

$$\delta Z_\lambda^{\overline{\text{MS}}} = \frac{3\lambda}{32\pi^2} \Delta \quad , \quad (6.25)$$

resulting in a finite scattering amplitude $i\mathcal{M}(p_1 p_2 \rightarrow p_3 p_4)$, which is still dependent on Q . Note that the counterterms are not dependent on the mass parameter Q , but only contain the UV divergent parts of the integrals.

On-shell scheme

In case of the on-shell scheme we want the mass and the scattering amplitude for a specific momentum to be physical quantities, so that they are not affected by one-loop corrections. Hence, the renormalization condition for the self-energy can be formulated as follows:

$$\text{---} \text{---} \text{---} \left|_{p^2=m^2} = \lim_{p^2 \rightarrow m^2} \frac{i}{p^2 - m^2} \left(1 + \frac{M(p^2)}{p^2 - m^2} \right) \stackrel{!}{=} \lim_{p^2 \rightarrow m^2} \frac{i}{p^2 - m^2} \quad (6.26)$$

A Taylor expansion of $M(p^2)$ according to

$$M(p^2) = M(m^2) + \frac{d^2}{dp^2} M(p^2) \Big|_{p^2=m^2} (p^2 - m^2) + \dots \quad (6.27)$$

results in the following conditions for $M(p^2)$:

$$M(p^2) \Big|_{p^2=m^2} = 0, \quad \frac{d^2}{dp^2} M(p^2) \Big|_{p^2=m^2} = 0 \quad (6.28)$$

For the scattering amplitude we demand:

$$i\mathcal{M}(p_1 p_2 \rightarrow p_3 p_4) \stackrel{!}{=} -i\lambda \quad \text{for} \quad s = 4m^2, \quad t = u = 0 \quad (6.29)$$

The second condition of Equation (6.28) is automatically fulfilled, whereas δZ_m^{OS} and $\delta Z_\lambda^{\text{OS}}$ can be fixed from the other conditions in Equations (6.28) and (6.29) to be:

$$\delta Z_m^{\text{OS}} = \frac{\lambda}{32\pi^2} \left(\Delta + 1 - \log \left(\frac{m^2}{Q^2} \right) \right) \quad (6.30)$$

$$\delta Z_\lambda^{\text{OS}} = \frac{\lambda}{32\pi^2} \left[3\Delta - \int_0^1 dx \log \left(\frac{m^2 - x(1-x)4m^2}{Q^2} \right) - 2 \log \left(\frac{m^2}{Q^2} \right) \right] \quad (6.31)$$

Whereas the renormalization constants are now dependent on Q , the mass correction $M(p^2) = 0$ vanishes for all p^2 and also the scattering amplitude is now independent of Q :

$$i\mathcal{M}(p_1p_2 \rightarrow p_3p_4) = -i\lambda - \frac{i\lambda^2}{32\pi^2} \int_0^1 dx \left[\log \left(\frac{m^2 - x(1-x)s}{m^2 - x(1-x)4m^2} \right) + \log \left(\frac{m^2 - x(1-x)t}{m^2} \right) + \log \left(\frac{m^2 - x(1-x)u}{m^2} \right) \right] \quad (6.32)$$

As demanded it yields $i\mathcal{M}(p_1p_2 \rightarrow p_3p_4) = -i\lambda$ for $s = 4m^2$ and $t = u = 0$.

Having pointed out the main differences between an on-shell scheme and the simple $\overline{\text{MS}}$ renormalization, we want to comment on some additional facts:

The reader might wonder about the existence of different renormalization schemes. However, it can be shown that results in n th order of perturbation theory differ only by parts of $(n + 1)$ th order in different renormalization schemes. Thus, calculating the full perturbation series leads to the same results independent of the choice of the renormalization procedure.

As we have seen the unphysical mass parameter Q is introduced as a result of dimensional regularization. Since it determines the mass scale of the renormalization procedure, it is usually called renormalization scale. In case of the $\overline{\text{MS}}$ scheme we showed that the final results are dependent on the renormalization scale, whereas in the on-shell scheme they are not. The same statements hold for the $\overline{\text{DR}}$ scheme (DRED) compared to the on-shell scheme in supersymmetric models. We didn't mention renormalization group equations yet, the reason being that in an on-shell scheme no dependence on Q is left. However we want to comment on this concept, which is based on [133]. When we define our theory to be valid at a certain renormalization scale Q , we can demand to have renormalized n -point functions $G^{(n)}$, which are independent of this scale. This concept results in the Callan-Symanzik equation [134], for which we refer to [1]. It includes masses, coupling constants and wave-function renormalizations being dependent on Q as well, such that the renormalized n -point function can be kept constant. In this sense the famous concept of running coupling constants has to be understood. However it is clear that a reference scale M , where the renormalization conditions were imposed, will always remain part of the result.

6.2. On-shell renormalization

In this section we work out the on-shell scheme for our purposes, namely for massive gauge bosons in R_ξ -gauge and neutralinos and charginos, which are mixed fermions. The latter case was first presented in our work [135] for the NMSSM and in [136] for BRpV and the $\mu\nu$ SSM with one right-handed neutrino superfield. Special emphasis is put on the gauge invariance of the masses and decay widths within the following discussion.

6.2.1. Renormalization of the gauge sector in R_ξ -gauge

We will first present the renormalization of a massive gauge boson in R_ξ -gauge, before discussing the renormalization of the gauge couplings and the Weinberg angle in accordance to [137].

Renormalization of a massive gauge boson

We introduced the R_ξ -gauge in Section 5.2, which will be used in the following discussion. We denoted the propagator of a massive gauge boson in this gauge as

$$iG_V^{\mu\nu}(k^2) = \frac{g^{\mu\nu}}{k^2 - m_V^2} - (1 - \xi_V) \frac{k^\mu k^\nu}{(k^2 - m_V^2)(k^2 - \xi_V m_V^2)} . \quad (6.33)$$

We call the inverse propagator at tree-level $i\Gamma_V^{\mu\nu}(k^2)$, which can be deduced according to

$$(iG_V^{\mu\nu}(k^2)) (i\Gamma_{V,\nu\rho}(k^2)) = \delta_\rho^\mu \quad \text{resulting in:} \quad (6.34)$$

$$i\Gamma_V^{\mu\nu}(k^2) = -ig^{\mu\nu}(k^2 - m_V^2) + i \left(1 - \frac{1}{\xi_V}\right) k^\mu k^\nu = -ig_T^{\mu\nu}(k^2 - m_V^2) + ig_L^{\mu\nu} \left(m_V^2 - \frac{k^2}{\xi_V}\right) \quad (6.35)$$

Therein we have used the transverse and longitudinal projectors:

$$g_T^{\mu\nu} = g^{\mu\nu} - \frac{k^\mu k^\nu}{k^2}, \quad g_L^{\mu\nu} = \frac{k^\mu k^\nu}{k^2} \quad (6.36)$$

Adding the one-loop corrections split in the transverse $\hat{\Sigma}_T^V(k^2)$ and longitudinal part $\hat{\Sigma}_L^V(k^2)$ the propagator reads

$$i\hat{\Gamma}_V^{\mu\nu}(k^2) = -ig_T^{\mu\nu}(k^2 - m_V^2) + ig_L^{\mu\nu} \left(m_V^2 - \frac{k^2}{\xi_V}\right) - ig_T^{\mu\nu} \hat{\Sigma}_T^V(k^2) - \frac{i}{\xi_V} g_L^{\mu\nu} \hat{\Sigma}_L^V(k^2) , \quad (6.37)$$

where the hat indicates renormalized one-loop contributions.

The generic Feynman diagrams contributing to $\hat{\Sigma}_T^V(k^2)$ and $\hat{\Sigma}_L^V(k^2)$ are depicted in Figure 6.2. The concrete formulas are not given within this thesis, since they are rather lengthy in R_ξ -gauge. However they can be taken from `CNNDecays`. Tadpole graphs are relevant for the scalar potential at one-loop level, but do not have to be included at this stage.

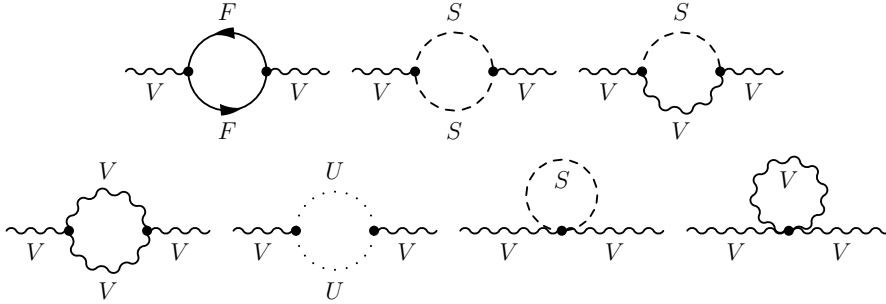


Figure 6.2.: Generic self-energy diagrams for vector bosons.

With this knowledge we can calculate the connection between the multiplicative renormalized parameters and the counterterms. First we split the bare Lagrangian density \mathcal{L}_0 in the physical Lagrangian density \mathcal{L}_{ph} and the corresponding counterterms \mathcal{L}_{ct} , the latter being parameterized by parameters C_1, \dots, C_4 . This procedure results in

$$-ig_T^{\mu\nu}(k^2 - m_{V0}^2)V_\mu^0 V_\nu^0 - ig_L^{\mu\nu} \left(m_{V0}^2 - \frac{k^2}{\xi_{V0}}\right) V_\mu^0 V_\nu^0 \quad (6.38)$$

$$\begin{aligned}
&= -ig_T^{\mu\nu}(k^2 - m_V^2)V_\mu V_\nu - ig_L^{\mu\nu}\left(m_V^2 - \frac{k^2}{\xi_V}\right)V_\mu V_\nu \\
&\quad - ig_T^{\mu\nu}(k^2 C_1 - C_2)V_\mu V_\nu - ig_L^{\mu\nu}(C_3 - k^2 C_4)V_\mu V_\nu \quad ,
\end{aligned}$$

where C_1, \dots, C_4 are functions of the following three multiplicative renormalization constants, which connect the bare and the physical parameters in the following form:

$$\begin{aligned}
m_{V0}^2 &\rightarrow Z_m m_V^2 = (1 + \delta Z_m)m_V^2 = m_V^2 + \delta m_V^2 & \text{with} & \quad \delta m_V^2 = m_V^2 \delta Z_m \\
V_\mu^0 &\rightarrow Z_V V_\mu = (1 + \frac{1}{2}\delta Z_V)V_\mu \\
\xi_{V0} &\rightarrow Z_{\xi_V}^{-1} \xi_V = (1 + \delta Z_{\xi_V})^{-1} \xi_V
\end{aligned} \tag{6.39}$$

Alternatively the multiplicative renormalization of the gauge fixing parameter could be done by $(1 + \delta Z_{\xi_V})\xi_V$, which corresponds to a simple replacement $\delta Z_{\xi_V} \leftrightarrow -\delta Z_{\xi_V}$. Inserting Equation (6.39) in the left-hand side of Equation (6.38) and expanding the result up to the first order in δZ , we can compare this expansion with the right-hand side of Equation (6.38). Thus, the parameters C_1, \dots, C_4 of the counterterms can be identified:

$$C_1 = \delta Z_V, \quad C_2 = \delta m_V^2 + m_V^2 \delta Z_V = C_3, \quad C_4 = \frac{1}{\xi_V}(\delta Z_{\xi_V} + \delta Z_V) \tag{6.40}$$

Therefore, we write the renormalized one-loop corrections as a function of the unrenormalized ones and the counterterms, now being functions of the multiplicative renormalization constants:

$$i\hat{\Gamma}^{V,\mu\nu}(k^2) = -ig_T^{\mu\nu}(k^2 - m_V^2) + ig_L^{\mu\nu}\left(m_V^2 - \frac{k^2}{\xi_V}\right) \tag{6.41}$$

$$\begin{aligned}
&- ig_T^{\mu\nu} \Sigma_T^V(k^2) - ig_T^{\mu\nu}(k^2 \delta Z_V - m_V^2 \delta Z_V - \delta m_V^2) \\
&- \frac{i}{\xi_V} g_L^{\mu\nu} \Sigma_L^V(k^2) - ig_L^{\mu\nu}\left(m_V^2 \delta Z_V + \delta m_V^2 - \frac{k^2}{\xi_V}(\delta Z_{\xi_V} + \delta Z_V)\right) \\
\implies \hat{\Sigma}_T^V(k^2) &= \Sigma_T^V(k^2) + k^2 \delta Z_V - m_V^2 \delta Z_V - \delta m_V^2 & (6.42) \\
\implies \hat{\Sigma}_L^V(k^2) &= \Sigma_L^V(k^2) + \xi_V m_V^2 \delta Z_V + \xi_V \delta m_V^2 - k^2(\delta Z_{\xi_V} + \delta Z_V) & (6.43)
\end{aligned}$$

Renormalization conditions

The renormalized propagator $i\hat{G}_V^{\mu\nu}$, which can be calculated from the renormalized two point function $i\hat{\Gamma}_V^{\mu\nu}$ in accordance to Equation (6.34), should have its pole at the physical, experimental squared mass m_V^2 . Therefore, an on-shell renormalization condition is imposed, namely the real part of the one-loop correction should vanish for $k^2 = m_V^2$:

$$\text{Re}\hat{\Gamma}_V^{\mu\nu}(k^2)\epsilon_\nu(k^2)\Big|_{k^2=m_V^2} = 0 \tag{6.44}$$

Moreover in order to get appropriate probabilities after a multiplicative renormalization of the fields the condition of having the residua of the renormalized propagators equal to 1 is demanded, precisely

$$\lim_{k^2 \rightarrow m_V^2} \frac{1}{-i(k^2 - m_V^2)} \text{Re}i\hat{\Gamma}_V^{\mu\nu}(k^2)\epsilon_\nu(k^2) = \epsilon^\mu(k^2) \quad . \tag{6.45}$$

Please note that taking the real part Re does only imply the real part of the one-loop corrections, but not the one of possible complex mixing matrices appearing in couplings or complex

chosen parameters in general. The two conditions in Equations (6.44) and (6.45) can be easily transformed to

$$\text{Re}\hat{\Sigma}_T^V(m_V^2) = 0 \quad (6.46)$$

$$\text{Re}\hat{\Sigma}_T^V(m_V^2) := \left. \frac{\partial \text{Re}\hat{\Sigma}_T^V(k^2)}{\partial k^2} \right|_{k^2=m_V^2} = 0 \quad , \quad (6.47)$$

where a simple expansion in k^2 around m_V^2 was used:

$$\text{Re}\hat{\Sigma}_T^V(k^2) = \text{Re}\hat{\Sigma}_T^V(m_V^2) + \left. \frac{\partial \text{Re}\hat{\Sigma}_T^V(k^2)}{\partial k^2} \right|_{k^2=m_V^2} (k^2 - m_V^2) \quad (6.48)$$

These on-shell renormalization conditions can now be used to derive δm_V^2 and δZ_V as a function of the unrenormalized one-loop contributions from Equation (6.42), resulting in:

$$\delta m_V^2 = \text{Re}\Sigma_T^V(m_V^2), \quad \delta Z_V = -\text{Re}\Sigma_T^V(m_V^2) \quad (6.49)$$

The Z_{ξ_V} s are fixed by the conditions that propagators mixing the Goldstone bosons with the vector bosons vanish [138] and will not be discussed further.

Renormalization of gauge couplings and the Weinberg angle

Having discussed the renormalization of a heavy gauge boson in general, we can use this knowledge for the renormalization of the Weinberg angle. For the Weinberg angle $\cos\theta_W$, which we defined as $m_W = m_Z \cos\theta_W$, yields:

$$\cos\theta_W \rightarrow \cos\theta_W + \delta \cos\theta_W \quad (6.50)$$

$$\delta \cos\theta_W = \frac{1}{2} \cos\theta_W \left(\frac{\delta m_W^2}{m_W^2} - \frac{\delta m_Z^2}{m_Z^2} \right) \quad (6.51)$$

For completeness we add the relations:

$$\frac{\delta \cos\theta_W}{\cos\theta_W} = \frac{\delta m_W}{m_W} - \frac{\delta m_Z}{m_Z} = -\tan^2\theta_W \frac{\delta \sin\theta_W}{\sin\theta_W} = \left(1 - \frac{m_W^2}{m_Z^2} \right) \frac{\delta \sin\theta_W}{\sin\theta_W} \quad (6.52)$$

The renormalization of the electric charge e is more tedious. It is based on the $ff\gamma$ -vertex for an on-shell fermion f in the Thomson limit in accordance to [137]. Using the following multiplicative renormalization constant

$$e \rightarrow \delta Z_e^{(0)} e = (1 + \delta Z_e^{(0)}) e \quad (6.53)$$

results in

$$\delta Z_e^{(0)} = \frac{1}{2} \Sigma_T^{\gamma\gamma}(0) - \frac{\tan\theta_W}{m_Z^2} \Sigma_T^{Z\gamma}(0) \quad , \quad (6.54)$$

so that we get the relation $e(0) = \sqrt{4\pi\alpha(0)}$ between the renormalized charge and the fine structure constant in the Thomson limit. Whereas we use $\alpha(0)$ for our tree-level calculations, the choice $\alpha(m_Z) = \alpha_{EM}$ is more convenient for the higher-order results. Necessarily we have to account for the shift $\Delta\alpha$ between $Q = 0$ and $Q = m_Z$, which we do in accordance to [139],

resulting in

$$\delta Z_e^{(m_Z)} = \delta Z_e^{(0)} - \frac{\Delta\alpha}{2} = \quad (6.55)$$

$$= \frac{1}{2}\Sigma_{T,\text{all}}^{\prime\gamma\gamma}(0) - \frac{1}{2}\Sigma_{T,\text{light f}}^{\prime\gamma\gamma}(0) + \frac{1}{2m_Z^2}\text{Re}\Sigma_{T,\text{light f}}^{\gamma\gamma}(m_Z^2) - \frac{\tan\theta_W}{m_Z^2}\Sigma_T^{Z\gamma}(0) \quad . \quad (6.56)$$

The equation is based on the relation

$$\left. \frac{\partial}{\partial k^2}\Sigma_{T,\text{light f}}^{\gamma\gamma}(0) \right|_{k^2=0} = \Delta\alpha + \frac{1}{m_Z^2}\text{Re}\Sigma_{T,\text{light f}}^{\gamma\gamma}(m_Z^2) \quad , \quad (6.57)$$

where ‘‘light f’’ denotes the light fermions in the loops, meaning leptons and the light quarks except from the top quark. Similarly in case of ‘‘all’’ we insert all particle combinations in the loops. The correction $\Delta\alpha$ can be split into a leptonic part $\Delta\alpha_{\text{leptonic}} = 0.031497687$ calculated to 3-loop order [140] and a hadronic part $\Delta\alpha_{\text{hadronic}} = 0.02755 \pm 0.0023$ [141], which is determined using a dispersion relation. However the usage of Equation (6.56) avoids the need of those calculated or measured values for our calculation. For the gauge coupling we introduce the following multiplicative renormalization constant

$$g \rightarrow \delta Z_g g = (1 + \delta Z_g)g = g + \delta g \quad (6.58)$$

which can be calculated by:

$$\delta g = \left(\delta Z_e^{(m_Z)} - \frac{\delta \sin\theta_W}{\sin\theta_W} \right) g \quad (6.59)$$

All these formulas imply that we do not only need the self-energy corrections to the W - and Z -boson and the photon, but also the ones mixing the Z boson with the photon, which can be calculated similarly. Due to the infrared divergences, we will calculate with a photon mass, so that also the photon can be considered to be a massive gauge boson.

6.2.2. Renormalization of Dirac fermions with mixing

In this section we will discuss the renormalization of Dirac fermions with mixing to apply them to neutralinos and charginos later. Starting point is the Lagrangian density

$$\mathcal{L} = \delta_{ij}\bar{f}_j(i\partial_\mu\gamma^\mu - m_{f,i})f_i \quad (6.60)$$

of the free fermion f_i in Dirac notation. The renormalized one particle irreducible two point functions for mixing fermions yield

$$\begin{array}{c} \text{---} \bullet \text{---} \\ \text{---} \bullet \text{---} \end{array} \equiv i\hat{\Gamma}_{ij}^f(p) \quad , \quad (6.61)$$

where the hat indicates that the considered quantity is already renormalized. This implies that the Feynman graph above not only includes the one-loop corrections, but also the counterterms and moreover the tree-level propagator. It enters the Lagrangian density in the form $\mathcal{L} = \bar{u}_i(p)\hat{\Gamma}_{ij}^f(p)u_j(p)$ and inversion of $i\hat{\Gamma}_{ij}^f$ results in the physical propagator. The full form can be

written as

$$i\hat{\Gamma}_{ij}^f(p) = i\delta_{ij}(\not{p} - m_{fi}) + i \left[\not{p} \left(P_L \hat{\Sigma}_{ij}^{fL}(p^2) + P_R \hat{\Sigma}_{ij}^{fR}(p^2) \right) + P_L \hat{\Sigma}_{ij}^{fSL}(p^2) + P_R \hat{\Sigma}_{ij}^{fSR}(p^2) \right] . \quad (6.62)$$

Similar to the case with a massive gauge boson the connection between the multiplicative renormalized parameters and the counterterms are deduced. Therefore, $\mathcal{L}_0 = \mathcal{L}_{ph} + \mathcal{L}_{ct}$ is imposed, resulting in

$$i\bar{f}_{i0}\delta_{ij}(\not{p} - m_{fj0})f_{j0} = i\bar{f}_i\delta_{ij}(\not{p} - m_{fj})f_j + i\bar{f}_i \left(C_{ij}^L P_L \not{p} + C_{ij}^R P_R \not{p} - C_{ij}^- P_L - C_{ij}^+ P_R \right) f_j , \quad (6.63)$$

where $C_{ij}^L, C_{ij}^R, C_{ij}^-$ and C_{ij}^+ parameterize the counterterms and can be identified with the following multiplicative renormalization constants:

$$f_{i0}^L \rightarrow (\delta_{ij} + \frac{1}{2}\delta Z_{ij}^L) f_i^L, \quad f_{i0}^R \rightarrow (\delta_{ij} + \frac{1}{2}\delta Z_{ij}^R) f_i^R \quad (6.64)$$

$$m_{fi0} \rightarrow m_{fi} + \delta m_{fi} \quad (6.65)$$

Inserting Equation (6.64) in the left-hand side of Equation (6.63) and expanding the result up to the first order in δZ , we obtain

$$i\bar{f}_{i0}\delta_{ij}(\not{p} - m_{fj0})f_{j0} \approx i\bar{f}_i\delta_{ij}(\not{p} - m_{fj})f_j - \bar{f}_i\delta_{ij}\delta m_{fj}f_j + i \left(\bar{f}_i^L \frac{1}{2}\delta Z_{ij}^{L\dagger} + \bar{f}_i^R \frac{1}{2}\delta Z_{ij}^{R\dagger} \right) (\not{p} - m_{fj})f_j + i\bar{f}_i(\not{p} - m_{fi}) \left(\frac{1}{2}\delta Z_{ij}^L f_j^L + \frac{1}{2}\delta Z_{ij}^R f_j^R \right) \quad (6.66)$$

where a summation over the indices i and j is implied. Using $\bar{f}_i = f_i^\dagger \gamma^0$ yields for example

$$\bar{f}_i C_{ij}^L \not{p} f_j^L = \bar{f}_i C_{ij}^L \not{p} P_L f_j = \bar{f}_i P_R C_{ij}^L \not{p} f_j = \bar{f}_i^L C_{ij}^L \not{p} f_j, \quad \bar{f}_i C_{ij}^- f_j^L = \bar{f}_i^R C_{ij}^- f_j \quad (6.67)$$

allowing to identify the counterterms on the right-hand side of Equation (6.63)

$$C_{ij}^L = \frac{1}{2}\delta Z_{ij}^L + \frac{1}{2}\delta Z_{ij}^{L\dagger}, \quad C_{ij}^- = \delta_{ij}\delta m_{fi} + m_{fi}\frac{1}{2}\delta Z_{ij}^L + m_{fj}\frac{1}{2}\delta Z_{ij}^{R\dagger} \quad (6.68)$$

$$C_{ij}^R = \frac{1}{2}\delta Z_{ij}^R + \frac{1}{2}\delta Z_{ij}^{R\dagger}, \quad C_{ij}^+ = \delta_{ij}\delta m_{fi} + m_{fi}\frac{1}{2}\delta Z_{ij}^R + m_{fj}\frac{1}{2}\delta Z_{ij}^{L\dagger} \quad (6.69)$$

without summation over i and j . Therefore, we can write the renormalized one-loop corrections as a function of the unrenormalized ones and the counterterms:

$$\hat{\Sigma}_{ij}^{fL}(p^2) = \Sigma_{ij}^{fL}(p^2) + \frac{1}{2} \left(\delta Z_{ij}^L + \delta Z_{ij}^{L\dagger} \right) \quad (6.70)$$

$$\hat{\Sigma}_{ij}^{fR}(p^2) = \Sigma_{ij}^{fR}(p^2) + \frac{1}{2} \left(\delta Z_{ij}^R + \delta Z_{ij}^{R\dagger} \right) \quad (6.71)$$

$$\hat{\Sigma}_{ij}^{fSL}(p^2) = \Sigma_{ij}^{fSL}(p^2) - \frac{1}{2} \left(m_{fi}\delta Z_{ij}^L + m_{fj}\delta Z_{ij}^{R\dagger} \right) - \delta_{ij}\delta m_{fi} \quad (6.72)$$

$$\hat{\Sigma}_{ij}^{fSR}(p^2) = \Sigma_{ij}^{fSR}(p^2) - \frac{1}{2} \left(m_{fi}\delta Z_{ij}^R + m_{fj}\delta Z_{ij}^{L\dagger} \right) - \delta_{ij}\delta m_{fi} \quad (6.73)$$

Renormalization conditions

The on-shell renormalization scheme sets conditions to $i\hat{\Gamma}_{ij}^f(p)$, since on the one hand the residues of the renormalized propagators should be equal to 1 and on the other hand the resulting propagators should have poles at the physical masses of the described particles. Therefore, we demand:

$$\bar{u}_i(p)\text{Re}\hat{\Gamma}_{ij}^f(p)\Big|_{p^2=m_{f_i}^2} = 0, \quad \lim_{p^2 \rightarrow m_{f_i}^2} \bar{u}_i(p)\text{Re}\hat{\Gamma}_{ii}^f(p) \frac{\not{p} + m_{f_i}}{p^2 - m_{f_i}^2} = \bar{u}_i(p) \quad (6.74)$$

$$\text{Re}\hat{\Gamma}_{ij}^f(p)u_j(p)\Big|_{p^2=m_{f_j}^2} = 0, \quad \lim_{p^2 \rightarrow m_{f_i}^2} \frac{\not{p} + m_{f_i}}{p^2 - m_{f_i}^2} \text{Re}\hat{\Gamma}_{ii}^f(p)u_i(p) = u_i(p) \quad (6.75)$$

Imposing these conditions guarantees to have no real contribution to the diagonal entries of the mass matrices by $i\hat{\Gamma}_{ij}^f(p)$ on the mass shell and therefore can be understood as on-shell renormalization scheme. The nondiagonal contributions vanish completely on-shell. The first two conditions in Equations (6.74) and (6.75) result in

$$\bar{u}_i(p) \left[P_L \left(m_{f_i} \text{Re}\hat{\Sigma}_{ij}^{fL}(m_{f_i}^2) + \text{Re}\hat{\Sigma}_{ij}^{fSL}(m_{f_i}^2) \right) + P_R \left(m_{f_i} \text{Re}\hat{\Sigma}_{ij}^{fR}(m_{f_i}^2) + \text{Re}\hat{\Sigma}_{ij}^{fSR}(m_{f_i}^2) \right) \right] = 0 \quad (6.76)$$

$$\left[P_L \left(m_{f_j} \text{Re}\hat{\Sigma}_{ij}^{fR}(m_{f_j}^2) + \text{Re}\hat{\Sigma}_{ij}^{fSL}(m_{f_j}^2) \right) + P_R \left(m_{f_j} \text{Re}\hat{\Sigma}_{ij}^{fL}(m_{f_j}^2) + \text{Re}\hat{\Sigma}_{ij}^{fSR}(m_{f_j}^2) \right) \right] u_j(p) = 0 \quad (6.77)$$

where $(\not{p} - m_{f_i})u_i(p) = \bar{u}_i(p)(\not{p} - m_{f_i}) = 0$ was used. Separated into left- and right-handed parts we get:

$$m_{f_i} \text{Re}\hat{\Sigma}_{ij}^{fL}(m_{f_i}^2) + \text{Re}\hat{\Sigma}_{ij}^{fSL}(m_{f_i}^2) = 0 \quad (6.78)$$

$$m_{f_i} \text{Re}\hat{\Sigma}_{ij}^{fR}(m_{f_i}^2) + \text{Re}\hat{\Sigma}_{ij}^{fSR}(m_{f_i}^2) = 0 \quad (6.79)$$

$$m_{f_j} \text{Re}\hat{\Sigma}_{ij}^{fR}(m_{f_j}^2) + \text{Re}\hat{\Sigma}_{ij}^{fSL}(m_{f_j}^2) = 0 \quad (6.80)$$

$$m_{f_j} \text{Re}\hat{\Sigma}_{ij}^{fL}(m_{f_j}^2) + \text{Re}\hat{\Sigma}_{ij}^{fSR}(m_{f_j}^2) = 0 \quad (6.81)$$

Please note that there is no summation over i and j in the above four equations. If we use Equations (6.78) and (6.79) in combination with Equations (6.70)–(6.73) in the case $i = j$ and add up the two equations, the system can be solved for δm_{f_i} .

$$\delta m_{f_i} = m_{f_i} \text{Re}\Sigma_{ii}^{fL}(m_{f_i}^2) + \text{Re}\Sigma_{ii}^{fSL}(m_{f_i}^2) + \frac{1}{2} m_{f_i} \left(\delta Z_{ii}^{L\dagger} - \delta Z_{ii}^{R\dagger} \right) \quad (6.82)$$

$$\delta m_{f_i} = m_{f_i} \text{Re}\Sigma_{ii}^{fR}(m_{f_i}^2) + \text{Re}\Sigma_{ii}^{fSR}(m_{f_i}^2) + \frac{1}{2} m_{f_i} \left(\delta Z_{ii}^{R\dagger} - \delta Z_{ii}^{L\dagger} \right) \quad (6.83)$$

$$\implies \delta m_{f_i} = \frac{1}{2} \left[m_{f_i} \text{Re}\Sigma_{ii}^{fL}(m_{f_i}^2) + m_{f_i} \text{Re}\Sigma_{ii}^{fR}(m_{f_i}^2) + \text{Re}\Sigma_{ii}^{fSL}(m_{f_i}^2) + \text{Re}\Sigma_{ii}^{fSR}(m_{f_i}^2) \right]$$

The same result can be obtained by using Equations (6.80) and (6.81) in combination with Equations (6.70)–(6.73). Moreover in the case $i \neq j$ the conditions in Equations (6.78)–(6.81) can be used to fix the nondiagonal elements of the field renormalizations δZ_{ij}^L and δZ_{ij}^R . From Equations (6.80) and (6.81) together with Equation (6.64) follows for $i \neq j$:

$$m_{f_j} \text{Re}\Sigma_{ij}^{fR}(m_{f_j}^2) + \text{Re}\Sigma_{ij}^{fSL}(m_{f_j}^2) + \frac{1}{2} (m_{f_j} \delta Z_{ij}^R - m_{f_i} \delta Z_{ij}^L) = 0 \quad (6.84)$$

$$m_{f_j} \text{Re}\Sigma_{ij}^{fL}(m_{f_j}^2) + \text{Re}\Sigma_{ij}^{fSR}(m_{f_j}^2) + \frac{1}{2} (m_{f_j} \delta Z_{ij}^L - m_{f_i} \delta Z_{ij}^R) = 0 \quad (6.85)$$

From Equations (6.84) and (6.85) we can deduce:

$$\delta Z_{ij}^L = \frac{2}{m_{f_i}^2 - m_{f_j}^2} \left[m_{f_j}^2 \text{Re} \hat{\Sigma}_{ij}^{fL}(m_{f_j}^2) + m_{f_i} m_{f_j} \text{Re} \hat{\Sigma}_{ij}^{fR}(m_{f_j}^2) \right. \\ \left. + m_{f_i} \text{Re} \hat{\Sigma}_{ij}^{fSL}(m_{f_j}^2) + m_{f_j} \text{Re} \hat{\Sigma}_{ij}^{fSR}(m_{f_j}^2) \right] \quad (6.86)$$

$$\delta Z_{ij}^R = \frac{2}{m_{f_i}^2 - m_{f_j}^2} \left[m_{f_i} m_{f_j} \text{Re} \hat{\Sigma}_{ij}^{fL}(m_{f_j}^2) + m_{f_j}^2 \text{Re} \hat{\Sigma}_{ij}^{fR}(m_{f_j}^2) \right. \\ \left. + m_{f_j} \text{Re} \hat{\Sigma}_{ij}^{fSL}(m_{f_j}^2) + m_{f_i} \text{Re} \hat{\Sigma}_{ij}^{fSR}(m_{f_j}^2) \right] \quad (6.87)$$

Starting with Equations (6.78) and (6.79) results in formulas for $\delta Z_{ij}^{L\dagger}$ and $\delta Z_{ij}^{R\dagger}$, which are in agreement with Equations (6.86) and (6.87), if we take into account the hermiticity of the Lagrangian. It implies the following symmetries for the unrenormalized self-energies:

$$\Sigma_{ij}^{fL}(p^2) = \hat{\Sigma}_{ij}^{fL\dagger}(p^2), \quad \Sigma_{ij}^{fR}(p^2) = \hat{\Sigma}_{ij}^{fR\dagger}(p^2), \\ \Sigma_{ij}^{fSL}(p^2) = \hat{\Sigma}_{ij}^{fSR\dagger}(p^2) \quad (6.88)$$

Therefore, δZ_{ij}^L or δZ_{ij}^R can be obtained from $\delta Z_{ij}^{L\dagger}$ or $\delta Z_{ij}^{R\dagger}$ by the replacements $m_i \leftrightarrow m_j$ and $\Sigma_{ij}^{fSL} \leftrightarrow \Sigma_{ij}^{fSR}$. These results are also in agreement with [142, 143, 144]. More tedious is the derivation of the diagonal entries δZ_{ii}^L and δZ_{ii}^R from Equation (6.75):

$$\lim_{p^2 \rightarrow m_{f_i}^2} \frac{\not{p} + m_{f_i}}{p^2 - m_{f_i}^2} \left[\not{p} P_L \text{Re} \hat{\Sigma}_{ii}^{fL}(p^2) + \not{p} P_R \text{Re} \hat{\Sigma}_{ii}^{fR}(p^2) \right. \\ \left. + P_L \text{Re} \hat{\Sigma}_{ii}^{fSL}(p^2) + P_R \text{Re} \hat{\Sigma}_{ii}^{fSR}(p^2) \right] u_i(p) = 0 \quad (6.89)$$

Taking into account $\not{p}\not{p} = p^2$, $\not{p}u_i(p) = m_{f_i}u_i(p)$ and $\not{p}P_L = P_R\not{p}$ this can be easily transformed:

$$\lim_{p^2 \rightarrow m_{f_i}^2} \frac{1}{p^2 - m_{f_i}^2} \left[(p^2 P_L + m_{f_i}^2 P_R) \text{Re} \hat{\Sigma}_{ii}^{fL}(p^2) + (p^2 P_R + m_{f_i}^2 P_L) \text{Re} \hat{\Sigma}_{ii}^{fR}(p^2) \right. \\ \left. + m_{f_i} \left(P_L \text{Re} \hat{\Sigma}_{ii}^{fSL}(p^2) + P_R \text{Re} \hat{\Sigma}_{ii}^{fSL}(p^2) \right. \right. \\ \left. \left. + P_L \text{Re} \hat{\Sigma}_{ii}^{fSR}(p^2) + P_R \text{Re} \hat{\Sigma}_{ii}^{fSR}(p^2) \right) \right] u_i(p) = 0 \quad (6.90)$$

Separating the left-handed and right-handed parts two conditions remain:

$$\lim_{p^2 \rightarrow m_{f_i}^2} \frac{1}{p^2 - m_{f_i}^2} \left[p^2 \text{Re} \hat{\Sigma}_{ii}^{fL}(p^2) + m_{f_i}^2 \text{Re} \hat{\Sigma}_{ii}^{fR}(p^2) \right. \\ \left. + m_{f_i} \left(\text{Re} \hat{\Sigma}_{ii}^{fSL}(p^2) + \text{Re} \hat{\Sigma}_{ii}^{fSR}(p^2) \right) \right] = 0 \quad (6.91)$$

$$\lim_{p^2 \rightarrow m_{f_i}^2} \frac{1}{p^2 - m_{f_i}^2} \left[m_{f_i}^2 \text{Re} \hat{\Sigma}_{ii}^{fL}(p^2) + p^2 \text{Re} \hat{\Sigma}_{ii}^{fR}(p^2) \right. \\ \left. + m_{f_i} \left(\text{Re} \hat{\Sigma}_{ii}^{fSL}(p^2) + \text{Re} \hat{\Sigma}_{ii}^{fSR}(p^2) \right) \right] = 0 \quad (6.92)$$

Similarly to the case of the massive gauge boson the nominators of the two conditions are expanded around $p^2 = m_{f_i}^2$ using the product rule. The constant terms cancel due to Equa-

tions (6.78)–(6.81) and we are left with the first order in p^2 coming with $(p^2 - m_{f_i}^2)$, which cancels the corresponding denominator:

$$\begin{aligned} & \hat{\Sigma}_{ii}^{fL}(m_{f_i}^2) + m_{f_i}^2 \left(\text{Re} \hat{\Sigma}'_{ii}{}^{fL}(m_{f_i}^2) + \text{Re} \hat{\Sigma}'_{ii}{}^{fR}(m_{f_i}^2) \right) \\ & + m_{f_i} \left(\text{Re} \hat{\Sigma}'_{ii}{}^{fSL}(m_{f_i}^2) + \text{Re} \hat{\Sigma}'_{ii}{}^{fSR}(m_{f_i}^2) \right) = 0 \end{aligned} \quad (6.93)$$

$$\begin{aligned} & \hat{\Sigma}_{ii}^{fR}(m_{f_i}^2) + m_{f_i}^2 \left(\text{Re} \hat{\Sigma}'_{ii}{}^{fL}(m_{f_i}^2) + \text{Re} \hat{\Sigma}'_{ii}{}^{fR}(m_{f_i}^2) \right) \\ & + m_{f_i} \left(\text{Re} \hat{\Sigma}'_{ii}{}^{fSL}(m_{f_i}^2) + \text{Re} \hat{\Sigma}'_{ii}{}^{fSR}(m_{f_i}^2) \right) = 0 \end{aligned} \quad (6.94)$$

with abbreviations like

$$\text{Re} \hat{\Sigma}'_{ij}{}^{fL}(m_{f_i}^2) := \left. \frac{\partial \text{Re} \hat{\Sigma}_{ij}{}^{fL}(p^2)}{\partial p^2} \right|_{p^2=m_{f_i}^2}. \quad (6.95)$$

Inserting Equations (6.70)–(6.73) in Equations (6.93) and (6.94) finally allows to calculate the diagonal entries of the field renormalization constants δZ_{ii}^L and δZ_{ii}^R :

$$\begin{aligned} \delta Z_{ii}^{fL} = & -\text{Re} \left[\Sigma_{ii}^{fL}(m_{f_i}^2) + m_{f_i}^2 \left(\Sigma'_{ii}{}^{fL}(m_{f_i}^2) + \Sigma'_{ii}{}^{fR}(m_{f_i}^2) \right) \right. \\ & \left. + m_{f_i} \left(\Sigma'_{ii}{}^{fSL}(m_{f_i}^2) + \Sigma'_{ii}{}^{fSR}(m_{f_i}^2) \right) \right] \end{aligned} \quad (6.96)$$

$$\begin{aligned} \delta Z_{ii}^{fR} = & -\text{Re} \left[\Sigma_{ii}^{fR}(m_{f_i}^2) + m_{f_i}^2 \left(\Sigma'_{ii}{}^{fL}(m_{f_i}^2) + \Sigma'_{ii}{}^{fR}(m_{f_i}^2) \right) \right. \\ & \left. + m_{f_i} \left(\Sigma'_{ii}{}^{fSL}(m_{f_i}^2) + \Sigma'_{ii}{}^{fSR}(m_{f_i}^2) \right) \right] \end{aligned} \quad (6.97)$$

Specification to neutralinos and charginos

In this section the case of neutralinos and charginos is worked out in more detail. The Feynman diagrams being relevant for the calculation of the one-loop self-energies are depicted in Figure 6.3. Again the formulas can be taken from `CNNDecays` and are not presented within this thesis.

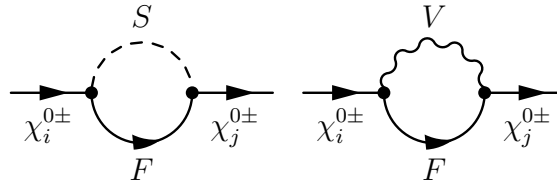


Figure 6.3.: Generic self-energy diagrams for neutralinos and charginos.

The tree-level mass matrices and their diagonalization were already presented in Section 5.3, where we have also shown the relations between the Weyl spinors ψ or F in gauge and mass eigenstates and the Dirac spinors $\tilde{\chi}$. Since the mass eigenstates $\tilde{\chi}_i^+$ and $\tilde{\chi}_i^-$ describe the same particle content, the renormalization constants defined by

$$\tilde{\chi}_i^0 \rightarrow \left(\delta_{ij} + \frac{1}{2} \delta Z_{ij}^{0L} P_L + \frac{1}{2} \delta Z_{ij}^{0R} P_R \right) \tilde{\chi}_j^0 \quad (6.98)$$

$$\tilde{\chi}_i^+ \rightarrow \left(\delta_{ij} + \frac{1}{2} \delta Z_{ij}^{+L} P_L + \frac{1}{2} \delta Z_{ij}^{+R} P_R \right) \tilde{\chi}_j^+ \quad (6.99)$$

$$\tilde{\chi}_i^- \rightarrow \left(\delta_{ij} + \frac{1}{2} \delta Z_{ij}^{-L} P_L + \frac{1}{2} \delta Z_{ij}^{-R} P_R \right) \tilde{\chi}_j^- \quad (6.100)$$

are connected in the following way:

$$\delta Z_{ij}^{0L} = \delta Z_{ij}^{0R*}, \quad \delta Z_{ij}^{+L} = \delta Z_{ij}^{-R*}, \quad \delta Z_{ij}^{-L} = \delta Z_{ij}^{+R*} \quad (6.101)$$

The combination of the mixing on tree-level with the nondiagonal field renormalization constants gives antihermitian parts, which are canceled by introducing counterterms for the mixing matrices defined in Equation (5.98). They read as follows [145]:

$$\delta \mathcal{N}_{ij} = \frac{1}{4} (\delta Z_{ik}^{0L} - \delta Z_{ki}^{0R}) \mathcal{N}_{kj} \quad (6.102)$$

$$\delta U_{ij} = \frac{1}{4} (\delta Z_{ik}^{+R*} - \delta Z_{ki}^{+R}) U_{kj}, \quad \delta V_{ij} = \frac{1}{4} (\delta Z_{ik}^{+L} - \delta Z_{ki}^{+L*}) V_{kj} \quad (6.103)$$

Inserting these additional corrections results in

$$\begin{aligned} \begin{pmatrix} \psi_k^0 \\ (\psi_k^0)^\dagger \end{pmatrix} &= \sum_{i,j} [(\mathcal{N}_{jk}^* + \delta \mathcal{N}_{jk}^* + \frac{1}{2} \mathcal{N}_{ik}^* \delta Z_{ij}^{0L}) P_L + (\mathcal{N}_{jk} + \delta \mathcal{N}_{jk} + \frac{1}{2} \mathcal{N}_{ik} \delta Z_{ij}^{0R}) P_R] \tilde{\chi}_i^0 \quad (6.104) \\ &= \sum_{i,j} [(\mathcal{N}_{jk}^* + \frac{1}{4} (\delta Z_{ij}^{0L} + \delta Z_{ij}^{0L*}) \mathcal{N}_{ik}^*) P_L + (\mathcal{N}_{jk} + \frac{1}{4} (\delta Z_{ij}^{0R} + \delta Z_{ij}^{0R*}) \mathcal{N}_{ik}) P_R] \tilde{\chi}_i^0 \end{aligned}$$

$$\begin{aligned} \begin{pmatrix} \psi_k^+ \\ (\psi_k^-)^\dagger \end{pmatrix} &= \sum_{i,j} [(V_{jk}^* + \delta V_{jk}^* + \frac{1}{2} V_{ik}^* \delta Z_{ij}^{+L}) P_L + (U_{jk} + \delta U_{jk} + \frac{1}{2} U_{ik} \delta Z_{ij}^{+R}) P_R] \tilde{\chi}_i^+ \quad (6.105) \\ &= \sum_{i,j} [(V_{jk}^* + \frac{1}{4} (\delta Z_{ij}^{+L} + \delta Z_{ij}^{+L*}) V_{ik}^*) P_L + (U_{jk} + \frac{1}{4} (\delta Z_{ij}^{+R} + \delta Z_{ij}^{+R*}) U_{ik}) P_R] \tilde{\chi}_i^+ \end{aligned}$$

This shows that a hermitian definition of the field renormalization constants in the form

$$\delta Z_{ij}^{0L/R} \rightarrow \frac{1}{2} (\delta Z_{ij}^{0L/R} + \delta Z_{ij}^{0L/R*}), \quad \delta Z_{ij}^{+L/R} \rightarrow \frac{1}{2} (\delta Z_{ij}^{+L/R} + \delta Z_{ij}^{+L/R*}) \quad (6.106)$$

cancels this problem and allows to set the counterterms of the mixing matrices to zero. However note that the procedure of renormalized mixing matrices, respectively nondiagonal contributions to δZ_{ij} does not allow to have gauge invariant masses or decay widths. Before discussing the case of on-shell masses of neutralinos and charginos, we address this problem in the following section.

Gauge invariance

In order to check gauge invariance we are using the general R_ξ -gauge introduced in Section 5.2. In the previous section we described the determination of the counterterms for the mixing matrices of the neutralinos and charginos in Equations (6.102) and (6.103) in accordance to [146]. This was done in such a way, that $\delta \mathcal{N}_{ij}, \delta U_{ij}$ and δV_{ij} cancel the UV divergences and avoid antihermitian parts in the Lagrangian.

Nevertheless it was pointed out in [147] that in case of the Cabibbo-Kobayashi-Maskawa (CKM) quark mixing matrix V_{CKM} [148] the corresponding counterterm δV_{CKM} is gauge dependent $\partial_\xi \delta V_{\text{CKM}} \neq 0$ using the on-shell scheme of [146], which in turn implies a gauge dependence for elementary processes like $t \rightarrow Wb$ at next-to-leading order level [149].

Since then, different solutions to the problem addressed above were proposed in the literature: Whereas [150] argued that missing absorptive parts due to the unstable nature of the external particles have to be included in the calculation, [149] proposed a method how to construct a

gauge invariant counterterm for the mixing matrices inspired by the pinch technique [151], which defines gauge independent form factors for gauge bosons. Another perspective is presented in [152], where the gauge variant on-shell renormalized mixing matrix is related to a gauge independent one in a generalized $\overline{\text{MS}}$ scheme of renormalization.

For the special case of the CKM matrix Q different methods were discussed in the literature: [147] proposed to set the momenta of the nondiagonal entries of the quark self-energies to zero, while [153] suggested new variants of renormalization in particular for the mixing matrices themselves partially based on physical processes which allows to get gauge independent decay widths. For lepton or neutrino mass matrices also [154] proposed useful renormalization conditions allowing gauge independent results.

Although the method of [149] inspired by the pinch technique has one weak point, namely a dependence on the choice of the gauge fixing for the mixing matrix counterterm, we will make use of this method, since it is model independent and does not rely on the concrete renormalization of physical parameters. Thus, it can be used for all models under consideration allowing gauge independent masses and decay widths at one-loop level.

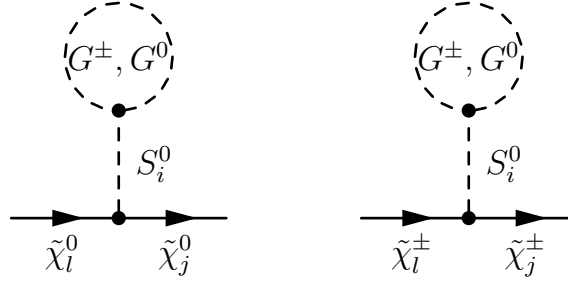


Figure 6.4.: Tadpole contributions including the Goldstone bosons $G_V = G^\pm, G^0$, which have to be added to the self-energies of the neutralinos $\tilde{\chi}^0$ and the charginos $\tilde{\chi}^\pm$ to achieve gauge invariance.

We explain the exact procedure being used in our formulation, which was published in [135, 136]: We calculate two variants of wave-function renormalization constants, namely in case of the neutralinos $\delta Z_{ij}^{0L}, \delta Z_{ij}^{0R}$ for arbitrary values of ξ_V and $\delta \check{Z}_{ij}^{0L}, \delta \check{Z}_{ij}^{0R}$ for $\xi_V = 1$ ('t Hooft-Feynman gauge). The same holds true for the wave-function renormalization constants of the charginos $\delta Z_{ij}^{\pm L}, \delta Z_{ij}^{\pm R}$ and $\delta \check{Z}_{ij}^{\pm L}, \delta \check{Z}_{ij}^{\pm R}$. The counterterms for the mixing matrices are calculated via the wave-function renormalization constants in the 't Hooft-Feynman gauge:

$$\delta \mathcal{N}_{ij} = \frac{1}{4} \left(\delta \check{Z}_{ik}^{0L} - \delta \check{Z}_{ki}^{0R} \right) \mathcal{N}_{kj} \quad (6.107)$$

$$\delta U_{ij} = \frac{1}{4} \left(\delta \check{Z}_{ik}^{+R*} - \delta \check{Z}_{ki}^{+R} \right) U_{kj}, \quad \delta V_{ij} = \frac{1}{4} \left(\delta \check{Z}_{ik}^{+L} - \delta \check{Z}_{ki}^{+L*} \right) V_{kj} \quad (6.108)$$

The ξ_V -dependent wave-function renormalization constants will be used for the counterterm of the considered processes. However note that this splitting in different wave-function renormalization constants forces us to include the additional contributions from the tadpole graphs with the Goldstone bosons of the massive gauge bosons shown in Figure 6.4. The contributions of the Goldstone bosons for $\xi_V = 1$ cancel each other. However for $\xi_V \neq 1$ they allow for a gauge invariant formulation of the considered processes as we will see in Chapter 9. Similarly they only contribute to the UV divergence for $\xi_V \neq 1$ proportional to $(\xi_V - 1)\Delta$ with Δ defined in Equation (6.10) and cancel exactly the ξ_V -dependent UV divergent parts of the vertex corrections and all other counterterms.

6.2.3. On-shell masses of neutralinos and charginos

A special feature of the chargino/neutralino sector is that the number of parameters is lower than the number of imposed on-shell conditions. This implies finite corrections to the tree-level masses of neutralinos and charginos. For the MSSM this was worked out in two different ways: Whereas [145] obtained the counterterms for the tree-level parameter from the individual elements in the mass matrix at one-loop level, [142] determined the counterterms from the mass eigenstates themselves. The latter calculation is simple for a (2×2) chargino mass matrix. In case of larger mass matrices, an analytic inversion is not possible anymore. Thus, we follow the more general concept of [145] to work out the corrections to neutralino and chargino masses in the NMSSM, BRpV and the $\mu\nu$ SMS and start with the one-loop contributions to neutralino masses $\delta\mathcal{M}_n^\otimes$ and chargino masses $\delta\mathcal{M}_c^\otimes$

$$(\delta\mathcal{M}_n^\otimes)_{ij} = \delta \left(\mathcal{N}^T \mathcal{M}_{n,dia.}^\otimes \mathcal{N} \right)_{ij} \quad (6.109)$$

$$= \sum_{n,l} \left[\delta\mathcal{N}_{ni} \left(\mathcal{M}_{n,dia.}^\otimes \right)_{nl} \mathcal{N}_{lj} + \mathcal{N}_{ni} \left(\delta\mathcal{M}_{n,dia.}^\otimes \right)_{nl} \mathcal{N}_{lj} + \mathcal{N}_{ni} \left(\mathcal{M}_{n,dia.}^\otimes \right)_{nl} \delta\mathcal{N}_{lj} \right]$$

$$(\delta\mathcal{M}_c^\otimes)_{ij} = \delta \left(U^T \mathcal{M}_{c,dia.}^\otimes V \right)_{ij} \quad (6.110)$$

$$= \sum_{n,l} \left[\delta U_{ni} \left(\mathcal{M}_{c,dia.}^\otimes \right)_{nl} V_{lj} + U_{ni} \left(\delta\mathcal{M}_{c,dia.}^\otimes \right)_{nl} V_{lj} + U_{ni} \left(\mathcal{M}_{c,dia.}^\otimes \right)_{nl} \delta V_{lj} \right]$$

with the diagonalized mass matrices $\mathcal{M}_{dia.}^\otimes$ and their counterterms $\delta\mathcal{M}_{dia.}^\otimes$:

$$\left(\mathcal{M}_{n,dia.}^\otimes \right)_{nl} = \delta_{nl} m_{\tilde{\chi}_l^0}, \quad \left(\delta\mathcal{M}_{n,dia.}^\otimes \right)_{nl} = \delta_{nl} \delta m_{\tilde{\chi}_l^0} \quad (6.111)$$

$$\left(\mathcal{M}_{c,dia.}^\otimes \right)_{nl} = \delta_{nl} m_{\tilde{\chi}_l^\pm}, \quad \left(\delta\mathcal{M}_{c,dia.}^\otimes \right)_{nl} = \delta_{nl} \delta m_{\tilde{\chi}_l^\pm} \quad (6.112)$$

The bare mass matrices of the neutralinos and charginos can be expressed as the full on-shell mass matrix with the corrections presented in Equations (6.109) and (6.110) or via the tree-level mass matrix expressed in physical parameters together with the renormalization constants of those:

$$\mathcal{M}_{n,c}^0 = \mathcal{M}_{n,c}^\otimes + \delta\mathcal{M}_{n,c}^\otimes = \mathcal{M}_{n,c} + \delta\mathcal{M}_{n,c} \quad (6.113)$$

Hence, the relations between tree-level and one-loop mass matrices take the form:

$$\mathcal{M}_{n,c}^\otimes = \mathcal{M}_{n,c} + \delta\mathcal{M}_{n,c} - \delta\mathcal{M}_{n,c}^\otimes =: \mathcal{M}_{n,c} + \Delta\mathcal{M}_{n,c} \quad (6.114)$$

In the following we will define the model dependent physical parameters, write down the renormalization of the mass matrices $\delta\mathcal{M}_{n,c}$ and identify the renormalization constants of the physical parameters, which are fixed in the neutralino or chargino sector. Some physical parameters, namely δm_W , δm_Z and thus $\delta \cos \theta_W$ are fixed in the gauge boson sector and $\delta \tan \beta$ in the Higgs sector. In particular for $\delta \tan \beta$ we take the $\overline{\text{DR}}$ renormalization [155], such that UV divergences in the masses and the considered process cancel

$$\frac{\delta \tan \beta}{\tan \beta} = \frac{1}{32\pi^2} \Delta \left(3\text{Tr}(Y_d Y_d^\dagger) - 3\text{Tr}(Y_u Y_u^\dagger) + \text{Tr}(Y_e Y_e^\dagger) - \text{Tr}(Y_\nu Y_\nu^\dagger) \right) \quad (6.115)$$

with Δ is defined in Equation (6.10) and Y_ν is only present in the $\mu\nu$ SMS. Note that this choice maintains also the gauge invariance of masses and the considered decay widths. We will also

need the renormalization constants for the sine and cosine of different angles, which are given by:

$$\frac{\delta \cos \beta}{\cos \beta} = -\sin^2 \beta \frac{\delta \tan \beta}{\tan \beta}, \quad \frac{\delta \sin \beta}{\sin \beta} = \cos^2 \beta \frac{\delta \tan \beta}{\tan \beta} \quad (6.116)$$

MSSM

In case of the MSSM we follow [145]. The tree-level neutralino mass matrix was presented in Equation (5.106), the chargino mass matrix was given in Equation (5.104). The variation of all given entries of the tree-level neutralino mass matrix leads to

$$\delta \mathcal{M}_n^{11} = \delta M_1 = \frac{\delta M_1}{M_1} \mathcal{M}_n^{11} \quad (6.117)$$

$$\delta \mathcal{M}_n^{13} = -\delta(m_Z \sin \theta_W \cos \beta) = \left(\frac{\delta m_Z}{m_Z} + \frac{\delta \sin \theta_W}{\sin \theta_W} + \frac{\delta \cos \beta}{\cos \beta} \right) \mathcal{M}_n^{13} \quad (6.118)$$

$$\delta \mathcal{M}_n^{14} = \delta(m_Z \sin \theta_W \sin \beta) = \left(\frac{\delta m_Z}{m_Z} + \frac{\delta \sin \theta_W}{\sin \theta_W} + \frac{\delta \sin \beta}{\sin \beta} \right) \mathcal{M}_n^{14} \quad (6.119)$$

$$\delta \mathcal{M}_n^{22} = \delta M_2 = \frac{\delta M_2}{M_2} \mathcal{M}_n^{22} \quad (6.120)$$

$$\delta \mathcal{M}_n^{23} = \delta(m_Z \cos \theta_W \cos \beta) = \left(\frac{\delta m_Z}{m_Z} + \frac{\delta \cos \theta_W}{\cos \theta_W} + \frac{\delta \cos \beta}{\cos \beta} \right) \mathcal{M}_n^{23} \quad (6.121)$$

$$\delta \mathcal{M}_n^{24} = -\delta(m_Z \cos \theta_W \sin \beta) = \left(\frac{\delta m_Z}{m_Z} + \frac{\delta \cos \theta_W}{\cos \theta_W} + \frac{\delta \sin \beta}{\sin \beta} \right) \mathcal{M}_n^{24} \quad (6.122)$$

$$\delta \mathcal{M}_n^{34} = -\delta \mu = \frac{\delta \mu}{\mu} \mathcal{M}_n^{34} \quad (6.123)$$

whereas all the other variations $\delta \mathcal{M}_n^{12} = \delta \mathcal{M}_n^{21} = \delta \mathcal{M}_n^{33} = \delta \mathcal{M}_n^{44} = 0$ necessarily vanish. The corrections in the chargino mass matrix read

$$\delta \mathcal{M}_c^{11} = \delta M_2 = \frac{\delta M_2}{M_2} \mathcal{M}_c^{11} \quad (6.124)$$

$$\delta \mathcal{M}_c^{12} = \sqrt{2} \delta(m_W \sin \beta) = \left(\frac{\delta m_W}{m_W} + \frac{\delta \sin \beta}{\sin \beta} \right) \mathcal{M}_c^{12} \quad (6.125)$$

$$\delta \mathcal{M}_c^{21} = \sqrt{2} \delta(m_W \cos \beta) = \left(\frac{\delta m_W}{m_W} + \frac{\delta \cos \beta}{\cos \beta} \right) \mathcal{M}_c^{21} \quad (6.126)$$

$$\delta \mathcal{M}_c^{22} = \delta \mu = \frac{\delta \mu}{\mu} \mathcal{M}_c^{22} \quad (6.127)$$

We will fix δM_2 and $\delta \mu$ in the chargino sector, whereas δM_1 is fixed in the neutralino sector by imposing the conditions

$$\Delta \mathcal{M}_c^{11} = \Delta \mathcal{M}_c^{22} = \Delta \mathcal{M}_n^{11} \stackrel{!}{=} 0 \quad (6.128)$$

resulting in:

$$\delta M_1 = \delta \mathcal{M}_n^{\otimes 11}, \quad \delta M_2 = \delta \mathcal{M}_c^{\otimes 11}, \quad \delta \mu = \delta \mathcal{M}_c^{\otimes 22} \quad (6.129)$$

For all the remaining entries of the neutralino and chargino mass matrices finite shifts $\Delta \mathcal{M}_{n,c}$ have to be taken into account.

NMSSM

Having the additional angles and parameters

$$\tan \beta_S = \frac{v_S}{v_u}, \quad \mu = \frac{1}{\sqrt{2}} \lambda v_S, \quad m_{\tilde{S}} = \sqrt{2} \kappa v_S \quad (6.130)$$

in mind, we refer to Equation (5.107) for the neutralino tree-level mass matrix, whereas the chargino mass matrix is equal to the one in the MSSM. Therefore, apart from the variations shown in Equations (6.117)–(6.123) and (6.124)–(6.127) already present in the MSSM we get in addition

$$\delta \mathcal{M}_n^{35} = \delta \left(-\frac{\mu}{\tan \beta_S} \right) = \left(\frac{\delta \mu}{\mu} - \frac{\delta \tan \beta_S}{\tan \beta_S} \right) \mathcal{M}_n^{35} \quad (6.131)$$

$$\delta \mathcal{M}_n^{45} = \delta \left(\frac{-\mu}{\tan \beta \tan \beta_S} \right) = \left(\frac{\delta \mu}{\mu} - \frac{\delta \tan \beta}{\tan \beta} - \frac{\delta \tan \beta_S}{\tan \beta_S} \right) \mathcal{M}_n^{45} \quad (6.132)$$

$$\delta \mathcal{M}_n^{55} = \frac{\delta m_{\tilde{S}}}{m_{\tilde{S}}} \mathcal{M}_n^{55} \quad , \quad (6.133)$$

whereas all the other variations $\delta \mathcal{M}_n^{12} = \delta \mathcal{M}_n^{15} = \delta \mathcal{M}_n^{21} = \delta \mathcal{M}_n^{25} = \delta \mathcal{M}_n^{33} = \delta \mathcal{M}_n^{44} = 0$ necessarily vanish. Similar to the MSSM we will fix δM_2 and $\delta \mu$ in the chargino sector. δM_1 , $\delta \tan \beta_S$ and $\delta m_{\tilde{S}}$ are determined from the neutralino sector by imposing the following conditions

$$\Delta \mathcal{M}_c^{11} = \Delta \mathcal{M}_c^{22} = \Delta \mathcal{M}_n^{11} = \Delta \mathcal{M}_n^{35} = \Delta \mathcal{M}_n^{55} \stackrel{!}{=} 0 \quad , \quad (6.134)$$

which result in:

$$\delta M_1 = \delta \mathcal{M}_n^{\otimes 11}, \quad \delta M_2 = \delta \mathcal{M}_c^{\otimes 11}, \quad \delta \mu = \delta \mathcal{M}_c^{\otimes 22} \quad (6.135)$$

$$\delta \tan \beta_S = \frac{\tan^2 \beta_S}{\mu} \left(\delta \mathcal{M}_n^{\otimes 35} - \frac{1}{\tan \beta_S} \delta \mathcal{M}_n^{\otimes 34} \right), \quad \delta m_{\tilde{S}} = \delta \mathcal{M}_n^{\otimes 55} \quad (6.136)$$

For all the remaining entries of the neutralino and chargino mass matrices finite shifts $\Delta \mathcal{M}_{n,c}$ have to be taken into account. Note that we could also fix $\delta \tan \beta_S$ in the Higgs sector.

BRpV

In case of bilinear R -parity breaking the renormalization of the physical parameters is more challenging. The masses of the Z and W bosons are defined in Equation (5.32), where not only the vacuum expectation values of the Higgs enter, but also the ones of the left-handed sneutrinos. As in the (N)MSSM the cosine of the given Weinberg angle $\cos \theta_W$ can be derived from $m_W = \cos \theta_W m_Z$. Apart from the already known $\tan \beta$ in the MSSM we define in addition

$$\tan \beta_i = \frac{v_i}{v_d} \quad \text{and} \quad \epsilon_i \quad (6.137)$$

as additional parameters at tree-level. We remind the reader once again of the form of the neutralino mass matrix

$$\mathcal{M}_n = \begin{pmatrix} M_n & m \\ m^T & 0 \end{pmatrix} \quad (6.138)$$

$$M_n = \begin{pmatrix} M_1 & 0 & -m_Z \sin \theta_W \cos \beta \Theta & m_Z \sin \theta_W \sin \beta \Theta \\ & M_2 & m_Z \cos \theta_W \cos \beta \Theta & -m_Z \cos \theta_W \sin \beta \Theta \\ & & 0 & -\mu \\ \text{sym.} & & & 0 \end{pmatrix} \quad (6.139)$$

$$(m^T)_i = (-m_Z \sin \theta_W \cos \beta \tan \beta_i \Theta \quad m_Z \cos \theta_W \cos \beta \tan \beta_i \Theta \quad 0 \quad \epsilon_i) \quad (6.140)$$

where Θ is defined in Equation (5.110). In this way we maintain the possibility to fix the renormalization constants of m_Z and $\cos \theta_W$ in the gauge boson sector, whereas the corrections from R -parity breaking are parameterized by $\tan \beta_i$ and ϵ_i and the parameter $\Theta(\beta, \beta_i)$. Defining in addition the lepton masses $m_e^{ij} = \frac{1}{\sqrt{2}} Y_e^{ij} v_d$ the chargino mass matrix, which we already presented in the previous chapter, is given by:

$$\mathcal{M}_c = \begin{pmatrix} M_2 & \sqrt{2} m_W \sin \beta \Theta & 0 & 0 & 0 \\ \sqrt{2} m_W \cos \beta \Theta & \mu & -\tan \beta_i m_e^{i1} & -\tan \beta_i m_e^{i2} & -\tan \beta_i m_e^{i3} \\ \sqrt{2} m_W \cos \beta \tan \beta_1 \Theta & -\epsilon_1 & m_e^{11} & m_e^{12} & m_e^{13} \\ \sqrt{2} m_W \cos \beta \tan \beta_2 \Theta & -\epsilon_2 & m_e^{21} & m_e^{22} & m_e^{23} \\ \sqrt{2} m_W \cos \beta \tan \beta_3 \Theta & -\epsilon_3 & m_e^{31} & m_e^{32} & m_e^{33} \end{pmatrix} \quad (6.141)$$

Using now the relations $\cos \beta^0 = \cos \beta + \delta \cos \beta$ and $\tan \beta_i^0 = \tan \beta_i + \delta \tan \beta_i$ we do a simple expansion in first order of $\delta \cos \beta$ and $\delta \tan \beta_i$:

$$\begin{aligned} \Theta_0 &= \sqrt{\frac{1}{1 + \cos^2 \beta^0 \sum_i \tan^2 \beta_i^0}} \approx \sqrt{\frac{1}{1 + \cos^2 \beta \sum_i \tan^2 \beta_i}} \\ &\quad - \left(\frac{1}{1 + \cos^2 \beta \sum_j \tan^2 \beta_j} \right)^{\frac{3}{2}} \sum_i \cos^2 \beta \tan \beta_i \delta \tan \beta_i \\ &\quad - \left(\frac{1}{1 + \cos^2 \beta \sum_j \tan^2 \beta_j} \right)^{\frac{3}{2}} \sum_i \cos \beta \delta \cos \beta \tan^2 \beta_i = \Theta + \delta \Theta \end{aligned} \quad (6.142)$$

The counterterm of Θ can therefore be expressed as a function of $\delta \tan \beta_i$ and $\delta \cos \beta$:

$$\begin{aligned} \delta \Theta &= -\cos \beta \delta \cos \beta \Theta^3 \sum_i \tan^2 \beta_i - \cos^2 \beta \Theta^3 \sum_i \tan \beta_i \delta \tan \beta_i \\ &= -\sum_i \cos^2 \beta \tan^2 \beta_i \Theta^3 \left(\frac{\delta \cos \beta}{\cos \beta} + \frac{\delta \tan \beta_i}{\tan \beta_i} \right) \xrightarrow{v_i \rightarrow 0} 0 \end{aligned} \quad (6.143)$$

The variation of all the given entries of the tree-level mass matrix leads to:

$$\delta \mathcal{M}_n^{11} = \delta M_1 = \frac{\delta M_1}{M_1} \mathcal{M}_n^{11} \quad (6.144)$$

$$\delta \mathcal{M}_n^{13} = -\delta(m_Z \sin \theta_W \cos \beta \Theta) = \left(\frac{\delta m_Z}{m_Z} + \frac{\delta \sin \theta_W}{\sin \theta_W} + \frac{\delta \cos \beta}{\cos \beta} + \frac{\delta \Theta}{\Theta} \right) \mathcal{M}_n^{13} \quad (6.145)$$

$$\delta \mathcal{M}_n^{14} = \delta(m_Z \sin \theta_W \sin \beta \Theta) = \left(\frac{\delta m_Z}{m_Z} + \frac{\delta \sin \theta_W}{\sin \theta_W} + \frac{\delta \sin \beta}{\sin \beta} + \frac{\delta \Theta}{\Theta} \right) \mathcal{M}_n^{14} \quad (6.146)$$

$$\delta \mathcal{M}_n^{1,4+i} = -\delta(m_Z \sin \theta_W \cos \beta \tan \beta_i \Theta) \quad (6.147)$$

$$= \left(\frac{\delta m_Z}{m_Z} + \frac{\delta \sin \theta_W}{\sin \theta_W} + \frac{\delta \cos \beta}{\cos \beta} + \frac{\delta \tan \beta_i}{\tan \beta_i} + \frac{\delta \Theta}{\Theta} \right) \mathcal{M}_n^{1,4+i}$$

$$\delta \mathcal{M}_n^{22} = \delta M_2 = \frac{\delta M_2}{M_2} \mathcal{M}_n^{22} \quad (6.148)$$

$$\delta \mathcal{M}_n^{23} = \delta(m_Z \cos \theta_W \cos \beta \Theta) = \left(\frac{\delta m_Z}{m_Z} + \frac{\delta \cos \theta_W}{\cos \theta_W} + \frac{\delta \cos \beta}{\cos \beta} + \frac{\delta \Theta}{\Theta} \right) \mathcal{M}_n^{23} \quad (6.149)$$

$$\delta \mathcal{M}_n^{24} = -\delta(m_Z \cos \theta_W \sin \beta \Theta) = \left(\frac{\delta m_Z}{m_Z} + \frac{\delta \cos \theta_W}{\cos \theta_W} + \frac{\delta \sin \beta}{\sin \beta} + \frac{\delta \Theta}{\Theta} \right) \mathcal{M}_n^{24} \quad (6.150)$$

$$\delta \mathcal{M}_n^{2,4+i} = \delta(m_Z \cos \theta_W \cos \beta \tan \beta_i \Theta) \quad (6.151)$$

$$= \left(\frac{\delta m_Z}{m_Z} + \frac{\delta \cos \theta_W}{\cos \theta_W} + \frac{\delta \cos \beta}{\cos \beta} + \frac{\delta \tan \beta_i}{\tan \beta_i} + \frac{\delta \Theta}{\Theta} \right) \mathcal{M}_n^{2,4+i}$$

$$\delta \mathcal{M}_n^{34} = -\delta \mu = \frac{\delta \mu}{\mu} \mathcal{M}_n^{34} \quad (6.152)$$

$$\delta \mathcal{M}_n^{4,4+i} = \delta \epsilon_i = \frac{\delta \epsilon_i}{\epsilon_i} \mathcal{M}_n^{4,4+i} \quad (6.153)$$

whereas all the other variations $\delta \mathcal{M}_n^{12} = \delta \mathcal{M}_n^{33} = \delta \mathcal{M}_n^{3,4+i} = \delta \mathcal{M}_n^{44} = 0$ necessarily vanish. The corrections in the chargino mass matrix read

$$\delta \mathcal{M}_c^{11} = \delta M_2 = \frac{\delta M_2}{M_2} \mathcal{M}_c^{11} \quad (6.154)$$

$$\delta \mathcal{M}_c^{12} = \sqrt{2} \delta(m_W \sin \beta \Theta) = \left(\frac{\delta m_W}{m_W} + \frac{\delta \sin \beta}{\sin \beta} + \frac{\delta \Theta}{\Theta} \right) \mathcal{M}_c^{12} \quad (6.155)$$

$$\delta \mathcal{M}_c^{21} = \sqrt{2} \delta(m_W \cos \beta \Theta) = \left(\frac{\delta m_W}{m_W} + \frac{\delta \cos \beta}{\cos \beta} + \frac{\delta \Theta}{\Theta} \right) \mathcal{M}_c^{21} \quad (6.156)$$

$$\delta \mathcal{M}_c^{22} = \delta \mu = \frac{\delta \mu}{\mu} \mathcal{M}_c^{22} \quad (6.157)$$

$$\delta \mathcal{M}_c^{2,2+i} = \delta(-\tan \beta_k m_{ki}) = \sum_k \left(\frac{\delta \tan \beta_k}{\tan \beta_k} - \frac{\delta m_e^{ki}}{m_e^{ki}} \right) \mathcal{M}_c^{2,2+i} \quad (6.158)$$

$$\delta \mathcal{M}_c^{2+i,1} = \sqrt{2} \delta(m_W \cos \beta \tan \beta_i \Theta) \quad (6.159)$$

$$= \left(\frac{\delta m_W}{m_W} + \frac{\delta \cos \beta}{\cos \beta} + \frac{\delta \tan \beta_i}{\tan \beta_i} + \frac{\delta \Theta}{\Theta} \right) \mathcal{M}_c^{2+i,1}$$

$$\delta \mathcal{M}_c^{2+i,2} = -\delta \epsilon_i = \frac{\delta \epsilon_i}{\epsilon_i} \mathcal{M}_c^{2+i,2} \quad (6.160)$$

$$\delta \mathcal{M}_c^{2+i,2+j} = \delta m_e^{ij} = \frac{\delta m_e^{ij}}{m_e^{ij}} \mathcal{M}_c^{2+i,2+j} \quad (6.161)$$

and $\delta \mathcal{M}_c^{1,2+i} = 0$ vanishes. Similar to the (N)MSSM we fix δM_1 in the neutralino and $\delta M_2, \delta \mu$ in the chargino sector. However, we still have to find appropriate renormalization conditions for $\delta \tan \beta_i, \delta \epsilon_i$ and δm_e^{ij} . Whereas δm_e^{ij} are fixed in the lepton sector, so that one-loop contributions to leptonic two-point functions vanish, we have several possibilities for $\delta \tan \beta_i$ and $\delta \epsilon_i$. Whereas $\delta \tan \beta_i$ could for example be determined from the Higgs sector together with the other angles $\tan \beta$ or $\tan \beta_S$, we could fix $\delta \epsilon_i$ with respect to an R -parity violating decay. We will focus on stable lepton masses, so that we calculate $\delta \tan \beta_i$ and $\delta \epsilon_i$ from the one-loop contributions in the chargino sector, which mix the well-known MSSM charginos with the leptons. In total we

impose the following conditions for the MSSM parameters

$$\Delta\mathcal{M}_n^{11} = \Delta\mathcal{M}_c^{11} = \Delta\mathcal{M}_c^{22} \stackrel{!}{=} 0 \quad , \quad (6.162)$$

which result in

$$\delta M_1 = \delta\mathcal{M}_n^{\otimes 11}, \quad \delta M_2 = \delta\mathcal{M}_c^{\otimes 11}, \quad \delta\mu = -\delta\mathcal{M}_c^{\otimes 22} \quad . \quad (6.163)$$

In a second step the conditions $\Delta\mathcal{M}_c^{2+i,2+j} \stackrel{!}{=} 0$ for the renormalization constants of the lepton masses m_e^{ij} are imposed:

$$\delta m_e^{ij} = \delta\mathcal{M}_c^{\otimes 2+i,2+j} \quad (6.164)$$

In a last step the R -parity violating sector with $\delta \tan \beta_i$ and $\delta \epsilon_i$ is considered, which can be fixed by imposing $\Delta\mathcal{M}_c^{2+i,2} = \Delta\mathcal{M}_c^{2,2+i} \stackrel{!}{=} 0$

$$\delta \tan \beta_i = \frac{1}{\det(m_e^{ij})} \frac{1}{2} \sum_{j,k,l,r,s} \epsilon_{ijk} \epsilon_{lrs} \Upsilon_l m_e^{jr} m_e^{ks} \quad (6.165)$$

$$\text{with } \Upsilon_i = - \sum_k \tan \beta_k \delta m_e^{ki} - \delta\mathcal{M}_n^{\otimes 2,2+i} \quad (6.166)$$

$$\delta \epsilon_i = \delta\mathcal{M}_c^{\otimes 2+i,2} \quad , \quad (6.167)$$

where ϵ_{ijk} is the Levi-Civita symbol. In case of vanishing nondiagonal lepton masses at tree-level $m_e^{ij} = 0$ for $i \neq j$ this simplifies to $\delta \tan \beta_i = \frac{1}{m_e^{ii}} \Upsilon_i$. Another possibility is to fix $\delta \tan \beta_i$ from $\Delta\mathcal{M}_c^{2+i,1}$. However, this induces a dependence on $\tan \beta$ and the other renormalization constants in the gauge sector, whereas in the described case the neutrino and lepton sector are “decoupled” from those.

For all the remaining entries of the neutralino and chargino mass matrices shifts $\Delta\mathcal{M}_{n,c}$ have to be taken into account. Due to the nonvanishing entries $\Delta\mathcal{M}_c^{2+i,1}$ also the lepton masses differ between tree- and one-loop level. However we will show that this difference is tiny, for reasonable neutrino masses far below the experimental uncertainties. Note that the Yukawa couplings of the leptons at tree-level of course have to be adopted, so that the tree-level lepton masses fit the experimental known values.

$\mu\nu$ SSM

Having in mind the additional parameters

$$\tan \beta_i = \frac{v_i}{v_d}, \quad \tan \beta_c = \frac{v_c}{v_u} \quad (6.168)$$

$$\mu = \frac{1}{\sqrt{2}} \lambda v_c, \quad m_c = \sqrt{2} \kappa v_c, \quad \epsilon_i = \frac{1}{\sqrt{2}} Y_\nu^i v_c \quad , \quad (6.169)$$

we refer to Equation (5.112) for the tree-level mass matrix of the neutralinos. The chargino mass matrix has the same form as in BRpV in Equation (6.141) and includes similar to the neutralino mass matrix the parameter Θ known from Equation (5.110). Apart from the variations already present in the bilinear model given in Equations (6.144)–(6.153), where the indices $4+i$ have to be shifted to $5+i$, $\delta\mathcal{M}_n$ has the following additional entries:

$$\delta\mathcal{M}_n^{35} = \delta \left(-\frac{\mu}{\tan \beta_c} \right) = \left(\frac{\delta\mu}{\mu} - \frac{\delta \tan \beta_c}{\tan \beta_c} \right) \mathcal{M}_n^{35} \quad (6.170)$$

$$\delta\mathcal{M}_n^{45} = \delta\left(\frac{\tan\beta_i\epsilon_i - \mu}{\tan\beta\tan\beta_c}\right) = \left(-\frac{\delta\tan\beta}{\tan\beta} - \frac{\delta\tan\beta_c}{\tan\beta_c} + \frac{\delta\tan\beta_i\epsilon_i + \tan\beta_i\delta\epsilon_i - \delta\mu}{\tan\beta_i\epsilon_i - \mu}\right)\mathcal{M}_n^{45} \quad (6.171)$$

$$\delta\mathcal{M}_n^{55} = \frac{\delta m_c}{m_c}\mathcal{M}_n^{55} \quad (6.172)$$

$$\delta\mathcal{M}_n^{5,5+i} = \delta\left(\frac{\epsilon_i}{\tan\beta_c}\right) = \left(\frac{\delta\epsilon_i}{\epsilon_i} - \frac{\delta\tan\beta_c}{\tan\beta_c}\right)\mathcal{M}_n^{55+i} \quad (6.173)$$

whereas all the other variations $\delta\mathcal{M}_n^{12} = \delta\mathcal{M}_n^{15} = \delta\mathcal{M}_n^{25} = \delta\mathcal{M}_n^{33} = \delta\mathcal{M}_n^{3,5+i} = \delta\mathcal{M}_n^{44} = 0$ necessarily vanish. The corrections in the chargino mass matrix are the same as in BRpV, presented in Equations (6.154)–(6.161). Similar to the MSSM, we fix δM_1 in the neutralino and $\delta M_2, \delta\mu$ in the chargino sector. Similar to the NMSSM, we fix $\delta\tan\beta_c$ and δm_c in the neutralino sector and similar to the BRpV case $\delta\tan\beta_i$ and $\delta\epsilon_i$ are determined in the chargino sector. However, we will summarize these results once again for the $\mu\nu$ SSM. We start with the conditions for the non- R -parity breaking variables

$$\Delta\mathcal{M}_c^{11} = \Delta\mathcal{M}_c^{22} = \Delta\mathcal{M}_n^{11} = \Delta\mathcal{M}_n^{35} = \Delta\mathcal{M}_n^{55} \stackrel{!}{=} 0 \quad , \quad (6.174)$$

which result in:

$$\delta M_1 = \delta\mathcal{M}_n^{\otimes 11}, \quad \delta M_2 = \delta\mathcal{M}_c^{\otimes 11}, \quad \delta\mu = \delta\mathcal{M}_c^{\otimes 22} \quad (6.175)$$

$$\delta\tan\beta_c = \frac{\tan^2\beta_c}{\mu} \left(\delta\mathcal{M}_n^{\otimes 35} - \frac{1}{\tan\beta_c} \delta\mathcal{M}_n^{\otimes 34} \right), \quad \delta m_c = \delta\mathcal{M}_n^{\otimes 55} \quad (6.176)$$

In a second step the conditions $\Delta\mathcal{M}_c^{2+i,2} = \Delta\mathcal{M}_c^{2,2+i} = \Delta\mathcal{M}_c^{2+i,2+j} \stackrel{!}{=} 0$ for the renormalization constants of the lepton masses m_e^{ij} , $\delta\tan\beta_i$ and $\delta\epsilon_i$ are imposed, resulting in:

$$\delta m_e^{ij} = \delta\mathcal{M}_c^{\otimes 2+i,2+j}, \quad \delta\epsilon_i = \delta\mathcal{M}_c^{\otimes 2+i,2} \quad (6.177)$$

$$\delta\tan\beta_i = \frac{1}{\det(m_e^{ij})} \frac{1}{2} \sum_{j,k,l,r,s} \epsilon_{ijk}\epsilon_{lrs} \Upsilon_l m_e^{jr} m_e^{ks} \quad (6.178)$$

$$\text{with } \Upsilon_i = - \sum_k \tan\beta_k \delta m_e^{ki} - \delta\mathcal{M}_n^{\otimes 2,2+i} \quad (6.179)$$

Definition of one-loop on-shell masses

With the procedure introduced in the last sections we calculate one-loop on-shell neutralino and chargino masses for the models under consideration namely by combining the full one-loop corrections $\delta\mathcal{M}_{n,c}^{\otimes}$ with the counterterms $\delta\mathcal{M}_{n,c}$ obtained according to Equation (6.114). This results in the one-loop mass matrix $\mathcal{M}_{n,c}^{\otimes}$, whose diagonalizations lead to one-loop neutralino $m^{1L}(\tilde{\chi}_i^0)$ and chargino masses $m^{1L}(\tilde{\chi}_i^\pm)$ and mixing matrices at the one-loop level $\mathcal{N}^{1L}, U^{1L}, V^{1L}$. Note that these masses are UV and IR finite as well as gauge independent if we take into account the gauge independent renormalization of the mixing matrices in Equations (6.107) and (6.108).

Effect on the considered processes

Instead of having the diagonal counterterm for the masses in Equation (6.65) we have to replace

$$\delta_{ij} m_{fi0} \rightarrow \delta_{ij} m_{fi} + \delta\tilde{\mathcal{M}}_{ij} P_L + \delta\tilde{\mathcal{M}}_{ji}^* P_R \quad , \quad (6.180)$$

where $\delta\tilde{\mathcal{M}} = D_R^* \delta\mathcal{M} D_L^\dagger$ with $\delta\mathcal{M}$ being the physical mass counterterm and D_L, D_R being the rotation matrices, which diagonalize the tree-level mass matrix $\mathcal{M}_{dia.} = D_R^* \mathcal{M} D_L^\dagger$ in the notation of [144]. With this counterterm contributions to the nondiagonal wave function renormalization constants arise:

$$\delta Z_{ij}^{fL} = \frac{2}{m_{f_i}^2 - m_{f_j}^2} \left[m_{f_j}^2 \text{Re}\Sigma_{ij}^{fL}(m_{f_j}^2) + m_{f_i} m_{f_j} \text{Re}\Sigma_{ij}^{fR}(m_{f_j}^2) \right. \\ \left. + m_{f_i} \text{Re}\Sigma_{ij}^{fSL}(m_{f_j}^2) + m_{f_j} \text{Re}\Sigma_{ij}^{fSR}(m_{f_j}^2) - m_i \delta\tilde{\mathcal{M}}_{ij} - m_j \delta\tilde{\mathcal{M}}_{ji}^* \right] \quad (6.181)$$

$$\delta Z_{ij}^{fR} = \frac{2}{m_{f_i}^2 - m_{f_j}^2} \left[m_{f_i} m_{f_j} \text{Re}\Sigma_{ij}^{fL}(m_{f_j}^2) + m_{f_j}^2 \text{Re}\Sigma_{ij}^{fR}(m_{f_j}^2) \right. \\ \left. + m_{f_j} \text{Re}\Sigma_{ij}^{fSL}(m_{f_j}^2) + m_{f_i} \text{Re}\Sigma_{ij}^{fSR}(m_{f_j}^2) - m_j \delta\tilde{\mathcal{M}}_{ij} - m_i \delta\tilde{\mathcal{M}}_{ji}^* \right] \quad (6.182)$$

However, it turns out that these additional contributions are canceled by the contributions to $\delta\mathcal{N}, \delta U$ and δV , which also have to be calculated using the new wave-function renormalization constants. This implies that the reduced number of physical parameters only has an impact on the calculated neutralino and chargino masses, but not directly on the considered processes itself.

6.3. Neutrino physics

We will later compare the one-loop on-shell masses of neutralinos and charginos with the corresponding $\overline{\text{DR}}$ masses, which should be mentioned briefly. Using our notation from Equation (6.62) we follow [97] and get the renormalized self-energies for neutralinos and charginos via

$$\hat{\Gamma}_{ij}^f(p) = \left[\Gamma_{ij}^f(p) \right]_{\Delta=0} \quad , \quad (6.183)$$

where Δ was defined in Equation (6.10). The corrections in mass eigenstates are then given by

$$\Delta M_{ij} = -\frac{1}{2} \left[\hat{\Sigma}_{ij}^{fS}(m_i^2) + \hat{\Sigma}_{ij}^{fS}(m_j^2) \right] - \frac{1}{2} \left[m_i \hat{\Sigma}_{ij}^f(m_i^2) + m_j \hat{\Sigma}_{ij}^f(m_j^2) \right] \quad (6.184)$$

$$\text{with } \hat{\Sigma}_{ij}^f(p^2) = \frac{1}{2} \left[\hat{\Sigma}_{ij}^{fL}(p^2) + \hat{\Sigma}_{ij}^{fR}(p^2) \right] \quad (6.185)$$

$$\text{and } \hat{\Sigma}_{ij}^{fS}(p^2) = \frac{1}{2} \left[\hat{\Sigma}_{ij}^{fSL}(p^2) + \hat{\Sigma}_{ij}^{fSR}(p^2) \right] \quad . \quad (6.186)$$

They can either be added to the diagonal mass matrix in mass eigenstates, which has to be diagonalized afterwards, so that the final mixing matrix is a product of the mixing matrices on tree-level and on one-loop level. Alternatively we can rotate back the mass corrections using the tree-level mixing matrices in gauge eigenstates, which can be diagonalized using one mixing matrix only. We will use the latter description for our calculations.

Independently from this choice, the effective neutrino mass matrix in Equation (5.130) for BRpV and the $\mu\nu$ SJM with one-right handed neutrino superfield take the form

$$(m_{\nu\nu}^{\text{eff},1L})_{ij} = a\Lambda_i\Lambda_j + b(\epsilon_i\Lambda_j + \Lambda_i\epsilon_j) + c\epsilon_i\epsilon_j \quad . \quad (6.187)$$

For a motivation of this structure we refer to [97]. Although the on-shell masses are more complicated and the simple motivation cannot be used a priori for them, we find a similar

structure for the on-shell neutrino masses. Thus, at one-loop level we can explain the full neutrino spectrum, since the presented effective neutrino mass matrix $m_{\nu\nu}^{\text{eff},1L}$ has at least two nonzero eigenvalues. All the neutrino parameters can be fitted by adopting the alignment parameters ϵ_i and Λ_i .

Since Λ_i determines the tree-level neutrino mass as shown in Equation (5.136), the most convenient choice for the explanation of neutrino data is the hierarchical spectrum, where ϵ_i determines the two lighter masses of the neutrinos at one-loop level. An inverted spectrum is possible, but requires some fine-tuning within the considered models. Due to the bounds to the absolute scale of neutrino masses as given in Section 2.3 the parameters $\vec{\Lambda}$ and $\vec{\epsilon}$ are constrained. For typical SUSY masses order $\mathcal{O}(100 \text{ GeV})$, we find $|\vec{\Lambda}|/\mu^2 \sim 10^{-7} - 10^{-6}$ and $|\vec{\epsilon}|/\mu \sim 10^{-5} - 10^{-4}$. This implies a ratio of $|\vec{\epsilon}|^2/|\vec{\Lambda}| \sim 10^{-3} - 10^{-1}$.

In Equation (5.139) we have shown the structure of the the neutrino mass matrix in case of the $\mu\nu$ SSM with two right-handed neutrino superfields. Within this section we want to comment on the importance respectively nonimportance of one-loop corrections to this tree-level mass matrix and explain two different ways of fitting the neutrino data:

Having two nonzero eigenvalues in the mass matrix at tree-level in Equation (5.139) two options arise to explain the experimental data:

- ▷ fit1: $\vec{\Lambda}$ generates the atmospheric mass scale, $\vec{\alpha}$ the solar mass scale
- ▷ fit2: $\vec{\alpha}$ generates the atmospheric mass scale, $\vec{\Lambda}$ the solar mass scale

Again both cases lead in general to a hierarchical spectrum. Thus, a strong fine-tuning would be necessary to generate an inverted hierarchy, which is not stable against small variations of the parameters. Moreover the absolute scale of neutrino mass requires both $|\vec{\Lambda}|/\mu^2$ and $|\vec{\alpha}|/\mu$ to be small. For typical SUSY masses of order $\mathcal{O}(100 \text{ GeV})$ we find in the first case $|\vec{\Lambda}|/\mu^2 \sim 10^{-7} - 10^{-6}$ and $|\vec{\alpha}|/\mu \sim 10^{-9} - 10^{-8}$, whereas in the second case we get $|\vec{\Lambda}|/\mu^2 \sim 10^{-8} - 10^{-7}$ and $|\vec{\alpha}|/\mu \sim 10^{-8} - 10^{-7}$. The ratios including $\vec{\epsilon}$ or $\vec{\alpha}$ are much smaller than those in the $1 \hat{\nu}^c$ case. Last but not least we comment on the one-loop corrections to Equation (5.139). They are negligible if

$$\frac{|\vec{\alpha}|^2}{|\vec{\Lambda}|} \lesssim 10^{-3} \quad \text{and} \quad \frac{|\vec{\epsilon}|^2}{|\vec{\Lambda}|} \lesssim 10^{-3} \quad (6.188)$$

are fulfilled. Note that the mixing of the neutrinos with the Higgsinos, given by the third column in the matrix ξ in Equation (B.9), depends not only on α_i but also on ϵ_i . Hence, the one-loop correction to the neutrino mass matrix contains parts proportional to the ϵ_i parameters similar to the $1 \hat{\nu}^c$ -model. Therefore, both conditions in Equation (6.188) need to be fulfilled. Finally, in models with more generations of right-handed neutrinos there will be more freedom due to additional contributions to the neutrino mass matrix. This also allows an inverted hierarchy spectrum due to the additional freedom as it is shown for three generations in [156].

Calculation of the neutrino parameters

With the one-loop on-shell masses $m_{\nu_i}^{1L}$ of the neutrinos and the mixing matrix \mathcal{N}^{1L} we can calculate the relevant parameters to be compared with experimental neutrino data:

$$\Delta m_{atm}^2 = (m^{1L}(\nu_3))^2 - (m^{1L}(\nu_1))^2, \quad \Delta m_{sol}^2 = (m^{1L}(\nu_2))^2 - (m^{1L}(\nu_1))^2 \quad (6.189)$$

$$\tan^2 \theta_{atm} = \left| \frac{\mathcal{N}_{3,6}^{1L}}{\mathcal{N}_{3,7}^{1L}} \right|^2, \quad \tan^2 \theta_{sol} = \left| \frac{\mathcal{N}_{2,5}^{1L}}{\mathcal{N}_{1,5}^{1L}} \right|^2, \quad U_{e3}^2 = |\mathcal{N}_{3,5}^{1L}|^2 \quad (6.190)$$

The formulas are valid for BRpV, in case of the $\mu\nu$ SSM with one right-handed neutrino superfield we have to replace $\mathcal{N}_{i,j}^{1L} \rightarrow \mathcal{N}_{i,j+1}^{1L}$. Similarly for the $\mu\nu$ SSM with more than one right-handed neutrino superfield the tree-level masses and mixing matrix are used and the indices of \mathcal{N} have to be adopted accordingly.

6.4. Decays $\tilde{\chi}_j^0 \rightarrow \tilde{\chi}_l^\pm W^\mp$ and $\tilde{\chi}_l^\pm \rightarrow \tilde{\chi}_j^0 W^\pm$

In Section 5.4 we discussed the tree-level decay width for the decays $\tilde{\chi}_j^0 \rightarrow \tilde{\chi}_l^\pm W^\mp$ and $\tilde{\chi}_l^\pm \rightarrow \tilde{\chi}_j^0 W^\pm$, for which we want to work out the one-loop corrections within this section.

6.4.1. Vertex corrections

The first piece of the one-loop corrections are the vertex corrections. In Figure 6.5 we depict the six generic contributions. In the Feynman diagrams a) and b) fermions and sfermions contribute as well as charginos/neutralinos together with the neutral and charged Higgs bosons. In diagrams c) and f) only charginos, neutralinos and the vector bosons (including the photon) contribute, whereas in diagrams d) and e) there are in addition the charged and neutral Higgs bosons as well as the Goldstone bosons. The individual contributions from the diagrams in Figure 6.5 to the matrix element M_V are given in Appendix D for the 't Hooft-Feynman gauge $\xi_V = 1$. The general case $\xi_V \neq 1$ leads to rather lengthy formulas, which are included in the program `CNNDecays` [157].

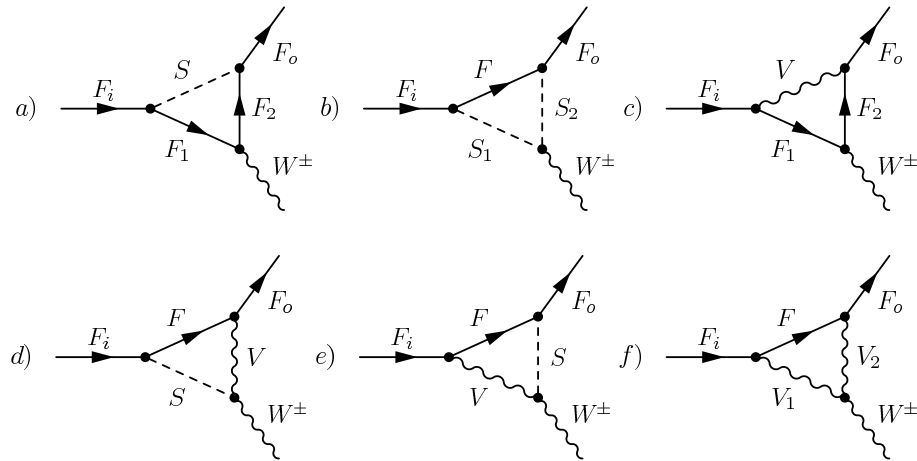


Figure 6.5.: Generic vertex corrections.

The matrix element squared at NLO is given by

$$\frac{1}{2} \sum_{pol} |M|^2 \approx \frac{1}{2} \sum_{pol} [|M_T|^2 + 2\text{Re}(M_V M_T^*) + 2\text{Re}(M_{WV} M_T^*)] \quad , \quad (6.191)$$

where M_V denotes the mentioned vertex corrections and M_{WV} includes the various counterterms, which will be discussed in the next section. In this notation the one-loop decay width is given

by

$$\Gamma^{1L} = \Gamma^0 + \frac{\sqrt{\kappa(m_i^2, m_o^2, m_W^2)}}{16\pi m_i^3} \frac{1}{2} \sum_{pol} 2\text{Re}((M_{WV} M_T^*) + (M_V M_T^*)) \quad . \quad (6.192)$$

This result is UV finite, gauge independent and also not dependent on the renormalization scale Q , which cancels between the contributions from M_V and M_{WV} . The IR finiteness is presented in all detail after having discussed the counterterm in the following section.

6.4.2. Counterterm corrections

The counterterm for the considered processes can be constructed using the tree-level couplings in the Lagrangian density

$$\mathcal{L} = \overline{\tilde{\chi}_l} \gamma^\mu (P_L O_{Llj} + P_R O_{Rlj}) \tilde{\chi}_j^0 W_\mu^- \quad . \quad (6.193)$$

In order to renormalize the vertex on NLO level, the counterterm has to be calculated using the wave function renormalization and the renormalization of the mixing matrices as presented in Section 6.2.2 and the gauge coupling as shown in Section 6.2.1. We obtain

$$\begin{aligned} \delta\mathcal{L} \supset \overline{\tilde{\chi}_l} \gamma^\mu \left(P_L \left[\delta O_{Llj} + \frac{1}{2} O_{Llj} \delta Z_W + \frac{1}{2} \sum_{k=1}^8 O_{Llk} \delta Z_{Lkj}^0 + \frac{1}{2} \sum_{k=1}^5 \delta Z_{Lkl}^{-*} O_{Lkj} \right] \right. \\ \left. + P_R \left[\delta O_{Rlj} + \frac{1}{2} O_{Rlj} \delta Z_W + \frac{1}{2} \sum_{k=1}^8 O_{Rlk} \delta Z_{Rkj}^0 + \frac{1}{2} \sum_{k=1}^5 \delta Z_{Rkl}^{-*} O_{Rkj} \right] \right) \tilde{\chi}_j^0 W_\mu^- \quad . \end{aligned} \quad (6.194)$$

Note that the sums are presented for the case of the $\mu\nu$ SSM with one-right handed neutrino superfield. According to the number of neutralinos and charginos they have to be adopted in the corresponding models.

The couplings δO_{Llj} and δO_{Rlj} for the $\mu\nu$ SSM (1 $\hat{\nu}^c$ -model) can be written in the form:

$$\begin{aligned} \delta O_{Llj} = & - (\delta g \mathcal{N}_{j2}^* U_{l1} + g \delta \mathcal{N}_{j2}^* U_{l1} + g \mathcal{N}_{j2}^* \delta U_{l1}) - \frac{1}{\sqrt{2}} (\delta g \mathcal{N}_{j3}^* U_{l2} + g \delta \mathcal{N}_{j3}^* U_{l2} + g \mathcal{N}_{j3}^* \delta U_{l2}) \\ & - \frac{1}{\sqrt{2}} (\delta g \mathcal{N}_{j6}^* U_{l3} + g \delta \mathcal{N}_{j6}^* U_{l3} + g \mathcal{N}_{j6}^* \delta U_{l3}) - \frac{1}{\sqrt{2}} (\delta g \mathcal{N}_{j7}^* U_{l4} + g \delta \mathcal{N}_{j7}^* U_{l4} + g \mathcal{N}_{j7}^* \delta U_{l4}) \\ & - \frac{1}{\sqrt{2}} (\delta g \mathcal{N}_{j8}^* U_{l5} + g \delta \mathcal{N}_{j8}^* U_{l5} + g \mathcal{N}_{j8}^* \delta U_{l5}) \end{aligned} \quad (6.195)$$

$$\delta O_{Rlj} = - (\delta g V_{l1}^* \mathcal{N}_{j2} + g \delta V_{l1}^* \mathcal{N}_{j2} + g V_{l1}^* \delta \mathcal{N}_{j2}) + \frac{1}{\sqrt{2}} (\delta g V_{l2}^* \mathcal{N}_{j4} + g \delta V_{l2}^* \mathcal{N}_{j4} + g V_{l2}^* \delta \mathcal{N}_{j4}) \quad (6.196)$$

For BRpV $\mathcal{N}_{j\{6,7,8\}}$ has to be replaced by $\mathcal{N}_{j\{5,6,7\}}$. In case of the MSSM and NMSSM the terms with projection on leptons or neutrinos are of course absent. Hence, we define

$$\delta A_{Llj} = i \left(\delta O_{Llj} + \frac{1}{2} O_{Llj} \delta Z_W + \frac{1}{2} \sum_{k=1}^8 O_{Llk} \delta Z_{Lkj}^0 + \frac{1}{2} \sum_{k=1}^5 \delta Z_{Lkl}^{-*} O_{Lkj} \right) \quad (6.197)$$

$$\delta A_{Rlj} = i \left(\delta O_{Rlj} + \frac{1}{2} O_{Rlj} \delta Z_W + \frac{1}{2} \sum_{k=1}^8 O_{Rlk} \delta Z_{Rkj}^0 + \frac{1}{2} \sum_{k=1}^5 \delta Z_{Rkl}^{-*} O_{Rkj} \right) \quad (6.198)$$

and obtain

$$M_{WV} = \bar{u}(p_1)\gamma^\mu (P_L\delta A_{Ll_j} + P_R\delta A_{Rl_j}) u(k)\epsilon_\mu^*(p_2) \quad . \quad (6.199)$$

Then the relevant contribution $2\text{Re}(M_{WV}M_T^*) \subset |M|^2$ for l and j being fixed is given by:

$$\begin{aligned} \frac{1}{2} \sum_{pol} 2\text{Re}(M_{WV}M_T^*) = & \quad (6.200) \\ \frac{1}{m_W^2} & \left[O_L^* \left(\delta A_L \left(m_W^2 (m_{\tilde{\chi}^-}^2 + m_{\tilde{\chi}^0}^2) - (m_{\tilde{\chi}^-}^2 - m_{\tilde{\chi}^0}^2)^2 + 2m_W^4 \right) - 6\delta A_R m_{\tilde{\chi}^-} m_{\tilde{\chi}^0} m_W^2 \right) \right. \\ & \left. + O_R^* \left(\delta A_R \left(m_W^2 (m_{\tilde{\chi}^-}^2 + m_{\tilde{\chi}^0}^2) - (m_{\tilde{\chi}^-}^2 - m_{\tilde{\chi}^0}^2)^2 + 2m_W^4 \right) - 6\delta A_L m_{\tilde{\chi}^-} m_{\tilde{\chi}^0} m_W^2 \right) \right] \end{aligned}$$

6.4.3. Real corrections

In this section we finally address the question of infrared (IR) divergences. The massless photon within loops generates such a divergence, which cancels with the divergence from the emission of a massless photon. Thus, we have to take into account the real corrections. The divergences are both regularized using the same photon mass, so that the final result has to be independent of this unphysical mass.

The cancellation of IR singularities between virtual and real soft corrections in quantum electrodynamics (QED) was already known before the invention of relativistic perturbation theory as Bloch-Nordsieck theorem [158]. The treatment was described more precisely by Yennie, Frautschi and Suura [159]. The most general framework applicable for the standard model is given by the Kinoshita-Lee-Nauenberg theorem [160]. We follow the approach presented by Weinberg [161].

We use the notation of Denner [137] for our Bremsstrahlung integrals. In contrast to the case of $t \rightarrow Wb$ the corrections do not factorize in the same form due to the presence of left- and right-handed couplings in Equation (5.142).

First we want to comment on the dependence on the linear R_ξ -gauge, which cancels out in the real photon emission. The contribution coming from the graph with the internal charged Goldstone boson exactly cancels with the contribution from the longitudinal part of the W boson, what can be seen on amplitude level analytically. Therefore, no gauge dependence on the linear R_ξ -gauge is left. The calculation of the squared amplitude performing all the polarization sums is tedious but straightforward.

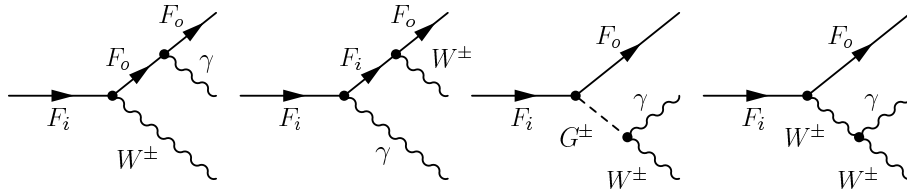


Figure 6.6.: Feynman diagrams for the real photon emission $F_i \rightarrow F_o W^\pm \gamma$.

We present the general result for the decay $F_i(k) \rightarrow F_o(p_1)W^\pm(p_2, \epsilon)\gamma(q, \eta)$ shown in Figure 6.6 with the two fermions F_i with mass m_i and charge Q_i , F_o with mass m_o and charge Q_o in Dirac notation, the W boson with mass m_W and polarization vector ϵ and the photon with

polarization vector η , where the following couplings are relevant:

$$\mathcal{L} \supset \bar{F}_o \gamma_\mu (O_{WL} P_L + O_{WR} P_R) F_i W^\mu + Q_o \bar{F}_o \gamma_\mu O_\gamma F_o A^\mu + Q_i \bar{F}_i \gamma_\mu O_\gamma F_i A^\mu \quad (6.201)$$

The first two diagrams in Figure 6.6, where the photon is emitted from the external fermion lines, result in the following matrix elements:

$$M_1 = \frac{Q_o}{2p_1 \cdot q} \bar{u}(p_1) \gamma^\nu O_\gamma (\not{p}_1 + \not{q} + m_o) \gamma^\mu (O_{WL} P_L + O_{WR} P_R) u(k) \eta_\nu^*(q) \epsilon_\mu^*(p_2) \quad (6.202)$$

$$M_2 = -\frac{Q_i}{2k \cdot q} \bar{u}(p_1) \gamma^\mu O_\gamma (\not{p}_1 + \not{p}_2 + m_i) \gamma^\nu (O_{WL} P_L + O_{WR} P_R) u(k) \eta_\nu^*(q) \epsilon_\mu^*(p_2) \quad (6.203)$$

The last two diagrams in Figure 6.6 add up to the transverse part of the W boson as internal particle, being:

$$M_3 = -\frac{1}{2p_2 \cdot q} O_\gamma \left(g^{\mu\nu} (p_2 - q)^\lambda + g^{\mu\lambda} (-2p_2 - q)^\nu + g^{\nu\lambda} (p_2 + 2q)^\mu \right) \cdot \left(-\frac{(p_2 + q)_\kappa (p_2 + q)_\lambda}{m_W^2} + g_{\kappa\lambda} \right) \bar{u}(p_1) \gamma^\kappa (O_{WL} P_L + O_{WR} P_R) u(k) \eta_\nu^*(q) \epsilon_\mu^*(p_2) \quad (6.204)$$

Therein we made already use of the following rewritten denominators

$$\frac{1}{(p_1 + q)^2 - m_o^2} = \frac{1}{p_1^2 + 2p_1 \cdot q + q^2 - m_o^2} \approx \frac{1}{2p_1 \cdot q} \quad (6.205)$$

$$\frac{1}{(p_1 + p_2)^2 - m_i^2} = \frac{1}{(k - q)^2 - m_i^2} = \frac{1}{k^2 - 2k \cdot q + q^2 - m_i^2} \approx -\frac{1}{2k \cdot q} \quad (6.206)$$

$$\frac{1}{(p_2 + q)^2 - m_W^2} = \frac{1}{p_2^2 + 2p_2 \cdot q + q^2 - m_W^2} \approx \frac{1}{2p_2 \cdot q} \quad (6.207)$$

with $k^2 = m_i^2$, $p_1^2 = m_o^2$, $p_2^2 = m_W^2$ and $q^2 = 0$. For the calculation of the squared amplitude the following sum rules for the gauge bosons are needed:

$$\sum \epsilon_\mu^*(p_2) \epsilon_\nu(p_2) \rightarrow -g_{\mu\nu} + \frac{p_{2\mu} p_{2\nu}}{m_W^2} \quad (6.208)$$

$$\sum \eta_\mu^*(q) \eta_\nu(q) \rightarrow -g_{\mu\nu} \quad (6.209)$$

The gauge dependent part of the sum rule for the photon cancels out and is therefore not included. This finally allows to re-express the result in terms of products of four-momenta with the four-momentum q of the photon. As a starting point for the decay width we take the general result for the three body decay being

$$\Gamma^R = \frac{1}{(4\pi)^3 m_i} \frac{1}{\pi^2} \int \frac{d^3 p_1}{2p_{10}} \frac{d^3 p_2}{2p_{20}} \frac{d^3 q}{2q_0} \delta^{(4)}(k - p_1 - p_2 - q) \frac{1}{2} \sum_{\text{pol}} |M|^2 \quad , \quad (6.210)$$

where the index R denotes the real emission of a photon. We will use the notation of Denner for the Bremsstrahlung integrals, which are defined for a decay of a particle with mass m_0 and momentum p_0 into two particles with masses m_1 and m_2 and momenta p_1 and p_2 and a photon

with momentum q by

$$I_{i_1 i_2}^{j_1 j_2}(m_0, m_1, m_2) = \frac{1}{\pi^2} \int \frac{d^3 p_1}{2p_{10}} \frac{d^3 p_2}{2p_{20}} \frac{d^3 q}{2q_0} \delta^{(4)}(p_0 - p_1 - p_2 - q) \frac{(\pm 2p_{j_1} \cdot q)(\pm 2p_{j_2} \cdot q)}{(\pm 2p_{i_1} \cdot q)(\pm 2p_{i_2} \cdot q)}, \quad (6.211)$$

where the minus signs refer to the momentum p_0 of the initial particle. In this context we need the integrals $I_{j_1 j_2}^{i_1 i_2}(m_i, m_o, m_W)$, allowing us to write the final result in the form:

$$\Gamma^R = \frac{1}{(4\pi)^3 m_i 2m_W^2} |O_\gamma|^2 [(|O_{WL}|^2 + |O_{WR}|^2) \Omega_1 + (O_{WL} O_{WR}^* + O_{WL}^* O_{WR}) \Omega_2] \quad , \quad (6.212)$$

where we have introduced abbreviations:

$$\begin{aligned} \Omega_1 &= Q_i^2 \Omega_{1ii} + 2Q_i Q_o \Omega_{1io} + Q_o^2 \Omega_{1oo} \\ \Omega_2 &= Q_i^2 \Omega_{2ii} + 2Q_i Q_o \Omega_{2io} + Q_o^2 \Omega_{2oo} \end{aligned} \quad (6.213)$$

The individual parts are given by:

$$\begin{aligned} \Omega_{1ii} &= 2I(m_i^2 + m_o^2 + 2m_W^2) - 4[m_W^2(m_i^2 + m_o^2) + (m_i^2 - m_o^2)^2 - 2m_W^4] \\ &\quad \cdot [I_0 + I_{00}m_i^2 + m_W^2(I_{02} + I_{22}) + I_{02}(m_i - m_o)(m_i + m_o) + I_2] \\ &\quad + 2I_0^2(m_i^2 + m_o^2 + 2m_W^2) - 8m_W^2(I_{22}^0 + I_2^1) \end{aligned} \quad (6.214)$$

$$\begin{aligned} \Omega_{1io} &= -3I(m_i^2 + m_o^2) + 2Im_W^2 - 2m_W^2 [2m_o^4(I_{01} + I_{02} - I_{22}) \\ &\quad + 2m_o^2(m_i^2(I_{01} + 2I_{22}) - I_2) - 2m_i^4(I_{02} + I_{22}) + I_0^1 - 2I_2m_i^2 - 4(I_{22}^0 + I_2^0 + I_2^1)] \\ &\quad + 4m_W^4(m_o^2(2(I_{01} + I_{02}) + I_{22}) + m_i^2(I_{22} - 2I_{02}) - 2I_2) - 4I_{01}m_i^4m_o^2 \\ &\quad + 8I_{01}m_i^2m_o^4 - 4I_{01}m_o^6 + 4I_{02}m_i^6 - 12I_{02}m_i^4m_o^2 + 12I_{02}m_i^2m_o^4 \\ &\quad - 4I_{02}m_o^6 - I_0^1m_i^2 - I_0^1m_o^2 - I_0^2(m_i^2 + m_o^2 + 2m_W^2) + 4I_2m_i^4 \\ &\quad - 8I_2m_i^2m_o^2 + 4I_2m_o^4 - 8I_{22}m_W^6 \end{aligned} \quad (6.215)$$

$$\begin{aligned} \Omega_{1oo} &= -8Im_W^2 - 4m_W^2 [m_o^2(m_i^2(2I_{01} + 2I_{02} + I_{11} - 2I_{22}) + I_1 + I_2) \\ &\quad + m_o^4(-2I_{01} - 2I_{02} + I_{11} + I_{22}) + m_i^2(I_1 + I_2 + I_{22}m_i^2) + I_1^0 + 2I_{22}^0 \\ &\quad + 4I_2^0 + 2I_2^1] \\ &\quad + 4m_W^4(-m_o^2(I_{01} + I_{02} - 2I_{11} + I_{22}) \\ &\quad + m_i^2(3(I_{01} + I_{02}) - I_{22}) + 2I_1 + 2I_2) - 8m_W^6(I_{01} + I_{02} - I_{22}) \\ &\quad - 4I_{01}m_i^6 + 12I_{01}m_i^4m_o^2 - 12I_{01}m_i^2m_o^4 + 4I_{01}m_o^6 - 4I_{02}m_i^6 \\ &\quad + 12I_{02}m_i^4m_o^2 - 12I_{02}m_i^2m_o^4 + 4I_{02}m_o^6 - 4I_1m_i^4 \\ &\quad + 8I_1m_i^2m_o^2 - 4I_1m_o^4 - 4I_{11}m_i^4m_o^2 + 8I_{11}m_i^2m_o^4 \\ &\quad - 4I_{11}m_o^6 - 2I_1^0m_i^2 - 2I_1^0m_o^2 - 4I_2m_i^4 + 8I_2m_i^2m_o^2 - 4I_2m_o^4 \end{aligned} \quad (6.216)$$

$$\begin{aligned} \Omega_{2ii} &= 2m_i m_o [-2I + 12m_W^2(I_0 + m_i^2(I_{00} + I_{02}) - I_{02}m_o^2 + I_2) \\ &\quad + 12m_W^4(I_{02} + I_{22}) - 2I_0^2] \end{aligned} \quad (6.217)$$

$$\Omega_{2io} = 2m_i m_o (3I - 12m_W^2(-m_o^2(I_{01} + I_{02}) + I_{02}m_i^2 + I_2) + I_0^1 + I_0^2 - 12I_{22}m_W^4) \quad (6.218)$$

$$\begin{aligned} \Omega_{2oo} &= 4m_i m_o [6m_W^2(-m_o^2(I_{01} + I_{02} - I_{11}) + m_i^2(I_{01} + I_{02}) + I_1 + I_2) \\ &\quad - 6m_W^4(I_{01} + I_{02} - I_{22}) + I_1^0] \end{aligned} \quad (6.219)$$

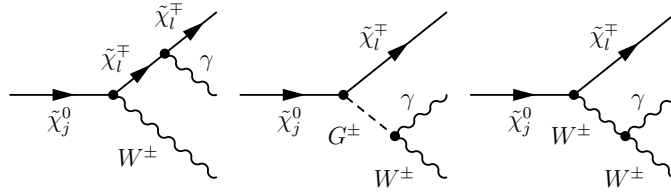


Figure 6.7.: Real corrections for $\tilde{\chi}_j^0 \rightarrow \tilde{\chi}_l^\mp W^\pm \gamma$.

This result was obtained by using `FeynArts` and `FormCalc` with all momentum replacements done automatically, which leads to a result written in a perhaps uncommon way. However the result was tested by a comparison with a numerical simulation based on a Monte Carlo integrated phase space. For our concrete processes we show an example of the relevant Feynman diagrams in Figure 6.7. The expressions can be easily obtained from the formulas above by plugging in the correct charges $Q_{\{i,o\}} = \{0, \pm 1\}$ for the neutralino and chargino. Thus, the IR finite decay width at NLO is given by

$$\Gamma^1 = \Gamma^{1L} + \Gamma^R \quad . \quad (6.220)$$

We add some comments on the calculation with a massive photon: First the usage of a massive photon explicitly breaks the gauge invariance in our calculations. However by choosing a small photon mass $m_\gamma < 1$ keV, this can be kept under control. In addition we can choose an external momentum of $p^2 = 0$ for the calculation of the photon and photon-Z self-energy, since $p^2 \rightarrow 0$ is well-defined and not divergent. The pinch technique for the renormalization of the fermionic mixing matrices does not affect the infrared finiteness, since the photon only contributes to the diagonal entries of fermionic self-energies.

Parameter choice for the models under consideration

In the subsequent chapters we work out collider signatures for various scenarios. To facilitate the comparison with existing studies we adopt the following strategy: We take existing benchmark points and augment them with the additional model parameters breaking R -parity at the electroweak scale. For the MSSM, BRpV and the $\mu\nu$ SMS we refer to the ‘‘Snowmass Points and Slopes’’ (SPS), in detail SPS 1a’ [162], SPS 3, SPS 4, SPS 9 [3] and the ATLAS SU4 point [163]. We summarize the relevant parameters of these models in Table 7.1. In addition we add SPS 2’, which we obtain from SPS 2 by setting $M_1 = M_2 = 600$ GeV at low energies, so that a Higgsino-like lightest neutralino is present. For all parameter sets we included a low-energy input file to the folder `/examples` of `CNNDecays`.

SPS 1a’ contains a light spectrum, SPS 3 has a somewhat heavier spectrum and in addition the lightest neutralino and the lighter stau are close in mass which affects also the R -parity violating decays of the lightest neutralino. SPS 4 is chosen because of the large $\tan\beta$ value and SPS 9 is an AMSB scenario where not only the lightest neutralino but also the lighter chargino has dominant R -parity violating decay modes. In all these points the lightest neutralino is so heavy that it can decay via two-body modes, as long as it is not a light ν^c . In contrast for the SU4 point all two-body decay modes (at tree-level) are kinematically forbidden. As the parameters of these points are given at different scales we use the program `SPheno` [71] to evaluate them at $Q = m_Z$, where we add the additional model parameters. Note that we allow μ to depart from their standard SPS values to be consistent with the LEP bounds on Higgs masses.

		SPS 1a’	SPS 2	SPS 3	SPS 4	SU4		SPS 9
GUT scale	M_0 (in GeV)	70	1450	90	400	200	M_0 (in GeV)	450
	$M_{1/2}$ (in GeV)	250	300	400	300	160	m_{aux} (in TeV)	60
	A_0 (in GeV)	-300	0	0	0	-400		
SUSY scale	$\tan\beta(m_Z)$	10	10	10	50	10	$\tan\beta(m_Z)$	10

Table 7.1.: Important parameters for SPS 1a’, SPS 2, SPS 3, SPS 4, SPS 9 [162, 3] and the ATLAS SU4 point [163].

In case of the NMSSM and the $\mu\nu$ SMS we have to specify the additional model parameters, which are λ_k, κ_k and the corresponding soft SUSY breaking terms T_λ^k and T_κ^{klm} . Those are subject to theoretical and experimental constraints. In [111] the question of color and charge breaking minima, perturbativity up to the GUT scale as well as the question of tachyonic states for the neutral scalar and pseudoscalars have been investigated. The last issue has already been addressed in Section 5.1.2 for the NMSSM where we derived conditions on the parameters. By choosing the coupling constants $\lambda, \kappa < 0.6$ in the 1 $\widehat{\nu}^c$ -model and $\lambda_k, \kappa_k < 0.5$ in the 2 $\widehat{\nu}^c$ -model,

perturbativity up to the GUT scale is guaranteed [111]. Note that choosing somewhat larger values for λ and/or κ up to 1 does not change any of the results presented below. We also address the question of color and charge breaking minima by choosing $\lambda_k > 0$, $\kappa_k > 0$, $T_\lambda^k > 0$, $T_\kappa^{klm} < 0$.

In case of BRpV we have to add the parameters ϵ_i and v_i , which are chosen such that the neutrino data is fulfilled within the 2σ bounds of Table 2.1, if not stated otherwise. As already explained the corresponding soft SUSY breaking parameters B_i are determined from the tadpole equations. They have to be chosen complex in addition to B_μ^I in case of complex ϵ_i as we have shown in Section 5.1.1. For the $\mu\nu$ SSM we set the Yukawa couplings Y_ν^{ik} and the VEVs v_i accordingly, implying small values $Y_\nu^{ik} < \mathcal{O}(10^{-5})$. The corresponding T_ν^{ik} determined from the tadpole equations are generally negative, so the condition (2.8) of [111] is easy to fulfill.

For the NMSSM and the $\mu\nu$ SSM with one right-handed neutrino superfield we refer in addition to the low-energy parameter sets of the NMSSM benchmark scenarios [164, 165] named mSUGRA i or GMSB j based on the soft SUSY breaking mechanism: minimal supergravity (mSUGRA) or gauge mediated SUSY breaking (GMSB). In Table 7.2 we recall the most important parameters of those scenarios. The parameter points can also be found within NMSSM-Tools [166]. For two of them, namely mSUGRA 3 and mSUGRA 4 we change the low-energy parameters $M_1 \leftrightarrow M_2$ and $\kappa \approx 0.1 \rightarrow 0.4$ resulting in mSUGRA 3' and 4', which show a wino- or a Higgsino-like lightest neutralino. Also the additional parameters Y_ν^i and v_i in the $\mu\nu$ SSM with one right-handed neutrino superfield are fixed by the neutrino constraints, which can be found in Table 2.1. For these NMSSM benchmark scenarios we add low-energy input files to the folder /examples of CNNDecays.

		mSUGRA 1	mSUGRA 3	mSUGRA 4
GUT scale	M_0 (in GeV)	180	178	780
	$M_{1/2}$ (in GeV)	500	500	775
	A_0 (in GeV)	-1500	-1500	-2250
SUSY scale	$\tan\beta(m_Z)$	10	10	2.6
	μ (in GeV)	969	938	-197
	λ, κ	0.10, 0.10	0.40, 0.30	0.52, 0.10
	A_λ, A_κ (in GeV)	-959, -1.6	-616, -11	-557, 20
		GMSB 1	GMSB 2	GMSB 5
Mess. scale	M_{Mess} (in GeV)	10^{13}	10^{13}	$5 \cdot 10^{14}$
	Λ (in GeV)	$1.7 \cdot 10^5$	$1.7 \cdot 10^5$	$7.5 \cdot 10^4$
SUSY scale	$\tan\beta(m_Z)$	8.5	1.63	50
	μ (in GeV)	1404	2351	1376
	λ, κ	0.020, 0.004	0.50, 0.43	0.010, -0.0007
	A_λ, A_κ (in GeV)	-52, -160	-446, -2300	118, 4645

Table 7.2.: Important parameters for the mSUGRA [164] and GMSB [165] benchmark scenarios.

Concerning experimental data we generally take the following constraints into account:

- ▷ As already pointed out we check that the neutrino data are fulfilled within the 2σ range given in Table 2.1 taken from [17] if not stated otherwise. For figures and tables published in [122] an older version of Table 2.1 from [167] is relevant. However, the update of the bounds three years ago to present bounds does not change the basic statements.

- ▷ Breaking lepton number implies that flavor violating decays like $\mu \rightarrow e\gamma$ of the leptons are possible, where strong experimental bounds exist [168]. R -parity violation induces those decays. However in the models under study, it turns out that these bounds are automatically fulfilled once the constraints from neutrino physics are taken into account [169].
- ▷ Bounds on the masses of the Higgs bosons [113, 168]. For this purpose we have added the dominant one-loop correction to the $(2, 2)$ -elements of the scalar mass matrices as described in Section 5.1.3.
- ▷ Constraints on the chargino and charged slepton masses given by the PDG [168].
- ▷ The bounds on squark and gluino masses from Tevatron [168] are automatically fulfilled by our choices of the study points. Recent bounds from LHC data might rule out some of the points under consideration, in particular SPS 1a' and SU4 potentially show a too light spectrum. However our statements are mostly generic and apply also for a mass spectrum shifted to slightly larger masses, so that the presented features remain accessible.

The smallness of the R -parity violating parameters guarantees that the direct production cross sections for the SUSY particles are very similar to the corresponding MSSM/NMSSM values.

LHC phenomenology of the $\mu\nu$ SSM

This chapter is dedicated to the LHC phenomenology of the $\mu\nu$ SSM with one or two right-handed neutrino superfields as we have discussed it in [122]. All the following statements are based on tree-level calculations, partially using one-loop corrected $\overline{\text{DR}}$ neutralino masses. Correlations between branching ratios and the neutrino mixing angles based on tree-level and one-loop calculations will be presented in Chapter 10.

8.1. Phenomenology of the 1 $\widehat{\nu}^c$ -model

First we will address the phenomenology of the $\mu\nu$ SSM with one right-handed neutrino superfield (1 $\widehat{\nu}^c$ -model), which includes mass hierarchies, the mixing in the scalar and fermionic sectors and decays of scalar and fermionic states. Within the discussion we call a neutralino mass eigenstates $\tilde{\chi}_i^0$ a bino \tilde{B} , if $|\mathcal{N}_{i+3,1}|^2 > 0.5$ is fulfilled. Similarly a singlino \tilde{S} is defined as $|\mathcal{N}_{i+3,5}|^2 > 0.5$. Note that the first three indices label the neutrinos. As we will see later, a light singlino as lightest neutralino also gives rise to light scalar S_i^0 and/or pseudoscalar states P_i^0 .

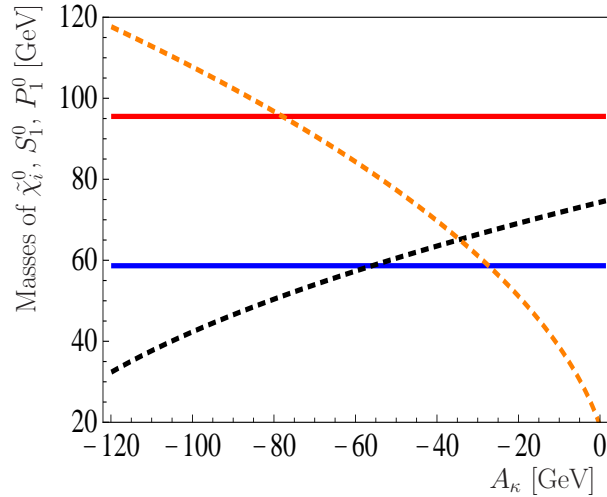


Figure 8.1.: Masses of the lightest neutralinos $\tilde{\chi}_{1,2}^0$ and the lightest scalar $S_1^0 = \text{Re}(\tilde{\nu}^c)$ /pseudoscalar $P_1^0 = \text{Im}(\tilde{\nu}_1^c)$ as a function of $A_\kappa = T_\kappa/\kappa$ for $\lambda = 0.24$, $\kappa = 0.060$, $\mu = 150$ GeV and $T_\lambda = 360$ GeV for SPS 1a'. The different colors refer to the singlino $\tilde{\chi}_1^0$ (blue), the bino $\tilde{\chi}_2^0$ (red), the singlet scalar S_1^0 (black, dashed) and the singlet pseudoscalar P_1^0 (orange, dashed).

According to Equation (5.73) the diagonal entry of the right-handed neutrino in the neutralino mass matrix is given by $m_c = \sqrt{2}\kappa v_c$. Hence, a singlino as lightest neutralino can be obtained by choosing small values for κ and/or v_c . In the discussion within this section we do not refer to the

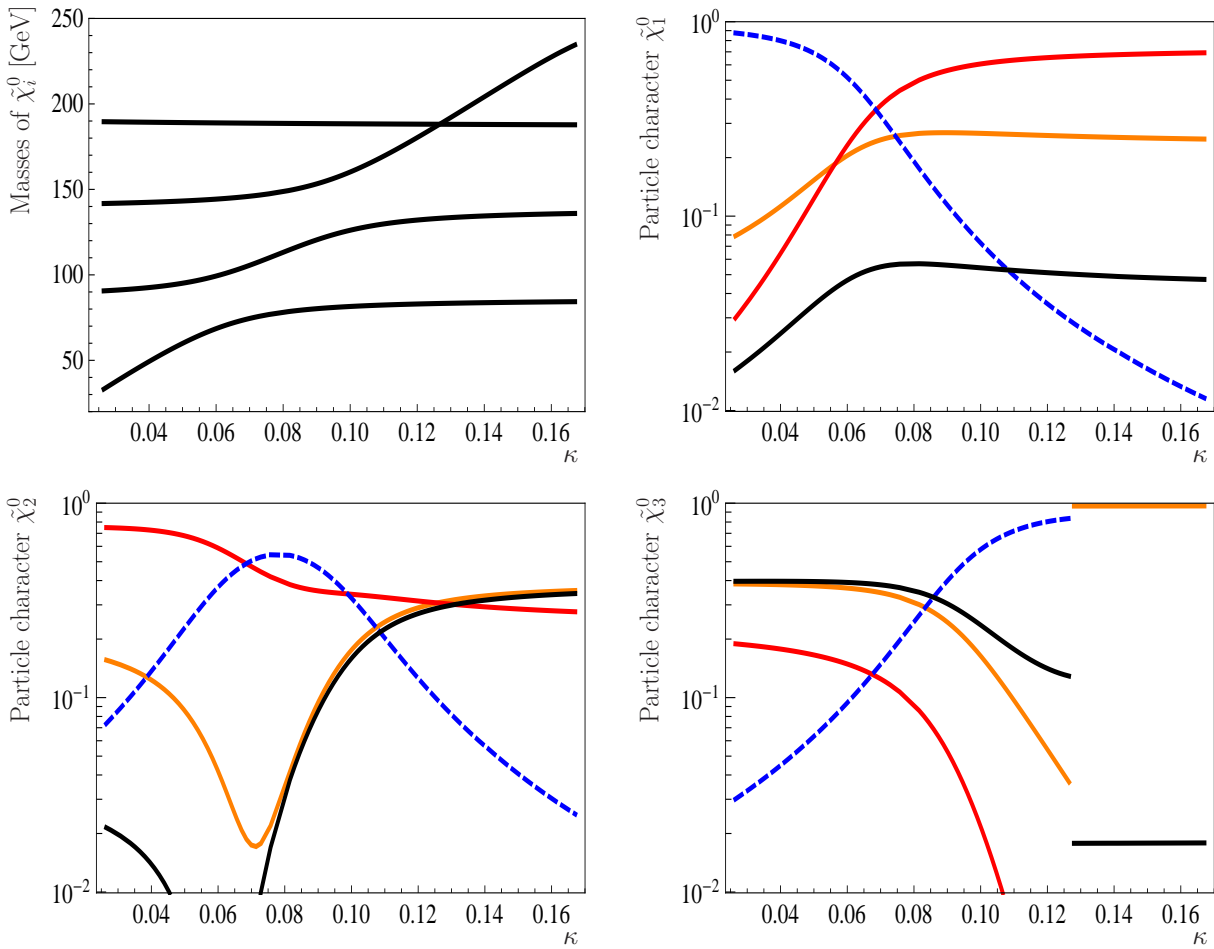


Figure 8.2.: One-loop $\overline{\text{DR}}$ masses and particle characters of the lightest neutralinos $\tilde{\chi}_i^0$ as a function of κ for $\lambda = 0.24$, $\mu = 170$ GeV, $T_\lambda = 360$ GeV and $T_\kappa = -\kappa \cdot 50$ GeV for SPS 1a'. The different colors refer to singlino purity $|\mathcal{N}_{i+3,5}|^2$ (blue, dashed), bino purity $|\mathcal{N}_{i+3,1}|^2$ (red), wino purity $|\mathcal{N}_{i+3,2}|^2$ (black) and Higgsino purity $|\mathcal{N}_{i+3,3}|^2 + |\mathcal{N}_{i+3,4}|^2$ (orange).

NMSSM benchmark scenarios adapted to the $\mu\nu$ SSM, but to MSSM benchmark scenarios and specify in addition the chosen values of λ, κ and an effective μ , from which we derive v_c using Equation (4.10). By appropriate choices of T_λ and T_κ a light singlet scalar and/or pseudoscalar can be obtained as it can be seen for an example spectrum in Figure 8.1.

We explained the determination of T_λ and T_κ for the NMSSM in Section 5.1.2, which exactly resembles the behavior in Figure 8.1, namely an increasing mass of the singlet scalar and a decreasing mass of the singlet pseudoscalar mass with growing T_κ . The MSSM parameters for this example spectrum are based on the benchmark scenario SPS 1a' except for the choice $\mu = 150$ GeV. Reducing μ helps to lower the mixing between the scalar state $S_2^0 = h^0$ and the lighter singlet scalar $S_1^0 = \tilde{\nu}^c$, so that S_2^0 is still consistent with experimental data from LEP. Note that the mixing with the singlet state also reduces the production rate $e^+e^- \rightarrow ZS_2^0$, however the bounds on h^0 remain strict.

For SPS 1a' with a reduced value of $\mu = 170$ GeV we present an example spectrum for neutral fermions using $\overline{\text{DR}}$ corrected one-loop masses in Figure 8.2. For reduced values of μ the neutralino mass eigenstates are rather mixed, what becomes important for their decay properties.

Note that the abrupt change in the composition of $\tilde{\chi}_3^0$ can be understood from a level-crossing in the mass eigenstates $\tilde{\chi}_3^0$ and $\tilde{\chi}_4^0$.

Before discussing the R -parity violating decay of the lightest supersymmetric particle, we want to focus on the decay properties of the lightest scalars/pseudoscalars in the 1 $\hat{\nu}^c$ -model, which are quite similar to those found in the NMSSM [110, 170]. The lightest doublet Higgs boson similar to the h^0 in the MSSM mainly decays into $b\bar{b}$ final states for masses $m_{h^0} < 140$ GeV. However, if there exists a light neutralino, the decay into $\tilde{\chi}_1^0\tilde{\chi}_1^0$ can be dominant. An example is presented in Figure 8.3, which displays the branching ratios of $S_2^0 = h^0$ as a function of the lightest neutralino mass $m(\tilde{\chi}_1^0)$ based on the parameter set of Figure 8.2 with a variation of κ . As it can be seen from Figure 8.2 the lightest neutralino is mainly singlino in this example. The variation of κ varies its mass, since v_c is kept fixed. This feature $h^0 \rightarrow \tilde{\chi}_1^0\tilde{\chi}_1^0$ is of course also possible in the NMSSM with $\tilde{\chi}_1^0 = \tilde{S}$ or even the MSSM with a very light bino state. However, in the (N)MSSM the lightest neutralino is stable, implying an invisible decay of the light doublet Higgs h^0 . In case of R -parity violation the lightest neutralino $\tilde{\chi}_1^0$ mainly decays to $b\bar{b}\nu$, resulting in 4 b -jets plus missing energy in the final state in combination with displaced vertices in our example. As we will show in Section 8.1.2 the lightest neutralino $\tilde{\chi}_1^0$ can have a long lifetime due to the small R -parity violating parameters, so that the decay of h^0 can result in displaced vertices. Note that the singlet scalar S_1^0 dominantly decay to $b\bar{b}$ final states, followed by $\tau^+\tau^-$ final states.

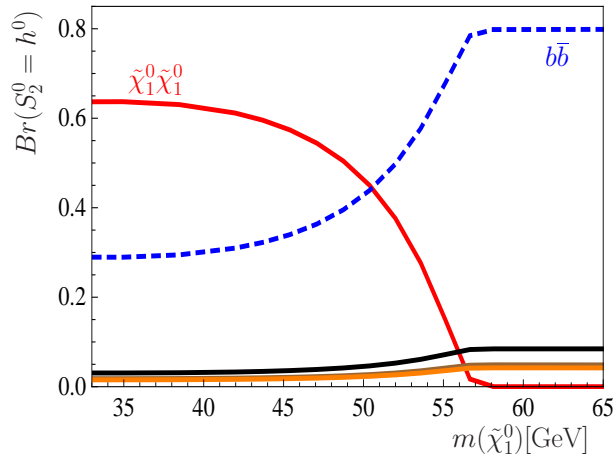


Figure 8.3.: Branching ratios $Br(S_2^0 = h^0)$ as a function of $m(\tilde{\chi}_1^0)$ for the parameter set of Figure 8.2 (variation of κ). The colors indicate the different final states: $\tilde{\chi}_1^0\tilde{\chi}_1^0$ (red), $b\bar{b}$ (blue, dashed), $\tau^+\tau^-$ (black), $c\bar{c}$ (orange) and $Wq\bar{q}$ (brown).

8.1.1. Decays of a gaugino-like lightest neutralino

Before addressing the dependence of the decays of the lightest neutralino on the particle character, we first want to show all possible decay modes of the lightest neutralino induced by lepton number violating terms: Beside the two-body decays $\tilde{\chi}_1^0 \rightarrow Z\nu$, $\tilde{\chi}_1^0 \rightarrow l^\pm W^\mp$ and $\tilde{\chi}_1^0 \rightarrow S_i^0\nu / P_i^0\nu$, which are generally but not necessarily dominant for larger masses of the neutralino, several tree-body decays into leptonic final states are possible, namely $\tilde{\chi}_1^0 \rightarrow l_i^\pm l_j^\mp \nu$, $\tilde{\chi}_1^0 \rightarrow q_i \bar{q}_j l$, $\tilde{\chi}_1^0 \rightarrow 3\nu$ or $\tilde{\chi}_1^0 \rightarrow q_i \bar{q}_j \nu$. If charged leptons are in the final state one can expect a correlation between neutrino physics and ratios of branching ratios, as we have indicated in Section 5.5.

Br in %	SPS 1a'	SPS 3	SPS 4
$Br(\tilde{\chi}_1^0 \rightarrow l^\pm W^\mp)$	23 – 80	12 – 55	68 – 72
$Br(\tilde{\chi}_1^0 \rightarrow l_i^\pm l_j^\mp \nu)$	11 – 75	2 – 31	2.6 – 3.9
$Br(\tilde{\chi}_1^0 \rightarrow Z\nu)$	2.2 – 8.9	5 – 28	25 – 28
$Br(\tilde{\chi}_1^0 \rightarrow S_i^0 \nu)$	–	15 – 53	< 2.0
Decay length [mm]	1.6 – 7.0	0.1 – 0.5	1.4 – 1.6

Table 8.1.: Branching ratios (in %) and total decay length in mm of the decay of the lightest bino-like neutralino for different values of $\lambda \in [0.02, 0.5]$ and $\kappa \in [0.05, 0.3]$ with a dependence of allowed $\kappa(\lambda)$ similar to [111] and to Figure 8.5 and $T_\lambda = \lambda \cdot 1.5$ TeV and $T_\kappa = -\kappa \cdot 100$ GeV.

We first stick to the case of a bino as lightest neutralino. For the SPS points under consideration it yields $m(\tilde{\chi}_1^0) > m_W$, so that the two-body decays $\tilde{\chi}_1^0 \rightarrow l^\pm W^\mp$ are dominant. However, the three-body decays, in particular $\tilde{\chi}_1^0 \rightarrow l_i l_j \nu$ dominated by a virtual $\tilde{\tau}$, can have a sizable branching ratio as it can be seen from Table 8.1 and Figure 8.5. The most important Feynman graph is shown in Figure 8.4, whose dominance can be understood from Higgsino \tilde{H}_d^- and lepton l_i mixing ($l_i = e, \mu$). For $l_i = \tau$ exists an additional contribution induced by \tilde{H}_d^0 - ν -mixing.

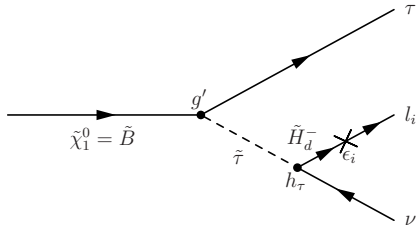


Figure 8.4.: Dominant Feynman graph for the decay $\tilde{\chi}_1^0 \rightarrow l_i \tau \nu$ with $l_i = e, \mu$.

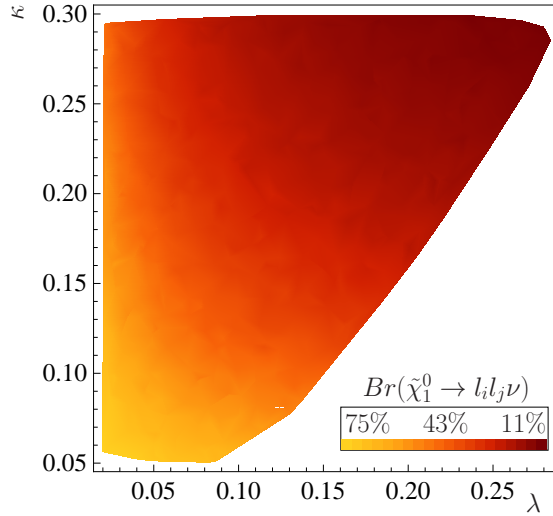


Figure 8.5.: Dependence of allowed $\kappa(\lambda)$ for values of $\lambda \in [0.02, 0.5]$ and $\kappa \in [0.05, 0.3]$ and $Br(\tilde{\chi}_1^0 \rightarrow l_i l_j \nu)$ as function of λ and κ exemplary for SPS 1a' with $\mu = 390$ GeV, $T_\lambda = \lambda \cdot 1.5$ TeV and $T_\kappa = -\kappa \cdot 100$ GeV.

Figure 8.5 shows the allowed parameter dependence of $\kappa(\lambda)$ due to tachyonic states. The figure also indicates the importance of the decay mode $\tilde{\chi}_1^0 \rightarrow l_i l_j \nu$ in comparison with $\tilde{\chi}_1^0 \rightarrow l^\pm W^\mp$ in the λ - κ -plane. The strong variation in the branching ratios for SPS 1a' is mainly induced by the strong dependence of the partial decay width of $\tilde{\chi}_1^0 \rightarrow l_i l_j \nu$, where both decays with $l_i = l_j = \tau$ and $l_i \neq l_j = \tau$ play a role. As demonstrated in Table 8.1 also the final states $\tilde{\chi}_1^0 \rightarrow Z\nu$ and in case of a light scalar with $m(\tilde{\chi}_1^0) > m(h^0)$ the decay $\tilde{\chi}_1^0 \rightarrow h^0 \nu$ can be important.

To stick to one example, where only three-body decay modes are allowed, we use the SU4 scenario of the ATLAS collaboration [163], which offers a very light SUSY spectrum with a

bino-like neutralino $m(\tilde{\chi}_1^0) \approx 60$ GeV. Figure 8.6 shows the most important branching ratios. The lightness of the bino-like neutralino $\tilde{\chi}_1^0$ results in a larger average decay length of (8–90) cm, strongly dependent on the parameter point in the λ - κ -plane. Generally the decay length scales as $L \propto m^{-4}(\tilde{\chi}_1^0)$ for $m(\tilde{\chi}_1^0) < m_W$. In addition the decay length becomes smaller for smaller values of λ and κ .

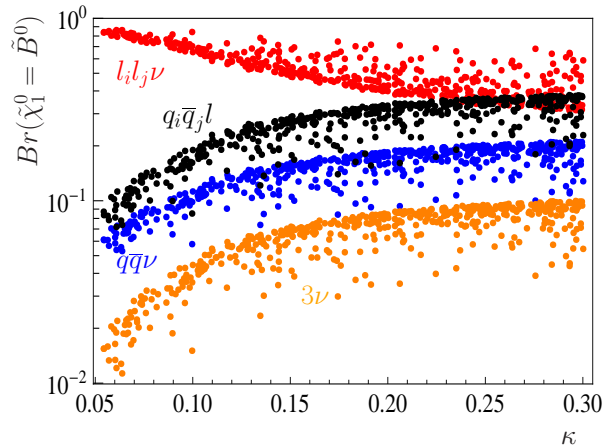


Figure 8.6.: Decay branching ratios for bino-like lightest neutralino as a function of κ for $\lambda \in [0.02, 0.5]$, $T_\lambda = \lambda \cdot 1.5$ TeV, $T_\kappa = -\kappa \cdot 100$ GeV and for MSSM parameters defined by the study point SU4 of the ATLAS collaboration [163]. The colors indicate the different final states: $l_i l_j \nu$ (red), $q_i \bar{q}_j l$ (black), $q \bar{q} \nu$ (blue) and 3ν (orange).

Last we want to mention that also chargino decays can be dominated by R -parity violating final states, for example in the AMSB point SPS 9. For this benchmark scenario exists a near degeneracy between the lightest neutralino and the lightest chargino. Varying λ and κ as before we find a total decay length of (0.12 – 0.16)mm with $Br(\tilde{\chi}_1^\pm \rightarrow W^\pm \nu) = (42 - 57)\%$, $Br(\tilde{\chi}_1^\pm \rightarrow Z l^\pm) = (20 - 26)\%$ and $Br(\tilde{\chi}_1^\pm \rightarrow h^0 l^\pm) = (17 - 40)\%$.

8.1.2. Decays of a singlino-like lightest neutralino

Having discussed the case of a gaugino-like LSP in great detail, we now turn to the case of a singlino-like lightest neutralino. As we have already shown in the previous sections, this scenario is connected to a light singlet scalar or pseudoscalar. Recall that in general the particles in the fermionic sector are strongly mixed for $\lambda, \kappa = \mathcal{O}(10^{-1})$ in combination with a low value of the effective μ -parameter as we have seen in Figure 8.2. Our primary focus for the singlino-like lightest neutralino is the average decay length, which we show in Figure 8.7 in meter for various SPS scenarios as a function of the lightest neutralino $m(\tilde{\chi}_1^0)$. The composition of the neutralino can be taken from the color code given in the caption. We varied λ , κ and μ to allow for different LSP masses and we have chosen T_κ in such a way, that all scalar and pseudoscalar states are heavier than the lightest neutralino. The singlino purity of the LSP increases with decreasing mass and for pure singlinos the decay length is mainly determined by its mass and the neutrino masses. However, for neutralino masses below 50 GeV the decay lengths become larger than 1 m, so that a large fraction of neutralinos does not decay within typical collider detectors. If we allow for lighter scalar and/or pseudoscalar states, so that the decays $\tilde{\chi}_1^0 \rightarrow S_1^0(P_1^0)\nu$ are kinematically allowed, the average decay length is easily reduced by several orders of magnitude. Similar to the case of a gaugino-like lightest neutralino typical final states are $l^\pm W^\mp$, $q_i \bar{q}_j l$, $Z\nu$, $q_i \bar{q}_j \nu$, $l_i^\pm l_j^\mp \nu$ and the invisible final state 3ν . For the region below the W threshold, meaning

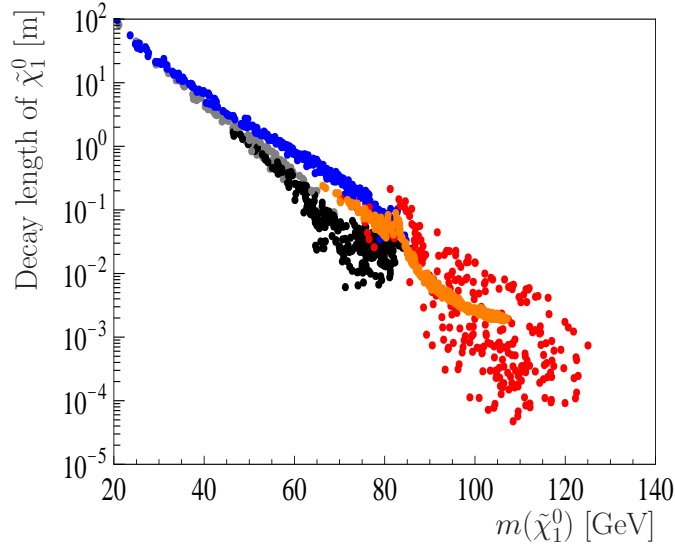


Figure 8.7.: Decay length of the lightest neutralino $\tilde{\chi}_1^0$ in m as a function of its mass $m(\tilde{\chi}_1^0)$ in GeV for different values of $\lambda \in [0.2, 0.5]$, $\kappa \in [0.0125, 0.1]$ and $\mu \in [110, 170]$ GeV with a dependence of allowed $\kappa(\lambda)$ similar to [111] and to Figure 8.5 and $T_\lambda = \lambda \cdot 1.5$ TeV, whereas $T_\kappa \in [-10, -0.025]$ GeV is chosen in such a way, that no lighter scalar or pseudoscalar states with $\{m(S_1^0), m(P_1^0)\} < m(\tilde{\chi}_1^0)$ appear. Note that the different colors stand for SPS 1a' (real singlino, $|\mathcal{N}_{45}|^2 > 0.5$) (gray), SPS 1a' (mixture state) (black), SPS 3 (real singlino) (blue), SPS 3 (mixture state) (red) and SPS 4 (mixture state) (orange).

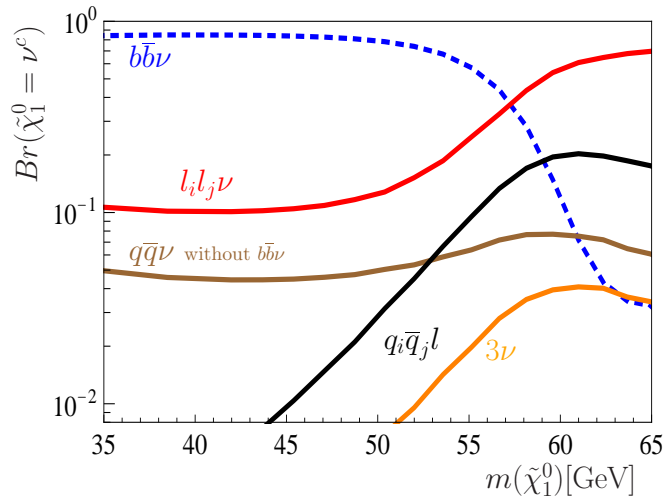


Figure 8.8.: Singlino decay branching ratios as a function of its mass, for the same parameter choices as in Figure 8.3. The colors indicate the different final states: $b\bar{b}\nu$ (blue, dashed), $l_i l_j \nu$ (red), $q_i \bar{q}_j l$ (black), 3ν (orange) and $q\bar{q}\nu$ ($q \neq b$, brown).

$m(\tilde{\chi}_1^0) < m_W$, we refer to Figure 8.8. The dominance of $b\bar{b}\nu$ for smaller values of $m(\tilde{\chi}_1^0)$ is induced by the decay chain $\tilde{\chi}_1^0 \rightarrow S_1^0 \nu \rightarrow b\bar{b}\nu$, whereas for larger values of $m(\tilde{\chi}_1^0)$ we have $m(S_1^0) > m(\tilde{\chi}_1^0)$ in this scenario.

Up to now we have considered values of λ and κ larger than 10^{-2} . However, for very small values of these couplings the singlet sector effectively decouples from the MSSM sector, although all singlet particles are very light. Necessarily the R -parity conserving decays of the second lightest neutralino $\tilde{\chi}_2^0$ to the final states $\tilde{\chi}_1^0 S_1^0$, $\tilde{\chi}_1^0 P_1^0$, $\tilde{\chi}_1^0 l^+ l^-$ or $\tilde{\chi}_1^0 q \bar{q}$ are suppressed in comparison to the R -parity violating decay modes, which implies a correlation between those decays and neutrino physics as in case of explicit BRpV.

8.2. Phenomenology of the $n \hat{\nu}^c$ -model

In the previous section the phenomenology of the $\mu\nu$ SSM with one right-handed neutrino superfield has been worked out in detail. In fact most of the signals discussed there are independent of the number of right-handed neutrinos. However, in case of n generations some additional features are possible, which we will discuss for the case of $n = 2$.

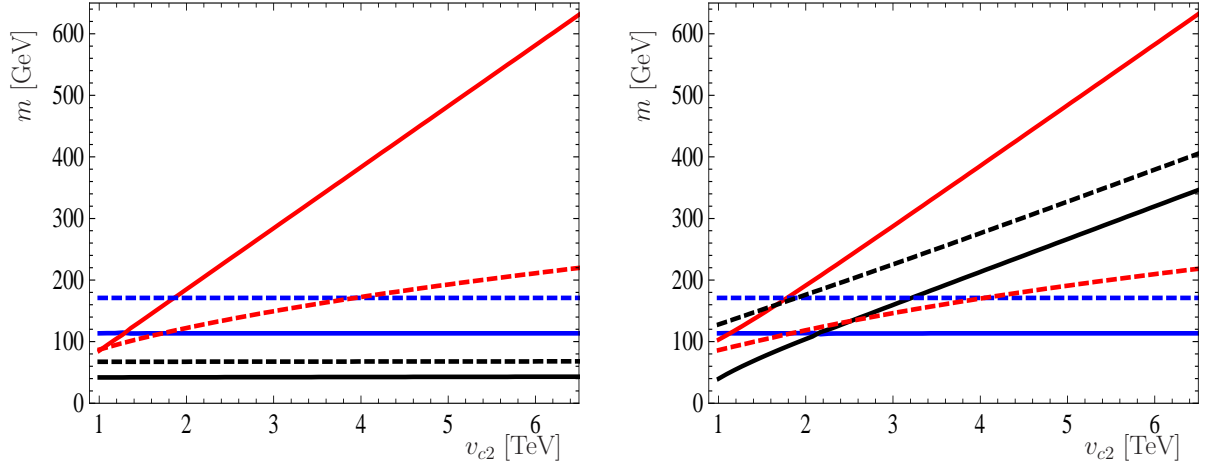


Figure 8.9.: Masses of the scalar states $\text{Re}(\tilde{\nu}_1^c)$ (black), $\text{Re}(\tilde{\nu}_2^c)$ (red) and h^0 (blue) and the pseudoscalar states $\text{Im}(\tilde{\nu}_1^c)$ (black, dashed), $\text{Im}(\tilde{\nu}_2^c)$ (dashed red) and $\text{Im}(\tilde{\nu}_1)$ (blue, dashed) as a function of v_{c2} for different values of $T_{\kappa}^{112} = T_{\kappa}^{122}$: **a)** (left) $T_{\kappa}^{112} = T_{\kappa}^{122} = 0$; **b)** (right) $T_{\kappa}^{112} = T_{\kappa}^{122} = -1$ GeV. The MSSM parameters have been taken such that the standard SPS 1a' point is reproduced. The light singlet parameters $\kappa_1 = 0.008$ and $v_{c1} = 500$ GeV ensure that in all points the lightest neutralino is mostly ν_1^c , with a mass of 47–48 GeV. In addition, $T_{\lambda}^1 = 300$ GeV and $T_{\lambda}^2 \in [10, 200]$ GeV.

As we have shown in accordance to the NMSSM [110, 171] a light singlino always implies a light scalar/pseudoscalar in the $\mu\nu$ SSM with one right-handed neutrino superfield. However, in case of more than one generation of singlets the off-diagonal T_{κ} terms in Equation (4.11) allow for additional mixing between the different generations of singlet scalars and pseudoscalars. Thus, the singlet scalars/pseudoscalars can be considerably heavier than the singlet fermions.

We illustrate this feature with an example. If we consider a scenario with a light singlino ν_1^c and a heavy singlino ν_2^c in a model with nonzero trilinear couplings T_{κ}^{112} , the contributions to the mass of the scalar or pseudoscalar $\tilde{\nu}_1^c$ coming together with the large value of v_{c2} are proportional to T_{κ}^{112} . Neglecting those contributions the mass of $\tilde{\nu}_1^c$ would only depend on the small v_{c1} . Hence it would be light like the corresponding singlino of the same generation.

However, with nonzero T_κ^{112} the mass of both $\tilde{\nu}_i^c$ are dominated by the larger values of v_{c_i} . Figure 8.9 demonstrates this feature. The lightest neutralino in both figures is the singlino ν_1^c with a mass of ~ 50 GeV. Both figures show the masses of the singlet scalar states $\text{Re}(\tilde{\nu}_1^c)$ and $\text{Re}(\tilde{\nu}_2^c)$ and the corresponding pseudoscalar states $\text{Im}(\tilde{\nu}_1^c)$ and $\text{Im}(\tilde{\nu}_2^c)$ as a function of the VEV v_{c2} for different values of $T_\kappa^{112} = T_\kappa^{122}$. For comparison also the masses of the light Higgs boson and the lightest left-handed sneutrino $\text{Im}(\tilde{\nu}_1)$ are shown. As expected the mass of the lightest singlet scalar does not depend on v_{c2} in case of $T_\kappa^{112} = T_\kappa^{122} = 0$, whereas for a nonzero $T_\kappa^{112} = T_\kappa^{122} = -1$ GeV $\text{Re}(\tilde{\nu}_1^c)$ becomes heavier for larger values of v_{c2} . In the pseudoscalar sector this effect is comparable, but even more pronounced.

8.2.1. $\tilde{\chi}_1^0$ decay length and type of fit

In Section 6.3 we presented two different possibilities to fit neutrino data, namely $\vec{\Lambda}$ can generate the atmospheric mass scale and $\vec{\alpha}$ the solar mass scale (fit1) or vice versa (fit2). In fact the decay length of the lightest neutralino is sensitive to the type of the fit, due to the proportionality between its couplings with gauge bosons and the R -parity violating parameters as indicated in Section 5.5.

To point out this feature we consider a simple example with a singlino-like neutralino, which couples to the gauge bosons proportional to the α_i parameters. Therefore, its decay length follows $L \propto 1/|\vec{\alpha}|^2$ and obeys the approximate relation

$$\frac{L(\text{fit1})}{L(\text{fit2})} \simeq \frac{m_{atm}}{m_{sol}} \simeq 6 \quad . \quad (8.1)$$

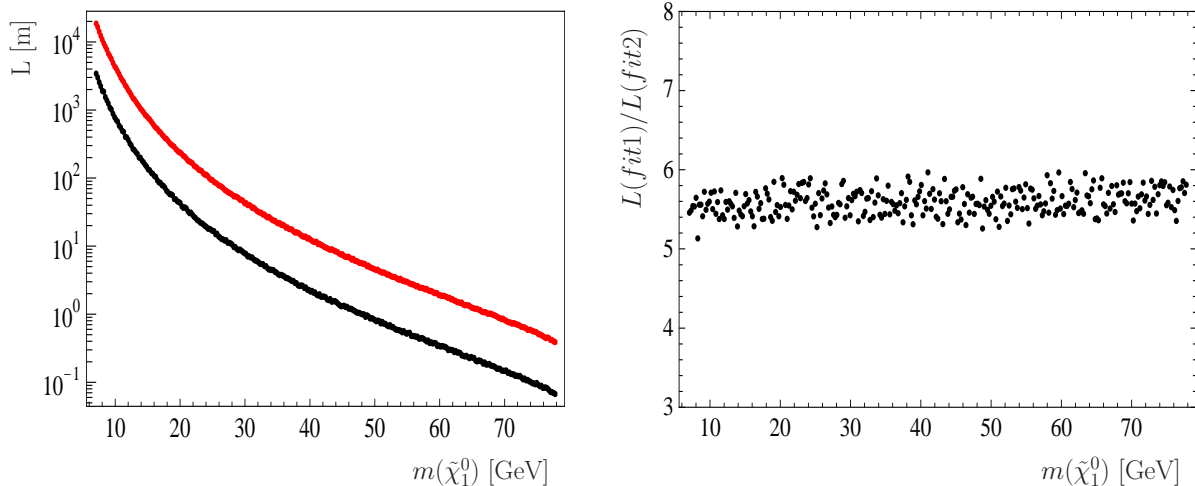


Figure 8.10.: Decay length of the lightest neutralino and its dependence on the type of fit to neutrino data: **a)** (left) the decay length of the lightest neutralino as a function of $m(\tilde{\chi}_1^0)$ for the case fit1 (red) and the case fit2 (blue); **b)** (right) the ratio $L(\text{fit1})/L(\text{fit2})$ as a function of $m(\tilde{\chi}_1^0)$. The MSSM parameters have been taken such that the standard SPS 1a' point is reproduced. The light singlet parameter κ is varied in the range $\kappa \in [0.005, 0.05]$. In all the points the lightest neutralino has a singlino purity higher than 0.99.

Figure 8.10 shows the decay length of the lightest neutralino and its dependence on the type of fit to neutrino data as a function of $m(\tilde{\chi}_1^0)$. Suppose the mass and decay length are known, this dependence allows to determine the type of fit. Note that this feature is independent of the MSSM parameters. However, it is lost in cases where the lightest neutralino has a sizable

gaugino or Higgsino component or lighter scalars/pseudoscalars are present opening additional decay channels.

8.2.2. Several light singlets

In case of two or even more light singlets the phenomenology of the $\mu\nu$ SSM can be even richer. Again the decays of the light Higgs boson h^0 can be strongly influenced by the presence of additional light singlets, namely it can decay with measurable branching ratios to pairs of right-handed neutrinos of different generations. Similarly also the MSSM neutralinos can decay to different light right-handed neutrinos.

We consider the case of two light singlinos and two light scalars/pseudoscalars. Then we obtain a mass spectrum with the singlets ν_1^c and ν_2^c as the two lightest neutralinos $\tilde{\chi}_{1,2}^0$ and a mass eigenstate $\tilde{\chi}_3^0$ being mostly a bino. The scalar sector contains two very light mostly singlet states S_1^0 and S_2^0 , which are consistent with the LEP bounds. Finally the state S_3^0 can be identified as the light doublet Higgs boson h^0 . Similarly the pseudoscalar sector can contain light singlet states.

It turns out that the decays of the bino-like neutralino $\tilde{\chi}_3^0$ can be very important to distinguish between the model with one light singlet and models with several ones. Since the decay channels strongly dependent on the particle spectrum including the masses of singlinos and scalars/pseudoscalars a general list of signals cannot be given. However, some features are always present: If they are kinematically allowed the decays $\tilde{\chi}_3^0 \rightarrow \tilde{\chi}_{1,2}^0 S_1^0 (P_1^0)$ will dominate with the sum of branching ratios typically larger than 50%. Therein kinematics mainly dictates the relative importance of the different decay channels.

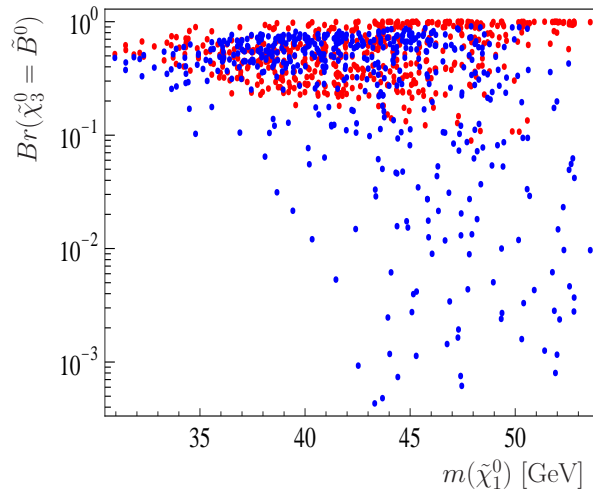


Figure 8.11.: Branching ratios $Br(\tilde{\chi}_3^0 = \tilde{B}^0 \rightarrow \tilde{\chi}_1^0)$ (red) and $Br(\tilde{\chi}_3^0 = \tilde{B}^0 \rightarrow \tilde{\chi}_2^0)$ (blue) as a function of the mass of the lightest neutralino for the scenario considered in Section 8.2.2. The MSSM parameters have been taken such that the standard SPS 1a' point is reproduced, whereas the singlet parameters are chosen randomly in the ranges $v_{c1}, v_{c2} \in [400, 600]$ GeV, $\lambda_1, \lambda_2 \in [0.0, 0.4]$, $T_\kappa^{111} = T_\kappa^{222} \in [-7.5, -0.5]$ GeV, $T_\kappa^{112} = T_\kappa^{122} \in [-0.75, -0.0025]$ GeV and $T_\lambda^1, T_\lambda^2 \in [0, 600]$ GeV. $\kappa_1 = \kappa_2 = 0.008$ is fixed to ensure the lightness of the two singlinos.

Figure 8.11 illustrates this feature, where we show both branching ratios as a function of the mass of the lightest neutralino. Whereas the singlet parameters are taken randomly, the rest of the spectrum is fixed by the benchmark scenario SPS 1a'. Both branching ratios are at least of order $10^{-3} - 10^{-4}$ allowing for enough statistics, although the relative importance of each singlino

cannot be predicted in general. For very light singlinos the two-body decays $\tilde{\chi}_3^0 \rightarrow \tilde{\chi}_1^0 S_1^0(P_1^0)$ and $\tilde{\chi}_3^0 \rightarrow \tilde{\chi}_2^0 S_1^0(P_1^0)$ are open, so that the branching ratios are close to 50% as expected if the singlet parameters of both generations are of the same size. If the mass of the lightest neutralino is increased, some of the two-body decays close, in particular the one involving $\tilde{\chi}_2^0$, which has to be produced through three-body decays, resulting in a suppression of $Br(\tilde{\chi}_3^0 \rightarrow \tilde{\chi}_2^0)$. Keep in mind that also the decay mode $\tilde{\chi}_3^0 \rightarrow \tilde{\chi}_{1,2}^0 S_2^0(P_2^0)$ might be relevant with branching ratios about 10% – 20% giving additional information.

Beside the singlet scalars/pseudoscalars appearing in the final states also the other usual bino decays of the NMSSM are possible, namely $\tilde{\chi}_{1,2}^0 l^+ l^-$ or $\tilde{\chi}_{1,2}^0 q \bar{q}$ final states, in particular when the decays to singlet scalars/pseudoscalars are kinematically forbidden.

As argued in the $\mu\nu$ SSM with one right-handed neutrino superfield the decays of the light Higgs boson h^0 are also strongly influenced by the presence of light singlet states, since final states can involve $\tilde{\chi}_1^0$ or $\tilde{\chi}_2^0$. In this case typically the standard Higgs boson decays are reduced to less than 40%, completely spoiling the usual search strategies.

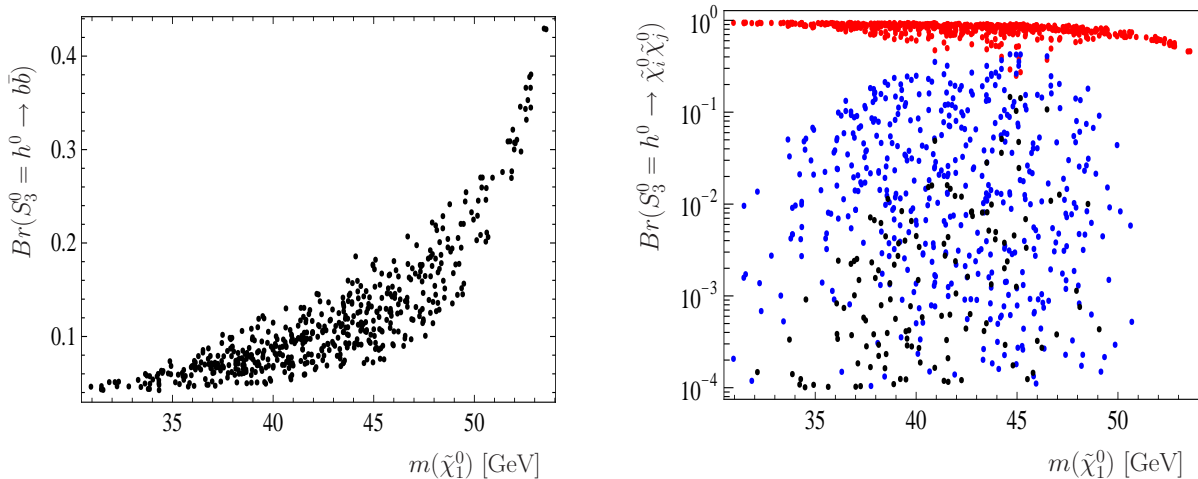


Figure 8.12.: Higgs boson decays as a function of the mass of the lightest neutralino for the scenario considered in Section 8.2.2: **a)** (left) the standard decay channel $h^0 \rightarrow b\bar{b}$; **b)** (right) the exotic decays to pairs of singlinos $h^0 \rightarrow \tilde{\chi}_1^0 \tilde{\chi}_1^0$ (red), $h^0 \rightarrow \tilde{\chi}_1^0 \tilde{\chi}_2^0$ (blue) and $h^0 \rightarrow \tilde{\chi}_2^0 \tilde{\chi}_2^0$ (black). The parameters are chosen as in Figure 8.11.

The branching ratios of the standard and exotic Higgs bosons are shown in Figure 8.12. Again the $b\bar{b}$ channel is more reduced compared to the main channel $\tilde{\chi}_1^0 \tilde{\chi}_1^0$ the lighter the neutralino mass $\tilde{\chi}_1^0$ gets. However, also the branching ratio to $\tilde{\chi}_1^0 \tilde{\chi}_2^0$ can be sizable. Note that $\tilde{\chi}_2^0$ decays dominantly to $\tilde{\chi}_1^0$ plus two SM fermions. Thus, we can distinguish between the 1 $\hat{\nu}^c$ -model and models with more than one generation of singlets. The decay to $\tilde{\chi}_2^0 \tilde{\chi}_2^0$ is small due to kinematics, but can lead to interesting final states with up to 8 b -jets and missing energy. We want to add that in those scenarios with many light singlets $\tilde{\chi}_1^0$ might dominantly decay to $b\bar{b}\nu$, which reduces statistics in the more interesting $l_i^\pm l_j^\mp \nu$ and $q_i \bar{q}_j l$ channels. Additionally mixing effects in the singlet sector might lead to less pronounced correlations.

One-loop calculations - Masses and total decay widths

This chapter is dedicated to the one-loop corrections for the neutralino and chargino masses and the processes under consideration for the various models. As we have pointed out in the previous sections the one-loop corrections to masses are crucial for the phenomenology of SUSY models and even necessary in case of BRpV and the $\mu\nu$ SSM with one right-handed neutrino superfield to explain the full neutrino spectrum. We show that also the corrections to the decay widths can be sizable and therefore important for SUSY cascade decays and the decays of the LSP in R -parity violation. The technical aspects of the one-loop calculations are presented in Appendix E, namely we show the UV and IR finiteness as well as the gauge independence of the masses and decay widths at one-loop level. In addition we comment on the renormalization scale dependence within the appendix.

9.1. One-loop masses of neutralinos and charginos

In this section we discuss the one-loop on-shell masses for neutralinos and charginos as explained in Section 6.2.3 for the various models under consideration. First we present the on-shell masses in case of the MSSM and NMSSM, before sticking to R -parity violating models. The corrections to the tree-level and one-loop on-shell masses of the heavy neutralinos and charginos (meaning the neutralinos and charginos present in the (N)MSSM) originating from the R -parity violating parameters are negligible. Therefore in case of the R -parity violating models we will focus on the neutrino and lepton masses and discuss the differences between their on-shell definition and the corresponding $\overline{\text{DR}}$ masses.

9.1.1. Heavy neutralinos and charginos

For the MSSM and the NMSSM benchmark scenarios, which we introduced in Chapter 7 we present the tree-level and one-loop on-shell masses in Tables 9.1 and 9.2. The mass corrections $m \rightarrow m^{1L}$ are generally small, in most cases in the per-mil range. Only the light singlino in the mSUGRA 4 scenario gets a large correction of 2.6% from squark and quark contributions.

9.1.2. Neutrino and lepton masses, neutrino mixing angles

In this section we discuss the one-loop corrections to the neutrino and lepton mass eigenstates in the neutralino and chargino mass matrices. As already indicated the effect of the R -parity violating parameters to the heavy neutralino and chargino masses is negligible. As starting point we illustrate the behavior of the absolute neutrino masses and emphasize that the on-shell renormalization allows a similar parameter dependence as the $\overline{\text{DR}}$ masses as they are defined in Section 6.3 or [97]. We stress once again that the one-loop on-shell corrections do not vanish due to the number of free parameters at tree-level.

	SPS 1a'	SPS 3	SPS 4	SPS 9	SPS 2'	SU4
$\tilde{\chi}_1^0 : m$	96.20	157.43	117.18	164.28	389.57	59.66
m^{1L}	95.88	157.19	117.00	164.30	389.20	59.23
C	\tilde{B}	\tilde{B}	\tilde{B}	\tilde{W}	\tilde{H}	\tilde{B}
$\tilde{\chi}_2^0 : m$	176.24	290.12	213.51	527.79	416.08	108.30
m^{1L}	176.32	290.47	213.92	527.64	416.04	108.27
C	\tilde{W}	\tilde{W}	\tilde{W}	\tilde{B}	\tilde{H}	\tilde{W}
$\tilde{\chi}_3^0 : m$	396.34	518.53	384.35	1024.68	600.00	313.23
m^{1L}	397.62	518.74	384.93	1023.90	599.87	315.36
C	\tilde{H}	\tilde{H}	\tilde{H}	\tilde{H}	\tilde{B}	\tilde{H}
$\tilde{\chi}_4^0 : m$	411.66	534.28	400.96	1028.75	626.51	328.49
m^{1L}	410.21	532.92	399.86	1029.53	626.18	326.30
C	\tilde{H}	\tilde{H}	\tilde{H}	\tilde{H}	\tilde{W}	\tilde{H}
$\tilde{\chi}_1^\pm : m$	175.86	289.89	213.31	164.28	396.53	107.64
m^{1L}	176.04	290.38	213.83	164.46	397.06	107.63
C	\tilde{W}^\pm	\tilde{W}^\pm	\tilde{W}^\pm	\tilde{W}^\pm	\tilde{H}^\pm	\tilde{W}^\pm
$\tilde{\chi}_2^\pm : m$	412.49	534.45	402.42	1028.71	621.36	330.17
m^{1L}	411.80	533.59	401.65	1028.35	620.57	329.53
C	\tilde{H}^\pm	\tilde{H}^\pm	\tilde{H}^\pm	\tilde{H}^\pm	\tilde{W}^\pm	\tilde{H}^\pm

Table 9.1.: Neutralino and chargino masses m at tree-level and m^{1L} at one-loop level in GeV and main particle character C for the MSSM using the ‘‘Snowmass Points and Slopes’’ [3] and the ATLAS SU4 point [163] benchmark scenarios.

	mSUGRA			mSUGRA		GMSB		
	1	3	4	3'	4'	1	2	5
$\tilde{\chi}_1^0 : m$	210.79	210.97	89.08	208.78	196.82	472.48	472.53	203.30
m^{1L}	210.61	210.77	91.45	208.55	199.51	472.38	472.39	203.30
C	\tilde{B}	\tilde{B}	\tilde{S}	\tilde{W}	\tilde{H}	\tilde{B}	\tilde{B}	\tilde{S}
$\tilde{\chi}_2^0 : m$	387.18	387.47	215.38	391.11	205.60	620.06	855.54	496.87
m^{1L}	387.10	387.37	215.58	390.82	205.24	620.06	855.53	496.81
C	\tilde{W}	\tilde{W}	\tilde{H}	\tilde{B}	\tilde{H}	\tilde{S}	\tilde{W}	\tilde{B}
$\tilde{\chi}_3^0 : m$	971.11	942.27	217.09	941.92	327.26	854.13	2352.36	899.60
m^{1L}	971.75	941.05	217.51	940.00	326.83	854.43	2352.49	899.98
C	\tilde{H}	\tilde{H}	\tilde{H}	\tilde{H}	\tilde{S}	\tilde{W}	\tilde{H}	\tilde{W}
$\tilde{\chi}_4^0 : m$	976.52	943.16	330.51	942.49	330.44	1405.44	2355.92	1377.67
m^{1L}	975.14	942.79	331.01	943.05	330.95	1405.15	2354.84	1377.45
C	\tilde{H}	\tilde{H}	\tilde{B}	\tilde{H}	\tilde{B}	\tilde{H}	\tilde{H}	\tilde{H}
$\tilde{\chi}_5^0 : m$	2101.57	1421.70	608.43	1421.70	608.43	1412.41	4062.82	1383.97
m^{1L}	2101.57	1421.67	607.64	1421.66	607.65	1411.46	4062.84	1383.04
C	\tilde{S}	\tilde{S}	\tilde{W}	\tilde{S}	\tilde{W}	\tilde{H}	\tilde{S}	\tilde{H}
$\tilde{\chi}_1^\pm : m$	387.16	387.48	201.36	208.83	201.36	854.11	855.53	899.59
m^{1L}	387.23	387.53	201.73	208.77	201.75	854.57	855.69	900.14
C	\tilde{W}^\pm	\tilde{W}^\pm	\tilde{H}^\pm	\tilde{W}^\pm	\tilde{H}^\pm	\tilde{W}^\pm	\tilde{W}^\pm	\tilde{W}^\pm
$\tilde{\chi}_2^\pm : m$	977.07	947.45	608.40	946.04	608.40	1412.29	2355.33	1384.24
m^{1L}	976.69	947.07	607.80	945.71	607.81	1411.62	2355.06	1383.51
C	\tilde{H}^\pm	\tilde{H}^\pm	\tilde{W}^\pm	\tilde{H}^\pm	\tilde{W}^\pm	\tilde{H}^\pm	\tilde{H}^\pm	\tilde{H}^\pm

Table 9.2.: Neutralino and chargino masses m at tree-level and m^{1L} at one-loop level in GeV and main particle character C for the NMSSM using the mSUGRA [164] and GMSB [165] benchmark scenarios.

The neutrino masses $m^{1L}(\nu_i)$ of the three left-handed neutrinos as a function of $|\vec{\epsilon}|^2/|\vec{\Lambda}|$ are shown in Figure 9.1. We set $\epsilon_1 = \epsilon_2 = \epsilon_3$ and $\Lambda_1 = \Lambda_2 = \Lambda_3$ and choose a fixed value of $|\vec{\Lambda}| = 0.235 \text{ GeV}^2$. In case of BRpV the scenario is based on SPS 3, in case of the $\mu\nu$ SSM with one right-handed neutrino superfield on mSUGRA 1. In contrast we fix $\Lambda_1 = -\Lambda_2 = \Lambda_3$ in Figure 9.2, so that the sign-condition

$$\frac{\epsilon_2 \Lambda_2}{\epsilon_3 \Lambda_3} < 0 \quad (9.1)$$

is fulfilled, resulting in a behavior described in [97, 121].

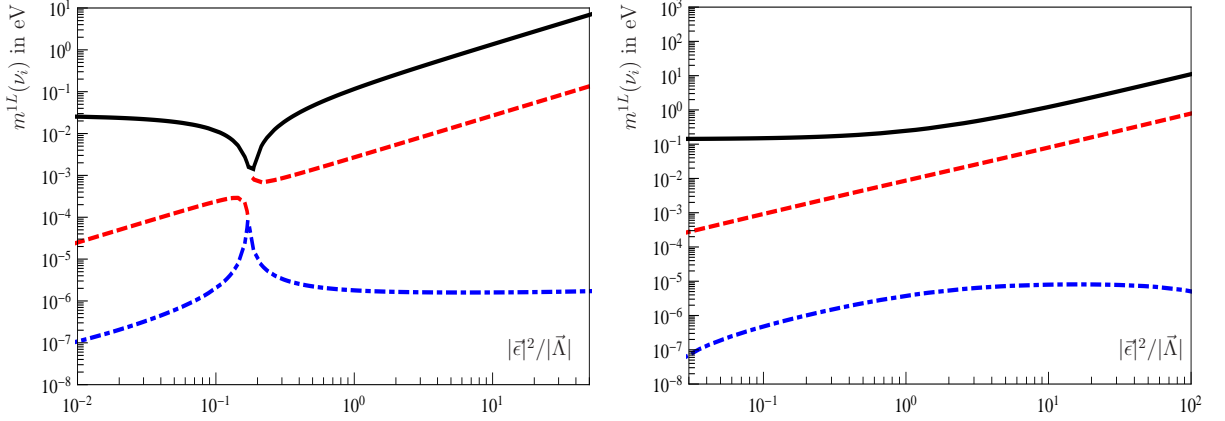


Figure 9.1.: Three on-shell neutrino masses $m^{1L}(\nu_i)$ in eV as a function of $|\vec{\epsilon}|^2/|\vec{\Lambda}|$ for a scenario in **a)** (left) the $\mu\nu$ SSM based on mSUGRA 1; **b)** (right) BRpV based on SPS 3.

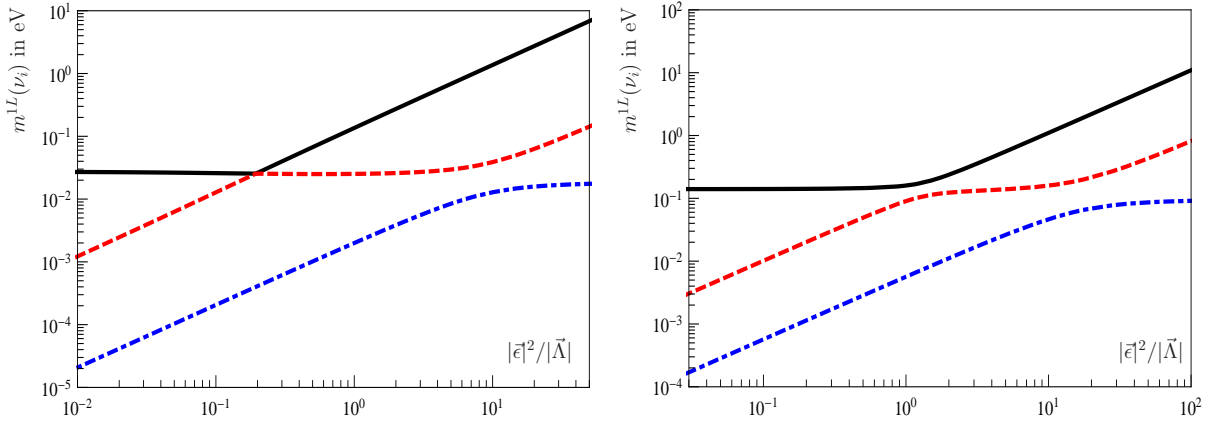


Figure 9.2.: Three on-shell neutrino masses $m^{1L}(\nu_i)$ in eV as a function of $|\vec{\epsilon}|^2/|\vec{\Lambda}|$ using the sign-condition defined in Equation (9.1) for a scenario in **a)** (left) $\mu\nu$ SSM based on mSUGRA 1; **b)** (right) BRpV based on SPS 3.

The sign-condition allows a simpler fit to the solar angle, since it helps to decouple the atmospheric and the solar problem by reducing the contributions from the b -term in the effective neutrino mass matrix at one-loop level in Equation (6.187). We will therefore make use of this sign-condition in the following. Both models show a similar behavior regarding the importance of one-loop corrections as a function of the (effective) parameter ϵ_i : The absolute value of $|\vec{\epsilon}|$ determines the neutrino masses $m^{1L}(\nu_1)$ and $m^{1L}(\nu_2)$, which are generated at one-loop level, whereas $|\vec{\Lambda}|$ sets the tree-level neutrino mass $m^{1L}(\nu_3)$ constant for small $|\vec{\epsilon}|$. m_{ν_3} is affected by the one-loop corrections only for large values of $|\vec{\epsilon}|$. For the explanation of the neutrino mixing

angles the individual ϵ_i and Λ_i have to be chosen differently. Dependent on the parameter point in the $\mu\nu$ SSM as well as in BRpV in case of scenarios without sign-condition a level-crossing as in Figure 9.1 **a**) can take place. It corresponds to a sign-flip between $m^{1L}(\nu_1)$ and $m^{1L}(\nu_3)$. At tree-level the Yukawa couplings Y_e of the leptons have to be adopted, such that the tree-level lepton masses coincide with the experimental values. After we have fitted the tree-level lepton masses m_e to the experimental values, we define the relative one-loop correction

$$\delta_e = \left| \frac{m_e^{1L} - m_e}{m_e} \right|. \quad (9.2)$$

Figure 9.3 shows the relative correction δ_e for the lepton masses at one-loop level for the scenarios already presented in Figures 9.1 **a**) and 9.2 **a**) with respect to the neutrino masses. For reasonable neutrino masses we find corrections to the lepton masses of $\delta_e < 10^{-10}$, which are so small that they are even for the electron below the experimental uncertainties. The shown dips have to be understood as sign change, since we present the absolute value of the correction.

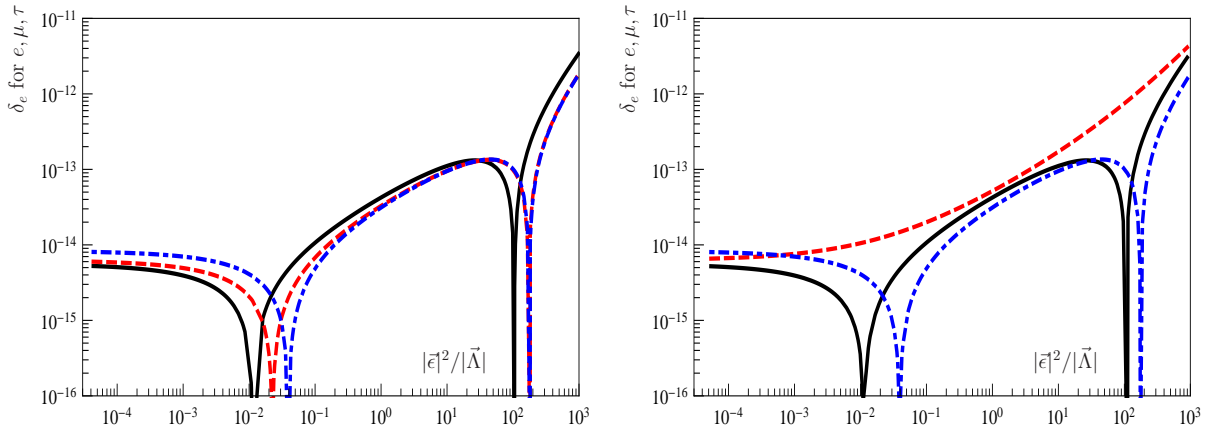


Figure 9.3.: Corrections δ_e defined in Equation (9.2) for the three lepton masses (τ (black, solid), μ (red, dashed), e (blue, dot-dashed)) as a function of $|\bar{\epsilon}|^2/|\bar{\Lambda}|$ for the $\mu\nu$ SSM as in Figure 9.1 **a**), in detail **a**) (left) without sign-condition in Equation (9.1); **b**) (right) with sign-condition in Equation (9.1).

To show the differences between the $\overline{\text{DR}}$ masses as defined in [97] or Section 6.3 and the on-shell masses as given in Section 6.2.3 we make use of the benchmark scenario SPS 3 in BRpV and refer to Figure 9.4 for the result.

Although there is a difference in the mass of the lightest neutrino $m^{1L}(\nu_1)$, the mass differences Δm_{atm}^2 and Δm_{sol}^2 defined in Equation (6.189) in both schemes are comparable, since they are determined by the absolute values of $m^{1L}(\nu_2)$ and $m^{1L}(\nu_3)$. Comparing the on-shell with the $\overline{\text{DR}}$ masses the largest mass $m^{1L}(\nu_3)$ is sometimes only for larger values $|\bar{\epsilon}|$ affected by the one-loop contributions, since the on-shell renormalization tends to reduce their impact. However, we can summarize that the two renormalization prescriptions are very similar for the neutrinos, whereas for the heavy neutralinos and charginos and the leptons the corrections are much smaller in the on-shell procedure in comparison to the $\overline{\text{DR}}$ renormalization. For the $\overline{\text{DR}}$ lepton masses δ_e is typically 0.3 – 2%, the corrections to the heavy neutralino and chargino masses are in the order of a few per-cent [172]. Here we have found $\delta_e < 10^{-10}$ and corrections to the heavy neutralinos and charginos in the per-mil range. As argued the mass differences due to the R -parity violating parameters in BRpV and the $\mu\nu$ SSM with one right-handed neutrino superfield in comparison to the MSSM and NMSSM for the heavy neutralinos and charginos are negligible.

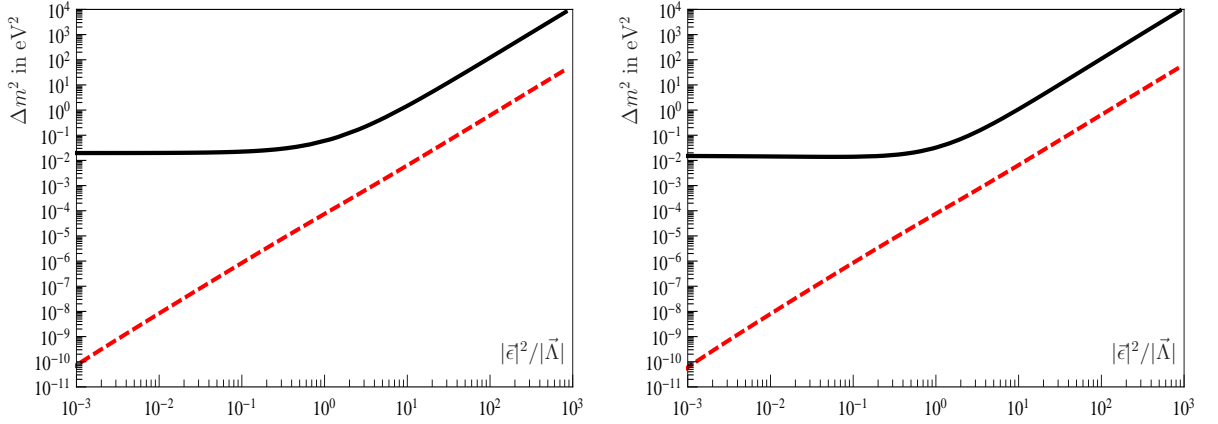


Figure 9.4.: Mass differences Δm_{atm}^2 (black, solid) and Δm_{sol}^2 (red, dashed) as a function of $|\vec{\epsilon}|^2/|\vec{\Lambda}|$ for BRpV based on SPS 3 using the **a)** (left) on-shell masses defined in Section 6.2.3; **b)** (right) DR masses as defined in [97].

9.1.3. Relation between $\vec{\Lambda}$, $\vec{\epsilon}$ and the neutrino mass differences/mixing angles

We are left with the discussion of the relations between the neutrino mass differences, the mixing angles and the (effective) alignment parameters $\vec{\epsilon}$ and $\vec{\Lambda}$. For all figures presented within this section we fit the alignment parameters, such that the neutrino data bounds are fulfilled except for the mass difference/mixing angle shown in the corresponding figure. We again refer to [17] for the current neutrino data, which can be found in Table 2.1.

After we have fitted the atmospheric mass difference and the atmospheric mixing angle at tree-level using $\vec{\Lambda}$ in accordance to [97], $\vec{\epsilon}$ respectively $\vec{\epsilon}^{\dagger}$ is used at the one-loop level to explain the solar mass difference and the solar mixing angle. The correlation to $\vec{\epsilon}$ is more distinct than the one to $\vec{\epsilon}^{\dagger}$, since a prerotation with the matrix \mathcal{N}_{ν} according to $\vec{\epsilon} = \mathcal{N}_{\nu} \vec{\epsilon}^{\dagger}$ was performed, where \mathcal{N}_{ν} diagonalizes the tree-level neutrino mass matrix $m_{\nu\nu}^{\text{eff}}$ given in Equation (5.130).

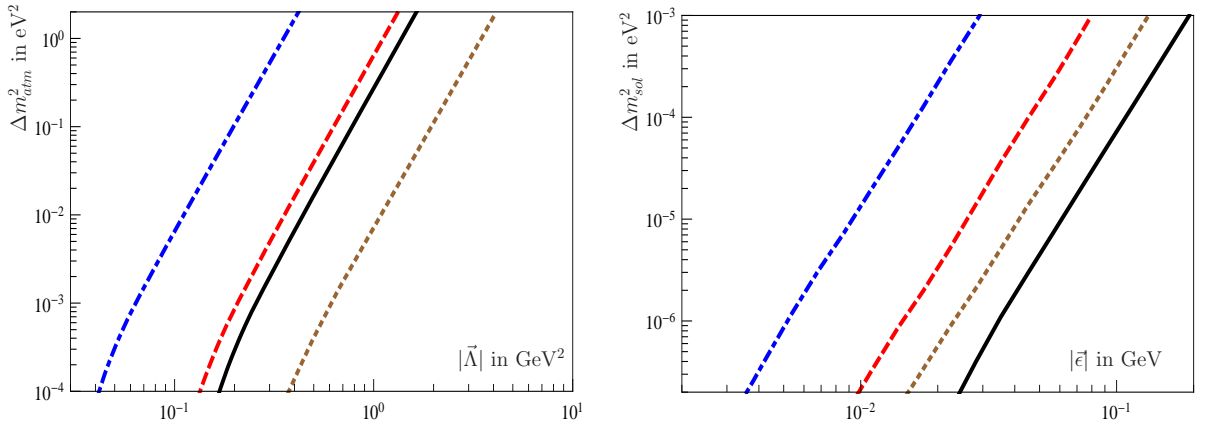


Figure 9.5.: Correlation between the alignment parameters and the neutrino mass differences for the $\mu\nu$ SSM based on mSUGRA 1 (black), 3' (red, dashed), 4' (blue, dot-dashed) and GMSB 5 (brown, dotted) given in Table 9.2, in detail: **a)** (left) Δm_{atm}^2 in eV^2 as a function of $|\vec{\Lambda}|$ in GeV^2 ; **b)** (right) Δm_{sol}^2 in eV^2 as a function of $|\vec{\epsilon}|$ in GeV .

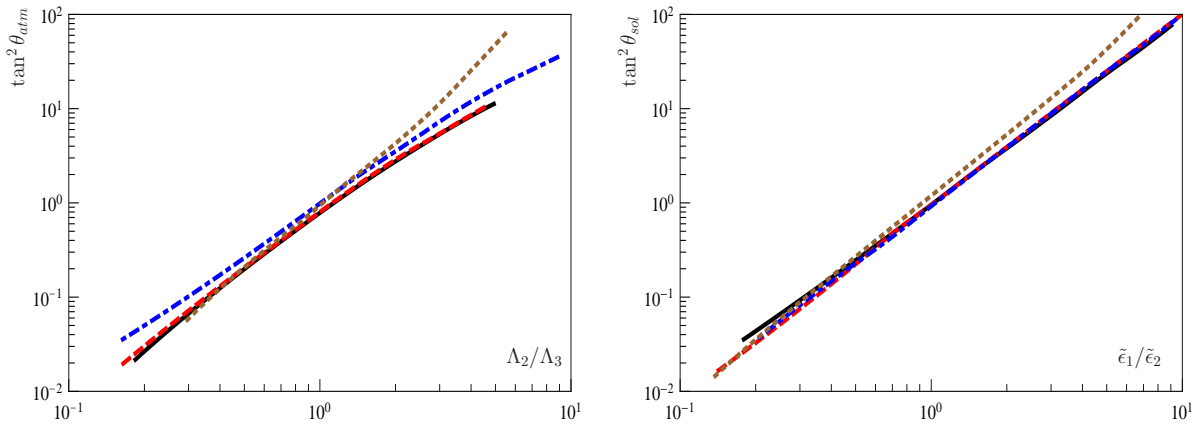


Figure 9.6.: Correlation between the alignment parameters and the neutrino mixing angles for the $\mu\nu$ SSM based on mSUGRA 1 (black), 3' (red, dashed), 4' (blue, dot-dashed) and GMSB 5 (brown, dotted) given in Table 9.2, in detail: **a)** (left) $\tan^2 \theta_{atm}$ as a function of Λ_2/Λ_3 ; **b)** (right) $\tan^2 \theta_{sol}$ as a function of $\tilde{\epsilon}_1/\tilde{\epsilon}_2$.

Thus, the vector $\vec{\tilde{\epsilon}}$ is perpendicular to $\vec{\Lambda}$. In the models under consideration the mixing matrix \mathcal{N}_ν is exactly given by [117]

$$\mathcal{N}_\nu = \begin{pmatrix} \frac{\sqrt{\Lambda_2^2 + \Lambda_3^2}}{|\vec{\Lambda}|} & -\frac{\Lambda_1 \Lambda_2}{\sqrt{\Lambda_2^2 + \Lambda_3^2} |\vec{\Lambda}|} & -\frac{\Lambda_1 \Lambda_3}{\sqrt{\Lambda_2^2 + \Lambda_3^2} |\vec{\Lambda}|} \\ 0 & \frac{\Lambda_3}{\sqrt{\Lambda_2^2 + \Lambda_3^2}} & -\frac{\Lambda_2}{\sqrt{\Lambda_2^2 + \Lambda_3^2}} \\ \frac{\Lambda_1}{|\vec{\Lambda}|} & \frac{\Lambda_2}{|\vec{\Lambda}|} & \frac{\Lambda_3}{|\vec{\Lambda}|} \end{pmatrix}. \quad (9.3)$$

First we comment on the atmospheric and solar mass differences Δm_{atm}^2 and Δm_{sol}^2 . By construction the atmospheric mass difference is correlated with $|\vec{\Lambda}|$, whereas the solar mass difference is determined by $|\vec{\tilde{\epsilon}}|$ as it can be seen in Figure 9.5 for various scenarios in the $\mu\nu$ SSM with one right-handed neutrino superfield. Using Equation (5.136) we estimate the absolute value of $\vec{\Lambda}$. Figure 9.6 presents the correlation between the alignment parameters Λ_i and $\tilde{\epsilon}_i$ and the neutrino mixing angles using the definitions of Equation (6.190) for the same scenarios as in Figure 9.5. The ratio Λ_2/Λ_3 fits the atmospheric angle, whereas $\tilde{\epsilon}_1/\tilde{\epsilon}_2$ determines the solar angle. The reactor angle is given by $\Lambda_1/\sqrt{\Lambda_2^2 + \Lambda_3^2}$ [97], which can receive sizable loop corrections.

9.2. Corrections to neutralino and chargino decays

In this section we show results for the corrections to the decays $\tilde{\chi}_j^0 \rightarrow \tilde{\chi}_i^- W^+$ and $\tilde{\chi}_i^+ \rightarrow \tilde{\chi}_j^0 W^+$ in the (N)MSSM, which play an important role in SUSY cascades. Afterwards we focus on the absolute corrections to the R -parity violating decays $\tilde{\chi}_1^0 \rightarrow l^+ W^-$. Their relation to neutrino mixing angles is worked out in the following chapter.

9.2.1. Two-body decays $\tilde{\chi}_j^0 \rightarrow \tilde{\chi}_i^- W^+$ and $\tilde{\chi}_i^+ \rightarrow \tilde{\chi}_j^0 W^+$ in the (N)MSSM

Sc.	Decay	Γ^0 (in GeV)	Γ^1 (in GeV)	$\delta_{1(\bar{q},q)}$	δ_2	δ_{1+2}
1	$\tilde{\chi}_3^0 \rightarrow \tilde{\chi}_1^- W^+$	2.153	2.234	1.8%	2.0%	3.8%
	$\tilde{\chi}_4^0 \rightarrow \tilde{\chi}_1^- W^+$	2.181	2.256	1.8%	1.6%	3.4%
	$\tilde{\chi}_5^0 \rightarrow \tilde{\chi}_1^- W^+$	$3.206 \cdot 10^{-3}$	$2.897 \cdot 10^{-3}$	-2.6%	-7.0%	-9.6%
	$\tilde{\chi}_5^0 \rightarrow \tilde{\chi}_2^- W^+$	$1.542 \cdot 10^{-1}$	$1.521 \cdot 10^{-1}$	-1.9%	0.5%	-1.4%
	$\tilde{\chi}_1^- \rightarrow \tilde{\chi}_1^0 W^-$	$2.575 \cdot 10^{-3}$	$2.561 \cdot 10^{-3}$	0.8%	-1.3%	-0.5%
	$\tilde{\chi}_2^- \rightarrow \tilde{\chi}_1^0 W^-$	$5.860 \cdot 10^{-1}$	$5.766 \cdot 10^{-1}$	0.2%	-1.8%	-1.6%
	$\tilde{\chi}_2^- \rightarrow \tilde{\chi}_2^0 W^-$	2.201	2.222	-0.3%	1.2%	0.9%
3	$\tilde{\chi}_3^0 \rightarrow \tilde{\chi}_1^- W^+$	2.085	2.153	1.8%	1.5%	3.3%
	$\tilde{\chi}_4^0 \rightarrow \tilde{\chi}_1^- W^+$	2.121	2.181	1.8%	1.0%	2.8%
	$\tilde{\chi}_5^0 \rightarrow \tilde{\chi}_1^- W^+$	$2.937 \cdot 10^{-2}$	$2.755 \cdot 10^{-2}$	-1.7%	-4.5%	-6.2%
	$\tilde{\chi}_5^0 \rightarrow \tilde{\chi}_2^- W^+$	1.302	1.352	-0.6%	4.5%	3.9%
	$\tilde{\chi}_1^- \rightarrow \tilde{\chi}_1^0 W^-$	$2.951 \cdot 10^{-3}$	$2.910 \cdot 10^{-1}$	0.7%	-2.1%	-1.4%
	$\tilde{\chi}_2^- \rightarrow \tilde{\chi}_1^0 W^-$	$5.684 \cdot 10^{-1}$	$5.552 \cdot 10^{-1}$	0.2%	-2.5%	-2.3%
	$\tilde{\chi}_2^- \rightarrow \tilde{\chi}_2^0 W^-$	2.115	2.141	0.6%	0.6%	1.2%
4	$\tilde{\chi}_4^0 \rightarrow \tilde{\chi}_1^- W^+$	$4.719 \cdot 10^{-2}$	$5.080 \cdot 10^{-2}$	-0.3%	7.9%	7.6%
	$\tilde{\chi}_5^0 \rightarrow \tilde{\chi}_1^- W^+$	$7.442 \cdot 10^{-1}$	$7.288 \cdot 10^{-1}$	0.2%	-2.3%	-2.1%
	$\tilde{\chi}_1^- \rightarrow \tilde{\chi}_1^0 W^-$	$1.623 \cdot 10^{-1}$	$1.650 \cdot 10^{-1}$	-0.9%	2.5%	1.6%
	$\tilde{\chi}_2^- \rightarrow \tilde{\chi}_1^0 W^-$	$2.357 \cdot 10^{-1}$	$2.291 \cdot 10^{-1}$	0.2%	-3.0%	-2.8%
	$\tilde{\chi}_2^- \rightarrow \tilde{\chi}_2^0 W^-$	$5.758 \cdot 10^{-1}$	$5.586 \cdot 10^{-1}$	0.2%	-3.2%	-3.0%
	$\tilde{\chi}_2^- \rightarrow \tilde{\chi}_3^0 W^-$	$6.024 \cdot 10^{-1}$	$5.875 \cdot 10^{-1}$	0.2%	-2.7%	-2.5%
	$\tilde{\chi}_2^- \rightarrow \tilde{\chi}_4^0 W^-$	$7.007 \cdot 10^{-2}$	$6.963 \cdot 10^{-2}$	-0.3%	-0.3%	-0.6%

Table 9.3.: NLO corrections for the mSUGRA benchmark scenarios; δ is defined in Equation (9.4).

We discuss the NLO corrections to the decay widths $\tilde{\chi}_j^0 \rightarrow \tilde{\chi}_i^- W^+$ and $\tilde{\chi}_i^+ \rightarrow \tilde{\chi}_j^0 W^+$ taking the NMSSM as example in this section. As long as the singlino is not involved, the discussed effects

are transferable to the MSSM. For the mSUGRA and GMSB scenarios we show our results for the decay widths in Tables 9.3 and 9.4 respectively. Beside the tree-level and one-loop corrected widths the correction factor

$$\delta = \frac{\Gamma^1 - \Gamma^0}{\Gamma^0} \quad , \quad (9.4)$$

is shown, which is split in the parts $\delta_1 = \delta_{1(\tilde{q},q)}$ due to squark and quark corrections and δ_2 containing the other contributions, which includes the hard photon emission for comparison with [173]. Please note that for the renormalization of the electric charge and the wave-function renormalization of δZ_W all light fermions are always taken into account, since otherwise the renormalization in the Thomson limit can not be guaranteed.

Sc.	Decay	Γ^0 (in GeV)	Γ^1 (in GeV)	$\delta_{1(\tilde{q},q)}$	δ_2	δ_{1+2}
1	$\tilde{\chi}_4^0 \rightarrow \tilde{\chi}_1^- W^+$	2.891	3.068	-0.2%	6.3%	6.1%
	$\tilde{\chi}_5^0 \rightarrow \tilde{\chi}_1^- W^+$	2.943	3.114	-0.1%	5.9%	5.8%
	$\tilde{\chi}_1^- \rightarrow \tilde{\chi}_1^0 W^-$	$1.027 \cdot 10^{-2}$	$1.028 \cdot 10^{-1}$	0.0%	0.1%	0.1%
	$\tilde{\chi}_1^- \rightarrow \tilde{\chi}_2^0 W^-$	$8.907 \cdot 10^{-5}$	$8.942 \cdot 10^{-5}$	-0.1%	0.5%	0.4%
	$\tilde{\chi}_2^- \rightarrow \tilde{\chi}_1^0 W^-$	$8.941 \cdot 10^{-1}$	$8.795 \cdot 10^{-1}$	0.2%	-1.8%	-1.6%
	$\tilde{\chi}_2^- \rightarrow \tilde{\chi}_2^0 W^-$	$3.787 \cdot 10^{-3}$	$3.697 \cdot 10^{-3}$	-0.5%	-1.9%	-2.4%
	$\tilde{\chi}_2^- \rightarrow \tilde{\chi}_3^0 W^-$	2.962	3.126	-0.1%	5.6%	5.5%
2	$\tilde{\chi}_3^0 \rightarrow \tilde{\chi}_1^- W^+$	7.431	7.241	0.2%	-2.8%	-2.6%
	$\tilde{\chi}_4^0 \rightarrow \tilde{\chi}_1^- W^+$	7.442	7.254	0.4%	-2.9%	-2.5%
	$\tilde{\chi}_5^0 \rightarrow \tilde{\chi}_1^- W^+$	$1.164 \cdot 10^{-2}$	$9.868 \cdot 10^{-3}$	-3.4%	-11.8%	-15.2%
	$\tilde{\chi}_5^0 \rightarrow \tilde{\chi}_2^- W^+$	1.890	1.851	-2.0%	-0.1%	-2.1%
	$\tilde{\chi}_1^- \rightarrow \tilde{\chi}_1^0 W^-$	$6.150 \cdot 10^{-3}$	$6.135 \cdot 10^{-3}$	0.0%	-0.2%	-0.2%
	$\tilde{\chi}_2^- \rightarrow \tilde{\chi}_1^0 W^-$	1.807	1.708	-0.7%	-4.8%	-5.5%
	$\tilde{\chi}_2^- \rightarrow \tilde{\chi}_2^0 W^-$	7.491	7.235	0.3%	-3.7%	-3.4%
5	$\tilde{\chi}_4^0 \rightarrow \tilde{\chi}_1^- W^+$	2.283	2.439	-0.3%	7.1%	6.8%
	$\tilde{\chi}_5^0 \rightarrow \tilde{\chi}_1^- W^+$	2.333	2.485	-0.1%	6.6%	6.5%
	$\tilde{\chi}_1^- \rightarrow \tilde{\chi}_1^0 W^-$	$1.462 \cdot 10^{-5}$	$1.453 \cdot 10^{-5}$	-0.3%	-0.3%	-0.6%
	$\tilde{\chi}_1^- \rightarrow \tilde{\chi}_2^0 W^-$	$8.424 \cdot 10^{-3}$	$8.407 \cdot 10^{-3}$	-0.1%	-0.1%	-0.2%
	$\tilde{\chi}_2^- \rightarrow \tilde{\chi}_1^0 W^-$	$1.279 \cdot 10^{-3}$	$1.242 \cdot 10^{-3}$	-0.6%	-2.2%	-2.9%
	$\tilde{\chi}_2^- \rightarrow \tilde{\chi}_2^0 W^-$	$7.898 \cdot 10^{-1}$	$7.775 \cdot 10^{-1}$	-0.1%	-1.5%	-1.6%
	$\tilde{\chi}_2^- \rightarrow \tilde{\chi}_3^0 W^-$	2.339	2.486	-0.1%	6.4%	6.3%

Table 9.4.: NLO corrections for the GMSB benchmark scenarios; δ is defined in Equation (9.4).

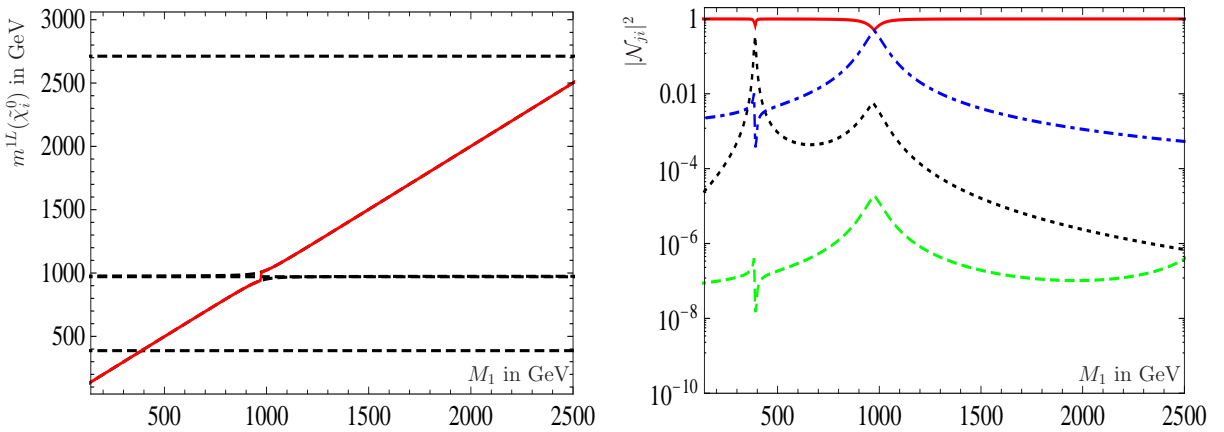


Figure 9.7.: **a)** (left): On-shell neutralino masses as a function of M_1 and the other parameters according to mSUGRA 1 apart from $\kappa = 0.14$. The red solid line marks \tilde{B} whereas the other states are shown with black dashed lines; **b)** (right): Particle character for the bino state \tilde{B} as a function of M_1 : red (solid): Bino character $|\mathcal{N}_{j1}|^2$, blue (dot-dashed): Higgsino character $|\mathcal{N}_{j3}|^2 + |\mathcal{N}_{j4}|^2$, black (dotted): Wino character $|\mathcal{N}_{j2}|^2$, green (dashed): Singlino character $|\mathcal{N}_{j5}|^2$.

In case that the neutralino has either large wino and/or Higgsino components the tree-level widths are larger, since from Equations (5.143) and (5.144) follows that the W boson couples either to a wino(\tilde{W}_3^0)-wino(\tilde{W}^\pm) or a Higgsino-Higgsino combination. This accounts for several at first glance surprising features like the fact that in mSUGRA scenarios 1 and 3 the width $\Gamma(\tilde{\chi}_5^0 \rightarrow \tilde{\chi}_2^+ W^-)$ is larger than $\Gamma(\tilde{\chi}_5^0 \rightarrow W^- \tilde{\chi}_1^+)$ despite the smaller phase space. Also the difference in δ_2 in the decay $\tilde{\chi}_2^- \rightarrow \tilde{\chi}_1^0 W^-$ in the scenarios mSUGRA 1 and 3 can be understood from differences in the scalar sector. In general the corrections are of order 1 – 3%, but can easily go up to 10%. Depending on the parameters the corrections can have both signs.

In the following we want to discuss the effects in case of a singlino or bino involved in the decays. If the neutralino involved is either pure bino or pure singlino, the partial widths into a W boson vanishes as it can be seen from the tree-level couplings in Equations (5.143) and (5.144). Therefore, processes containing states, which are to a large extent bino or singlino in Tables 9.3 and 9.4 have small widths at tree-level. However, the corresponding couplings are induced at one-loop level, which we investigate in more detail in the following. Note that we partially consider a wide mass range being aware that neutralinos with masses above 1 TeV will hardly be produced at LHC and might only be accessible at a multi-TeV lepton collider such as CLIC. All the figures showing decay widths are based on tree-level masses $m(\tilde{\chi}_i^{\pm 0})$ for neutralinos and charginos ensuring that the final decay widths are UV and IR finite as well as gauge independent. Taking into account the one-loop corrected masses $m^{1L}(\tilde{\chi}_i^{\pm 0})$, which are nearly identical to the tree-level masses, for the one-loop decay width results in slight differences, which are hardly visible in the shown figures.

Bino decays

We start with the consideration of a bino-like neutralino \tilde{B} , which is the neutralino mass eigenstate with $|\mathcal{N}_{j1}|^2 > 0.5$. Taking benchmark point mSUGRA 1 we vary the gaugino mass M_1 for our subsequent numerical investigations. In addition we shift κ from 0.11 to 0.14 to disentangle different effects and to simplify our discussion. Figure 9.7 **a)** shows the corresponding neutralino mass spectrum as a function of M_1 . The particle character of the bino-like state \tilde{B} is presented in Figure 9.7 **b)**. At the various crossings in Figure **a)** the index of the corresponding neutralino mass eigenstate changes.

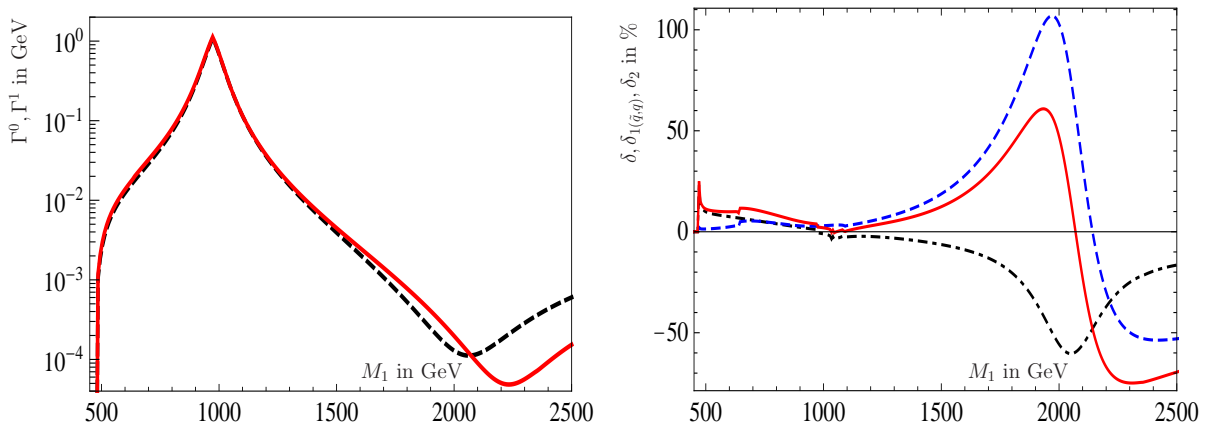


Figure 9.8.: **a)** (left): LO (black, dashed) and NLO (red, solid) decay widths for $\tilde{B} \rightarrow \tilde{\chi}_1^- W^+$ as a function of M_1 for the spectrum of Figure 9.7; **b)** (right): Correction factor δ in % defined in Equation (9.4) for $\tilde{B} \rightarrow \tilde{\chi}_1^- W^+$ as a function of M_1 : blue (dashed): Squark and quark contributions, black (dot-dashed): Other sectors, red (solid): Full correction.

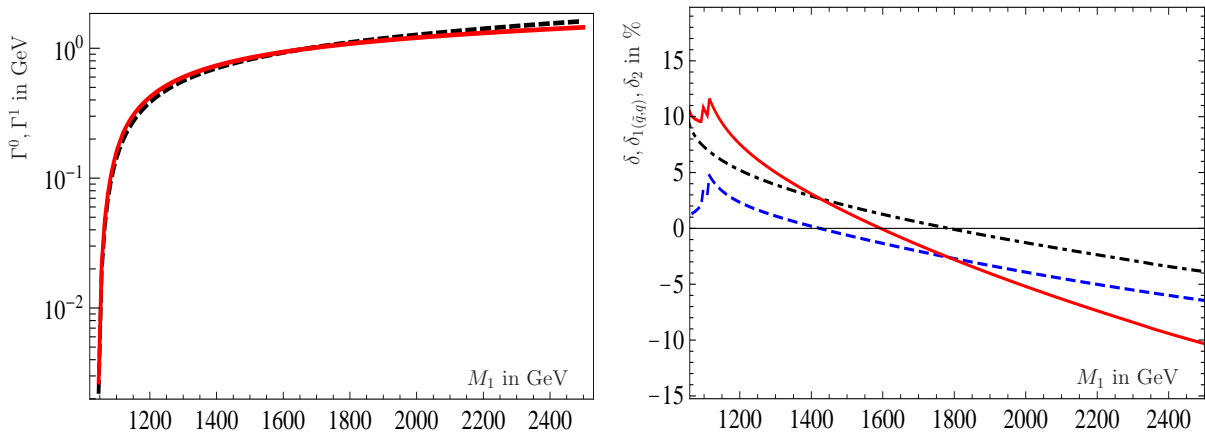


Figure 9.9.: **a)** (left): LO (black, dashed) and NLO (red, solid) decay widths for $\tilde{B} \rightarrow \tilde{\chi}_2^- W^+$ as a function of M_1 for the spectrum of Figure 9.7; **b)** (right): Correction factor δ in % defined in Equation (9.4) for $\tilde{B} \rightarrow \tilde{\chi}_2^- W^+$ as a function of M_1 : blue (dashed): Squark and quark contributions, black (dot-dashed): Other sectors, red (solid): Full correction.

In Figure 9.8 **a)** we show the LO and NLO decay width of $\tilde{B} \rightarrow \tilde{\chi}_1^- W^+$ as a function of M_1 . At $M_1 \simeq 1$ TeV the bino crosses the Higgsino state resulting in a rise of the width with M_1 and the subsequent decrease. With further increasing M_1 a negative interference of the Higgsino and wino parts at tree-level occurs, so that a small LO decay width suffers large NLO corrections. We note that here and in the following figures a Coulomb singularity occurs close to the kinematical threshold, meaning close to $m(\tilde{B}) = m(\tilde{\chi}_1^\pm) + m_W$, which has to be resummed. As this has not been done, our plots start slightly above this region.

The relative size of the corrections are presented in Figure 9.8 **b)**, where we again split the squark/quark contributions from the additional ones. Kinks occur at the level-crossings in Figure 9.7. Note that both parts of the correction can be of equal importance and that they can either partly cancel each other or point in the same direction depending on the regions of the parameter space. The fact, that the loop induced corrections can be of the same order of magnitude as the tree-level widths, does not imply a break-down of perturbation theory, but can

be understood as a consequence that in the limit of a pure bino the tree-level coupling vanishes but the one-loop induced one is nonzero.

The LO and NLO widths for the decay $\tilde{B} \rightarrow \tilde{\chi}_2^- W^+$ with $\tilde{\chi}_2^-$ being a Higgsino are shown in Figure 9.9 **a**) as a function of M_1 . In contrast to the decay discussed before there is a positive interference of the wino-wino and Higgsino-Higgsino components in the LO couplings given in Equations (5.143) and (5.144). The decrease of the couplings for increasing M_1 is compensated by a phase space factor $(m(\tilde{B})/m_W)^2$ according to Equations (5.146) and (5.149). Therefore, a slight increase of the width with increasing M_1 can be observed. Again the corrections can be sizable amounting up to about 15%.

Singlino decays

We define a neutralino to be singlino-like \tilde{S} in case of $|\mathcal{N}_{j5}|^2 > 0.5$ resulting in similar features as in case of a bino-like neutralino. However, there is one important difference: For a pure singlino exists only a coupling to the doublet Higgs/Higgsino states and the singlet Higgs boson. Hence, the squark/quark contributions should be of less importance compared to the bino case.

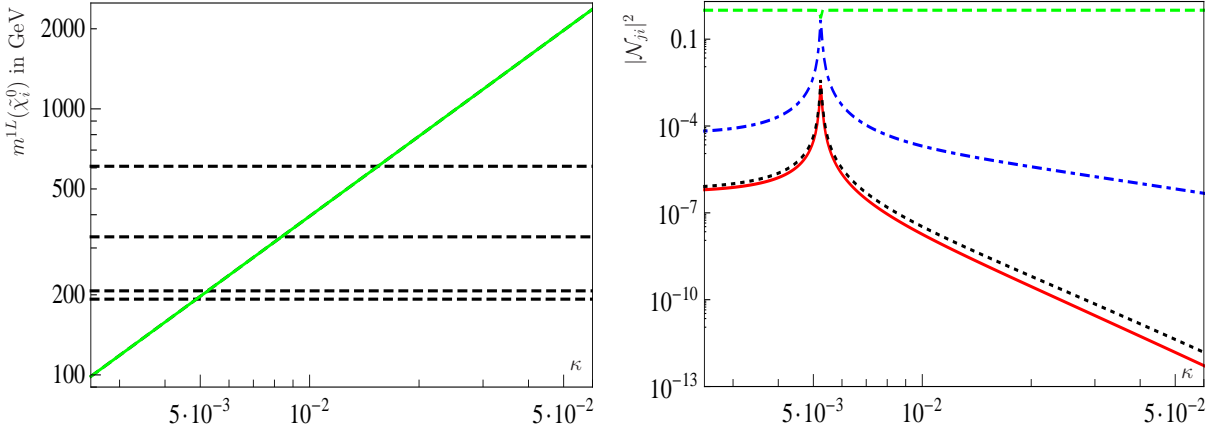


Figure 9.10.: **a)** (left): On-shell neutralino masses as a function of κ and the other parameters according to mSUGRA 4 apart from $\lambda = 0.01$. The green solid line marks \tilde{S} whereas the other states are shown with black dashed lines; **b)** (right): Particle character for the singlino state \tilde{S} as a function of κ : red (solid): Bino character $|\mathcal{N}_{j1}|^2$, blue (dot-dashed): Higgsino character $|\mathcal{N}_{j3}|^2 + |\mathcal{N}_{j4}|^2$, black (dotted): Wino character $|\mathcal{N}_{j2}|^2$, green (dashed): Singlino character $|\mathcal{N}_{j5}|^2$.

The benchmark scenario mSUGRA 4 with a reduced λ of 0.01 is convenient for our numerical investigation, since it allows to have a relatively pure light singlino mass eigenstate. We vary κ between $2 \cdot 10^{-3}$ and $6 \cdot 10^{-2}$ leading to singlino masses between 100 GeV and 2.5 TeV. In this rather light particle spectrum the Higgsino-like chargino has a fixed mass of $m(\tilde{\chi}_1^\pm) = 201$ GeV and the wino-like chargino has a mass of $m(\tilde{\chi}_2^\pm) = 608$ GeV. Figure 9.10 **a**) shows the mass spectrum of the neutralinos, the particle character is presented in Figure 9.10 **b**).

We show the details for the decay $\tilde{S} \rightarrow \tilde{\chi}_1^- W^+$ in Figure 9.11. Again the decrease of the coupling due to the decrease in the wino and Higgsino components is compensated by an increase of the phase space factor $(m(\tilde{S})/m_W)^2$ with increasing κ . Figure 9.11 **b**) clearly shows that the contributions of the quarks and squarks are less important compared to the bino case. However the remaining contribution can amount up to 10%. The decay into the heavier chargino shows similar features as it can be seen from Figure 9.12. The threshold effects due to on-shell

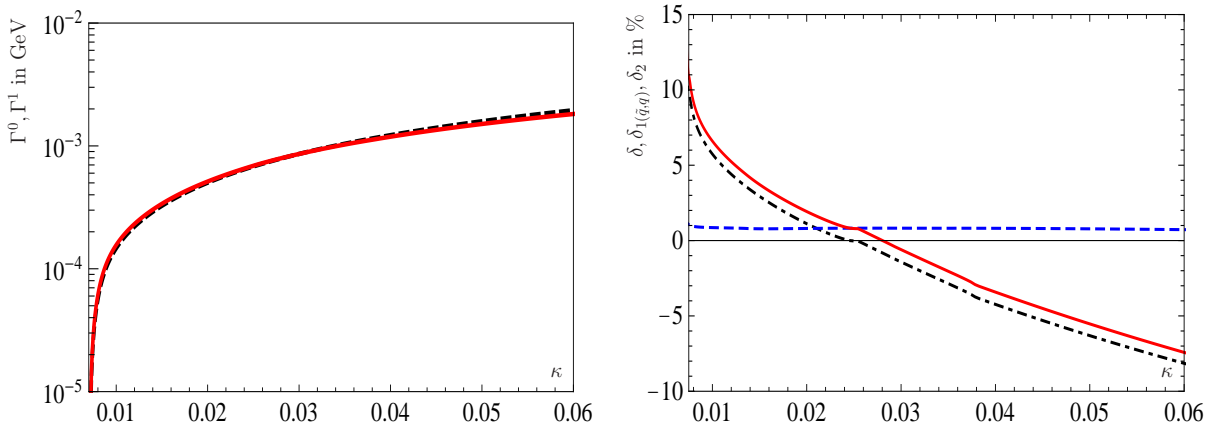


Figure 9.11.: **a)** (left): LO (black, dashed) and NLO (red, solid) decay widths for $\tilde{S} \rightarrow \tilde{\chi}_1^- W^+$ as a function of κ for the spectrum of Figure 9.10; **b)** (right): Correction factor δ in % defined in Equation (9.4) for $\tilde{S} \rightarrow \tilde{\chi}_1^- W^+$ as a function of κ : blue (dashed): Squark and quark contributions, black (dot-dashed): Other sectors, red (solid): Full correction.

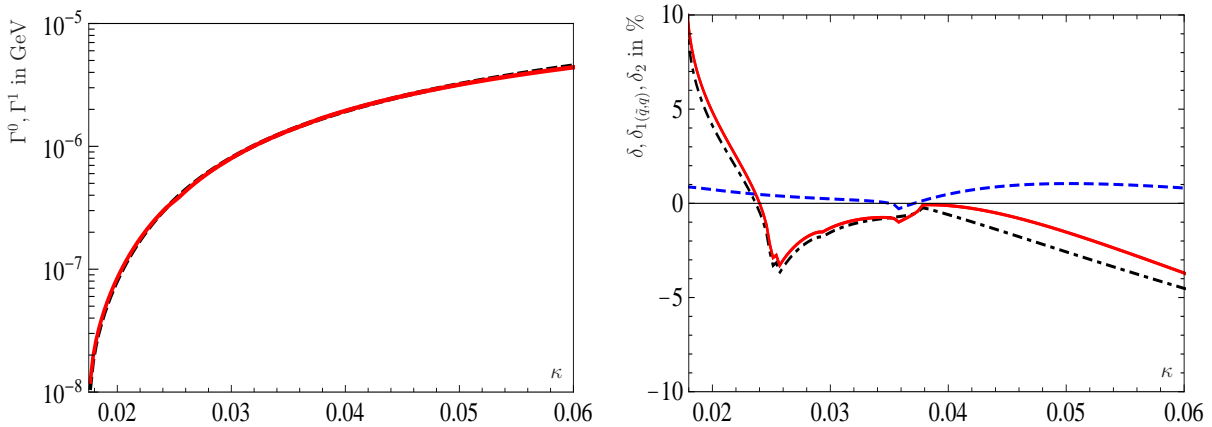


Figure 9.12.: **a)** (left) LO (black, dashed) and NLO (red, solid) decay widths for $\tilde{S} \rightarrow \tilde{\chi}_2^- W^+$ as a function of κ for the spectrum of Figure 9.10; **b)** (right): Correction factor δ in % defined in Equation (9.4) for $\tilde{S} \rightarrow \tilde{\chi}_2^- W^+$ as a function of κ : blue (dashed): Squark and quark contributions, black (dot-dashed): Other sectors, red (solid): Full correction.

intermediate states in the loops are more pronounced in this case, mainly caused by sleptons and Higgs bosons at $m(\tilde{S}) \approx 1$ TeV and by squarks at $m(\tilde{S}) \approx 1.6$ TeV.

Chargino decays

Next we want to address the corrections to the chargino decays taking the example of a wino-like chargino \tilde{W}^+ decaying into a bino- or singlino-like neutralino $\tilde{\chi}_{1,2}^0$, being the two lightest neutralinos in the benchmark scenario GMSB 5. We depart from the original parameters by setting $M_1 = 300$ GeV and $\mu = 600$ GeV to lower the particle masses further. Then we vary the gaugino mass M_2 between 100 and 2000 GeV. The resulting neutralino mass spectrum can be found in Figure 9.13 **a)** and the chargino mass spectrum is shown in Figure 9.13 **b)**. The two light neutralinos have a nearly fixed mass of $m(\tilde{\chi}_1^0) = 89$ GeV for the singlino-like neutralino and $m(\tilde{\chi}_2^0) = 298$ GeV for the bino-like neutralino.

The two Figures 9.14 and 9.15 present the decays $\tilde{W}^+ \rightarrow \tilde{\chi}_{1,2}^0 W^+$. Note that the peaks close to $M_2 \approx 620$ GeV can be explained by the level-crossing of the wino-like states with the Higgsino-like states. The overall features of the widths and corrections are of course similar to the case of the neutralino decays. The corrections are in the order of a few per-cent except for a region close to $M_2 = 1.15$ TeV for the decay $\tilde{W}^+ \rightarrow \tilde{\chi}_2^0 W^+$ in Figure 9.15 where the tree-level couplings to $\tilde{\chi}_2^0$ nearly vanish due to a negative interference between the wino and Higgsino contributions. We find that the squark/quark contributions are smaller than the remaining ones.

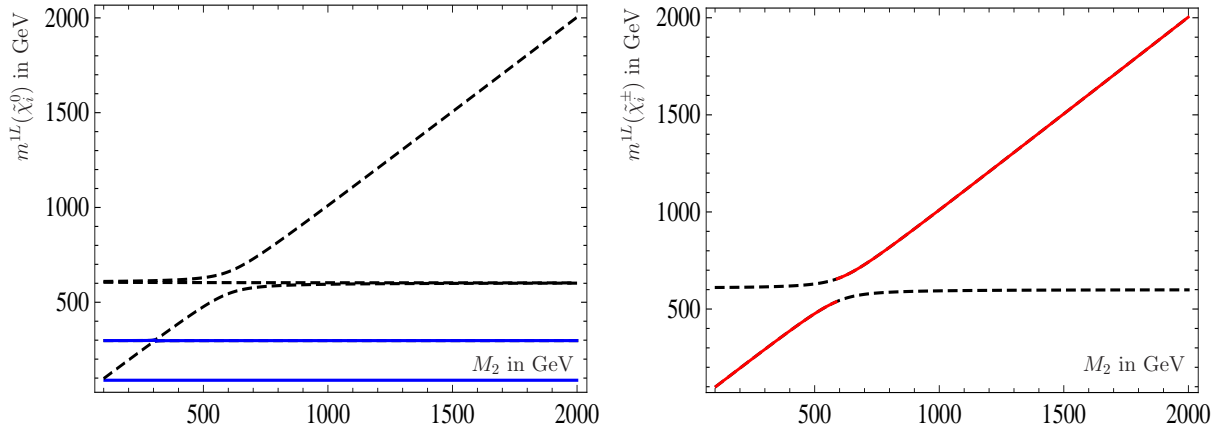


Figure 9.13.: a) (left): On-shell neutralino masses and b) (right): On-shell chargino masses as a function of M_2 . The other parameters are as GMSB 5 apart from $M_1 = 300$ GeV and $\mu = 600$ GeV. The red lines in b) correspond to the wino-like states and the two blue ones in a) to the singlino state $\tilde{\chi}_1^0$ and bino state $\tilde{\chi}_2^0$.

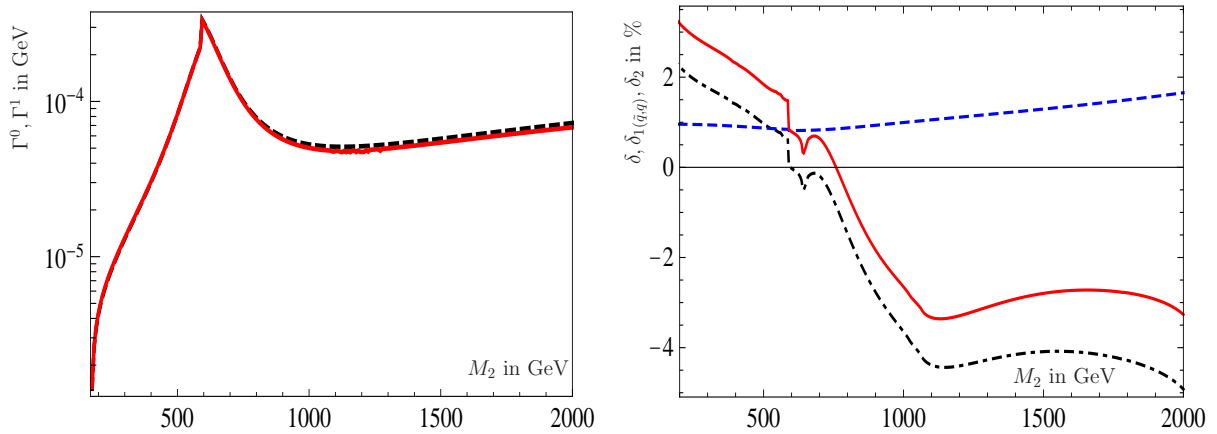


Figure 9.14.: a) (left): LO (black, dashed) and NLO (red, solid) decay widths for $\tilde{W}^+ \rightarrow \tilde{\chi}_1^0 W^+$ as a function of M_2 for the spectrum of Figure 9.13; b) (right): Correction factor δ in % defined in Equation (9.4) for $\tilde{W}^+ \rightarrow \tilde{\chi}_1^0 W^+$ as a function of M_2 : blue (dashed): Squark and quark contributions, black (dot-dashed): Other sectors, red (solid): Full correction.

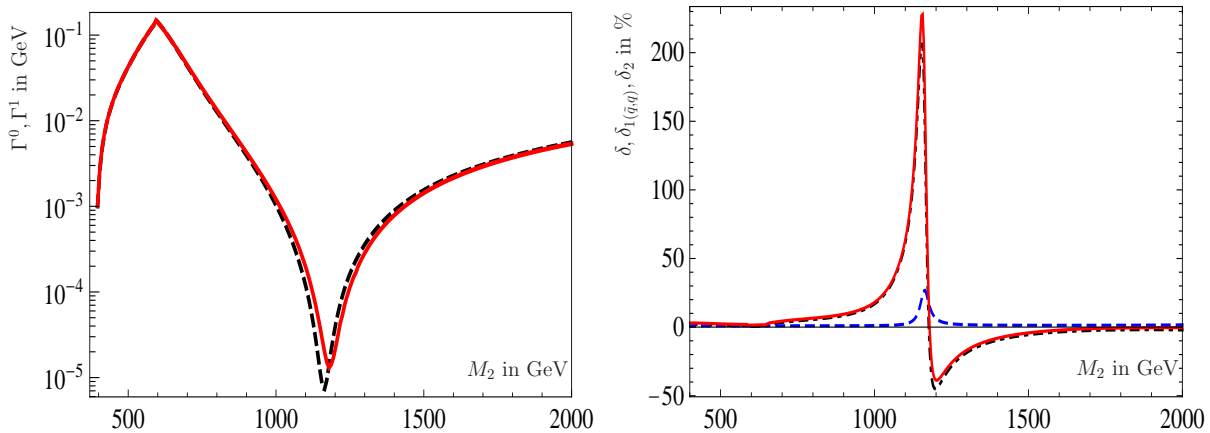


Figure 9.15.: **a)** (left): LO (black, dashed) and NLO (red, solid) decay widths for $\tilde{W}^+ \rightarrow \tilde{\chi}_2^0 W^+$ as a function of M_2 for the spectrum of Figure 9.13; **b)** (right): Correction factor δ in % defined in Equation (9.4) for $\tilde{W}^+ \rightarrow \tilde{\chi}_2^0 W^+$ as a function of M_2 : blue (dashed): Squark and quark contributions, black (dot-dashed): Other sectors, red (solid): Full correction.

9.2.2. Two-body decays $\tilde{\chi}_1^0 \rightarrow l^+ W^-$ in R -parity violating models

In this section we want to discuss the absolute corrections to the R -parity violating decay $\tilde{\chi}_1^0 \rightarrow l^+ W^-$ taking the example of the $\mu\nu$ SSM with one-right handed neutrino superfield. We use the NMSSM inspired scenario mSUGRA 4, where we vary $\kappa \in [0.1, 0.5]$ in order to have a singlino- and a Higgsino-like lightest neutralino $\tilde{\chi}_1^0$ in comparison. Note that for $\kappa \lesssim 0.1$ the decay is near the kinematical threshold and for $\kappa \gg 0.5$ a Landau pole appears. Figure 9.16 **a)** contains the particle spectrum of the neutralinos as a function of κ , whereas **b)** shows the particle character of the lightest neutralino. In Figure 9.16 **c)** one can find the NLO decay width for the decay $\tilde{\chi}_1^0 \rightarrow l^+ W^-$ and **d)** presents the relative correction as defined in Equation (9.4).

Of course, the choice of mSUGRA 4 does not fix the R -parity violating parameters. In fact, the size and the sign of the corrections is strongly dependent on those parameters, either v_{Li} and Y_ν^i or Λ_i and ϵ_i . For our example we fixed $\vec{\Lambda} = (0.31, 5.21, 2.02) \cdot 10^{-2} \text{ GeV}^2$ and $\vec{\epsilon} = (7.49, 9.61, -6.57) \cdot 10^{-3} \text{ GeV}$ in Figure 9.16. Since the solar mass difference and mixing angle are induced at one-loop level, the corrections to the decay $\tilde{\chi}_1^0 \rightarrow e^+ W^-$ are sizable and can be of the order of the tree-level decay width or even larger. In contrast the corrections to the second or third generation leptons $\tilde{\chi}_1^0 \rightarrow \mu^+ W^-$ or $\tau^+ W^-$ are generally smaller, but remain of order 10%. Note that the neutrino bounds from Table 2.1 are only fulfilled for small values of κ in Figure 9.16.

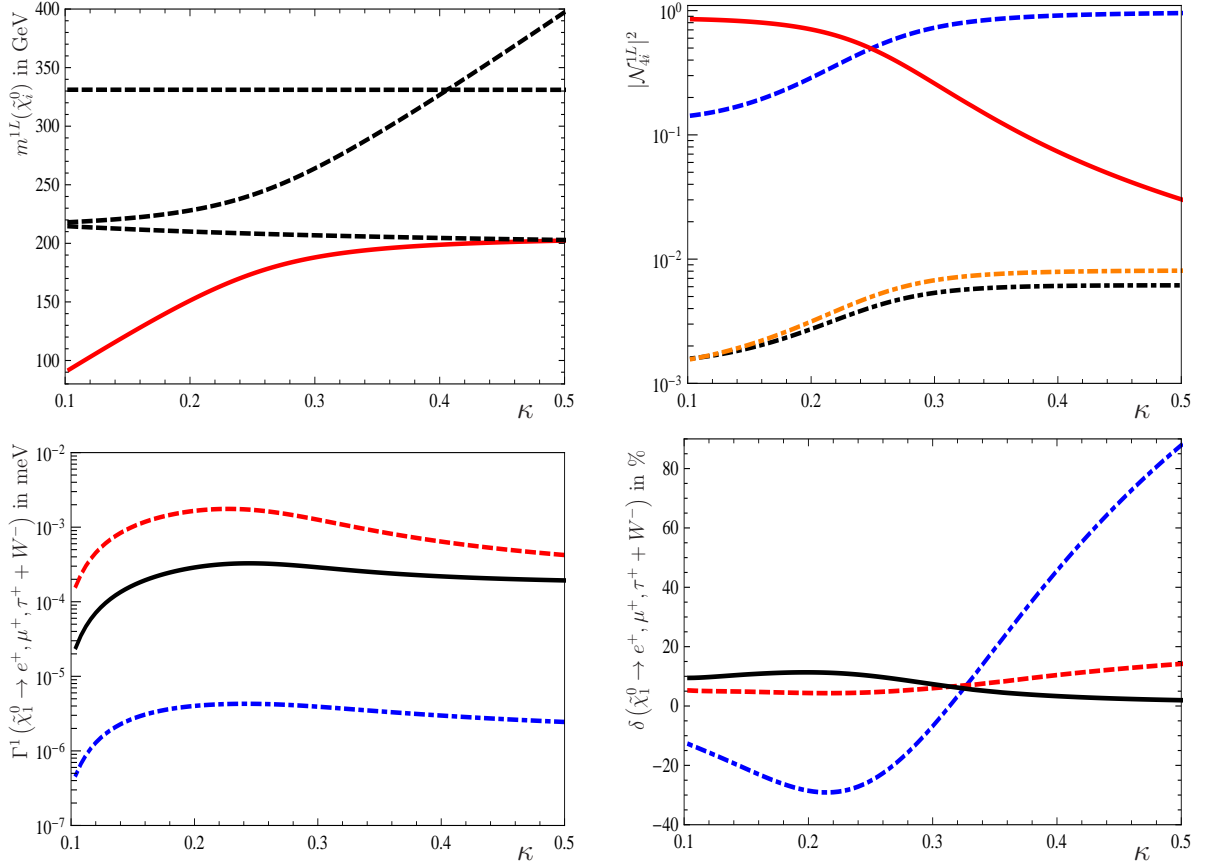


Figure 9.16.: On-shell neutralino masses, particle content of the lightest neutralino and decay widths $\Gamma^1(\tilde{\chi}_1^0 \rightarrow l^+ W^-)$ as a function of κ within the $\mu\nu$ SSM based on the mSUGRA 4 scenario and $\vec{\Lambda} = (0.31, 5.21, 2.02) \cdot 10^{-2}$ GeV² and $\vec{\epsilon} = (7.49, 9.61, -6.57) \cdot 10^{-3}$ GeV: **a)** (upper left) Neutralino masses $m^{1L}(\tilde{\chi}_i^0)$ ($m^{1L}(\tilde{\chi}_1^0)$ (red, solid), $m^{1L}(\tilde{\chi}_{2,3,4}^0)$ (black, dashed)); **b)** (upper right) Particle character $|N_{4i}^{1L}|^2$ ($\tilde{\nu}^c$ (red, solid), $\tilde{H}_u + \tilde{H}_d$ (blue, dashed), \tilde{B} (black, dot-dashed), \tilde{W} (orange, dot-dashed)); **c)** (lower left) NLO decay width Γ^1 (e (blue, dot-dashed), μ (red, dashed), τ (black)); **d)** (lower right) Relative correction δ defined in Equation (9.4) (e (blue, dot-dashed), μ (red, dashed), τ (black)).

Neutrino mixing angles and leptonic branching ratios

In this chapter we discuss the interesting feature of a correlation between branching ratios of different leptonic final states in the R -parity violating decays of the LSP and the neutrino mixing angles. This feature is specific to the class of BRpV schemes, since neutrino data fixes all R -parity violating couplings in sufficiently small intervals. In case of explicit BRpV this has been shown for a (bino-dominated) neutralino LSP in [118, 174, 175], for charged scalar LSPs in [176], for sneutrino LSPs in [177, 178], and for chargino, gluino and squark LSPs in [177]. In case of trilinear and bilinear couplings such a tight connection between LSP decays and neutrino physics is lost to some extent. The question, whether those relations are also present in models with effectively generated bilinear terms, was addressed in [100] for spontaneous R -parity breaking and in [122, 156] for the $\mu\nu$ SSM confirming the behavior in explicit BRpV.

In the first section we focus on our work done in [122] presenting the correlations for the $\mu\nu$ SSM with one right-handed neutrino superfields using tree-level decay widths in combination with one-loop corrected $\overline{\text{DR}}$ masses and mixing matrices for the neutralinos including the neutrinos. However, we pointed out already that in case of a singlino LSP the usage of one-loop mixing matrices for the tree-level decay width results in an unexpected behavior, so that in the second section we follow our work in [136]. Hence, we present the ratios of the full one-loop decay width for $\tilde{\chi}_1^0 \rightarrow l^\pm W^\mp$ not only for the 1 $\hat{\nu}^c$ -model of the $\mu\nu$ SSM, but in addition for BRpV. In the last section of this chapter we focus on the $\mu\nu$ SSM with two right-handed neutrino superfields, where a tree-level calculation can be done consistently under the assumption that the conditions in Equation (6.188) are fulfilled.

10.1. Tree-level correlations in the $\mu\nu$ SSM with 1 $\hat{\nu}^c$

We will start our discussion with the consideration of a gaugino-like neutralino focusing on the two-body decay $\tilde{\chi}_1^0 \rightarrow l^+ W^-$. Figure 10.1 **a**) shows the predicted correlation of the branching ratios respectively decay widths to the atmospheric angle for various MSSM scenarios varying the additional parameters of the $\mu\nu$ SSM, namely λ, κ . Note that the correlation gets more pronounced using the full one-loop decay width in the next section or in the n generation case without the need of one-loop contributions. In Chapter 8 we discussed in addition SPS 9, where the degeneracy between the lightest neutralino and lightest chargino results in chargino decays dominated by R -parity violating final states. Also these decays are correlated to neutrino mixing angles: Figure 10.1 **b**) shows the ratio of decay widths $\Gamma(\tilde{\chi}_1^+ \rightarrow Z\mu^+)/\Gamma(\tilde{\chi}_1^+ \rightarrow Z\tau^+)$ as a function of the atmospheric angle similar to the $l^+ W^-$ final states in case of a neutralino LSP. This dependence is of course equal to the one of the branching ratios.

For some benchmark scenarios with a very light particle spectrum three-body decays are dominant, which we will only consider at tree-level in combination with the one-loop corrected

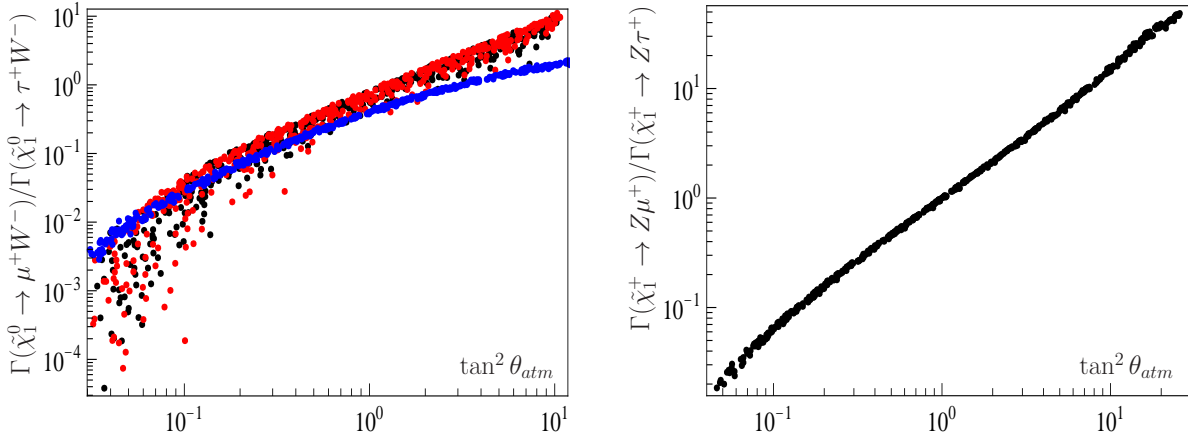


Figure 10.1.: **a)** (left) Ratio $\Gamma(\tilde{\chi}_1^0 \rightarrow \mu^+ W^-) / \Gamma(\tilde{\chi}_1^0 \rightarrow \tau^+ W^-)$ as a function of $\tan^2 \theta_{atm}$ for different SPS scenarios (SPS 1a' (black), SPS 3 (red), SPS 4 (blue)) and for different values of $\lambda \in [0.02, 0.5]$ and $\kappa \in [0.05, 0.3]$ with a dependence of allowed $\kappa(\lambda)$ similar to [111] and to Figure 8.5 and $T_\lambda = \lambda \cdot 1.5$ TeV and $T_\kappa = -\kappa \cdot 100$ GeV; **b)** (right) Ratio $\Gamma(\tilde{\chi}_1^+ \rightarrow Z \mu^+) / \Gamma(\tilde{\chi}_1^+ \rightarrow Z \tau^+)$ as a function of $\tan^2 \theta_{atm}$ for the AMSB scenario SPS 9 and for different values of $\lambda \in [0.02, 0.5]$, $\kappa \in [0.1, 0.6]$, $T_\lambda = \lambda \cdot 1.5$ TeV and $T_\kappa = -\kappa \cdot 100$ GeV.

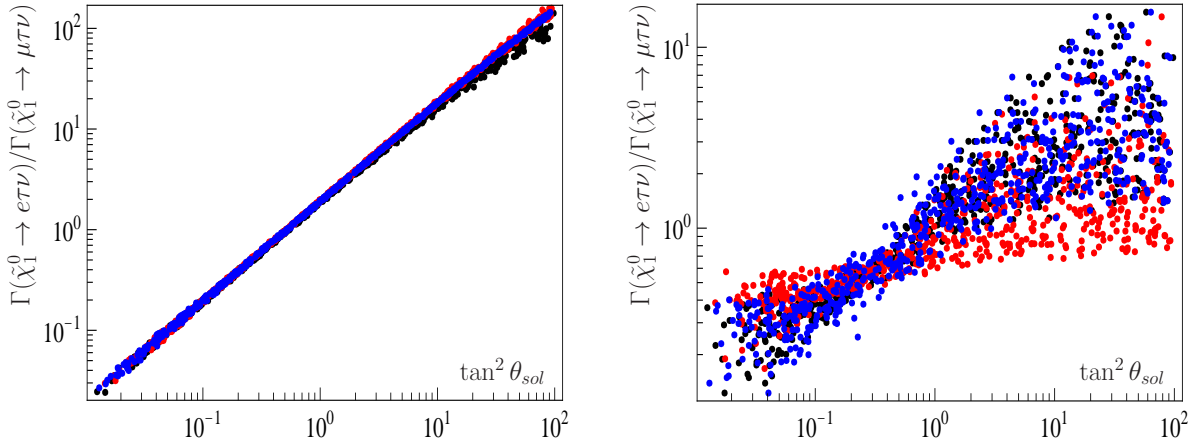


Figure 10.2.: Ratio $\Gamma(\tilde{\chi}_1^0 \rightarrow e \tau \nu) / \Gamma(\tilde{\chi}_1^0 \rightarrow \mu \tau \nu)$ as a function of $\tan^2 \theta_{sol}$ with same set of parameters as Figure 10.1. Bino purity $|\mathcal{N}_{41}|^2 > 0.97$. **a)** (left) Three-body contributions only; **b)** (right) Two-body plus three-body contributions. For a discussion see text.

$\overline{\text{DR}}$ mixing matrix \mathcal{N}^{1L} . As it can be seen from Figure 10.2 the three-body decay $\tilde{\chi}_1^0 \rightarrow l_i l_j \nu$ exemplifies a correlation to the solar mixing angle, where ν denotes all three generations of left-handed neutrinos. However, there are two main contributions to this final state, namely $\tilde{\chi}_1^0 \rightarrow l^\pm W^\mp \rightarrow l_i l_j \nu$ and $\tilde{\chi}_1^0 \rightarrow \tilde{\tau}^* l \rightarrow l_i l_j \nu$. The former is dominated by the alignment parameter Λ_i , the latter is sensitive to ϵ_i , which induces the correlation to the solar angle in accordance to Figure 10.2 **a)**. Both contributions are shown in Figure 10.2 **b)**. In case the W is on-shell the observance of hadronic final states allows to calculate the leptonic final states to reduce the two-body contribution. This improves the quality of the correlation significantly.

In case of the ATLAS SU4 point [163] (see Chapter 7) the LSP decays are dominated by three-body decays $\tilde{\chi}_1^0 \rightarrow q_i \bar{q}_j \mu$ and $\tilde{\chi}_1^0 \rightarrow l_i l_j \nu$, whose decay widths are related to the neutrino mixing angles as shown in Figure 10.3.

Finally we present the correlation for a singlino-like LSP using the three-body final state $l_i l_j \nu$. The relation to the solar mixing angle for a singlino purity of $|\mathcal{N}_{45}|^2 \in [0.75, 0.83]$ and a singlino mass $m(\tilde{\chi}_1^0) \in [22, 53]$ GeV is illustrated in Figure 10.4 without adding the contributions from

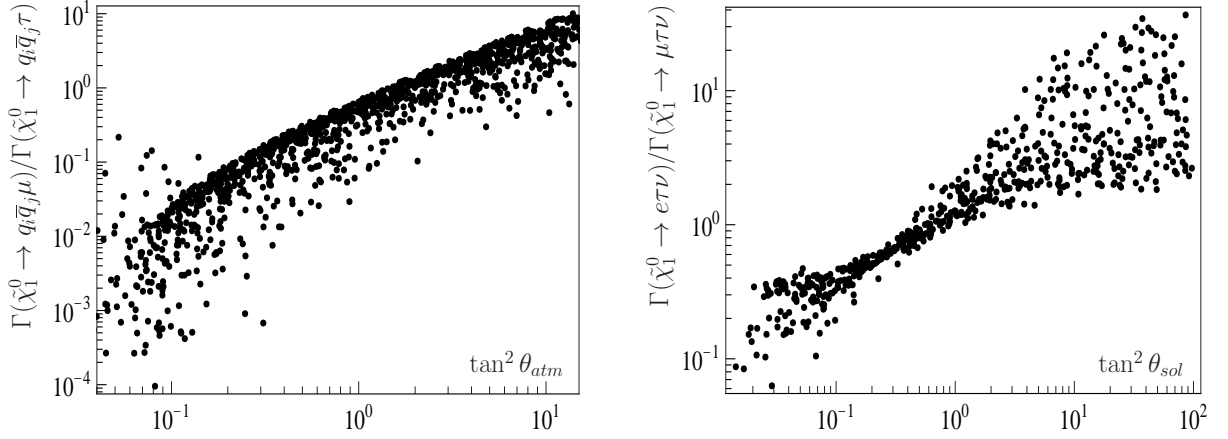


Figure 10.3.: a) (left) Ratio $\Gamma(\tilde{\chi}_1^0 \rightarrow q_i \bar{q}_j \mu) / \Gamma(\tilde{\chi}_1^0 \rightarrow q_i \bar{q}_j \tau)$ as a function of $\tan^2 \theta_{atm}$ for the SU4 scenario of the ATLAS collaboration [163]; b) (right) Ratio $\Gamma(\tilde{\chi}_1^0 \rightarrow e \tau \nu) / \Gamma(\tilde{\chi}_1^0 \rightarrow \mu \tau \nu)$ as a function of $\tan^2 \theta_{sol}$ with same set of parameters as a). Bino purity $|\mathcal{N}_{41}|^2 > 0.94$.

the two-body decay in $l^\pm W^\mp$. The absolute values for the branching ratios are comparable to the ones of the described SU4 scenario with a bino-like lightest neutralino. We want to add that for the shown example the light Higgs $S_2^0 = h^0$ decays to $\tilde{\chi}_1^0 \tilde{\chi}_1^0$ with a branching ratio of $Br(S_2^0 = h^0 \rightarrow \tilde{\chi}_1^0 \tilde{\chi}_1^0) = (21 - 91)\%$. However, we note that this result has to be taken advisedly, since the two-body final states do not show the relations we expect from the consideration of tree-level couplings using the one-loop corrected mixing matrices as we will see in the next section.

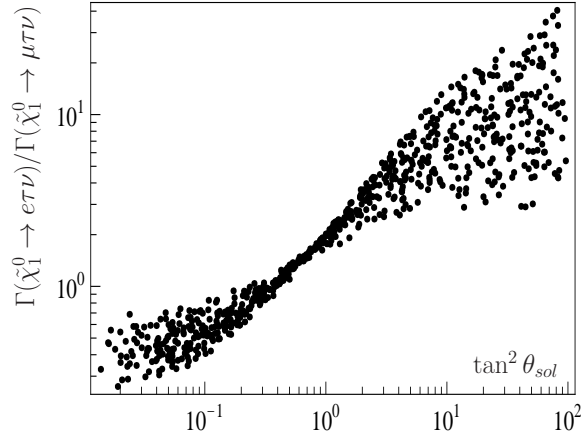


Figure 10.4.: Ratio $\Gamma(\tilde{\chi}_1^0 \rightarrow e \tau \nu) / \Gamma(\tilde{\chi}_1^0 \rightarrow \mu \tau \nu)$ as a function of $\tan^2 \theta_{sol}$ for the SPS 1a' scenario and $\lambda \in [0.2, 0.5]$, $\mu \in [110, 170]$ GeV, $\kappa = 0.035$, $T_\lambda = \lambda \cdot 1.5$ TeV and $T_\kappa = -0.7$ GeV.

10.2. One-loop correlations in the $\mu\nu$ SSM with 1 $\hat{\nu}^c$ and BRpV

After focusing on tree-body decay modes we will now discuss the correlations for the two-body decays $\tilde{\chi}_1^0 \rightarrow l^+ W^-$ in more detail using the full one-loop decay width as theoretically explained in Section 6.4 for the $\mu\nu$ SSM with one right-handed neutrino superfield and for BRpV. The absolute size of the corrections compared to the pure tree-level calculation was already illustrated in Section 9.2.2.

In accordance to Section 5.5 the tree-level couplings can be approximated in terms of the alignment parameters $\vec{\Lambda}$ and $\vec{\epsilon}$, which are connected to the neutrino mixing angles as shown in Section 9.1.3. Therefore, one can expect the following tree-level relation:

$$\frac{\Gamma^0(\tilde{\chi}_1^0 \rightarrow \mu^+ W^-)}{\Gamma^0(\tilde{\chi}_1^0 \rightarrow \tau^+ W^-)} \propto \left(\frac{O_{L21}}{O_{L31}} \right)^2 \approx \left(\frac{\Lambda_2}{\Lambda_3} \right)^2 \approx \tan^2 \theta_{atm} \quad (10.1)$$

However, it is a priori not clear, whether this relation also holds at the one-loop level. It turns out that using one-loop corrected $\overline{\text{DR}}$ masses and mixing matrices \mathcal{N}^{1L} for the tree-level decay width partially spoils the relation to the neutrino mixing angles and even further leads to unphysical large corrections compared to the tree-level decay width. Performing the full one-loop correction including the real corrections from photon emission in the on-shell scheme described in this thesis retains the predictions at tree-level, resulting in:

$$\frac{\Gamma^1(\tilde{\chi}_1^0 \rightarrow \mu^+ W^-)}{\Gamma^1(\tilde{\chi}_1^0 \rightarrow \tau^+ W^-)} \propto \left(\frac{\Lambda_2}{\Lambda_3} \right)^2 \approx \tan^2 \theta_{atm} \quad . \quad (10.2)$$

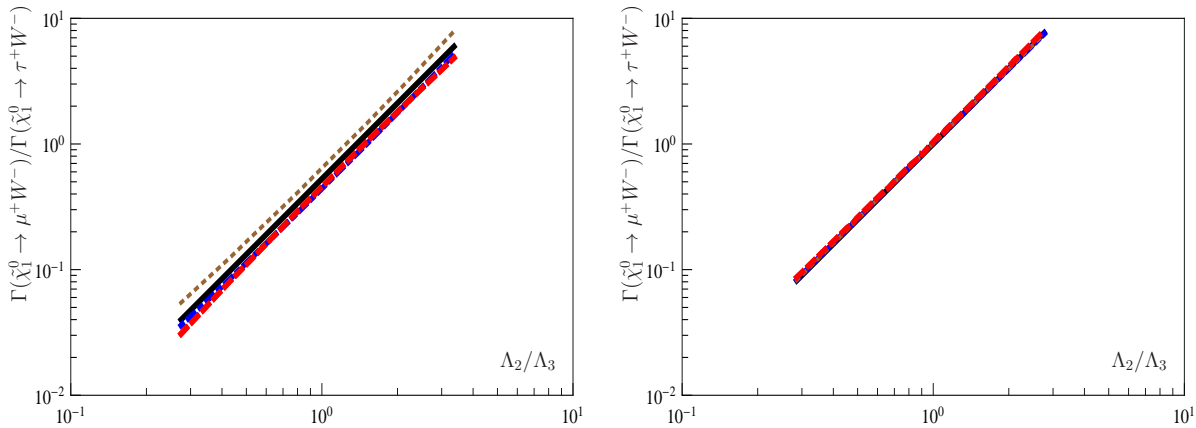


Figure 10.5.: Ratios $\Gamma(\tilde{\chi}_1^0 \rightarrow \mu^+ W^-)/\Gamma(\tilde{\chi}_1^0 \rightarrow \tau^+ W^-)$ with $\Gamma = \Gamma^0$ in black, $\Gamma = \Gamma^1$ in red, dashed, $\Gamma = \Gamma^0$ with \mathcal{N}^{1L} in blue, dot-dashed, $\Gamma = \Gamma^0$ with \mathcal{N}^{1L} , U^{1L} and V^{1L} in brown, dotted as a function of Λ_2/Λ_3 for the BRpV scenarios of Chapter 7: **a)** (left) SPS 2'; **b)** (right) SPS 3.

We start with BRpV taking two scenarios, where the lightest neutralino is either mainly a bino (scenario SPS 3) or Higgsino (scenario SPS 2'), and present the results in Figure 10.5. The figures do not only illustrate the tree-level and one-loop relations, but in addition the potentially false relations obtained by using the one-loop mixing matrices for the neutralinos \mathcal{N}^{1L} or in addition the charginos U^{1L} and V^{1L} within the tree-level decay width $\Gamma^0(\tilde{\chi}_1^0 \rightarrow l^+ W^-)$ presented in Equation (5.146). Instead of showing the relation to the atmospheric mixing angle $\tan^2 \theta_{atm}$, we show the ratios as a function of Λ_2/Λ_3 , which are connected to the mixing angle in accordance to Figure 9.6. The reason is the more pronounced connection to the alignment parameters itself. Note that the other R -parity violating parameters are fixed in such a way, that the neutrino data are within their 2σ bounds as given in Table 2.1. For the Higgsino-like neutralinos the NLO corrections are generally more important than for gaugino-like neutralinos. In fact the correlations using one-loop masses and mixing matrices can be off by a factor of 2 compared to the complete NLO calculation. The latter one shifts the correlations up to 30% compared to the tree-level result.

For the $\mu\nu$ SSM we highlight the correlation using the scenarios mSUGRA 1, mSUGRA 3',

mSUGRA 4' and GMSB 5 presented in Chapter 7 in Figure 10.6. In case of the mSUGRA 4' scenario the width originates from the variation of the neutrino parameters within the 2σ bounds.

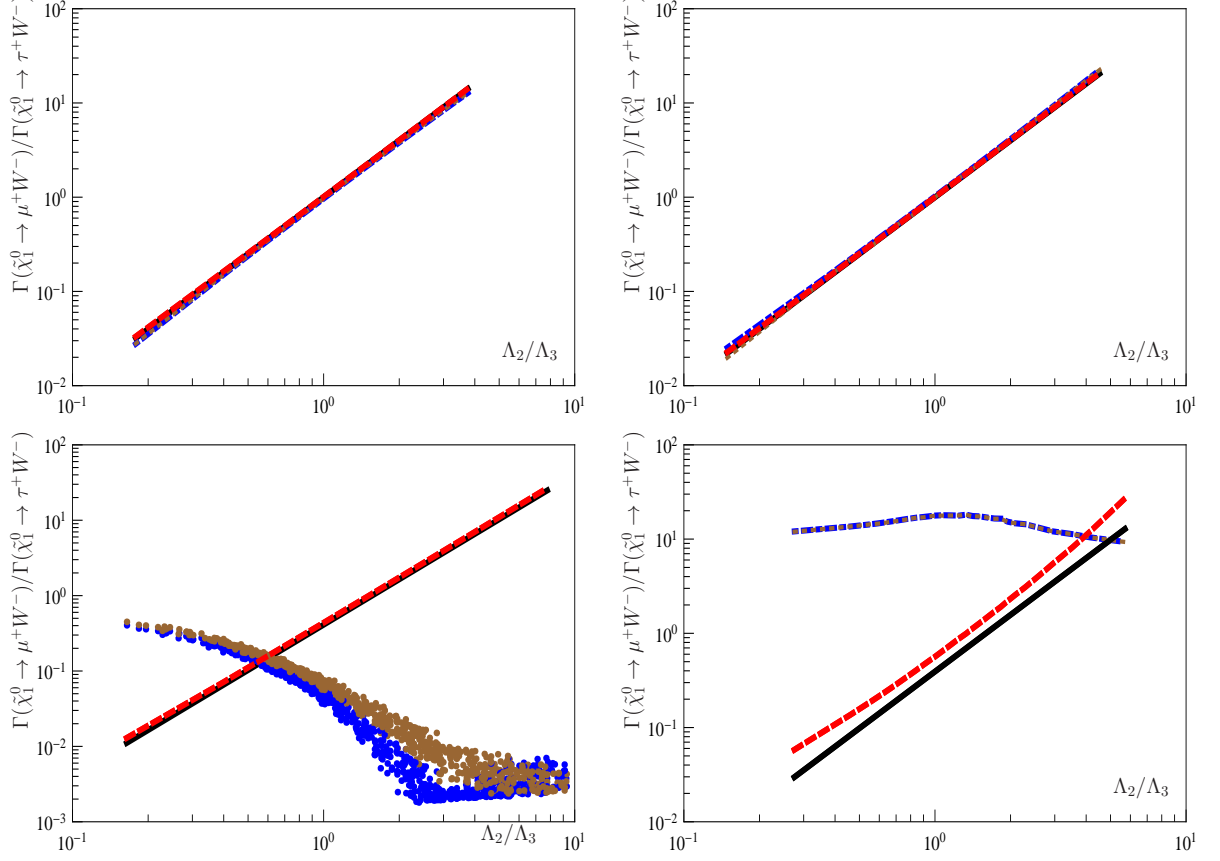


Figure 10.6.: Ratios $\Gamma(\tilde{\chi}_1^0 \rightarrow \mu^+W^-)/\Gamma(\tilde{\chi}_1^0 \rightarrow \tau^+W^-)$ with $\Gamma = \Gamma^0$ in black, $\Gamma = \Gamma^1$ in red, dashed, $\Gamma = \Gamma^0$ with \mathcal{N}^{1L} in blue, dot-dashed, $\Gamma = \Gamma^0$ with \mathcal{N}^{1L}, U^{1L} and V^{1L} in brown, dotted as a function of Λ_2/Λ_3 for the $\mu\nu$ SSM scenarios in Chapter 7: **a)** (upper left) mSUGRA 1; **b)** (upper right) mSUGRA 3'; **c)** (lower left) mSUGRA 4'; **d)** (lower right) GMSB 5.

If the lightest neutralino is either mainly a bino, wino or pure Higgsino, we know from BRpV that the approximated one-loop contributions using Γ^0 in combination with the one-loop corrected mixing matrices show the expected behavior. As soon as the singlino component of the neutralino gets sizable or even dominant, these approximations obviously fail and we have to refer to the complete one-loop decay width Γ^1 to obtain a reliable result. Figure 10.6 **d)** presents the case of a singlino-like LSP using the scenario GMSB 5, where clearly the complete one-loop decay width is needed for reasonable correlations. Figure 10.6 **c)** shows the relation for a Higgsino with a purity of 91.7% and a subdominant singlino component of 6.9%. Also in this case the full one-loop decay width is advisable.

The reader might wonder about the reason for this misleading ratios in case of a singlino component of the lightest neutralino. In case of a pure singlino the second and the last term of the left-handed coupling O_{LL1} shown in Equation (5.143) cancel at tree-level. If the tree-level mixing matrix \mathcal{N} is replaced by the one-loop mixing matrix \mathcal{N}^{1L} this cancellation is spoiled, leading to unreasonable results for the decay widths and necessarily the ratios of decay widths. However, taking into account the complete one-loop corrections restores this effect.

10.3. Tree-level correlations in the $\mu\nu$ SSM with 2 $\widehat{\nu}^c$

In this last section we want to consider the connection between LSP decays and neutrino mixing angles for the $\mu\nu$ SSM with two right-handed neutrino superfields, which can be done consistently on tree-level without the need of one-loop corrections in case the conditions of Equation (6.188) hold. Since the structure of the approximated couplings in Section 5.5 is different, some additional features show up in case of $n = 2$.

According to Section 6.3 we have two possibilities to fit neutrino data, which was already important for the decay length of a singlino-like neutralino as seen in Section 8.2.1. For completeness we recall that in case of fit1 Λ_i was used to fit the atmospheric scale and α_i for the solar scale, whereas fit2 was working vice versa.

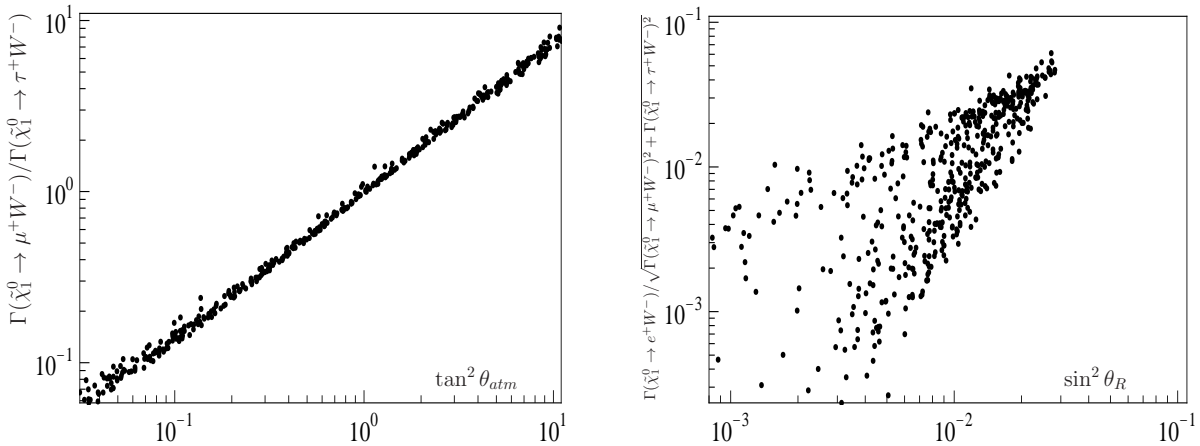


Figure 10.7.: **a)** (left) Ratio $\Gamma(\tilde{\chi}_1^0 \rightarrow \mu^+W^-)/\Gamma(\tilde{\chi}_1^0 \rightarrow \tau^+W^-)$ as a function of $\tan^2 \theta_{atm}$; **b)** (right) Ratio $\Gamma(\tilde{\chi}_1^0 \rightarrow e^+W^-)/\sqrt{\Gamma(\tilde{\chi}_1^0 \rightarrow \mu^+W^-)^2 + \Gamma(\tilde{\chi}_1^0 \rightarrow \tau^+W^-)^2}$ as a function of $\sin^2 \theta_R$ for a bino-like LSP. Bino purity $|\mathcal{N}_{41}|^2 > 0.9$. Neutrino data is fitted using option fit1.

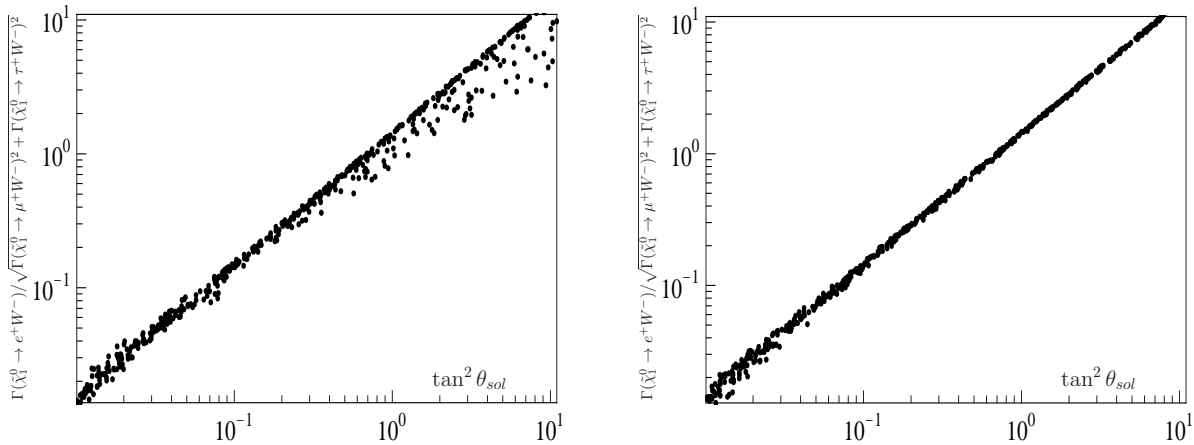


Figure 10.8.: **a)** (left) Ratio $\Gamma(\tilde{\chi}_1^0 \rightarrow e^+W^-)/\sqrt{\Gamma(\tilde{\chi}_1^0 \rightarrow \mu^+W^-)^2 + \Gamma(\tilde{\chi}_1^0 \rightarrow \tau^+W^-)^2}$ as a function of $\tan^2 \theta_{sol}$ for a bino-like LSP. Bino purity $|\mathcal{N}_{41}|^2 > 0.9$. Neutrino data is fitted using option fit2; **b)** (right) Ratio $\Gamma(\tilde{\chi}_1^0 \rightarrow e^+W^-)/\sqrt{\Gamma(\tilde{\chi}_1^0 \rightarrow \mu^+W^-)^2 + \Gamma(\tilde{\chi}_1^0 \rightarrow \tau^+W^-)^2}$ as a function of $\tan^2 \theta_{sol}$ for a singlino-like LSP. Singlino purity $|\mathcal{N}_{45}|^2 > 0.9$. Neutrino data is fitted using option fit1.

Given the approximated couplings in Section 5.5 a bino-like lightest neutralino couples proportional to Λ_i , whereas for a singlino-like neutralino the coupling is proportional to the alignment

parameter α_i . Using fit1 we show the ratios $\Gamma(\tilde{\chi}_1^0 \rightarrow \mu^+ W^-)/\Gamma(\tilde{\chi}_1^0 \rightarrow \tau^+ W^-)$ as a function of $\tan^2 \theta_{atm}$ and $\Gamma(\tilde{\chi}_1^0 \rightarrow e^+ W^-)/\sqrt{\Gamma(\tilde{\chi}_1^0 \rightarrow \mu^+ W^-)^2 + \Gamma(\tilde{\chi}_1^0 \rightarrow \tau^+ W^-)^2}$ as a function of $\sin^2 \theta_R$ for a bino-like neutralino in Figure 10.7. The correlation using a pure tree-level calculation is more pronounced than in the 1 $\hat{\nu}^c$ -model, implying that the ratio $|\tilde{\epsilon}|^2/|\tilde{\Lambda}|$ is much smaller. In case of fit2 a correlation of $\Gamma(\tilde{\chi}_1^0 \rightarrow e^+ W^-)/\sqrt{\Gamma(\tilde{\chi}_1^0 \rightarrow \mu^+ W^-)^2 + \Gamma(\tilde{\chi}_1^0 \rightarrow \tau^+ W^-)^2}$ to the solar mixing angle is induced as shown in Figure 10.8 a).

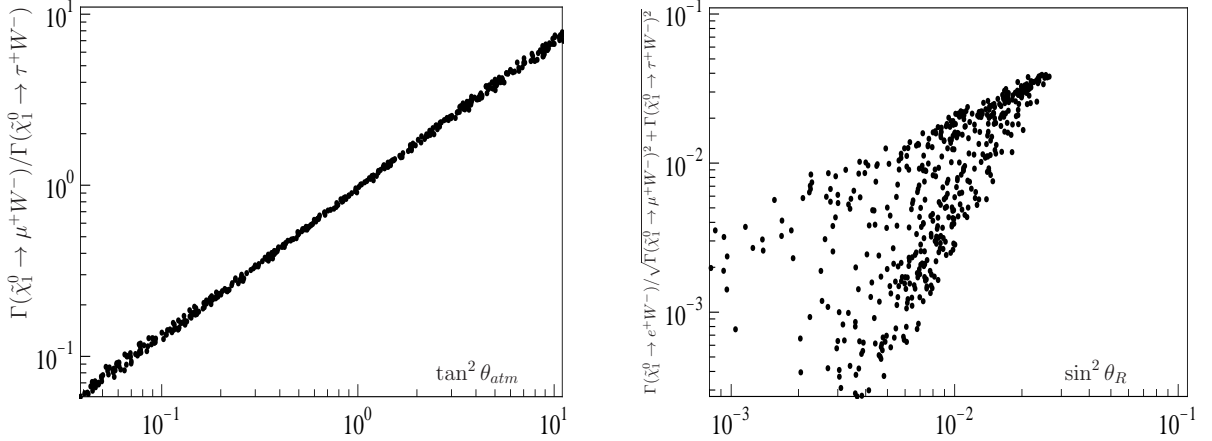


Figure 10.9.: **a)** (left) Ratio $\Gamma(\tilde{\chi}_1^0 \rightarrow \mu^+ W^-)/\Gamma(\tilde{\chi}_1^0 \rightarrow \tau^+ W^-)$ as a function of $\tan^2 \theta_{atm}$; **b)** (right) Ratio $\Gamma(\tilde{\chi}_1^0 \rightarrow e^+ W^-)/\sqrt{\Gamma(\tilde{\chi}_1^0 \rightarrow \mu^+ W^-)^2 + \Gamma(\tilde{\chi}_1^0 \rightarrow \tau^+ W^-)^2}$ as a function of $\sin^2 \theta_R$ for a singlino-like LSP. Singlino purity $|\mathcal{N}_{45}|^2 > 0.9$. Neutrino data is fitted using option fit2.

For the case of a singlino-like neutralino the correlations and types of fit to neutrino data are swapped with respect to the gaugino-like LSP case: The couplings in Equations (5.143) and (5.144) are proportional to α_i instead of Λ_i , so that a scenario with a singlino-like LSP and fit1 (fit2) is similar to a bino-like LSP and fit2 (fit1). This is demonstrated for the solar angle in Figure 10.8 b) and the atmospheric and reactor angle in Figure 10.9. In order to determine the case of fit the particle character of the lightest neutralino is crucial. Its determination is possible to a good accuracy at CLIC or the ILC, but might be difficult at the LHC. Note that the correlations for a singlino-like LSP presented in [156] for the 3 $\hat{\nu}^c$ -model cannot be reproduced completely in the 2 $\hat{\nu}^c$ -model.

Although all shown results in this section were based on SPS 1a' we checked that for the other benchmark scenarios the results do not change. Similarly to the two-body decay modes also three-body decays like $\tilde{\chi}_1^0 \rightarrow q_i \bar{q}_j l$, mediated by a virtual W boson, are correlated to neutrino mixing angles.

Lets us add a final comment: In case of $n > 2$ right-handed neutrino superfields, the effective neutrino mass matrix will have additional terms with respect to the one given in Equation (5.139). However, these contributions from additional right-handed neutrinos might be sub-dominant. Thus, if these additional right-handed neutrinos produce a negligible contribution to the neutrino masses but are at the same time the LSP ν_3^c , the correlations between the decays of ν_3^c and the neutrino mixing angles is lost.

Conclusion

As pointed out in the introduction fundamental questions about the origin of masses for particles and physics beyond the standard model might be answered in the near very exciting future for particle physics. This thesis contributes to the understanding of extensions of the minimal supersymmetrization of the standard model and their phenomenology at colliders like the LHC. We presented the scalar and fermionic sectors of the NMSSM, bilinear R -parity violation and the $\mu\nu$ SSM at tree-level highlighting the physical parameters of each model. For the LHC phenomenology of supersymmetric models the mass spectra of the squarks and sleptons, the scalars and pseudoscalars as well as the neutralinos and charginos are crucial, since they determine the detailed form of SUSY cascade decays. Therefore we worked out the one-loop contributions for the neutralino and chargino mass matrices including neutrinos and leptons and two-body decays of the form $\tilde{\chi}_j^0 \rightarrow \tilde{\chi}_l^\pm W^\mp$ using an on-shell scheme. Whereas for the MSSM on-shell one-loop corrections were discussed in various publications, the corrections in the MSSM extensions under consideration were not yet known. Since the number of free parameters at tree-level in the neutralino and chargino sector is lower than the number of conditions imposed in an on-shell scheme, one-loop mass corrections to the neutralinos and charginos in the MSSM and NMSSM had to be taken into account. Within this discussion we put special emphasis on the gauge invariance of our calculation by choosing a pinch technique for the renormalization of the mixing matrices, the reason being that the pinch technique is easily extendable to the discussed models. The two-body decays contain the real emission of a photon to obtain an infrared finite result. Due to the presence of left- and right-handed couplings the real emission does not factorize in the two-body decay width times a factor containing the Bremsstrahlung of the photon.

After the analytical formulas we also presented numerical results for the one-loop contributions in the various models under consideration: In the MSSM and NMSSM the mass corrections to neutralinos and charginos in the on-shell scheme are small of order per-mil, whereas in a $\overline{\text{DR}}$ scheme they are known to be of order per-cent. In R -parity violating models the limited number of physical parameters in the neutralino and chargino sector at tree-level also induces corrections to lepton and neutrino masses in the on-shell scheme: We have shown that the corrections to lepton masses are tiny, below the experimental uncertainties, whereas the neutrino masses obtain similar corrections as in case of $\overline{\text{DR}}$ calculations. Thus, the full neutrino spectrum can be explained at one-loop level in bilinear R -parity violation and the $\mu\nu$ SSM with one right-handed neutrino superfield using an on-shell scheme, where at tree-level only one neutrino acquires a mass, so that finite one-loop corrections are needed.

For various particle characters we illustrated that the two-body decays $\tilde{\chi}_j^0 \rightarrow \tilde{\chi}_l^\pm W^\mp$ can receive sizable corrections at the one-loop level in the (N)MSSM. In case of small tree-level decay width due to a cancellation of wino and Higgsino contributions the corrections can be even larger than the tree-level decay width itself. Moreover for a pure singlino or bino the tree-level width vanishes, such that one-loop contributions had to be considered to make reliable predictions. In

case of the R -parity violating decays $\tilde{\chi}_1^0 \rightarrow l^\pm W^\mp$ of the lightest neutralino in bilinear R -parity violation and the $\mu\nu$ SSM with one right-handed neutrino superfield the one-loop corrections can also be large, in particular for an electron in the final state. For the numerical analysis of the one-loop corrections carried out in this thesis we developed the programs `MaCoR` and `CNNDecays`, which are described in the appendix.

For the $\mu\nu$ SSM with one and two right-handed neutrino superfields we presented the LHC phenomenology with special focus on light singlet states in the scalar/pseudoscalar as well as the fermionic sector. Since the R -parity violating couplings are small compared to the (N)MSSM soft SUSY breaking parameters, the $\mu\nu$ SSM, but also BRpV, provide similar SUSY production cross sections and decay chains. The phenomenological difference to the (N)MSSM is the final decay of the lightest neutralino and decays of the lightest Higgs. We calculated the decay length of the lightest neutralino, which can result in displaced vertices within the detectors of the LHC. However, if a singlino-like lightest neutralino has a mass below 30 GeV the decay length might exceed several meter, so that a measurement of the final decay might not be possible. For the latter feature the masses of the lightest singlet scalar/pseudoscalar states are crucial, since the decay $\tilde{\chi}_1^0 \rightarrow S_i^0(P_i^0)\nu$ significantly reduces the decay length of the lightest neutralino, if kinematically allowed. Apart from a scalar/pseudoscalar final state the lightest neutralino decays are either dominated by two-body decays involving a heavy gauge boson or in particular for smaller masses of a bino- or singlino-like neutralino by the three-body decays into $l_i l_j \nu$ or $q_i \bar{q}_j l/\nu$. Another interesting difference compared to the MSSM phenomenology are non-standard Higgs decays like $S_i^0 \rightarrow \tilde{\chi}_1^0 \tilde{\chi}_1^0$ into a pair of lightest neutralinos, which further decay. Hence, non-standard Higgs decays into up to six leptons or quarks in combination with displaced vertices and missing energy are possible. However, from the phenomenological point of view the $\mu\nu$ SSM with one right-handed neutrino superfield is identical to the NMSSM in combination with bilinear R -parity violation. In case of more than one right-handed neutrino superfield we pointed out that in specific scenarios of a singlino-like neutralino the decay length is correlated to the neutrino mass scale. Whereas for one right-handed neutrino superfield the singlet scalar/pseudoscalar states are close to the singlino in mass, in case of more fields the soft SUSY breaking terms allow for the decoupling of the sectors. If several light scalars are present in particular the decays of the MSSM-like lightest Higgs h and the bino-like neutralino might help to determine the number of right-handed neutrino superfields in the $\mu\nu$ SSM.

Finally we discussed in great detail the pronounced correlation between branching ratios of the lightest neutralino decay and the neutrino mixing angles in BRpV and in the $\mu\nu$ SSM with one and two right-handed neutrino superfields. This feature is mainly independent of the SUSY parameter point, but determined by neutrino physics only. Apart from the tree-level results for the three-body decays in the $\mu\nu$ SSM with one right-handed neutrino superfield we focused on the correlations of the two-body decays $\tilde{\chi}_1^0 \rightarrow l^\pm W^\mp$ in BRpV and the $\mu\nu$ SSM at one-loop level, the reason being that one-loop corrected masses are needed for the explanation of the full neutrino spectrum. We demonstrated that in particular for singlinos as lightest neutralino full one-loop corrections for the decays have to be taken into account to obtain the expected tree-level correlations. Lastly the distinct correlations in the $\mu\nu$ SSM with two right-handed neutrino superfields were worked out, where a pure tree-level calculation can be performed consistently.

Tadpole equations and mass matrices in the $\mu\nu$ SSM

In this section we summarize the tadpole equations and mass matrices for the $\mu\nu$ SSM with n right-handed neutrino superfields. The superpotential of the $\mu\nu$ SSM can be found in Equation (4.9), the soft SUSY breaking Lagrangian in Equation (4.11). All the results can be reproduced with **MaCoR**, which we present in Appendix F.1. Except from the squarks the rotation from gauge to mass eigenstates was already described in Section 5. The masses of the neutralinos including the neutrinos and the charginos including the leptons are part of Section 5.3.

A.1. Tadpole equations

Using the scalar potential of the $\mu\nu$ SSM, which can be deduced from Equation (5.1), results in following minimization conditions:

$$\begin{aligned}
 t_d^0 = \frac{\partial V}{\partial v_d} = & \frac{1}{8}(g^2 + g'^2)u^2 v_d + m_{H_d}^2 v_d + \frac{1}{2}v_d \lambda_k \lambda_l^* v_{ck} v_{cl} + \frac{1}{2}v_d v_u^2 \lambda_k \lambda_k^* \\
 & - \frac{1}{8}v_{cs}^2 v_u (\kappa_k \lambda_k^* + \kappa_k^* \lambda_k) - \frac{1}{4}v_i v_{ck} v_{cl} (\lambda_k^* Y_\nu^{il} + \lambda_k (Y_\nu^{il})^*) - \frac{1}{4}v_u^2 v_i (\lambda_k^* Y_\nu^{ik} + \lambda_k (Y_\nu^{ik})^*) \\
 & - \frac{1}{2\sqrt{2}}v_u v_{ck} (T_\lambda^k + (T_\lambda^k)^*) = 0
 \end{aligned} \tag{A.1}$$

$$\begin{aligned}
 t_u^0 = \frac{\partial V}{\partial v_u} = & -\frac{1}{8}(g^2 + g'^2)u^2 v_u + m_{H_u}^2 v_u + \frac{1}{2}v_u \lambda_k \lambda_l^* v_{ck} v_{cl} + \frac{1}{2}v_d^2 v_u \lambda_k \lambda_k^* - \frac{1}{8}v_{ci}^2 v_d (\kappa_k \lambda_k^* + \kappa_k^* \lambda_k) \\
 & + \frac{1}{8}v_i v_{ck}^2 (\kappa_k^* Y_\nu^{ik} + \kappa_k (Y_\nu^{ik})^*) - \frac{1}{2}v_d v_u v_i (\lambda_k^* Y_\nu^{ik} + \lambda_k (Y_\nu^{ik})^*) + \frac{1}{2}v_u v_i v_j Y_\nu^{ik} (Y_\nu^{jk})^* \\
 & + \frac{1}{2}v_u Y_\nu^{ik} (Y_\nu^{il})^* v_{ck} v_{cl} - \frac{1}{2\sqrt{2}}v_d v_{ck} (T_\lambda^k + (T_\lambda^k)^*) \\
 & + \frac{1}{2\sqrt{2}}v_i v_{ck} (T_\nu^{ik} + (T_\nu^{ik})^*) = 0
 \end{aligned} \tag{A.2}$$

$$\begin{aligned}
 t_i^0 = \frac{\partial V}{\partial v_i} = & \frac{1}{8}(g^2 + g'^2)u^2 v_i + \frac{1}{2}(m_{L_{ij}}^2 + m_{L_{ji}}^2)v_j - \frac{1}{4}v_d v_u^2 (\lambda_k^* Y_\nu^{ik} + \lambda_k (Y_\nu^{ik})^*) \\
 & + \frac{1}{8}v_{ck}^2 v_u (\kappa_k^* Y_\nu^{ik} + \kappa_k (Y_\nu^{ik})^*) - \frac{1}{4}v_d v_{ck} v_{cl} (\lambda_k^* Y_\nu^{il} + \lambda_k (Y_\nu^{il})^*) \\
 & + \frac{1}{4}v_j v_{ck} v_{cl} (Y_\nu^{ik} (Y_\nu^{jl})^* + (Y_\nu^{ik})^* Y_\nu^{jl}) + \frac{1}{4}v_u^2 v_j (Y_\nu^{ik} (Y_\nu^{jk})^* + (Y_\nu^{ik})^* Y_\nu^{jk}) \\
 & + \frac{1}{2\sqrt{2}}v_u v_{ck} (T_\nu^{ik} + (T_\nu^{ik})^*) = 0
 \end{aligned} \tag{A.3}$$

$$t_{ck}^0 = \frac{\partial V}{\partial v_{ck}} = m_{\tilde{\nu}^c k k}^2 v_{ck} - \frac{1}{4}v_d v_u v_{ck} (\kappa_k \lambda_k^* + \kappa_k^* \lambda_k) + \frac{1}{4}\kappa_k \kappa_k^* v_{ck}^3 + \frac{1}{4}v_u v_{ck} v_i (\kappa_k^* Y_\nu^{ik} + \kappa_k (Y_\nu^{ik})^*)$$

$$\begin{aligned}
& + \frac{1}{4}(v_u^2 + v_d^2)v_{cl}(\lambda_k\lambda_l^* + \lambda_k^*\lambda_l) + \frac{1}{4}v_u^2v_{cl}(Y_\nu^{ik}(Y_\nu^{il})^* + (Y_\nu^{ik})^*Y_\nu^{il}) \\
& + \frac{1}{4}v_iv_jv_{cl}((Y_\nu^{ik})^*Y_\nu^{jl} + Y_\nu^{ik}(Y_\nu^{jl})^*) - \frac{1}{2\sqrt{2}}v_dv_u(T_\lambda^k + (T_\lambda^k)^*) \\
& - \frac{1}{4}v_dv_iv_{cl}(\lambda_l^*Y_\nu^{ik} + \lambda_l(Y_\nu^{ik})^* + \lambda_k^*Y_\nu^{il} + \lambda_k(Y_\nu^{il})^*) + \frac{1}{2\sqrt{2}}v_uv_i(T_\nu^{ik} + (T_\nu^{ik})^*) \\
& + \frac{1}{4\sqrt{2}}v_{cl}v_{cm} \left(T_\kappa^{klm} + (T_\kappa^{klm})^* \right) = 0
\end{aligned} \tag{A.4}$$

These equations imply a summation over $i, j = 1, \dots, 3$ and $k, l, m = 1, \dots, n$, only i is fixed in case of t_i^0 and k in case of t_{ck}^0 .

A.2. Scalar matrices

Here we give the mass matrices of the scalars and pseudoscalars including the sneutrinos and the charged scalars including the sleptons.

A.2.1. Charged Scalars

The quadratic part of the scalar potential, which contains the charged scalars, is of the form

$$V_{S^\pm} = S^{-'T} M_{S^\pm}^2 S^{+'} \tag{A.5}$$

with the following particle content:

$$S^{+'T} = ((H_d^-)^*, H_u^+, \tilde{e}^*, \tilde{\mu}^*, \tilde{\tau}^*, \tilde{e}^c, \tilde{\mu}^c, \tilde{\tau}^c) \tag{A.6}$$

$$S^{-'T} = (H_d^-, (H_u^+)^*, \tilde{e}, \tilde{\mu}, \tilde{\tau}, (\tilde{e}^c)^*, (\tilde{\mu}^c)^*, (\tilde{\tau}^c)^*) \tag{A.7}$$

$M_{S^\pm}^2$ is the (8×8) -mass matrix of the charged scalars, which is presented in Landau gauge $\xi_V = 0$, resulting in a massless Goldstone boson. For the general case of R_ξ -gauges the contributions in Section 5.2 have to be added. It can be split in the following form:

$$M_{S^\pm}^2 = \begin{pmatrix} M_{HH}^2 & (M_{H\tilde{l}}^2)^\dagger \\ M_{H\tilde{l}}^2 & M_{\tilde{l}\tilde{l}}^2 \end{pmatrix} \tag{A.8}$$

The (2×2) -matrix M_{HH}^2 is given by:

$$\begin{aligned}
(M_{HH}^2)_{11} &= m_{H_d}^2 + \frac{1}{8}((g^2 + g'^2)v_d^2 + (g^2 - g'^2)(v_u^2 - v_1^2 - v_2^2 - v_3^2)) \\
&\quad + \frac{1}{2}\lambda_k\lambda_l^*v_{ck}v_{cl} + \frac{1}{2}v_i(Y_e Y_e^\dagger)_{ij}v_j \\
(M_{HH}^2)_{12} &= \frac{1}{4}g^2v_uv_d - \frac{1}{2}\lambda_k\lambda_k^*v_uv_d + \frac{1}{4}\lambda_k\kappa_k^*v_{ck}^2 + \frac{1}{2}v_uv_i\lambda_k(Y_\nu^{ik})^* + \frac{1}{\sqrt{2}}v_{ck}T_\lambda^k \\
(M_{HH}^2)_{21} &= (M_{HH}^2)_{12}^* \\
(M_{HH}^2)_{22} &= m_{H_u}^2 + \frac{1}{8}[(g^2 + g'^2)v_u^2 + (g^2 - g'^2)(v_d^2 + v_1^2 + v_2^2 + v_3^2)] \\
&\quad + \frac{1}{2}\lambda_k\lambda_l^*v_{ck}v_{cl} + \frac{1}{2}v_{ck}v_{cl}Y_\nu^{ik}(Y_\nu^{il})^*
\end{aligned} \tag{A.9}$$

Again a summation over $i, j, i', j' = 1, 2, 3$ and $k, l, m = 1, \dots, n$ numbering the right-handed neutrino superfields has to be performed, if one of the indices does not show up on the left-hand side of an equation. The (6×2) -matrix, that mixes the charged Higgs bosons with the charged sleptons, is given by

$$M_{H\bar{l}}^2 = \begin{pmatrix} M_{HL}^2 \\ M_{HR}^2 \end{pmatrix} \quad (\text{A.10})$$

with:

$$\begin{aligned} (M_{HL}^2)_{i1} &= \frac{1}{4}g^2 v_d v_i - \frac{1}{2}\lambda_k^* Y_\nu^{il} v_{ck} v_{cl} - \frac{1}{2}v_d \left(Y_e Y_e^\dagger \right)_{ij} v_j \\ (M_{HL}^2)_{i2} &= \frac{1}{4}g^2 v_u v_i - \frac{1}{4}\kappa_k^* v_{ck}^2 Y_\nu^{ik} + \frac{1}{2}v_u v_d \lambda_k^* h_\nu^{ik} - \frac{1}{2}v_u v_j Y_\nu^{ik} (Y_\nu^{jk})^* - \frac{1}{\sqrt{2}}v_{ck} T_\nu^{ik} \\ (M_{HR}^2)_{i1} &= -\frac{1}{2}v_u v_{ck} (Y_e^{ji})^* Y_\nu^{jk} - \frac{1}{\sqrt{2}}v_j (T_e^{ji})^* \\ (M_{HR}^2)_{i2} &= -\frac{1}{2}\lambda_k v_{ck} v_j (Y_e^{ji})^* - \frac{1}{2}v_d (Y_e^{ji})^* Y_\nu^{jk} v_{ck} \end{aligned} \quad (\text{A.11})$$

Finally, the (6×6) -mass matrix of the charged sleptons can be decomposed as follows

$$M_{\bar{l}l}^2 = \begin{pmatrix} M_{LL}^2 & M_{LR}^2 \\ M_{RL}^2 & M_{RR}^2 \end{pmatrix} \quad (\text{A.12})$$

with:

$$\begin{aligned} (M_{LL}^2)_{ij} &= \left(m_{\bar{L}}^2 \right)_{ij} + \frac{1}{8}(g'^2 - g^2)(v_d^2 - v_u^2 + v_1^2 + v_2^2 + v_3^2)\delta_{ij} + \frac{1}{4}g^2 v_i v_j \\ &\quad + \frac{1}{2}v_d^2 \left(Y_e Y_e^\dagger \right)_{ij} + \frac{1}{2}v_{ck} v_{cl} Y_\nu^{ik} (Y_\nu^{jl})^* \\ M_{LR}^2 &= -\frac{1}{2}\lambda_k^* v_{ck} v_u Y_e + \frac{1}{\sqrt{2}}v_d T_e \\ M_{RL}^2 &= (M_{LR}^2)^\dagger \\ (M_{RR}^2)_{ij} &= \left(m_{\bar{R}}^2 \right)_{ij} + \frac{1}{4}g'^2(v_u^2 - v_d^2 - v_1^2 - v_2^2 - v_3^2)\delta_{ij} \\ &\quad + \frac{1}{2}v_d^2 \left(Y_e^\dagger Y_e \right)_{ij} + \frac{1}{2}v_{i'} v_{j'} (Y_e^{i'i})^* Y_e^{j'j} \end{aligned} \quad (\text{A.13})$$

A.2.2. Neutral Scalars

In the basis

$$S^{0'T} = (\sigma_d^0, \sigma_u^0, \tilde{\nu}_k^{cR}, \tilde{\nu}_i^R) \quad (\text{A.14})$$

the scalar potential includes the following term

$$V_{S^0} = \frac{1}{2}S^{0'T} M_{S^0}^2 S^{0'} \quad , \quad (\text{A.15})$$

with the $((5+n) \times (5+n))$ -matrix $M_{S^0}^2$ of the neutral scalars, which we decompose in the following form:

$$M_{S^0}^2 = \begin{pmatrix} M_{HH}^2 & M_{HS}^2 & M_{H\bar{L}}^2 \\ (M_{HS}^2)^T & M_{SS}^2 & M_{\bar{L}S}^2 \\ (M_{H\bar{L}}^2)^T & (M_{\bar{L}S}^2)^T & M_{\bar{L}\bar{L}}^2 \end{pmatrix} . \quad (\text{A.16})$$

The matrix elements are given as follows:

$$\begin{aligned}
(M_{HH}^2)_{11} &= m_{H_d}^2 + \frac{1}{8}(g^2 + g'^2)(3v_d^2 - v_u^2 + v_1^2 + v_2^2 + v_3^2) \\
&\quad + \frac{1}{2}\lambda_k\lambda_l^*v_{ck}v_{cl} + \frac{1}{2}v_u^2\lambda_k\lambda_k^* \\
(M_{HH}^2)_{12} &= -\frac{1}{4}(g^2 + g'^2)v_dv_u + \lambda_s\lambda_s^*v_dv_u - \frac{1}{8}v_{ck}^2(\lambda_k\kappa_k^* + \lambda_k^*\kappa_k) \\
&\quad - \frac{1}{2}v_uv_i(\lambda_k^*Y_\nu^{ik} + \lambda_k(Y_\nu^{ik})^*) - \frac{1}{2\sqrt{2}}v_{ck}(T_\lambda^k + (T_\lambda^k)^*) \\
(M_{HH}^2)_{21} &= (M_{HH}^2)_{12} \\
(M_{HH}^2)_{22} &= m_{H_u}^2 - \frac{1}{8}(g^2 + g'^2)(v_d^2 - 3v_u^2 + v_1^2 + v_2^2 + v_3^2) \\
&\quad + \frac{1}{2}\lambda_k\lambda_l^*v_{ck}v_{cl} + \frac{1}{2}v_d^2\lambda_k\lambda_k^* + \frac{1}{2}v_{ck}v_{cl}Y_\nu^{ik}(Y_\nu^{il})^* + \frac{1}{2}v_iv_j(Y_\nu^{ik})^*Y_\nu^{jk} \\
&\quad - \frac{1}{2}v_dv_i(\lambda_k^*Y_\nu^{ik} + \lambda_k(Y_\nu^{ik})^*) \tag{A.17}
\end{aligned}$$

$$\begin{aligned}
(M_{HS}^2)_{1k} &= -\frac{1}{4}v_uv_{ck}(\lambda_k^*\kappa_k + \lambda_k\kappa_k^*) + \frac{1}{2}v_dv_{cl}(\lambda_k\lambda_l^* + \lambda_k^*\lambda_l) \\
&\quad - \frac{1}{2\sqrt{2}}v_u(T_\lambda^k + (T_\lambda^k)^*) - \frac{1}{4}v_iv_{cl}(\lambda_k^*Y_\nu^{il} + \lambda_k(Y_\nu^{il})^* + \lambda_l^*Y_\nu^{ik} + \lambda_l(Y_\nu^{ik})^*) \\
(M_{HS}^2)_{2k} &= -\frac{1}{4}v_dv_{ck}(\lambda_k^*\kappa_k + \lambda_k\kappa_k^*) + \frac{1}{2}v_uv_{cl}(\lambda_k\lambda_l^* + \lambda_k^*\lambda_l) \\
&\quad - \frac{1}{2\sqrt{2}}v_d(T_\lambda^k + (T_\lambda^k)^*) + \frac{1}{2\sqrt{2}}v_i(T_\nu^{ik} + (T_\nu^{ik})^*) + \frac{1}{4}v_{ck}v_i(\kappa_k^*Y_\nu^{ik} + \kappa_k(Y_\nu^{ik})^*) \\
&\quad + \frac{1}{2}v_uv_{cl}[Y_\nu^{ik}(Y_\nu^{il})^* + (Y_\nu^{ik})^*Y_\nu^{il}] \tag{A.18}
\end{aligned}$$

$$\begin{aligned}
(M_{H\bar{L}}^2)_{1i} &= \frac{1}{4}(g^2 + g'^2)v_dv_i - \frac{1}{4}v_u^2(\lambda_k^*Y_\nu^{ik} + \lambda_k(Y_\nu^{ik})^*) - \frac{1}{4}v_{ck}v_{cl}(\lambda_k^*Y_\nu^{il} + \lambda_k(Y_\nu^{il})^*) \\
(M_{H\bar{L}}^2)_{2i} &= -\frac{1}{4}(g^2 + g'^2)v_uv_i + \frac{1}{8}v_{ck}^2(\kappa_k^*Y_\nu^{ik} + \kappa_k(Y_\nu^{ik})^*) - \frac{1}{2}v_uv_d(\lambda_k^*Y_\nu^{ik} + \lambda_k(Y_\nu^{ik})^*) \\
&\quad + \frac{1}{2}v_uv_j(Y_\nu^{jk}(Y_\nu^{ik})^* + (Y_\nu^{jk})^*Y_\nu^{ik}) + \frac{1}{2\sqrt{2}}v_{ck}(T_\nu^{ik} + (T_\nu^{ik})^*) \tag{A.19}
\end{aligned}$$

$$\begin{aligned}
(M_{SS}^2)_{kl} &= \frac{1}{2}((m_{\bar{\nu}c}^2)_{kl} + (m_{\bar{\nu}c}^2)_{lk}) + \frac{1}{4}(\lambda_k\lambda_l^* + \lambda_k^*\lambda_l)(v_d^2 + v_u^2) - \frac{1}{4}v_dv_u(\lambda_k^*\kappa_k + \lambda_k\kappa_k^*)\delta_{kl} \\
&\quad + \frac{3}{4}\kappa_k\kappa_l^*v_{ck}^2\delta_{kl} + \frac{1}{4}v_uv_i(\kappa_k^*Y_\nu^{ik} + \kappa_k(Y_\nu^{ik})^*)\delta_{kl} + \frac{1}{4}v_u^2[(Y_\nu^{ik})^*Y_\nu^{il} + Y_\nu^{ik}(Y_\nu^{il})^*] \\
&\quad + \frac{1}{4}v_iv_j[(Y_\nu^{ik})^*Y_\nu^{jl} + Y_\nu^{ik}(Y_\nu^{jl})^*] - \frac{1}{4}v_dv_i(\lambda_k^*Y_\nu^{il} + \lambda_l(Y_\nu^{ik})^* + \lambda_k(Y_\nu^{il})^* + \lambda_l^*Y_\nu^{ik}) \\
&\quad + \frac{1}{2\sqrt{2}}v_{cm}(T_\kappa^{klm} + (T_\kappa^{klm})^*) \tag{A.20}
\end{aligned}$$

$$\begin{aligned}
(M_{LS}^2)_{ki} &= \frac{1}{4}v_u v_{ck}(\kappa_k^* Y_\nu^{ik} + \kappa_k(Y_\nu^{ik})^*) - \frac{1}{4}v_d v_{cl}(\lambda_k^* Y_\nu^{il} + \lambda_l^* Y_\nu^{ik} + \lambda_k(Y_\nu^{il})^* + \lambda_l(Y_\nu^{ik})^*) \\
&\quad + \frac{1}{4}v_j v_{cl} \left(Y_\nu^{jl}(Y_\nu^{ik})^* + Y_\nu^{jk}(Y_\nu^{il})^* + (Y_\nu^{jl})^* Y_\nu^{ik} + (Y_\nu^{jk})^* Y_\nu^{il} \right) \\
&\quad + \frac{1}{2\sqrt{2}}v_u(T_\nu^{ik} + (T_\nu^{ik})^*)
\end{aligned} \tag{A.21}$$

$$\begin{aligned}
(M_{\bar{L}\bar{L}}^2)_{ij} &= \frac{1}{2} \left((m_{\bar{L}}^2)_{ij} + (m_{\bar{L}}^2)_{ji} \right) + \frac{1}{8}(g^2 + g'^2)(v_d^2 - v_u^2 + v_1^2 + v_2^2 + v_3^2)\delta_{ij} \\
&\quad + \frac{1}{4}(g^2 + g'^2)v_i v_j + \frac{1}{4}v_u^2 \left(Y_\nu^{ik}(Y_\nu^{jk})^* + (Y_\nu^{ik})^* Y_\nu^{jk} \right) \\
&\quad + \frac{1}{4}v_{ck} v_{cl} \left(Y_\nu^{ik}(Y_\nu^{jl})^* + (Y_\nu^{ik})^* Y_\nu^{jl} \right)
\end{aligned} \tag{A.22}$$

A.2.3. Pseudoscalars

In the basis

$$P^{0'T} = (\phi_d^0, \phi_u^0, \tilde{\nu}_k^I, \tilde{\nu}_i^I) \tag{A.23}$$

the scalar potential includes the following term

$$V_{P^0} = \frac{1}{2}P^{0'T} M_{P^0}^2 P^{0'} \quad , \tag{A.24}$$

with the $((5+n) \times (5+n))$ -matrix $M_{P^0}^2$ of the pseudoscalars, which we decompose in the following form:

$$M_{P^0}^2 = \begin{pmatrix} M_{HH}^2 & M_{HS}^2 & M_{H\bar{L}}^2 \\ (M_{HS}^2)^T & M_{SS}^2 & M_{LS}^2 \\ (M_{H\bar{L}}^2)^T & (M_{LS}^2)^T & M_{\bar{L}\bar{L}}^2 \end{pmatrix} . \tag{A.25}$$

The individual elements are given by:

$$\begin{aligned}
(M_{HH}^2)_{11} &= m_{H_d}^2 + \frac{1}{8}(g^2 + g'^2)(v_d^2 - v_u^2 + v_1^2 + v_2^2 + v_3^2) \\
&\quad + \frac{1}{2}\lambda_k \lambda_l^* v_{ck} v_{cl} + \frac{1}{2}v_u^2 \lambda_k \lambda_k^* \\
(M_{HH}^2)_{12} &= \frac{1}{8}v_{ck}^2 (\lambda_k \kappa_k^* + \lambda_k^* \kappa_k) + \frac{1}{2\sqrt{2}}v_{ck}(T_\lambda^k + (T_\lambda^k)^*) \\
(M_{HH}^2)_{21} &= (M_{HH}^2)_{12} \\
(M_{HH}^2)_{22} &= m_{H_u}^2 - \frac{1}{8}(g^2 + g'^2)(v_d^2 - v_u^2 + v_1^2 + v_2^2 + v_3^2) \\
&\quad + \frac{1}{2}\lambda_k \lambda_l^* v_{ck} v_{cl} + \frac{1}{2}v_d^2 \lambda_k \lambda_k^* + \frac{1}{2}v_{ck} v_{cl} Y_\nu^{ik}(Y_\nu^{il})^* + \frac{1}{2}v_i v_j (Y_\nu^{ik})^* Y_\nu^{jk} \\
&\quad - \frac{1}{2}v_d v_i (\lambda_k^* Y_\nu^{ik} + \lambda_k(Y_\nu^{ik})^*)
\end{aligned} \tag{A.26}$$

$$\begin{aligned}
(M_{HS}^2)_{1k} &= -\frac{1}{4}v_u v_{ck}(\lambda_k^* \kappa_k + \text{h.c.}) + \frac{1}{4} \sum_{l \neq k} v_i v_{cl}(\lambda_k^* Y_\nu^{il} - \lambda_l^* Y_\nu^{ik} + \lambda_k(Y_\nu^{il})^* - \lambda_l(Y_\nu^{ik})^*) \\
&\quad + \frac{1}{2\sqrt{2}}v_u(T_\lambda^k + (T_\lambda^k)^*) \\
(M_{HS}^2)_{2k} &= -\frac{1}{4}v_d v_{ck}(\lambda_k^* \kappa_k + \lambda_k \kappa_k^*) + \frac{1}{4}v_{ck} v_i(\kappa_k^* Y_\nu^{ik} + \kappa_k(Y_\nu^{ik})^*) \\
&\quad + \frac{1}{2\sqrt{2}}v_d(T_\lambda^k + (T_\lambda^k)^*) - \frac{1}{2\sqrt{2}}v_i(T_\nu^{ik} + (T_\nu^{ik})^*)
\end{aligned} \tag{A.27}$$

$$\begin{aligned}
(M_{H\tilde{L}}^2)_{1i} &= -\frac{1}{4}v_u^2(\lambda_k^* Y_\nu^{ik} + \lambda_k(Y_\nu^{ik})^*) - \frac{1}{4}v_{ck} v_{cl}(\lambda_k^* Y_\nu^{il} + \lambda_k(Y_\nu^{il})^*) \\
(M_{H\tilde{L}}^2)_{2i} &= -\frac{1}{8}v_{ck}^2(\kappa_k^* Y_\nu^{ik} + \kappa_k(Y_\nu^{ik})^*) - \frac{1}{2\sqrt{2}}v_{ck}(T_\nu^{ik} + (T_\nu^{ik})^*)
\end{aligned} \tag{A.28}$$

$$\begin{aligned}
(M_{SS}^2)_{kl} &= \frac{1}{2}((m_{\tilde{\nu}c}^2)_{kl} + (m_{\tilde{\nu}c}^2)_{lk}) + \frac{1}{4}(\lambda_k \lambda_l^* + \lambda_k^* \lambda_l)(v_d^2 + v_u^2) + \frac{1}{4}v_d v_u(\lambda_k^* \kappa_k + \lambda_k \kappa_k^*)\delta_{kl} \\
&\quad + \frac{1}{4}\kappa_k \kappa_k^* v_{ck}^2 \delta_{kl} - \frac{1}{4}v_u v_i(\kappa_k^* Y_\nu^{ik} + \kappa_k(Y_\nu^{ik})^*)\delta_{kl} + \frac{1}{4}v_u^2 \left((Y_\nu^{ik})^* Y_\nu^{il} + Y_\nu^{ik} (Y_\nu^{il})^* \right) \\
&\quad + \frac{1}{4}v_i v_j \left((Y_\nu^{ik})^* Y_\nu^{jl} + Y_\nu^{ik} (Y_\nu^{jl})^* \right) - \frac{1}{4}v_d v_i \left(\lambda_k^* Y_\nu^{il} + \lambda_l(Y_\nu^{ik})^* + \lambda_k(Y_\nu^{il})^* + \lambda_l^* Y_\nu^{ik} \right) \\
&\quad - \frac{1}{2\sqrt{2}}v_{cm}(T_\kappa^{klm} + (T_\kappa^{klm})^*)
\end{aligned} \tag{A.29}$$

$$\begin{aligned}
(M_{LS}^2)_{ki} &= \frac{1}{4}v_u v_{ck}(\kappa_k^* Y_\nu^{ik} + \kappa_k(Y_\nu^{ik})^*) + \frac{1}{4} \sum_{l \neq k} v_d v_{cl}(\lambda_l^* Y_\nu^{ik} - \lambda_k^* Y_\nu^{il} + \lambda_l(Y_\nu^{ik})^* - \lambda_k(Y_\nu^{il})^*) \\
&\quad + \frac{1}{4} \sum_{l \neq k} v_j v_{cl} \left(Y_\nu^{jk} (Y_\nu^{il})^* - Y_\nu^{jl} (Y_\nu^{ik})^* + (Y_\nu^{jk})^* Y_\nu^{il} - (Y_\nu^{jl})^* Y_\nu^{ik} \right) \\
&\quad - \frac{1}{2\sqrt{2}}v_u(T_\nu^{ik} + (T_\nu^{ik})^*)
\end{aligned} \tag{A.30}$$

$$\begin{aligned}
(M_{\tilde{L}\tilde{L}}^2)_{ij} &= \frac{1}{2} \left((m_{\tilde{L}}^2)_{ij} + (m_{\tilde{L}}^2)_{ji} \right) + \frac{1}{8}(g^2 + g'^2)(v_d^2 - v_u^2 + v_1^2 + v_2^2 + v_3^2)\delta_{ij} \\
&\quad + \frac{1}{4}v_u^2 \left(Y_\nu^{ik} (Y_\nu^{jk})^* + (Y_\nu^{ik})^* Y_\nu^{jk} \right) + \frac{1}{4}v_{ck} v_{cl} \left(Y_\nu^{ik} (Y_\nu^{jl})^* + (Y_\nu^{ik})^* Y_\nu^{jl} \right)
\end{aligned} \tag{A.31}$$

A.2.4. Squarks

We have not yet addressed the impact of R -parity violating couplings in the $\mu\nu$ SSM for the squark mass matrices, which should be done in this short section. Using the gauge eigenstates $(\tilde{u}'_i)^T = (\tilde{u}_{Li}, \tilde{u}_{Ri}) = (\tilde{u}_i, \tilde{u}_i^{c*})$ and a similar one for \tilde{d}'_i we can write the quadratic part of the scalar potential containing the squarks in the form

$$V_{\tilde{u},\tilde{d}} = \tilde{u}'^\dagger M_{\tilde{u}}^2 \tilde{u}' + \tilde{d}'^\dagger M_{\tilde{d}}^2 \tilde{d}' \quad , \quad (\text{A.32})$$

where the hermitian (6×6) -matrix $M_{\tilde{q}}^2$ with $\tilde{q} = \tilde{u}$ or \tilde{d} is given by

$$M_{\tilde{q}}^2 = \begin{pmatrix} M_{\tilde{q}LL}^2 & M_{\tilde{q}LR}^2 \\ M_{\tilde{q}RL}^2 & M_{\tilde{q}RR}^2 \end{pmatrix} . \quad (\text{A.33})$$

Using the (3×3) -identity matrix I_3 the individual blocks for \tilde{u} and \tilde{d} are

$$\begin{aligned} M_{\tilde{u}LL}^2 &= \frac{1}{2}v_u^2 (Y_u^* Y_u^T) + m_{\tilde{Q}}^2 + \left(\frac{1}{8}g^2 - \frac{1}{24}g'^2\right) u^2 I_3 \\ M_{\tilde{u}LR}^2 &= -\frac{1}{2}v_{ck}v_d\lambda_k (Y_u^*) + \frac{1}{2}v_{ck}v_i Y_\nu^{ik} (Y_u) + \frac{1}{\sqrt{2}}v_u (T_u^*) \\ M_{\tilde{u}RL}^2 &= (M_{\tilde{u}LR}^2)^\dagger \\ M_{\tilde{u}RR}^2 &= \frac{1}{2}v_u^2 (Y_u^T Y_u^*) + (m_{\tilde{u}c}^2)^T + \frac{1}{6}g'^2 u^2 I_3 \end{aligned} \quad (\text{A.34})$$

and

$$\begin{aligned} M_{\tilde{d}LL}^2 &= \frac{1}{2}v_d^2 (Y_d^* Y_d^T) + m_{\tilde{Q}}^2 - \left(\frac{1}{8}g^2 + \frac{1}{24}g'^2\right) u^2 I_3 \\ M_{\tilde{d}LR}^2 &= -\frac{1}{2}v_{ck}v_d\lambda_k (Y_d^*) + \frac{1}{\sqrt{2}}v_d (T_d^*) \\ M_{\tilde{d}RL}^2 &= (M_{\tilde{d}LR}^2)^\dagger \\ M_{\tilde{d}RR}^2 &= \frac{1}{2}v_d^2 (Y_d^T Y_d^*) + (m_{\tilde{d}c}^2)^T - \frac{1}{12}g'^2 u^2 I_3 \end{aligned} \quad (\text{A.35})$$

The mass eigenstates of the squarks are obtained by

$$\tilde{q} = R^{\tilde{q}} \tilde{q}' \quad \text{and} \quad \tilde{q}_i = R_{ij}^{\tilde{q}} \tilde{q}'_j \quad , \quad (\text{A.36})$$

where the unitary rotation matrices diagonalize the hermitian mass matrices according to

$$M_{\tilde{q},\text{diag.}}^2 = R^{\tilde{q}} M_{\tilde{q}}^2 (R^{\tilde{q}})^\dagger \quad . \quad (\text{A.37})$$

Expansion matrices in BRpV and the $\mu\nu$ SSM

In this section we present the expansion matrices ξ , ξ_L and ξ_R as they appear in the approximated diagonalization matrices of the neutralinos and charginos of Section 5.3

$$\mathcal{N} = \begin{pmatrix} N & N\xi^T \\ -V^T\xi & V^T \end{pmatrix}, \quad U = \begin{pmatrix} U_c & U_c\xi_L^T \\ -\xi_L & I_3 \end{pmatrix}, \quad V = \begin{pmatrix} V_c & V_c\xi_R^T \\ -\xi_R & I_3 \end{pmatrix}. \quad (\text{B.1})$$

Using the abbreviations in Equations (4.10), (5.132) and (5.133) and the determinant shown in Equation (5.134), the elements of ξ in case of BRpV are given by:

$$\xi_{i1} = \frac{g'M_2\mu}{2\text{Det}_0}\Lambda_i \qquad \xi_{i2} = -\frac{gM_1\mu}{2\text{Det}_0^{\text{BRpV}}}\Lambda_i \quad (\text{B.2})$$

$$\xi_{i3} = -\frac{\epsilon_i}{\mu} + \frac{m_\gamma v_u}{4\text{Det}_0^{\text{BRpV}}}\Lambda_i \qquad \xi_{i4} = -\frac{m_\gamma v_d}{4\text{Det}_0^{\text{BRpV}}}\Lambda_i \quad (\text{B.3})$$

With the determinant in Equation (5.135) instead of Equation (5.134) we get for the $\mu\nu$ SSM with one right-handed neutrino superfield:

$$\xi_{i1} = \frac{g'M_2}{2\text{Det}_0^{1\mu\nu\text{SSM}}}(v_d v_u \lambda^2 + m_R \mu)\Lambda_i \quad (\text{B.4})$$

$$\xi_{i2} = -\frac{gM_1}{2\text{Det}_0^{1\mu\nu\text{SSM}}}(v_d v_u \lambda^2 + m_R \mu)\Lambda_i \quad (\text{B.5})$$

$$\xi_{i3} = -\frac{\epsilon_i}{\mu} + \frac{m_\gamma}{8\mu\text{Det}_0^{1\mu\nu\text{SSM}}}(\lambda^2 v_d (v_d^2 + v_u^2) + 2m_R \mu v_u)\Lambda_i \quad (\text{B.6})$$

$$\xi_{i4} = -\frac{m_\gamma}{8\mu\text{Det}_0^{1\mu\nu\text{SSM}}}(\lambda^2 v_u (v_d^2 + v_u^2) + 2m_R \mu v_d)\Lambda_i \quad (\text{B.7})$$

$$\xi_{i5} = \frac{\lambda m_\gamma}{4\sqrt{2}\text{Det}_0^{1\mu\nu\text{SSM}}}(v_u^2 - v_d^2)\Lambda_i \quad (\text{B.8})$$

In case of the $\mu\nu$ SSM with two right-handed neutrino superfields the expansion matrix ξ is of the form

$$\xi_{ij} = K_\Lambda^j \Lambda_i + K_\alpha^j \alpha_i - \frac{\epsilon_i}{\mu} \delta_{j3} \quad (\text{B.9})$$

with ϵ_i , Λ_i and α_i defined in Equations (4.10), (5.132) and (5.138). The K_Λ and K_α using the definitions of a, b, c in Equation (5.140) can be obtained from

$$K_\Lambda^1 = \frac{2g'M_2\mu}{m_\gamma}a, \quad K_\alpha^1 = \frac{2g'M_2\mu}{m_\gamma}b$$

$$\begin{aligned}
K_\Lambda^2 &= -\frac{2gM_1\mu}{m_\gamma}a, & K_\alpha^2 &= -\frac{2gM_1\mu}{m_\gamma}b \\
K_\Lambda^3 &= \frac{m_\gamma}{8\mu\text{Det}_0^{2\mu\nu\text{SSM}}} [v_d v^2 (M_{R1}\lambda_2^2 + M_{R2}\lambda_1^2) + 2v_u M_{R1} M_{R2}\mu] \\
K_\alpha^3 &= \frac{b}{m_\gamma(v_u^2 - v_d^2)} (m_\gamma v^2 v_u - 4M_1 M_2 \mu v_d) \\
K_\Lambda^4 &= -\frac{m_\gamma}{8\mu\text{Det}_0^{2\mu\nu\text{SSM}}} [v_u v^2 (M_{R1}\lambda_2^2 + M_{R2}\lambda_1^2) + 2v_d M_{R1} M_{R2}\mu] \\
K_\alpha^4 &= \frac{b}{m_\gamma(v_u^2 - v_d^2)} (m_\gamma v^2 v_d - 4M_1 M_2 \mu v_u) \\
K_\Lambda^5 &= \frac{M_{R2}\lambda_1 m_\gamma}{4\sqrt{2}\text{Det}_0^{2\mu\nu\text{SSM}}} (v_u^2 - v_d^2), & K_\alpha^5 &= -\sqrt{2}\lambda_2 c - \frac{4\text{Det}_0^{\text{BRpV}} v_{R1}}{\mu m_\gamma (v_u^2 - v_d^2)} b \\
K_\Lambda^6 &= \frac{M_{R1}\lambda_2 m_\gamma}{4\sqrt{2}\text{Det}_0^{2\mu\nu\text{SSM}}} (v_u^2 - v_d^2), & K_\alpha^6 &= \sqrt{2}\lambda_1 c - \frac{4\text{Det}_0^{\text{BRpV}} v_{R2}}{\mu m_\gamma (v_u^2 - v_d^2)} b
\end{aligned} \tag{B.10}$$

with the determinants from Equations (5.134) and (5.141). The expansion matrices ξ_L and ξ_R in U and V are in all models given by

$$\begin{aligned}
(\xi_L)_{i1} &= \frac{g\Lambda_i}{\sqrt{2}\text{Det}_+} \\
(\xi_L)_{i2} &= -\frac{\epsilon_i}{\mu} - \frac{g^2 v_u \Lambda_i}{2\mu\text{Det}_+} \\
(\xi_R)_{i1} &= \frac{g v_d Y_e^{ii}}{2\text{Det}_+} \left[\frac{v_u \epsilon_i}{\mu} + \frac{(2\mu^2 + g^2 v_u^2) \Lambda_i}{2\mu\text{Det}_+} \right] \\
(\xi_R)_{i2} &= -\frac{\sqrt{2} v_d Y_e^{ii}}{2\text{Det}_+} \left[\frac{M_2 \epsilon_i}{\mu} + \frac{g^2 (v_d \mu + M_2 v_u) \Lambda_i}{2\mu\text{Det}_+} \right] ,
\end{aligned} \tag{B.11}$$

where the determinant Det_+ of the chargino mass matrix yields

$$\text{Det}_+ = M_2 \mu - \frac{1}{2} g^2 v_d v_u \quad . \tag{B.12}$$

Passarino-Veltman integrals

In this section we will provide the necessary information about one- and two-point functions in the notation of Passarino and Veltman. In particular the derivatives of the two-point functions \dot{B}_{001} and \dot{B}_{111} - being relevant when using R_ξ -gauge - should be presented in all detail.

C.1. Notation and basic integral

The notation of Passarino-Veltman integrals in their general form $T_n^{\mu_1 \dots \mu_p}$ was presented in Section 6.1.2. We emphasized the important role of the special integral $I_n(f^2)$ for our calculations:

$$\begin{aligned} I_n(f^2) &:= \frac{(2\pi Q)^{4-d}}{i\pi^2} \int d^d k \frac{1}{(k^2 - f^2)^n} = \frac{(4\pi Q^2)^{2-\frac{d}{2}}}{i\pi^{d/2}} \int d^d k \frac{1}{(k^2 - f^2)^n} \\ &= (-1)^n (4\pi Q^2)^{2-\frac{d}{2}} \frac{\Gamma(n - \frac{d}{2})}{\Gamma(n)} f^{d-2n} \end{aligned} \quad (\text{C.1})$$

The last equality should be deduced in all details. Therefore some basic formulas are needed:

▷ $\Gamma(z)$ function with expansion for $z \rightarrow 0$:

$$\begin{aligned} \Gamma(z) &= \int_0^\infty dt t^{z-1} e^{-t} \quad \text{with} \quad \Gamma(z+1) = z\Gamma(z) \quad \text{and} \quad \Gamma(1) = \Gamma(2) = 1 \\ \Gamma(z) &\xrightarrow{z \rightarrow 0} \frac{1}{z} - \gamma_E + \mathcal{O}(z) \quad \text{with} \quad \gamma_E = - \int_0^\infty dt \ln t e^{-t} \end{aligned} \quad (\text{C.2})$$

▷ d -dimensional unit sphere:

$$\int d^d \Omega = \frac{2\pi^{d/2}}{\Gamma(\frac{d}{2})} \quad (\text{C.3})$$

▷ special integral:

$$\int_0^\infty dt \frac{t^{g-1}}{(t+1)^f} = \frac{\Gamma(g)\Gamma(f-g)}{\Gamma(f)} \quad (\text{C.4})$$

At first we perform a Wick rotation to get from Minkowski to Euclidean space to be able to use d -dimensional polar coordinates:

$$\int_{-\infty}^\infty dk^0 = - \int_{+i\infty}^{-i\infty} dk^0 = i \int_{+i\infty}^{-i\infty} d(ik^0) = i \int_{-\infty}^\infty dk_E^0 \quad (\text{C.5})$$

$$k^2 = k^{02} - \sum_i k^{i2} = -k_E^{02} - \sum_i k^{i2} = -k_E^2 \quad (\text{C.6})$$

With this Wick rotation (k_E again called k) we get:

$$\begin{aligned}
I_n(f^2) &= \frac{(4\pi Q^2)^{2-\frac{d}{2}}}{\pi^{d/2}} \int d^d k \frac{1}{(-k^2 - f^2)^n} = (-1)^n \frac{(4\pi Q^2)^{2-\frac{d}{2}}}{\pi^{d/2}} \int d^d k \frac{1}{(k^2 + f^2)^n} \\
&= (-1)^n \frac{(4\pi Q^2)^{2-\frac{d}{2}}}{\pi^{d/2}} \int d^d \Omega \int_0^\infty dk k^{d-1} \frac{1}{(k^2 + f^2)^n} \\
&= (-1)^n (4\pi Q^2)^{2-\frac{d}{2}} \frac{2}{\Gamma(\frac{d}{2})} (f^2)^{-n} \int_0^\infty dk k^{d-1} \frac{1}{\left(\frac{k^2}{f^2} + 1\right)^n} \\
&= (-1)^n (4\pi Q^2)^{2-\frac{d}{2}} \frac{2}{\Gamma(\frac{d}{2})} (f^2)^{-n} \int_0^\infty dt f^2 \frac{1}{2} (t f^2)^{\frac{1}{2}(d-2)} \frac{1}{(t+1)^n} \\
&= (-1)^n (4\pi Q^2)^{2-\frac{d}{2}} \frac{2}{\Gamma(\frac{d}{2})} (f^2)^{\frac{d}{2}-n} \int_0^\infty dt \frac{t^{\frac{d}{2}-1}}{(t+1)^n} \\
&= (-1)^n (4\pi Q^2)^{2-\frac{d}{2}} \frac{\Gamma(n - \frac{d}{2})}{\Gamma(n)} f^{d-2n} \tag{C.7}
\end{aligned}$$

To regularize the UV divergences we set $d = 4 - 2\epsilon$ with $\epsilon > 0$ in the following sections. Regarding the special cases $n = 1, 2, 3$, one gets:

$$I_1(f^2) = -(4\pi Q^2)^\epsilon \Gamma(-1 + \epsilon) f^{2-2\epsilon} \xrightarrow{\epsilon \rightarrow 0} f^2 \left(\Delta + 1 + \ln \left(\frac{Q^2}{f^2} \right) \right) + \mathcal{O}(\epsilon) \tag{C.8}$$

$$I_2(f^2) = (4\pi Q^2)^\epsilon \Gamma(\epsilon) f^{-2\epsilon} \xrightarrow{\epsilon \rightarrow 0} \Delta + \ln \left(\frac{Q^2}{f^2} \right) + \mathcal{O}(\epsilon) \tag{C.9}$$

$$I_3(f^2) = -(4\pi Q^2)^\epsilon \frac{1}{2} \Gamma(1 + \epsilon) f^{-2-2\epsilon} \xrightarrow{\epsilon \rightarrow 0} -\frac{1}{2f^2} + \mathcal{O}(\epsilon) \tag{C.10}$$

where we have defined

$$\Delta = \frac{1}{\epsilon} - \gamma_E + \ln(4\pi) \tag{C.11}$$

with the Euler-Mascheroni constant γ_E from Equation (6.10).

C.2. Scalar integrals

Next we want to calculate the scalar integrals A_0 , B_0 and \dot{B}_0 before focusing on the tensor reduction in the following section. The scalar 1-point function A_0 is given by $A_0(m^2) = I_1(m^2)$. Therefore the result is:

$$A_0(m^2) = \frac{(2\pi Q)^{4-d}}{i\pi^2} \int d^d k \frac{1}{k^2 - m^2} = m^2 \left[\Delta + 1 + \ln \left(\frac{Q^2}{m^2} \right) \right] \tag{C.12}$$

Some more work has to be done for the scalar 2-point function, which is defined by:

$$B_0(p^2, m_1^2, m_2^2) = \frac{(2\pi Q)^{4-d}}{i\pi^2} \int d^d k \frac{1}{(k^2 - m_1^2)((k+p)^2 - m_2^2)} \tag{C.13}$$

To be able to use $I_2(f^2)$, we have to linearize the denominator by using the Feynman parametrization, which is generally defined by:

$$\frac{1}{g_1^{\alpha_1} \cdots g_n^{\alpha_n}} = \frac{\Gamma(\alpha_1 + \cdots + \alpha_n)}{\Gamma(\alpha_1) \cdots \Gamma(\alpha_n)} \int_0^1 dx_1 \cdots \int_0^1 dx_n \frac{\delta(x_1 + \cdots + x_n - 1) x_1^{\alpha_1 - 1} \cdots x_n^{\alpha_n - 1}}{(x_1 g_1 + \cdots + x_n g_n)^{\alpha_1 + \cdots + \alpha_n}} \quad (\text{C.14})$$

In this simple case we obtain:

$$\begin{aligned} B_0(p^2, m_1^2, m_2^2) &= \frac{(2\pi Q)^{4-d}}{i\pi^2} \int d^d k \int_0^1 dx \int_0^1 dy \frac{\delta(x+y-1)}{(x(k^2 - m_1^2) + y((k+p)^2 - m_2^2))^2} \\ &= \frac{(2\pi Q)^{4-d}}{i\pi^2} \int d^d k \int_0^1 dx \frac{1}{(x(k^2 - m_1^2) + (1-x)((k+p)^2 - m_2^2))^2} \\ &= \frac{(2\pi Q)^{4-d}}{i\pi^2} \int_0^1 dx \int d^d k \frac{1}{((k+p-xp)^2 - x^2 p^2 + xp^2 + x(m_2^2 - m_1^2) - m_2^2)^2} \end{aligned} \quad (\text{C.15})$$

Substituting $k + xp \rightarrow k$ leads to $I_2(f^2)$ with $f^2 = x^2 p^2 - xp^2 + x(m_1^2 - m_2^2) + m_2^2$:

$$B_0(p^2, m_1^2, m_2^2) = (4\pi Q^2)^\epsilon \Gamma(\epsilon) \int_0^1 dx (x^2 p^2 - xp^2 + x(m_1^2 - m_2^2) + m_2^2)^{-\epsilon} \quad (\text{C.16})$$

Now we can use an expansion in the parameter ϵ :

$$x^{-\epsilon} = \sum_{n=0}^{\infty} \frac{(-\epsilon \ln x)^n}{n!} \quad (\text{C.17})$$

Thus, for B_0 a straightforward calculation shows:

$$B_0(p^2, m_1^2, m_2^2) = \Delta - \int_0^1 dx \ln \frac{x^2 p^2 - xp^2 + x(m_1^2 - m_2^2) + m_2^2}{Q^2} \quad (\text{C.18})$$

Please note that the integral over x is symmetric in m_1 and m_2 by substituting $x \rightarrow 1-x$, which becomes obvious when writing $f^2 = -p^2 x(1-x) + xm_1^2 + (1-x)m_2^2$. This already implies $B_0(p^2, m_1^2, m_2^2) = B_0(p^2, m_2^2, m_1^2)$. At the very end this leads to

$$B_0(p^2, m_1^2, m_2^2) = \Delta + 2 + \ln \left(\frac{Q^2}{m_1 m_2} \right) + \frac{m_1^2 - m_2^2}{p^2} \ln \left(\frac{m_2}{m_1} \right) - \frac{m_1 m_2}{p^2} \left(\frac{1}{r} - r \right) \ln r, \quad (\text{C.19})$$

where r and $\frac{1}{r}$ denote the negative roots of the polynomial

$$x^2 + \frac{m_1^2 + m_2^2 - p^2}{m_1 m_2} x + 1 = (x+r) \left(x + \frac{1}{r} \right) \quad .$$

The derivative of B_0 with respect to p^2 yields:

$$\begin{aligned} \dot{B}_0(p^2, m_1^2, m_2^2) &:= \frac{\partial}{\partial p^2} B_0(p^2, m_1^2, m_2^2) \\ &= -\frac{m_1^2 - m_2^2}{p^4} \ln \left(\frac{m_2}{m_1} \right) + \frac{m_1 m_2}{p^4} \left(\frac{1}{r} - r \right) \ln r - \frac{1}{p^2} \left(1 + \frac{r^2 + 1}{r^2 - 1} \ln r \right) \end{aligned} \quad (\text{C.20})$$

C.3. Tensor integrals

Lorentz covariance in d dimensions allows us to decompose the tensor integrals in terms of scalar integrals. We want to present a simple example. Starting with

$$B^\mu(p^2, 0, m^2) = \frac{(2\pi Q)^{4-d}}{i\pi^2} \int d^d k \frac{k^\mu}{k^2((k+p)^2 - m^2)} \quad (\text{C.21})$$

we use Lorentz covariance to write:

$$B^\mu(p^2, 0, m^2) = p^\mu B_1(p^2, 0, m^2) \quad (\text{C.22})$$

The calculation of B_1 can now easily be done by contraction with p_μ , yielding:

$$p_\mu B^\mu = p^2 B_1 = \frac{(2\pi Q)^{4-d}}{i\pi^2} \int d^d k \frac{pk}{k^2((k+p)^2 - m^2)} \quad (\text{C.23})$$

Re-expressing $pk = \frac{1}{2} [((k+p)^2 - m^2) - k^2 - (p^2 - m^2)]$ we get:

$$p^2 B_1 = \frac{1}{2} \left[\frac{(2\pi Q)^{4-d}}{i\pi^2} \int d^d k \frac{1}{k^2} - \frac{(2\pi Q)^{4-d}}{i\pi^2} \int d^d k \frac{1}{(k+p)^2 - m^2} - (p^2 - m^2) \frac{(2\pi Q)^{4-d}}{i\pi^2} \int d^d k \frac{1}{k^2((k+p)^2 - m^2)} \right] \quad (\text{C.24})$$

Therefore B_1 can be written in the form:

$$B_1(p^2, 0, m^2) = \frac{1}{2p^2} [A_0(0) - A_0(m^2) - (p^2 - m^2)B_0(p^2, 0, m^2)] \quad (\text{C.25})$$

In this way we get for the A and B tensor integrals in terms of scalar integrals:

$$A_{00}(m^2) = \frac{1}{4}m^2 A_0(m^2) + \frac{1}{8}m^4 \quad (\text{C.26})$$

$$B_1(p^2, m_1^2, m_2^2) = \frac{1}{2p^2} [(m_2^2 - m_1^2)(B_0(p^2, m_1^2, m_2^2) - B_0(0, m_1^2, m_2^2)) - \frac{1}{2}B_0(p^2, m_1^2, m_2^2)] \quad (\text{C.27})$$

$$B_{00}(p^2, m_1^2, m_2^2) = \frac{1}{6} \left[A_0(m_2^2) + (p^2 - m_2^2 + m_1^2)B_1(p^2, m_1^2, m_2^2) + 2m_1^2 B_0(p^2, m_1^2, m_2^2) + m_0^2 + m_1^2 - \frac{1}{3}p^2 \right] \quad (\text{C.28})$$

$$B_{11}(p^2, m_1^2, m_2^2) = \frac{1}{3p^2} \left[A_0(m_2^2) - m_1^2 B_0(p^2, m_1^2, m_2^2) - 2(p^2 - m_2^2 + m_1^2)B_1(p^2, m_1^2, m_2^2) + \frac{1}{6}(p^2 - 3m_1^2 - 3m_2^2) \right] \quad (\text{C.29})$$

$$B_{001}(p^2, m_1^2, m_2^2) = \frac{1}{8} \left[2m_1^2 B_1(p^2, m_1^2, m_2^2) - A_0(m_2^2) + (p^2 - m_2^2 + m_1^2)B_{11}(p^2, m_1^2, m_2^2) - \frac{1}{6}(2m_1^2 + 4m_2^2 - p^2) \right] \quad (\text{C.30})$$

$$B_{111}(p^2, m_1^2, m_2^2) = -\frac{1}{4p^2} \left[A_0(m_2^2) + 3(p^2 - m_2^2 + m_1^2)B_{11}(p^2, m_1^2, m_2^2) \right. \\ \left. + 2m_1^2 B_1(p^2, m_1^2, m_2^2) - \frac{1}{6}(2m_1^2 + 4m_2^2 - p^2) \right] \quad (\text{C.31})$$

C.4. Special cases for B functions

PV integral	UV behavior	PV integral	UV behavior
A_0	$m^2 \Delta$	A_{00}	$\frac{1}{4}m^4 \Delta$
B_0	Δ	B_1	$-\frac{1}{2}\Delta$
B_{00}	$\frac{1}{12}(3m_1^2 + 3m_2^2 - p^2)\Delta$	B_{11}	$\frac{1}{3}\Delta$
B_{001}	$\frac{1}{24}(-2m_1^2 - 4m_2^2 + p^2)\Delta$	B_{111}	$-\frac{1}{4}\Delta$
C_{00}	$\frac{1}{4}\Delta$	C_{001}	$-\frac{1}{12}\Delta$
C_{002}	$-\frac{1}{12}\Delta$		
\dot{B}_{00}	$-\frac{1}{12}\Delta$	\dot{B}_{001}	$\frac{1}{24}\Delta$

Table C.1.: UV divergent parts of the Passarino-Veltman integrals.

The following special cases turn out to be useful in the numerical evaluation. Here we give only the finite parts and summarize the UV divergent parts of the functions appearing in the calculation in Table C.1.

$$B_0(0, 0, m^2) = B_0(0, m^2, 0) = 1 + \ln \left(\frac{Q^2}{m^2} \right) \quad (\text{C.32})$$

$$B_0(0, m_1^2, m_2^2) = 1 + \frac{1}{m_1^2 - m_2^2} \left[m_1^2 \ln \left(\frac{Q^2}{m_1^2} \right) - m_2^2 \ln \left(\frac{Q^2}{m_2^2} \right) \right] \quad (\text{C.33})$$

$$B_0(0, m^2, m^2) = \ln \left(\frac{Q^2}{m^2} \right) \quad (\text{C.34})$$

$$B_0(p^2, 0, 0) = 2 + \ln \left(\frac{Q^2}{p^2} \right) + i\pi \quad (\text{C.35})$$

$$B_0(p^2, 0, m^2) = B_0(p^2, m^2, 0) = 2 + \ln \left(\frac{Q^2}{m^2} \right) + \frac{m^2 - p^2}{p^2} \ln \left(1 - \frac{p^2}{m^2} \right) \quad (\text{C.36})$$

$$B_0(p^2, m^2, m^2) = 2 + \ln \left(\frac{Q^2}{m^2} \right) - \frac{m^2}{p^2} \left(\frac{1}{r} - r \right) \ln r \quad (\text{C.37})$$

$$B_0(m^2, m^2, m^2) = 2 + \ln \left(\frac{Q^2}{m^2} \right) - \pi \quad (\text{C.38})$$

C.5. Derivatives of the B functions

First we present the general results for the derivatives and afterwards the special cases. Again we only show the finite parts, whereas the UV divergent parts can be found in Table C.1. $\dot{B}_0(p^2, m_1^2, m_2^2)$ is given in Equation (C.20).

$$\begin{aligned} \dot{B}_1(p^2, m_1^2, m_2^2) = & \frac{1}{2p^4} \left[(m_1^2 - m_2^2)B_0(p^2, m_1^2, m_2^2) + (m_2^2 - m_1^2)B_0(0, m_1^2, m_2^2) \right. \\ & \left. - p^2(m_1^2 - m_2^2 + p^2)\dot{B}_0(p^2, m_1^2, m_2^2) \right] \end{aligned} \quad (\text{C.39})$$

$$\begin{aligned} \dot{B}_{00}(p^2, m_1^2, m_2^2) = & \frac{1}{36p^4} \left[-3(m_1^2 - m_2^2)^2 B_0(0, m_1^2, m_2^2) \right. \\ & + 3(m_1^4 - 2m_1^2 m_2^2 + m_2^4 - p^4) B_0(p^2, m_1^2, m_2^2) \\ & \left. - p^2(3\kappa(p^2, m_1^2, m_2^2)\dot{B}_0(p^2, m_1^2, m_2^2) + 2p^2) \right] \end{aligned} \quad (\text{C.40})$$

$$\begin{aligned} \dot{B}_{11}(p^2, m_1^2, m_2^2) = & \frac{1}{6p^6} \left[2(m_1 - m_2)(m_1 + m_2)(2m_1^2 - 2m_2^2 + p^2) B_0(0, m_1^2, m_2^2) \right. \\ & - 2(p^2(m_1^2 - 2m_2^2) + 2(m_1^2 - m_2^2)^2) B_0(p^2, m_1^2, m_2^2) \\ & + 2p^2(p^2(m_1^2 - 2m_2^2) + (m_1^2 - m_2^2)^2 + p^4)\dot{B}_0(p^2, m_1^2, m_2^2) \\ & \left. - 2p^2 A_0(m_2^2) + p^2(m_1^2 + m_2^2) \right] \end{aligned} \quad (\text{C.41})$$

$$\begin{aligned} \dot{B}_{001}(p^2, m_1^2, m_2^2) = & \frac{1}{144p^6} \left[6(m_1^2 - m_2^2)(2(m_1^2 - m_2^2)^2 - p^2(m_1^2 + 2m_2^2)) B_0(0, m_1^2, m_2^2) \right. \\ & + 6(p^2(m_1^2 - m_2^2)(m_1^2 + 3m_2^2) - 2(m_1^2 - m_2^2)^3 + p^6) B_0(p^2, m_1^2, m_2^2) \\ & + 6p^2(m_1^2 - m_2^2 + p^2) \\ & \quad \left. (-2p^2(m_1^2 + m_2^2) + (m_1^2 - m_2^2)^2 + p^4)\dot{B}_0(p^2, m_1^2, m_2^2) \right. \\ & \left. + 6p^2(m_2^2 - m_1^2)A_0(m_2^2) + p^2(3m_1^4 - 3m_2^4 + 4p^4) \right] \end{aligned} \quad (\text{C.42})$$

$$\begin{aligned} \dot{B}_{111}(p^2, m_1^2, m_2^2) = & \frac{1}{12p^8} \left[3(m_1^2 - m_2^2)(2p^2(m_1^2 - 2m_2^2)) \right. \\ & + 3(m_1^2 - m_2^2)^2 + p^4) B_0(0, m_1^2, m_2^2) \\ & - 3(p^4(m_1^2 - 3m_2^2) + 2p^2(m_1^2 - 3m_2^2)(m_1^2 - m_2^2) \\ & \quad \left. + 3(m_1^2 - m_2^2)^3) B_0(p^2, m_1^2, m_2^2) \right. \\ & + 3p^2(m_1^2 - m_2^2 + p^2)((m_1^2 - m_2^2)^2 - 2m_2^2 p^2 + p^4)\dot{B}_0(p^2, m_1^2, m_2^2) \\ & - 6p^2 A_0(m_2^2)(m_1^2 - m_2^2 + p^2) \\ & \left. + p^2(3m_1^4 + 2m_1^2 p^2 - 3m_2^4 + 4m_2^2 p^2) \right] \end{aligned} \quad (\text{C.43})$$

In subsequent formulas for $p^2 = 0$ we use the abbreviations

$$K_1 = \log\left(\frac{Q^2}{m_1^2}\right), K_2 = \log\left(\frac{Q^2}{m_2^2}\right), K_3 = \log\left(\frac{m_2^2}{m_1^2}\right) \quad . \quad (\text{C.44})$$

Thus we get for $m_1 \neq m_2 \neq 0$

$$\dot{B}_0(0, m_1^2, m_2^2) = \frac{1}{2(m_1^2 - m_2^2)^2} \left[m_1^2 + m_2^2 + \frac{2m_1^2 m_2^2 K_3}{m_1^2 - m_2^2} \right] \quad (\text{C.45})$$

$$\dot{B}_1(0, m_1^2, m_2^2) = \frac{1}{6(m_1^2 - m_2^2)^4} [-3m_1^4 m_2^2 (2K_3 + 1) - 2m_1^6 + 6m_1^2 m_2^4 - m_2^6] \quad (\text{C.46})$$

$$\begin{aligned} \dot{B}_{00}(0, m_1^2, m_2^2) &= \frac{1}{72(m_1^2 - m_2^2)^3} [-(6K_1 + 5) m_1^6 + 9(2K_1 + 3) m_1^4 m_2^2 \\ &\quad - 9(2K_2 + 3) m_1^2 m_2^4 + (6K_2 + 5) m_2^6] \end{aligned} \quad (\text{C.47})$$

$$\begin{aligned} \dot{B}_{11}(0, m_1^2, m_2^2) &= \frac{1}{24(m_1^2 - m_2^2)^5} [4m_1^6 m_2^2 (6K_3 + 5) \\ &\quad + 6m_1^8 - 36m_1^4 m_2^4 + 12m_1^2 m_2^6 - 2m_2^8] \end{aligned} \quad (\text{C.48})$$

$$\begin{aligned} \dot{B}_{001}(0, m_1^2, m_2^2) &= \frac{1}{288(m_1^2 - m_2^2)^4} [(12K_1 + 13) m_1^8 - 8(6K_1 + 11) m_1^6 m_2^2 \\ &\quad + 36(2K_2 + 3) m_1^4 m_2^4 - 8(6K_2 + 5) m_1^2 m_2^6 \\ &\quad + (12K_2 + 7) m_2^8] \end{aligned} \quad (\text{C.49})$$

$$\begin{aligned} \dot{B}_{111}(0, m_1^2, m_2^2) &= \frac{1}{60(m_1^2 - m_2^2)^6} [-5m_1^8 m_2^2 (12K_3 + 13) \\ &\quad - 12m_1^{10} - 120m_1^6 m_2^4 - 60m_1^4 m_2^6 + 20m_1^2 m_2^8 - 3m_2^{10}] \end{aligned} \quad (\text{C.50})$$

and for the remaining cases:

$$\dot{B}_0(0, m^2, m^2) = -\frac{1}{6m^2} \quad \dot{B}_1(0, m^2, m^2) = -\frac{1}{12m^2} \quad (\text{C.51})$$

$$\dot{B}_0(0, 0, m^2) = \frac{1}{2m^2} \quad \dot{B}_1(0, 0, m^2) = -\frac{1}{6m^2} \quad (\text{C.52})$$

$$\dot{B}_0(0, m^2, 0) = \frac{1}{2m^2} \quad \dot{B}_1(0, m^2, 0) = \frac{1}{3m^2} \quad (\text{C.53})$$

$$\dot{B}_{00}(0, m^2, m^2) = -\frac{1}{12} \log\left(\frac{Q^2}{m^2}\right) \quad \dot{B}_{11}(0, m^2, m^2) = \frac{1}{20m^2} \quad (\text{C.54})$$

$$\dot{B}_{00}(0, 0, m^2) = -\frac{1}{72} \left[6 \log\left(\frac{Q^2}{m^2}\right) + 5 \right] \quad \dot{B}_{11}(0, 0, m^2) = \frac{1}{12m^2} \quad (\text{C.55})$$

$$\dot{B}_{00}(0, m^2, 0) = -\frac{1}{72} \left[6 \log\left(\frac{Q^2}{m^2}\right) + 5 \right] \quad \dot{B}_{11}(0, m^2, 0) = \frac{1}{4m^2} \quad (\text{C.56})$$

$$\dot{B}_{001}(0, m^2, m^2) = \frac{1}{24} \log\left(\frac{Q^2}{m^2}\right) \quad \dot{B}_{111}(0, m^2, m^2) = -\frac{1}{30m^2} \quad (\text{C.57})$$

$$\dot{B}_{001}(0, 0, m^2) = \frac{1}{288} \left[12 \log\left(\frac{Q^2}{m^2}\right) + 7 \right] \quad \dot{B}_{111}(0, 0, m^2) = -\frac{1}{20m^2} \quad (\text{C.58})$$

$$\dot{B}_{001}(0, m^2, 0) = \frac{1}{288} \left[12 \log\left(\frac{Q^2}{m^2}\right) + 13 \right] \quad \dot{B}_{111}(0, m^2, 0) = -\frac{1}{5m^2} \quad (\text{C.59})$$

Vertex corrections for the decays $F_i \rightarrow F_o W^\pm$

In this chapter we show the generic formulas for the NLO vertex contributions to the decays $F_i \rightarrow F_o W^\pm$ in the 't Hooft-Feynman gauge $\xi_V = 1$. The program `CNNDecays` [157] also contains the formulas for the general R_ξ -gauge, however their presentation would spoil this thesis. The formulas for the self-energies can for example be taken from [179] allowing to calculate the derivatives with respect to p^2 . Within `CNNDecays` they can be found in the folder `corrections` and the particle insertions in `callcorrections`.

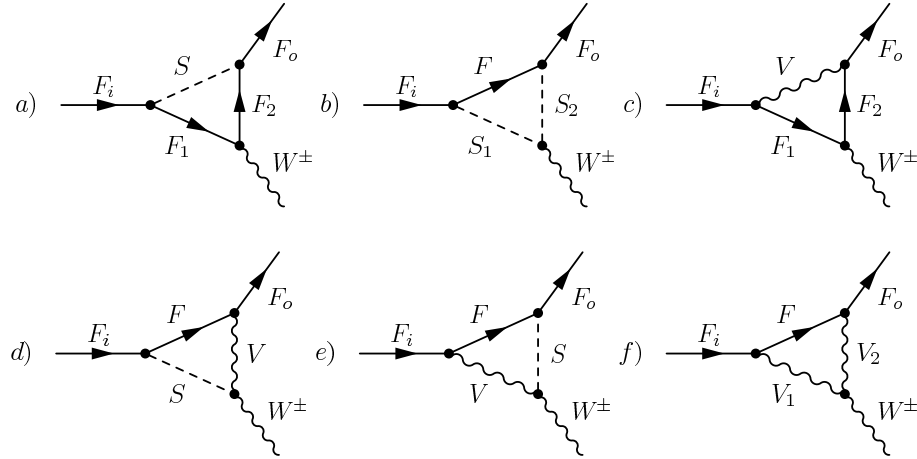


Figure D.1.: Generic Vertex NLO corrections.

Figure D.1 illustrates the generic contributions to the matrix element M_V . All contributions have the same generic structure:

$$\begin{aligned}
 M_V = & \frac{i}{16\pi^2} \bar{u}(p_1) \gamma^\mu (P_L M_1 + P_R M_2) u(k) \epsilon_\mu^*(p_2) \\
 & + \frac{i}{16\pi^2} \bar{u}(p_1) (P_L M_3^\mu + P_R M_4^\mu) u(k) \epsilon_\mu^*(p_2)
 \end{aligned}
 \tag{D.1}$$

Together with the individual matrix elements for the six Feynman diagrams we denote in addition the particle combinations to be inserted in these diagrams for the decay $\tilde{\chi}^0 \rightarrow \tilde{\chi}^- W^+$ neglecting generation indices. The following notation is used: S^0 stands for one of the scalar states, P^0 for one of the pseudoscalars including the Goldstone boson and S^\pm for one of the charged scalars including the Goldstone boson. Note that scalars, pseudoscalars, charged scalars and the neutralinos and charginos are supposed to contain the (s)neutrinos and (s)leptons. The indices of couplings and masses in the generic formulas have to be understood in the following

form: F_i and F_o denote the decaying and outgoing fermion, W the external W -boson, whereas F , $F_{1,2}$, S , $S_{1,2}$, V or $V_{1,2}$ represent possible internal fermionic, scalar or vector particles. It is understood implicitly that one has to sum over possible flavor and generation indices of the internal particles.

The vertex in Figure 6.5 a) contains two internal fermions and one scalar. The couplings are abbreviated as follows:

$$O_1 = O_{FFV,L}(F_2, F_1, W), \quad O_2 = O_{FFV,R}(F_2, F_1, W) \quad (D.2)$$

$$O_3 = O_{FFS,L}(F_1, F_i, S), \quad O_4 = O_{FFS,R}(F_1, F_i, S) \quad (D.3)$$

$$O_5 = O_{FFS,L}(F_o, F_2, S), \quad O_6 = O_{FFS,R}(F_o, F_2, S) \quad (D.4)$$

The arguments of the Passarino-Veltman integrals in the following formulas are as follows: $B_0(m_W^2, m_{F_2}^2, m_{F_1}^2)$ and $C_i, C_{ij}(m_W^2, m_i^2, m_o^2, m_{F_2}^2, m_{F_1}^2, m_S^2)$. Possible particle insertions in the notation SF_1F_2 are given by $S^0\tilde{\chi}^0\tilde{\chi}^\pm$, $P^0\tilde{\chi}^0\tilde{\chi}^\pm$, $S^\pm\tilde{\chi}^\pm\tilde{\chi}^0$, $\tilde{u}ud$, $\tilde{d}du$. The individual contributions are:

$$\begin{aligned} M_{1,a} = & -O_1 [O_3 m_{F_1} (O_6 m_{F_2} C_0 - O_5 m_o C_1) + O_4 O_6 m_{F_2} m_i (C_0 + C_1)] \\ & + O_1 O_5 m_o C_2 (O_3 m_{F_1} + O_4 m_i) + O_2 [O_3 (O_6 (m_S^2 C_0 + m_i^2 C_1 + B_0 - 2C_{00}) \\ & - m_o^2 (C_0 + C_1 + C_2)) - O_5 m_{F_2} m_o (C_0 + C_1 + C_2)] + O_4 O_6 m_{F_1} m_i C_1] \end{aligned} \quad (D.5)$$

$$\begin{aligned} M_{2,a} = & O_1 \{O_3 O_5 m_{F_1} m_i C_1 + O_4 [O_5 (m_S^2 C_0 + m_i^2 C_1 - m_o^2 (C_0 + C_1 + C_2) \\ & + B_0 - 2C_{00}) - O_6 m_{F_2} m_o (C_0 + C_1 + C_2)]\} \\ & + O_2 \{O_3 m_i (O_6 m_o C_2 - O_5 m_{F_2} (C_0 + C_1)) \\ & + O_4 m_{F_1} (O_6 m_o (C_1 + C_2) - O_5 m_{F_2} C_0)\} \end{aligned} \quad (D.6)$$

$$\begin{aligned} M_{3,a}^\mu = & p_1^\mu 2 \{O_1 O_4 [O_5 m_o (C_{12} + C_2 + C_{22}) - O_6 m_{F_2} (C_0 + C_1 + C_2)] \\ & + O_2 O_6 (O_4 m_{F_1} C_1 - O_3 m_i C_{12})\} \\ & + p_2^\mu 2 \{O_2 O_6 [O_3 m_i (C_1 + C_{12}) + O_4 m_{F_1} C_1] - O_1 O_4 O_5 m_o (C_1 + 2C_{12})\} \end{aligned} \quad (D.7)$$

$$\begin{aligned} M_{4,a}^\mu = & p_1^\mu 2 \{O_1 O_5 (O_3 m_{F_1} C_1 - O_4 m_i C_{12}) \\ & + O_2 O_3 [O_6 m_o (C_{12} + C_2 + C_{22}) - O_5 m_{F_2} (C_0 + C_1 + C_2)]\} \\ & + p_2^\mu 2 \{O_1 O_5 (O_3 m_{F_1} C_1 + O_4 m_i (C_1 + C_{12})) - O_2 O_3 O_6 m_o (C_1 + 2C_{12})\} \end{aligned} \quad (D.8)$$

For the vertex in Figure 6.5 b) we define:

$$O_1 = O_{SSV}(S_1, S_2, V) \quad (D.9)$$

$$O_2 = O_{FFS,L}(F, F_i, S_1), \quad O_3 = O_{FFS,R}(F, F_i, S_1) \quad (D.10)$$

$$O_4 = O_{FFS,L}(F_o, F, S_2), \quad O_5 = O_{FFS,R}(F_o, F, S_2) \quad (D.11)$$

For completeness we note that in case of O_1 the following internal momentum combination appears ($p_{S_1} - p_{S_2}$) over which of course has been integrated. The Passarino-Veltman integrals below have the arguments $C_i, C_{ij}(m_o^2, m_W^2, m_i^2, m_F^2, m_{S_2}^2, m_{S_1}^2)$. Possible particle insertions in the notation FS_1S_2 are given by $\tilde{\chi}^0 S^0 S^\pm$, $\tilde{\chi}^\pm S^\pm S^0$, $\tilde{\chi}^0 P^0 S^\pm$, $\tilde{\chi}^\pm S^\pm P^0$, $u\tilde{u}\tilde{d}$, $\tilde{d}\tilde{u}$. The different parts are:

$$M_{1,b} = 2O_1 O_2 O_5 C_{00} \quad (D.12)$$

$$M_{2,b} = 2O_1 O_3 O_4 C_{00} \quad (D.13)$$

$$\begin{aligned}
M_{3,b}^\mu = & p_2^\mu O_1 \{ O_3 (O_5 m_F (C_0 + 2C_2) - O_4 m_o (C_1 + 2C_{12})) \\
& - O_2 O_5 m_i (C_2 + 2C_{22}) \} - 2p_1^\mu O_1 \{ O_2 O_5 m_i (C_{12} + C_2 + C_{22}) \\
& + O_3 [O_4 m_o (C_1 + C_{11} + C_{12}) - O_5 m_F (C_0 + C_1 + C_2)] \} \quad (D.14)
\end{aligned}$$

$$\begin{aligned}
M_{4,b}^\mu = & 2p_1^\mu O_1 \{ O_2 [O_4 m_F (C_0 + C_1 + C_2) - O_5 m_o (C_1 + C_{11} + C_{12})] \\
& - O_3 O_4 m_i (C_{12} + C_2 + C_{22}) \} + p_2^\mu O_1 \{ O_2 [O_4 m_F (C_0 + 2C_2) \\
& - O_5 m_o (C_1 + 2C_{12})] - O_3 O_4 m_i (C_2 + 2C_{22}) \} \quad (D.15)
\end{aligned}$$

For the vertex in Figure 6.5 c) we define:

$$O_1 = O_{FFV,L}(F_1, F_i, V), \quad O_2 = O_{FFV,R}(F_1, F_i, V) \quad (D.16)$$

$$O_3 = O_{FFV,L}(F_2, F_1, W), \quad O_4 = O_{FFV,R}(F_2, F_1, W) \quad (D.17)$$

$$O_5 = O_{FFV,L}(F_o, F_2, V), \quad O_6 = O_{FFV,R}(F_o, F_2, V) \quad (D.18)$$

The arguments of the Passarino-Veltman integrals are $C_i, C_{ij}(m_W^2, m_i^2, m_o^2, m_{F_2}^2, m_{F_1}^2, m_V^2)$ and $B_0(m_W^2, m_{F_2}^2, m_{F_1}^2)$. Possible particle insertions in the notation $V F_1 F_2$ are given by $Z\tilde{\chi}^0\tilde{\chi}^\pm, W\tilde{\chi}^\pm\tilde{\chi}^0$. The final result is:

$$\begin{aligned}
M_{1,c} = & 2O_1 O_5 \{ O_3 [m_V^2 C_0 + m_i^2 (C_1 - C_2) - m_o^2 (C_0 + C_1 + 2C_2) \\
& + m_W^2 C_2 + B_0 - 2C_{00}] - O_4 m_{F_1} m_{F_2} C_0 \} - 2O_2 O_4 O_6 m_i m_o C_2 \quad (D.19)
\end{aligned}$$

$$\begin{aligned}
M_{2,c} = & 2O_2 O_6 \{ O_4 [m_V^2 C_0 + m_i^2 (C_1 - C_2) - m_o^2 (C_0 + C_1 + 2C_2) \\
& + m_W^2 C_2 + B_0 - 2C_{00}] - O_3 m_{F_1} m_{F_2} C_0 \} - 2O_1 O_3 O_5 m_i m_o C_2 \quad (D.20)
\end{aligned}$$

$$\begin{aligned}
M_{3,c}^\mu = & 4p_1^\mu \{ O_2 [O_3 O_5 m_{F_1} C_2 + O_4 (O_5 m_{F_2} C_2 + O_6 m_o (C_2 + C_{22}))] \\
& - O_1 O_3 O_5 m_i (C_2 + C_{12}) \} - 4p_2^\mu \{ O_2 [O_3 O_5 m_{F_1} C_1 + O_4 (O_5 m_{F_2} (C_0 + C_1) \\
& + O_6 m_o (C_1 + C_{11} + C_{12} + C_2))] - O_1 O_3 O_5 m_i (C_1 + C_{11}) \} \quad (D.21)
\end{aligned}$$

$$\begin{aligned}
M_{4,c}^\mu = & 4p_1^\mu \{ O_1 [O_3 (O_5 m_o (C_{12} + C_{22}) + O_6 m_{F_2} C_2) + O_4 O_6 m_{F_1} C_2] \\
& - O_2 O_4 O_6 m_i (C_2 + C_{12}) \} - 4p_2^\mu \{ O_1 [O_3 (O_5 m_o (C_1 + C_{11} + C_{12} + C_2) \\
& + O_6 m_{F_2} (C_0 + C_1)) + O_4 O_6 m_{F_1} C_1] - O_2 O_4 O_6 m_i (C_1 + C_{11}) \} \quad (D.22)
\end{aligned}$$

For the vertex in Figure 6.5 d) we define:

$$O_1 = O_{FFV,L}(F_o, F, V), \quad O_2 = O_{FFV,R}(F_o, F, V) \quad (D.23)$$

$$O_3 = O_{FFS,L}(F, F_i, S), \quad O_4 = O_{FFS,R}(F, F_i, S) \quad (D.24)$$

$$O_5 = O_{SVV}(S, W, V) \quad (D.25)$$

The arguments of the Passarino-Veltman integrals are $C_i, C_{ij}(m_o^2, m_W^2, m_i^2, m_F^2, m_V^2, m_S^2)$ in the following formulas. Possible particle insertions in the notation FSV are given by $\tilde{\chi}^\pm S^\pm \gamma, \tilde{\chi}^\pm S^\pm Z, \tilde{\chi}^0 S^0 W, \tilde{\chi}^0 P^0 W$. It yields:

$$M_{1,d} = O_5 (O_1 O_3 m_F C_0 - O_1 O_4 m_i C_2 + O_2 O_3 m_o C_1) \quad (D.26)$$

$$M_{2,d} = O_5 (O_1 O_4 m_o C_1 - O_2 O_3 m_i C_2 + O_2 O_4 m_F C_0) \quad (D.27)$$

$$M_{3,d}^\mu = 2p_1^\mu O_1 O_4 O_5 C_1 \quad (D.28)$$

$$M_{4,d}^\mu = 2p_1^\mu O_2 O_3 O_5 C_1 \quad (D.29)$$

We define for the vertex in Figure 6.5 e):

$$O_1 = O_{FFV,L}(F, F_i, V), \quad O_2 = O_{FFV,R}(F, F_i, V) \quad (\text{D.30})$$

$$O_3 = O_{FFS,L}(F_o, F, S), \quad O_4 = O_{FFS,R}(F_o, F, S) \quad (\text{D.31})$$

$$O_5 = O_{SVV}(S, W, V) \quad (\text{D.32})$$

The Passarino-Veltman integrals, which appear in the following formulas, have as arguments $C_i, C_{ij}(m_i^2, m_W^2, m_o^2, m_F^2, m_V^2, m_S^2)$. Possible particle insertions in the notation FVS are given by $\tilde{\chi}^0 Z S^\pm, \tilde{\chi}^\pm W S^0, \tilde{\chi}^\pm W P^0$. The individual contributions are given by:

$$M_{1,e} = O_5(-O_1 O_3 m_o C_2 + O_1 O_4 m_F C_0 + O_2 O_4 m_i C_1) \quad (\text{D.33})$$

$$M_{2,e} = O_5(O_1 O_3 m_i C_1 + O_2 O_3 m_F C_0 - O_2 O_4 m_o C_2) \quad (\text{D.34})$$

$$M_{3,e}^\mu = 2(p_1^\mu + p_2^\mu) O_2 O_4 O_5 C_1 \quad (\text{D.35})$$

$$M_{4,e}^\mu = 2(p_1^\mu + p_2^\mu) O_1 O_3 O_5 C_1 \quad (\text{D.36})$$

Finally for the vertex in Figure 6.5 f) we define:

$$O_1 = O_{FFV,L}(F, F_i, V_1), \quad O_2 = O_{FFV,R}(F, F_i, V_1) \quad (\text{D.37})$$

$$O_3 = O_{FFV,L}(F_o, F, V_2), \quad O_4 = O_{FFV,R}(F_o, F, V_2) \quad (\text{D.38})$$

$$O_5 = O_{VVV}(W, V_1, V_2) \quad (\text{D.39})$$

For completeness we note that O_5 has the following internal momentum contribution over which has been integrated: $((p_{V_1}^\mu - p_W^\mu)g^{\nu\sigma} + \dots)$. The arguments of the Passarino-Veltman integrals are $C_i, C_{ij}(m_o^2, m_W^2, m_i^2, m_F^2, m_{V_2}^2, m_{V_1}^2)$ and $B_0(m_W^2, m_{V_2}^2, m_{V_1}^2)$. Possible particle insertions in the notation FV_1V_2 are given by $\tilde{\chi}^\pm W \gamma, \tilde{\chi}^0 Z W, \tilde{\chi}^\pm W Z$. In this case the vertex contributions have the form:

$$\begin{aligned} M_{1,f} = & O_5 \{ O_1 [O_3 (2m_F^2 C_0 + m_i^2 (2C_1 + 3C_2) \\ & + m_o^2 (3C_1 + 2C_2) - 2m_W^2 (C_1 + C_2) + 2B_0 + 4C_{00}) + 3O_4 m_F m_o C_0] \\ & + 3O_2 m_i [O_3 m_F C_0 + O_4 m_o (C_1 + C_2)] \} \end{aligned} \quad (\text{D.40})$$

$$\begin{aligned} M_{2,f} = & O_5 \{ 3O_1 m_i (O_3 m_o (C_1 + C_2) + O_4 m_F C_0) + O_2 [3O_3 m_F m_o C_0 \\ & + O_4 (2m_F^2 C_0 + m_i^2 (2C_1 + 3C_2) \\ & + m_o^2 (3C_1 + 2C_2) - 2m_W^2 (C_1 + C_2) + 2B_0 + 4C_{00})] \} \end{aligned} \quad (\text{D.41})$$

$$\begin{aligned} M_{3,f}^\mu = & -2O_5 \{ p_1^\mu [O_1 O_3 m_i (2(C_{12} + C_{22}) - C_1) + O_2 (3O_3 m_F (C_1 + C_2) \\ & + O_4 m_o (2(C_{11} + C_{12}) - C_2))] + p_2^\mu [O_1 O_3 m_i (C_2 + 2C_{22}) \\ & - O_2 (O_4 m_o (C_1 - 2C_{12} + C_2) - 3O_3 m_F C_2)] \} \end{aligned} \quad (\text{D.42})$$

$$\begin{aligned} M_{4,f}^\mu = & -2O_5 \{ p_1^\mu [O_1 (O_3 m_o (2(C_{11} + C_{12}) - C_2) + 3O_4 m_F (C_1 + C_2)) \\ & + O_2 O_4 m_i (2(C_{12} + C_{22}) - C_1)] + p_2^\mu [O_2 O_4 m_i (C_2 + 2C_{22}) \\ & - O_1 (O_3 m_o (C_1 - 2C_{12} + C_2) - 3O_4 m_F C_2)] \} \end{aligned} \quad (\text{D.43})$$

Technical aspects of one-loop calculations

We present the technical aspects of our calculations of masses and decay widths at one-loop level for the NMSSM using the mSUGRA 3 scenario and focus on the arbitrarily chosen decay $\tilde{\chi}_3^0 \rightarrow \tilde{\chi}_1^- W^+$, for proofing the UV and IR finiteness and the gauge independence.

E.1. Masses

The on-shell masses as we have defined them in Section 6.2.3 are UV and IR finite as well as gauge independent. For the mSUGRA 3 scenario under consideration we show the one-loop masses of the neutralinos and charginos in Figure E.1 as a function of the UV parameter Δ as defined in Equation (6.10) and as a function of the photon mass m_γ . In both cases no dependence on the parameters for the individual masses can be seen, meaning the masses are constant, which implies they are UV and IR finite.

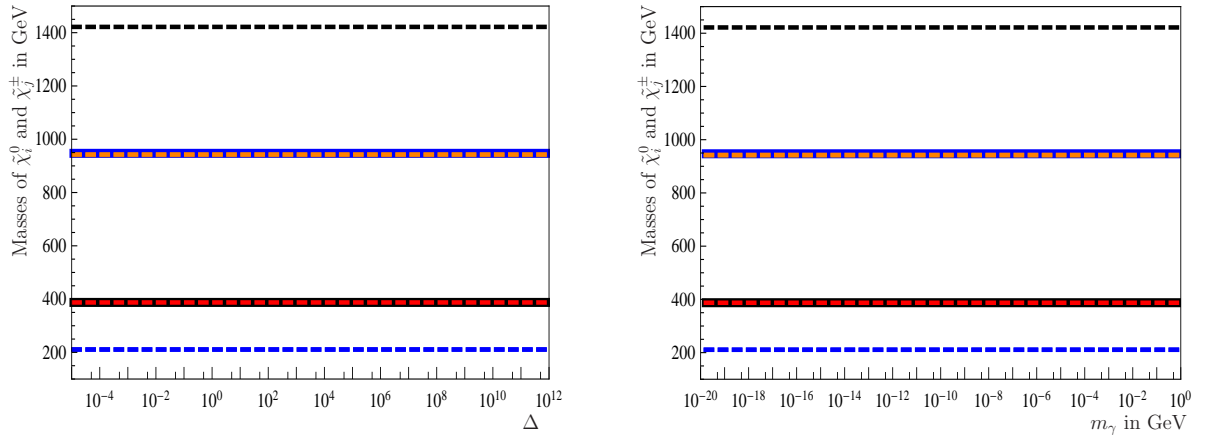


Figure E.1.: One-loop on-shell masses of neutralinos $m^{1L}(\tilde{\chi}_i^0)$ (dashed) and charginos $m^{1L}(\tilde{\chi}_j^\pm)$ (solid) as a function of: **a)** (left) the UV parameter Δ as defined in Equation (6.10); **b)** (right) the photon mass m_γ . In both cases the masses are constant and independent of the Δ and m_γ .

Since we have used a $\overline{\text{DR}}$ renormalization of $\tan\beta$ as defined in Equation (6.115) the masses of neutralinos and charginos are dependent on the renormalization scale Q as it can be seen from Figure E.2 **a)**. Since the renormalization of $\tan\beta$ only enters nondiagonal elements in the neutralino mass matrix, the sum of the neutralino masses is independent of Q . This statement is not valid for the chargino masses, since those are calculated from the squared chargino mass matrix, implying that the dependence of nondiagonal elements enters the trace of diagonal elements of the squared matrix. However, note that the residual Q dependence is small, typically

only $\mathcal{O}(0.1)$ GeV over several orders of magnitude in Q . In case of R -parity violation we checked that for the neutrino and lepton masses the relative dependence on Q is comparable to the one of neutralino and chargino masses. By construction the calculated masses are also gauge independent as it is shown in Figure E.2 b).

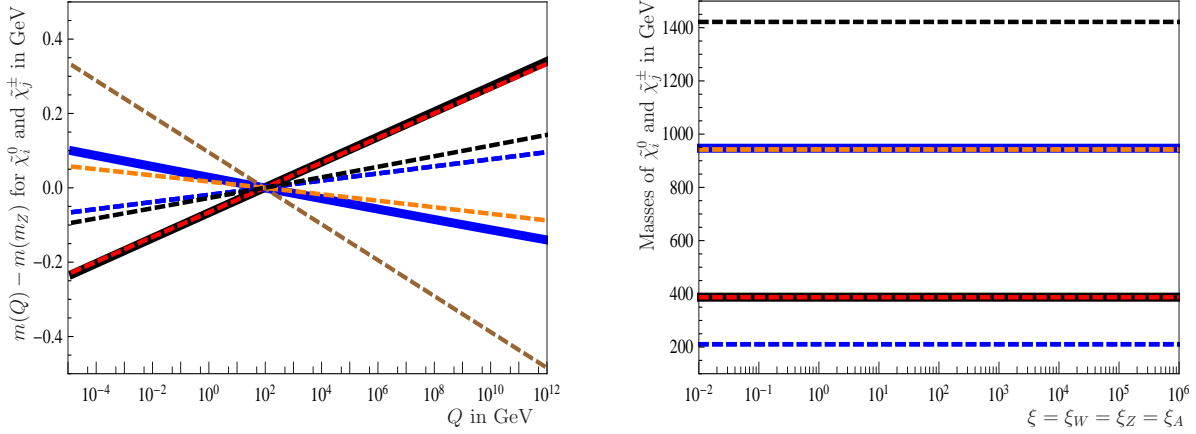


Figure E.2.: **a)** (left) Mass difference $m(Q) - m(m_Z)$ for the one-loop on-shell masses of neutralinos $m^{1L}(\tilde{\chi}_i^0)$ (dashed) and charginos $m^{1L}(\tilde{\chi}_j^\pm)$ (solid) as a function of the renormalization scale Q in GeV; **b)** (right) One-loop on-shell masses of neutralinos $m^{1L}(\tilde{\chi}_i^0)$ (dashed) and charginos $m^{1L}(\tilde{\chi}_j^\pm)$ (solid) as a function of the gauge parameters $\xi = \xi_W = \xi_Z = \xi_A$.

E.2. Decay widths

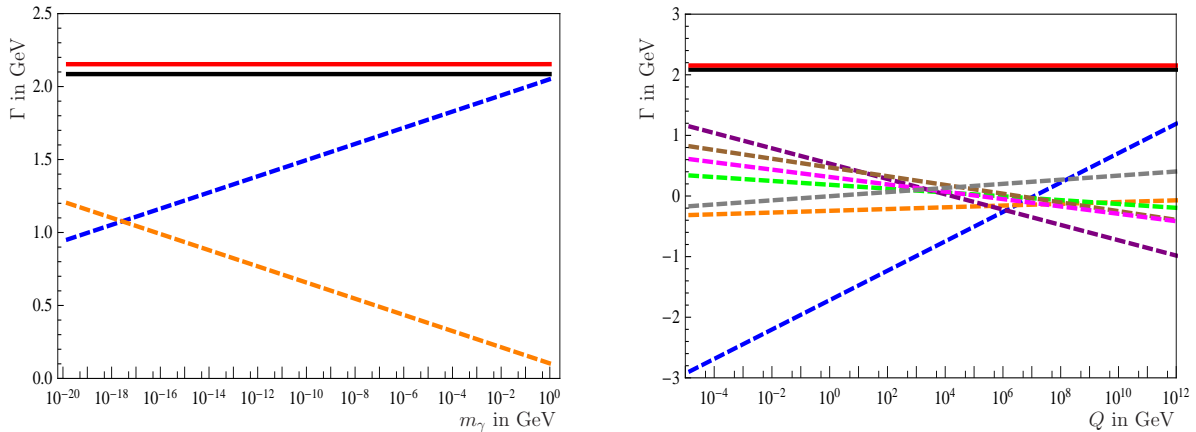


Figure E.3.: **a)** (left) Individual contributions to Γ^1 in GeV as a function of m_γ in GeV, in detail: Γ^0 (black, solid), $\Gamma^0 + \Gamma_V^1 + \Gamma_{CT}^1$ (blue, dashed), Γ^R (orange, dashed), Γ^1 (red, solid); **b)** (right) Individual contributions to Γ^1 in GeV as a function of Q in GeV, in detail: $\Gamma_{CT}^1(\delta g)$ (orange, dashed); $\Gamma_{CT}^1(\delta U, \delta V)$ (purple, dashed); $\Gamma_{CT}^1(\delta \mathcal{N})$ (green, dashed); $\Gamma_{CT}^1(\delta Z_W)$ (brown, dashed); $\Gamma_{CT}^1(\delta Z^0)$ (magenta, dashed); $\Gamma_{CT}^1(\delta Z^\pm)$ (gray, dashed); Γ_V^1 (blue, dashed); Γ^0 (black, solid); Γ^1 (red, solid).

Similar to the masses we want to discuss the technical aspects of the one-loop calculations concerning the decay widths taking the example $\tilde{\chi}_3^0 \rightarrow \tilde{\chi}_1^- W^+$. In Figure E.3 a) we show the cancellation of the photon mass dependence between the vertex and counterterm contributions

Γ_V^1 and Γ_{CT}^1 and the real emission of a photon Γ^R , implying that the final one-loop decay width $\Gamma^1 = \Gamma^0 + \Gamma_V^1 + \Gamma_{CT}^1 + \Gamma^R$ is an IR finite quantity.

Next we focus on the dependence on the renormalization scale Q , which vanishes for the decay width Γ^1 , since the $\overline{\text{DR}}$ renormalization of $\tan\beta$ does not enter the one-loop correction as long as the one-loop masses are not used for the calculation. The cancellation of the individual contributions to the counterterm and the vertex correction, which are dependent on Q , can be seen in Figure E.3 b) together with the fact, that the sum is a renormalization scale independent result.

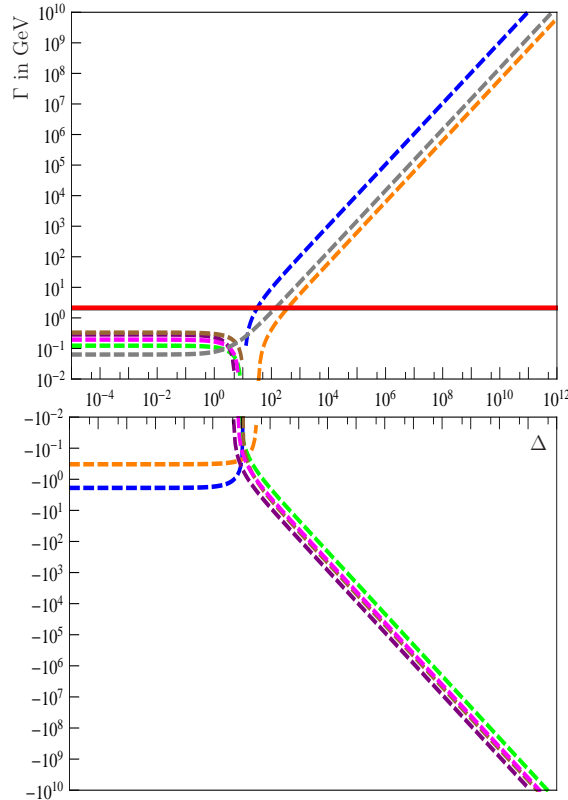


Figure E.4.: Individual contributions to Γ^1 in GeV as a function of the UV parameter Δ , in detail: $\Gamma_{CT}^1(\delta g)$ (orange, dashed); $\Gamma_{CT}^1(\delta U, \delta V)$ (purple, dashed); $\Gamma_{CT}^1(\delta \mathcal{N})$ (green, dashed); $\Gamma_{CT}^1(\delta Z_W)$ (brown, dashed); $\Gamma_{CT}^1(\delta Z^0)$ (magenta, dashed); $\Gamma_{CT}^1(\delta Z^\pm)$ (gray, dashed); Γ_V^1 (blue, dashed); Γ^0 (black, solid); Γ^1 (red, solid).

We are now left with the cancellation of the UV divergences between the various contributions, which we show in Figure E.4. All individual counterterms and the vertex correction are dependent on the UV parameter Δ , which we defined in Equation (6.10). However, the sum results in a UV finite decay width Γ^1 . Last but not least we want to focus on the gauge independence of our calculation, which can be seen from Figure E.5. In Figure E.5 a) we varied $\xi = \xi_W = \xi_Z$, whereas we fixed $\xi_A = 1$. In contrast Figure E.5 b) shows the variation of all gauge parameters. Please note that δg is gauge independent, since the individual contributions from the renormalization of the electric charge and the Weinberg angle cancel. Moreover the contributions from $\delta \mathcal{N}$ and $\delta U, \delta V$ are gauge independent by construction. All the other contributions can show a gauge dependence, which cancels after summing up to the full decay width Γ^1 .

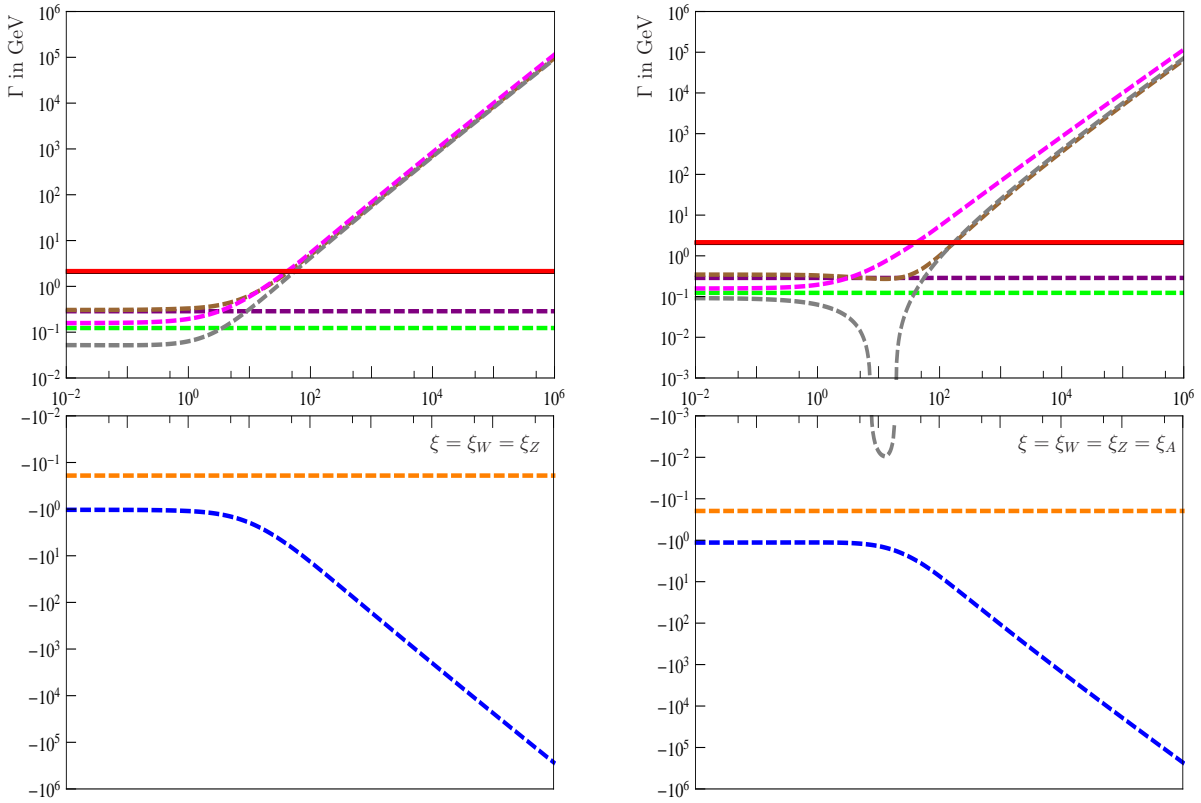


Figure E.5.: Individual contributions to Γ^1 in GeV as a function of the gauge parameters ξ , **a)** (left) $\xi = \xi_W = \xi_Z$; **b)** (right) $\xi = \xi_W = \xi_Z = \xi_A$, in detail: $\Gamma_{CT}^1(\delta g)$ (orange, dashed); $\Gamma_{CT}^1(\delta U, \delta V)$ (purple, dashed); $\Gamma_{CT}^1(\delta \mathcal{N})$ (green, dashed); $\Gamma_{CT}^1(\delta Z_W)$ (brown, dashed); $\Gamma_{CT}^1(\delta Z^0)$ (magenta, dashed); $\Gamma_{CT}^1(\delta Z^\pm)$ (gray, dashed); Γ_V^1 (blue, dashed); Γ^0 (black, solid); Γ^1 (red, solid).

Programs

In this chapter we describe the two programs, which were developed for the presented work and thereafter we list all public and commercial programs being used in the context of this thesis.

F.1. The Mathematica package MaCoR

In the context of R -parity violating models the Mathematica package MaCoR (Masses and Couplings in R-parity violating SUSY) was written, which calculates the mass matrices and couplings for bilinear R -parity violation and the $\mu\nu$ SSM with n right-handed neutrino superfields. It provides in addition the scalar potential and allows to calculate the tadpole equations. Moreover MaCoR handles the MSSM and the NMSSM and is easily extendable to an arbitrary field content as long as no additional gauge groups are added. For the $\mu\nu$ SSM with one right-handed neutrino superfield and BRpV the results were cross-checked against the program SARAH [180] except from the 4-point scalar interactions, which were not needed within this thesis. In the following we will explain the basic features of the program, which can be downloaded from [181] for the NMSSM or can be obtained from the author for the various other models:

```

2 | MaCoRNMSSM.nb

SetDirectory[NotebookDirectory[]]
/home/stefan/uni/MaCoR
<< "LagrangianNMSSM.m"

Model file for the generation of the Lagrangian of the NMSSM, S. Liebler 2010
Definitions
Generating kinetic Lagrangian
Generating Superpotential, D-Terms and Gaugino interactions
Generating Soft -breaking Lagrangian
Generating Lagrangian, Please hold on!
- Lagrangian without kinetic terms
- Lagrangian with kinetic terms
- Partial Lagrangians
- Scalar potential
Definition of particles
Definition of ThreePointCouplings
Definition of MassMatrixFunction
Ready for takeoff!
Use the following particle content "Particle[i,H]" with i being
the generation index/number of particles in species and H being:
1: S_i^- , 2: S_i^+ , 3: s1lep_i^- , 4: s1lep_i^+
5: S_i^0 , 6: P_i^0 , 7: Re(smi_i) , 8: Im(smi_i),
9: nu_i , 10: snu_i^dag , 11: sd_i , 12: sdi_i^dag
13: A[0] , 14: A[1]

By default the gauge bosons have lower indices, namely e, l, e, e, e for A, Z, W+, W-. For vertices
with more than one equal gauge bosons, a new index omega is introduced automatically.
Use the following particle content "ParticleWeyl[i,H]" with i being
the generation index/number of particles in species and H being for fermionic
particles, if you want to calculate mass matrices:
1: P_i^0(1) , 2: P_i^0(2) , 3: P_i^0(1)^dag , 4: P_i^0(2)^dag
5: nu_i(1) , 6: nu_i(2) , 7: nu_i(1)^dag , 8: nu_i(2)^dag
9: P_i^+(1) , 10: P_i^+(2) , 11: P_i^+(1)^dag , 12: P_i^+(2)^dag
13: P_i^-(1) , 14: P_i^-(2) , 15: P_i^-(1)^dag , 16: P_i^-(2)^dag
17: lep_i^+(1) , 18: lep_i^+(2) , 19: lep_i^+(1)^dag , 20: lep_i^+(2)^dag
21: lep_i^-(1) , 22: lep_i^-(2) , 23: lep_i^-(1)^dag , 24: lep_i^-(2)^dag
25: u_i(1) , 26: u_i(2) , 27: u_i(1)^dag , 28: u_i(2)^dag

29: u_i^c(1) , 30: u_i^c(2) , 31: u_i^c(1)^dag , 32: u_i^c(2)^dag
33: d_i(1) , 34: d_i(2) , 35: d_i(1)^dag , 36: d_i(2)^dag
37: d_i^c(1) , 38: d_i^c(2) , 39: d_i^c(1)^dag , 40: d_i^c(2)^dag

Moreover the following
Dirac particles can be used for the calculation of couplings "DiracParticle[i,H]":
1: chi_i^0*bar , 2: chi_i^0
3: chi_i^+-*bar (= chi_i^+*T), 4: chi_i^- (= chi_i^-*barT)
5: nu_i*bar , 6: nu_i
7: lep_i^+*bar (= lep_i^+*T), 8: lep_i^- (= lep_i^-*barT)
9: u_i^*bar (= u_i^cT) , 10: u_i (= u_i^cbarT)
11: d_i^*bar (= d_i^cT) , 12: d_i (= d_i^cbarT)

Some comments:
- This program cannot handle ghosts
and VVV, SSSS interactions (possible, but not checked)!!
- In this version no color indices are included!!
- To get towards a FeynArts model file the couplings have to be multiplied:
CorrFFS = i, CorrFPV = i, CorrSSS = i, CorrSSV = 1, CorrSVV = -i
CorrSFFV = -i, CorrFVV = 1

(*!Mass matrices!*)
(*Neutralino Mass Matrix*)
MassMatrixFunction[ParticleWeyl[t1, 1], ParticleWeyl[t2, 1]]
( M1 0 -g1*vev1/2 g1*vev1/2 0
0 M2 g1*vev1/2 -g1*vev1/2 0
-g1*vev1/2 g1*vev1/2 0 -g1*vev1/2 -g1*vev1/2
g1*vev1/2 -g1*vev1/2 -g1*vev1/2 0 -g1*vev1/2
0 0 -g1*vev1/2 -g1*vev1/2 sqrt(2)*vev1*ks )
(*Scalar Mass Matrix*)
MassMatrixFunction[Particle[t1, 5], Particle[t2, 5]][[1, 1]]
1/2*vev1^2*Lambda*Conj(1) + 1/2*vev1^2*Lambda*Conj(1) + 3/8*g1^2*vev1^2 - g^2*vev1^2/8 - 3/8*g1^2*vev1^2 - g1^2*vev1^2/8 + MHd2

```

```

MacCoRMSM.nb | 3
4 | MacCoRMSM.nb

MassMatrixFunction[Particle[t1, 5], Particle[t2, 5]][[1, 2]]

$$\frac{\text{vevS Conig(Ta)}}{2\sqrt{2}} + \text{vevd vevu } \lambda \text{ Conig}(\lambda) - \frac{1}{4} \text{vevS}^2 \lambda \text{ Conig}(\epsilon) - \frac{1}{4} \text{vevS}^2 \kappa \text{ Conig}(\lambda) - \frac{1}{4} g^2 \text{vevd vevu} - \frac{1}{4} g^2 \text{vevd vevu} - \frac{\text{Ta vevS}}{2\sqrt{2}}$$

MassMatrixFunction[Particle[t1, 5], Particle[t2, 5]][[1, 3]]

$$\frac{\text{vevu Conig(Ta)}}{2\sqrt{2}} + \text{vevd vevS } \lambda \text{ Conig}(\lambda) - \frac{1}{2} \text{vevS vevu } \lambda \text{ Conig}(\epsilon) - \frac{1}{2} \text{vevS vevu } \kappa \text{ Conig}(\lambda) - \frac{\text{Ta vevu}}{2\sqrt{2}}$$

(*!!Tadpole equations!*)
D[Vscalar, vevS] /. vec[a_][b_] -> 0
(*Note the momentum structure!*)
Simplify[ThreePointCouplings[Particle[t1, 6], Particle[t2, 1], Particle[t3, 13], Ga[3]]]

$$\frac{1}{2} g (\text{Rpl}(t2, 1) \text{Rpsc}(t1, 1) + \text{Rpl}(t2, 2) \text{Rpsc}(t1, 2)) ((P(\text{PO}(t1))(\sigma))(1) - (P(\text{Spn}(t2))(\sigma))(1))$$

(*!!Four point couplings!*)
(*S0, S0, W, W*)
FourPointCouplings[Particle[t1, 5], Particle[t2, 5], Particle[t3, 13], Particle[t3, 13], Ga[3], Ga[4]]

$$\frac{1}{2} (g^2 \text{Rsc}(t1, 1) \text{Rsc}(t2, 1) (-g(\zeta, \sigma)) - g^2 \text{Rsc}(t1, 2) \text{Rsc}(t2, 2) g(\zeta, \sigma))$$

(*!!Three point couplings with fermions!*)
(*structure has to be DiracParticle,DiracParticle,Particle*)

```

We briefly want to present the basic functions of the Mathematica package MaCoR: The derivative $D[\text{Vscalar}, \text{vev}]$ with $\text{vev} = \text{vevd}$, vevu , vevS respectively allows to calculate the tadpole equations. Fermionic mass matrices can be obtained by $\text{MassMatrixFunction}[\dots]$ inserting two Weyl spinors $\text{ParticleWeyl}[\text{gen}, \text{par}]$, whereas $\text{Particle}[\text{gen}, \text{par}]$ specifies scalar/pseudoscalar particles and gauge bosons. Therein gen denotes the generation index of the particle under consideration and par determines the particle itself. For example the charged scalars S_i^- are given by $\text{Particle}[\text{t}, 1]$, the neutral scalars S_j^0 by $\text{Particle}[\text{j}, 5]$. Loading the Lagrangian of a model gives the list of all available particles and their antiparticles and the corresponding numbering. Three or four point interactions can be derived using $\text{ThreePointCouplings}[\dots]$ or $\text{FourPointCouplings}[\dots]$, where in case of a gauge boson $\text{Particle}[\text{t1}, 13]$ the additional argument $\text{Ga}[\text{i}]$ with $i = 1$ for the photon γ , $i = 2$ for the Z boson and $i = 3, 4$ for the W^\pm bosons has to be added. Three point couplings involving fermions can be calculated by $\text{DiracThreePointCouplings}[\dots]$, where the first two particles have to be the fermions and the last particle can either be a scalar or gauge boson, where in the latter case again $\text{Ga}[\text{i}]$ specifies the gauge boson.

MaCoR has been used to calculate all the couplings and mass matrices for **CNNDecays**, where they are included in the folder `couplings` and the file `oneloop/treemasses.f90` as explained in the next section.

F.2. The program CNNDecays

For the calculation of the on-shell masses as described in Section 6.2.3 and the full NLO corrections for the decays $\tilde{\chi}_j^\pm \rightarrow \tilde{\chi}_l^0 W^\pm$ and $\tilde{\chi}_i^0 \rightarrow \tilde{\chi}_k^\mp W^\pm$ including the R -parity violating decays $\tilde{\chi}_i^0 \rightarrow \tilde{l}_k^\mp W^\pm$ we provide the program **CNNDecays**, which was published in [135] and can be obtained from [157]. Recently also the neutralino decays $\tilde{\chi}_j^0 \rightarrow \tilde{\chi}_i^0 Z$ were added. It is written in Fortran 95 and based on SPheno [71].

The program folder contains the following sub-folders:

- ▷ `callcorrections`: routines to combine the generic routines contained in `corrections` with the model dependent information concerning masses and couplings.
- ▷ `corrections`: generic NLO routines, which are provided in R_ξ -gauge and 't Hooft-Feynman gauge, as well as the loop functions which are not contained in the `SPheno` package.
- ▷ `couplings`: couplings organized in three sub-folders, namely `NMSSMunuSSM` containing the couplings for the NMSSM and the $\mu\nu$ SSM with one right-handed neutrino superfield, `MSSMbilinear` for the MSSM and bilinear R -parity violation and `bilinearcomplex` for bilinear R -parity violation with complex parameters as described in Section 5.1.1. The couplings were cross-checked with the program `SARAH` [180].
- ▷ `oneloop`: contains the main program `CNNDecays.f90` and the main module for the calculation `Renormbasic.f90`. The latter one can also be used to implement the package in other programs. In `treemasses.f90` the matrices for all considered models on tree-level can be found, whereas `loopmasses.f90` contains the two routines `NeutralinoMassLoopOS` and `CharginoMassLoopOS`, which perform the calculation of on-shell one-loop masses for neutralinos and charginos. The tadpole equations for the models under consideration can be found in `tadpoles.f90`. The calculation of wave-function renormalization constants and counterterms is included in `wavemassrenorm.f90`. Moreover `addtools.f90` contains different routines for the fit of lepton masses at tree-level in R -parity violating supersymmetry, the check of the neutrino data and bounds on Higgs masses. In the module `Bremsstrahlung.f90` the user finds the relevant routines for the calculation of hard photon emission.
- ▷ `sphenooriginal`: necessary parts of `SPheno`.
- ▷ `examples`: This folder contains various example input files, whose general form we present in the following. In the sub-folder `MSSM-SPS-SU4` MSSM input files based on the SPS scenarios and the ATLAS SU4 point are included, whereas `NMSSM-mSUGRA-GMSB` provides NMSSM benchmark scenarios, which were described in Chapter 7. In addition example input files for the $\mu\nu$ SSM and bilinear R -parity violation with real or complex parameters can be found.

Before compiling it might be necessary to adjust the `f90`-compiler and the corresponding flags in the `Makefile` which is placed in the main folder. In addition the number of processors can be specified to allow for a faster compilation of the routines, which contain the one-loop corrections. The program `CNNDecays` can then be created by performing `make` in the main folder. It is stored in the sub-folder `bin` and runs with `./CNNDecays`, if an input file named `LesHouches.in` is accessible.

The input and output files in `examples` are based on the SUSY Les Houches Accord (SLHA) [182, 183]. Concerning the input, which is expected to be given at the electroweak scale, there are two main differences with respect to the SLHA:

1. The entries of the block `EXTPAR` are interpreted as effective on-shell values for the masses and mixing entries. Therefore the entry 0 setting the scale is ignored.
2. A new block called `NLOPAR` has been created containing the information to check for the gauge and renormalization scale independence of the results. The program allows to use

only the UV divergent parts of the Passarino-Veltman integrals. Moreover the divergence itself can be set to an arbitrary value. By varying the photon mass we can simply check the IR finiteness. In addition the gauge parameter ξ_V can be set to an arbitrary value and it can be chosen, whether R_ξ -gauge or 't Hooft-Feynman gauge should be used for the photon, the Z -boson and the W -boson independently. Note that the renormalization scale Q in NLOPAR only affects the scale within the Passarino-Veltman integrals and does not imply any running of the parameters of the block **EXTPAR**. Last but not least, the user can choose whether LO or NLO neutralino and chargino on-shell masses are used for the calculation of the processes, meaning they enter as external as well as internal masses.

As already mentioned the folder **examples** contains such example input files for the MSSM, the NMSSM, bilinear R -parity violation as well as the $\mu\nu$ SSM with one right-handed neutrino superfield. In all models the (effective) parameter μ has to be provided in the block **EXTPAR**, either as entry 23 or as entry 65 in case it is an effective parameter. Thus, in case of the NMSSM and the $\mu\nu$ SSM this value is used together with entry 61 to calculate the singlet or right-handed sneutrino vacuum expectation value v_S respectively v_c . A couple of parameters is fixed by the tadpole equations, namely $m_{H_d}^2, m_{H_u}^2$ in case of the MSSM and in addition B_i in case of BRpV, whereas in the NMSSM we fix m_S^2 and in the $\mu\nu$ SSM the diagonal elements of $m_{\nu^c}^2$ and T_ν^i in addition. For BRpV with complex μ and ϵ also the imaginary parts of B_i and B_μ are deduced from tadpole equations. Below we give an example input file **LesHouches.in** based on the benchmark scenario mSUGRA 1 for the $\mu\nu$ SSM:

```

Block MODSEL                # Select model
 3   6                       # mnuSSM
 4   1                       # RPviolation
Block SMINPUTS              # Standard Model inputs
 1   1.27920000E+02         # ALPHA_EM^-1(MZ)
 2   1.16639000E-05        # GF
 3   1.17200000E-01        # ALPHA_S(MZ)
 4   9.11870000E+01        # MZ
 5   4.21400000E+00        # MB(MB)
 6   1.71400000E+02        # MTOP (POLE MASS)
 7   1.77700000E+00        # MTAU
Block MINPAR                # Input parameters
 3   10                      # tanb
 4   1                       # sign(mu)
BLOCK EXTPAR
 1   2.11635141E+02         # M1
 2   3.91898115E+02         # M2
 3   1.11230823E+03         # M3
11  -1.42395369E+03         # ATOP
12  -2.61046378E+03         # ABOT
13  -1.77741018E+03         # ATAU
31   3.77391179E+02         # M_eL
32   3.77391179E+02         # M_muL
33   3.65780798E+02         # M_tauL
34   2.57517852E+02         # M_eR
35   2.57517852E+02         # M_muR
36   2.21138594E+02         # M_tauR
41   1.02413355E+03         # M_q1L
42   1.02413355E+03         # M_q2L
43   8.46048325E+02         # M_q3L
44   9.86146013E+02         # M_uR
45   9.86146013E+02         # M_cR
46   5.65558510E+02         # M_tR
47   9.81632542E+02         # M_dR
48   9.81632542E+02         # M_sR
49   9.66133394E+02         # M_bR
61   1.00000000E-01         # LAMBDA

```

```

62  1.08485437E-01  # KAPPA/2
63  -9.59966990E+02 # TLAMBDA/LAMBDA = ALAMBDA
64  -1.58051889E+00 # T_KAPPA/KAPPA = A_KAPPA
65  9.68523016E+02  # EFFMU
73  5.71920838E-06  # hnu_1
74  6.20206893E-06  # hnu_2
75  -6.20206893E-06 # hnu_3
BLOCK RVSNEVIN
  1  -1.35445088E-03 # v_L_1
  2  -1.27271724E-03 # v_L_2
  3  1.71364110E-03  # v_L_3
BLOCK NLOPAR
  1  0                # UV divergence: 1 = only UV div. parts
  2  0.00000000E+00  # UV divergence: Delta
  3  1.00000000E-05  # IR divergence: Photon regulator mass
  4  9.11870000E+01  # Renormalization scale: Q for NLO calc.
  5  1.00000000E+05  # Gauge dependence: Xi
  6  1                # Xi = 1 for photon, otherwise set to 0
  7  1                # Xi = 1 for Z, otherwise set to 0
  8  1                # Xi = 1 for W\pm, otherwise set to 0
  9  0                # NLO masses for process: 0 LO masses, 1 uses NLO masses

```

In BRpV ϵ_i and v_i can be chosen as input parameters

```

Block MODSEL                # Select model
  1  0                      # bilinear model
  4  1                      # RPviolation
....
BLOCK RVKAPPAIN
  1  1.45660382E-02        # kappa_1 = eps_1
  2  9.01765562E-03        # kappa_2 = eps_2
  3  -3.16131217E-03       # kappa_3 = eps_3
BLOCK RVSNEVIN
  1  -8.68089903E-04       # v_L_1
  2  -4.50162251E-04       # v_L_2
  3  4.19592513E-04        # v_L_3
....

```

whereas in the $\mu\nu$ SSM Y_ν^i and v_i are input variables:

```

Block MODSEL                # Select model
  3  6                      # mnuSSM
  4  1                      # RPviolation
....
BLOCK EXTPAR
  73  5.71920838E-06       # hnu_1
  74  6.20206893E-06       # hnu_2
  75  -6.20206893E-06      # hnu_3
BLOCK RVSNEVIN
  1  -1.35445088E-03       # v_L_1
  2  -1.27271724E-03       # v_L_2
  3  1.71364110E-03        # v_L_3
....

```

A successful run creates the output file `CNNDecays.dec`. We store in the SLHA block `MASS` the NLO masses of neutralinos and charginos, whereas the LO masses are only part of the screen output. In the SLHA block `DECAYTREE` the LO decay widths Γ^0 in GeV are shown. The corresponding NLO decay width Γ^1 in GeV are given in the SLHA block `DECAY`. For the lightest neutralino $\tilde{\chi}_1^0$ we also give the R -parity violating decays in case of BRpV and the $\mu\nu$ SSM. In those cases the block `SPhenoRP` contains all the relevant parameters for neutrino physics. In case of light scalars or pseudoscalars, which violate the LEP bounds, a warning is part of the screen output, which also informs about a successful description of the neutrino data according to [17], if R -parity is broken. In the example output file we give only the crucial information:

```

# SUSY Les Houches Accord 2 - Neutralino + Chargino NLO Decays into W boson
# S. Liebler, published in arXiv:1011.6163
# in case of problems send email to sliebler@physik.uni-wuerzburg.de
# Created: 23.08.2011, 18:17
Block SPINFO # Program information
  1 CNNDecays # spectrum calculator
.....
Block MODSEL # Model selection
  3 6 # mnuSSM
  4 1 # add R-parity
.....
Block EXTPAR #
.....
.....
Block MASS # Mass spectrum
# PDG code mass particle
.....
  12 -3.32997778E-14 # nu_1
  14 8.80228020E-12 # nu_2
  16 -4.82129947E-11 # nu_3
 1000022 2.10611052E+02 # chi01
 1000023 3.87101530E+02 # chi02
 1000025 -9.71754987E+02 # chi03
 1000035 9.75135419E+02 # chi04
 1000045 2.10157308E+03 # nu_R
  11 5.10999060E-04 # e+
  13 1.05658000E-01 # mu +
  15 1.77700000E+00 # tau+
 1000024 3.87225368E+02 # chi1+
 1000037 9.76694005E+02 # chi2+
.....
DECAYTREE 1000022 5.71681505E-13 # chi01
# BR NDA ID1 ID2
  1.66867238E-01 2 -15 24 # BR(chi01 -> tau- W+)
  1.66867238E-01 2 15 -24 # BR(chi01 -> tau+ W-)
  1.64601716E-01 2 -13 24 # BR(chi01 -> mu- W+)
  1.64601716E-01 2 13 -24 # BR(chi01 -> mu + W-)
  1.61639201E-03 2 -11 24 # BR(chi01 -> e- W+)
  1.61639201E-03 2 11 -24 # BR(chi01 -> e+ W-)
  3.33829308E-01 2 16 23 # BR(chi01 -> nu_3 Z)
  1.23762944E-60 2 14 23 # BR(chi01 -> nu_2 Z)
  1.14818350E-60 2 12 23 # BR(chi01 -> nu_1 Z)
.....
DECAY 1000022 6.10147635E-13 # chi01 on NLO
# BR NDA ID1 ID2
  1.66206979E-01 2 -15 24 # BR(chi01 -> tau- W+)
  1.66206979E-01 2 15 -24 # BR(chi01 -> tau+ W-)
  1.65219418E-01 2 -13 24 # BR(chi01 -> mu- W+)
  1.65219418E-01 2 13 -24 # BR(chi01 -> mu + W-)
  1.73036516E-03 2 -11 24 # BR(chi01 -> e- W+)
  1.73036516E-03 2 11 -24 # BR(chi01 -> e+ W-)
  3.33686476E-01 2 16 23 # BR(chi01 -> nu_3 Z)
  2.68286001E-33 2 14 23 # BR(chi01 -> nu_2 Z)
  1.00157839E-33 2 12 23 # BR(chi01 -> nu_1 Z)
.....
Block SPhenoRP # additional RP parameters
  1 5.53918495E-02 # Re(eps_1)
  2 6.00684651E-02 # Re(eps_2)
  3 -6.00684651E-02 # Re(eps_3)
  4 2.10857140E-02 # Re(Lambda_1) = Re(v_d epsilon_1 + mu v_L1) [GeV^2]
  5 2.12780743E-01 # Re(Lambda_2) = Re(v_d epsilon_2 + mu v_L2) [GeV^2]
  6 2.14264164E-01 # Re(Lambda_3) = Re(v_d epsilon_3 + mu v_L3) [GeV^2]
  7 2.24701272E-03 # m^2_atm [eV^2]
  8 7.74790278E-05 # m^2_sol [eV^2]
  9 9.27404289E-01 # tan^2 theta_atm
 10 4.08145879E-01 # tan^2 theta_sol
.....
Block NLOPAR # Renormalization parameters
  1 0 # UV divergence: 1 = only UV div. parts

```

2	0.00000000E+00	# UV divergence: Delta
3	1.00000000E-05	# IR divergence: Photon regulator mass
4	9.11870000E+01	# Renormalization scale: Q for NLO calc.
5	1.00000000E+05	# Gauge dependence: Xi
6	1	# Special choice of gauge for photon
7	1	# Special choice of gauge for Z boson
8	1	# Special choice of gauge for W boson
9	0	# NLO masses used for process: 0 LO, 1 NLO masses

F.3. Used commercial programs/public codes

Since MaCoR is written as `Mathematica` package it is based on a commercial program. Also parts of `CNNDecays` were written by the use of other public codes. In the following we list all programs used in the context of this thesis:

- ▷ `Mathematica` [184]: The `Mathematica` packages `FeynArts`, `FormCalc` and `MaCoR` are processed with `Mathematica 7`. Moreover plots and diagrams are generated with the various plot functions within `Mathematica`.
- ▷ `FeynArts` and `FormCalc` [131, 185]: Both programs were used to provide the generic routines for the one-loop calculations as they appear in `CNNDecays` and for basic calculations of two- and three-body decays.
- ▷ `SARAH` [180]: The couplings and mass matrices of `MaCoR` were cross-checked with the results of `SARAH` in case of the $\mu\nu$ SSM with one right-handed neutrino superfield and BRpV.
- ▷ `SPheno` [71]: In `CNNDecays` the basic routines for the in- and output, the loop functions and the diagonalization of matrices are taken from `SPheno`, which can be found in the folder `sphenooriginal` within `CNNDecays`. Moreover the results involving decay widths of particles in the $\mu\nu$ SSM were generated with a modified version of `SPheno`.
- ▷ This thesis is written in $\text{\LaTeX}2\epsilon$ with the help of Kile 2.0 and BibTeX.
- ▷ `feynmf/mp`: All Feynman diagrams were generated with this \LaTeX program of Thorsten Ohl based on `MetaPost` [186].
- ▷ GNU Image Manipulation Program GIMP: Some diagrams and pictures were processed with the help of GIMP.

List of Figures

2.1.	Illustration of electroweak symmetry breaking	7
2.2.	Allowed regions for the neutrino differences of squared masses and mixing angles	11
2.3.	Constraints on the reactor angle	12
3.1.	Illustration of interactions arising from terms in the superpotential	21
3.2.	Contribution to the proton decay via couplings λ' and λ''	25
5.1.	LEP exclusion plots for scalar and pseudoscalar states	45
6.1.	Definition and notation of Passarino-Veltman integrals	61
6.2.	Generic self-energy diagrams for vector bosons.	66
6.3.	Generic self-energy diagrams for neutralinos and charginos.	73
6.4.	Tadpole contributions including the Goldstone bosons	75
6.5.	Generic vertex corrections.	85
6.6.	Feynman diagrams for the real photon emission $F_i \rightarrow F_o W^\pm \gamma$	87
6.7.	Real corrections for $\tilde{\chi}_j^0 \rightarrow \tilde{\chi}_l^\mp W^\pm \gamma$	90
8.1.	Neutralino and lightest scalar/pseudoscalar masses versus A_κ in 1 $\hat{\nu}^c$ - $\mu\nu$ SSM . .	95
8.2.	One-loop $\overline{\text{DR}}$ neutralino masses and particle characters versus κ in 1 $\hat{\nu}^c$ - $\mu\nu$ SSM .	96
8.3.	Branching ratios of h^0 versus $m(\tilde{\chi}_1^0)$ in 1 $\hat{\nu}^c$ - $\mu\nu$ SSM	97
8.4.	Dominant Feynman graph for the decay $\tilde{\chi}_1^0 \rightarrow l_i \tau \nu$ with $l_i = e, \mu$	98
8.5.	Branching ratios of h^0 versus $m(\tilde{\chi}_1^0)$ in 1 $\hat{\nu}^c$ - $\mu\nu$ SSM	98
8.6.	Branching ratios of $\tilde{\chi}_1^0$ versus κ in 1 $\hat{\nu}^c$ - $\mu\nu$ SSM	99
8.7.	Decay length of $\tilde{\chi}_1^0$ versus $m(\tilde{\chi}_1^0)$ in 1 $\hat{\nu}^c$ - $\mu\nu$ SSM	100
8.8.	Singlino branching ratios versus $m(\tilde{\chi}_1^0)$ in 1 $\hat{\nu}^c$ - $\mu\nu$ SSM	100
8.9.	Masses of scalars S_i^0 and pseudoscalars P_j^0 versus v_{e2} for different T_κ in 2 $\hat{\nu}^c$ - $\mu\nu$ SSM	101
8.10.	Decay length of $\tilde{\chi}_1^0$ dependent on type of fit versus $m(\tilde{\chi}_1^0)$ in 2 $\hat{\nu}^c$ - $\mu\nu$ SSM	102
8.11.	Branching ratios of $\tilde{\chi}_3^0$ versus $m(\tilde{\chi}_1^0)$ in 2 $\hat{\nu}^c$ - $\mu\nu$ SSM	103
8.12.	Higgs boson decays versus $m(\tilde{\chi}_1^0)$ in 2 $\hat{\nu}^c$ - $\mu\nu$ SSM	104
9.1.	On-shell neutrino masses versus $ \vec{e} ^2/ \vec{\Lambda} $ in $\mu\nu$ SSM and BRpV	107
9.2.	On-shell neutrino masses with sign-condition versus $ \vec{e} ^2/ \vec{\Lambda} $ in $\mu\nu$ SSM and BRpV	107
9.3.	One-loop corrections to lepton masses versus $ \vec{e} ^2/ \vec{\Lambda} $ in $\mu\nu$ SSM	108
9.4.	Mass differences Δm_{atm}^2 and Δm_{sol}^2 versus $ \vec{e} ^2/ \vec{\Lambda} $ for BRpV	109
9.5.	Mass differences Δm_{atm}^2 and Δm_{sol}^2 versus alignment parameters in $\mu\nu$ SSM . . .	109
9.6.	Neutrino mixing angles versus ratios of alignment parameters in $\mu\nu$ SSM	110
9.7.	On-shell neutralino masses and particle characters versus M_1 in $\mu\nu$ SSM	113
9.8.	(N)LO decay widths and correction factor for $\tilde{B} \rightarrow \tilde{\chi}_1^- W^+$ versus M_1 in $\mu\nu$ SSM	114
9.9.	(N)LO decay widths and correction factor for $\tilde{B} \rightarrow \tilde{\chi}_2^- W^+$ versus M_1 in $\mu\nu$ SSM	114
9.10.	On-shell neutralino masses and particle characters versus κ in $\mu\nu$ SSM	115

9.11. (N)LO decay widths and correction factor for $\tilde{S} \rightarrow \tilde{\chi}_1^- W^+$ versus κ in $\mu\nu$ SSM	116
9.12. (N)LO decay widths and correction factor for $\tilde{S} \rightarrow \tilde{\chi}_2^- W^+$ versus κ in $\mu\nu$ SSM	116
9.13. On-shell neutralino and chargino masses versus M_2 in $\mu\nu$ SSM	117
9.14. (N)LO decay widths and correction factor for $\tilde{W}^+ \rightarrow \tilde{\chi}_1^0 W^+$ versus M_2 in $\mu\nu$ SSM	117
9.15. (N)LO decay widths and correction factor for $\tilde{W}^+ \rightarrow \tilde{\chi}_2^0 W^+$ versus M_2 in $\mu\nu$ SSM	118
9.16. On-shell neutralino masses, particle content of the lightest neutralino, decay widths $\Gamma^1(\tilde{\chi}_1^0 \rightarrow l^+ W^-)$ and correction factor versus κ in $\mu\nu$ SSM	119
10.1. Ratio of decay widths $\Gamma(\tilde{\chi}_1^0 \rightarrow l^+ W^-)$ and ratio of decay widths $\Gamma(\tilde{\chi}_1^+ \rightarrow Z l^+)$ versus $\tan^2 \theta_{atm}$ in 1 $\hat{\nu}^c$ - $\mu\nu$ SSM	122
10.2. Ratios of decay widths $\Gamma(\tilde{\chi}_1^0 \rightarrow l_i l_j \nu)$ versus $\tan^2 \theta_{sol}$ in 1 $\hat{\nu}^c$ - $\mu\nu$ SSM	122
10.3. Ratio of decay widths $\Gamma(\tilde{\chi}_1^0 \rightarrow q_i \bar{q}_j l)$ versus $\tan^2 \theta_{atm}$ and $\Gamma(\tilde{\chi}_1^0 \rightarrow l_i l_j \nu)$ versus $\tan^2 \theta_{sol}$ in 1 $\hat{\nu}^c$ - $\mu\nu$ SSM	123
10.4. Ratio of decay widths $\Gamma(\tilde{\chi}_1^0 \rightarrow l_i l_j \nu)$ versus $\tan^2 \theta_{sol}$ in 1 $\hat{\nu}^c$ - $\mu\nu$ SSM	123
10.5. Ratios of decay widths $\Gamma(\tilde{\chi}_1^0 \rightarrow l^+ W^-)$ versus Λ_2/Λ_3 in BRpV	124
10.6. Ratios of decay widths $\Gamma(\tilde{\chi}_1^0 \rightarrow l^+ W^-)$ versus Λ_2/Λ_3 in 1 $\hat{\nu}^c$ - $\mu\nu$ SSM	125
10.7. Ratios of decay widths $\Gamma(\tilde{\chi}_1^0 \rightarrow l^+ W^-)$ versus $\tan^2 \theta_{atm}$ and $\sin^2 \theta_R$ for bino-like LSP in 2 $\hat{\nu}^c$ - $\mu\nu$ SSM	126
10.8. Ratios of decay widths $\Gamma(\tilde{\chi}_1^0 \rightarrow l^+ W^-)$ versus $\tan^2 \theta_{sol}$ for bino- and singlino-like LSP in 2 $\hat{\nu}^c$ - $\mu\nu$ SSM	126
10.9. Ratios of decay widths $\Gamma(\tilde{\chi}_1^0 \rightarrow l^+ W^-)$ versus $\tan^2 \theta_{atm}$ and $\sin^2 \theta_R$ for singlino-like LSP in 2 $\hat{\nu}^c$ - $\mu\nu$ SSM	127
D.1. Generic Vertex NLO corrections.	149
E.1. Neutralino and chargino masses versus UV parameter and photon mass	153
E.2. Neutralino and chargino masses/mass differences versus renormalization scale and gauge parameters	154
E.3. Individual contributions to one-loop decay widths versus photon mass	154
E.4. Individual contributions to one-loop decay widths versus UV parameter	155
E.5. Individual contributions to one-loop decay widths versus gauge parameters	156

Bibliography

- [1] M. E. Peskin and D. V. Schroeder, *An Introduction to quantum field theory*, Reading, USA: Addison-Wesley (1995) 842 p.
- [2] S. P. Martin, *A Supersymmetry Primer*, (1997), arXiv:hep-ph/9709356.
- [3] B. C. Allanach et al., *The Snowmass points and slopes: Benchmarks for SUSY searches*, Eur. Phys. J. **C25**, 113–123 (2002), arXiv:hep-ph/0202233.
- [4] F. Mandl and G. Shaw, *Quantum field theory*, Chichester, UK: Wiley (1984) 354 p. (A Wiley-interscience Publication).
- [5] O. Nachtmann, *Elementary particle physics: concepts and phenomena*, Berlin, Germany: Springer (1990) 559 p.
- [6] M. Bohm, A. Denner and H. Joos, *Gauge theories of the strong and electroweak interaction*, Stuttgart, Germany: Teubner (2001) 784 p.
- [7] P. W. Higgs, *Broken Symmetries and the Masses of Gauge Bosons*, Phys. Rev. Lett. **13**(16), 508–509 (Oct 1964).
- [8] F. Englert and R. Brout, *Broken Symmetry and the Mass of Gauge Vector Mesons*, Phys. Rev. Lett. **13**(9), 321–323 (Aug 1964).
- [9] H. Yukawa, *On the Interaction of Elementary Particles*, Proc. Phys.-Math. Soc. Jpn. (17), 48–57 (1935).
- [10] Y. Nambu, *Quasi-Particles and Gauge Invariance in the Theory of Superconductivity*, Phys. Rev. **117**(3), 648–663 (Feb 1960).
J. Goldstone, *Field theories with superconductor solutions*, Il Nuovo Cimento (1955-1965) **19**, 154–164 (1961), 10.1007/BF02812722.
- [11] R. Davis, *A review of the Homestake solar neutrino experiment*, Prog. Part. Nucl. Phys. **32**, 13–32 (1994).
B. T. Cleveland et al., *Measurement of the solar electron neutrino flux with the Homestake chlorine detector*, Astrophys. J. **496**, 505–526 (1998).
J. N. Abdurashitov et al. (SAGE Collaboration), *Measurement of the solar neutrino capture rate with gallium metal*, Phys. Rev. **C60**, 055801 (1999), arXiv:astro-ph/9907113.
C. M. Cattadori (GNO Collaboration), *Update of solar neutrino interaction rate measurements from GNO at LNGS*, Nucl. Phys. Proc. Suppl. **110**, 311–314 (2002).
W. Hampel et al. (GALLEX Collaboration), *GALLEX solar neutrino observations: Results for GALLEX IV*, Phys. Lett. **B447**, 127–133 (1999).

- M. Altmann et al. (GNO Collaboration), *GNO solar neutrino observations: Results for GNO I*, Phys. Lett. **B490**, 16–26 (2000), arXiv:hep-ex/0006034.
- S. Fukuda et al. (Super-Kamiokande Collaboration), *Determination of solar neutrino oscillation parameters using 1496 days of Super-Kamiokande-I data*, Phys. Lett. **B539**, 179–187 (2002), arXiv:hep-ex/0205075.
- Q. R. Ahmad et al. (SNO Collaboration), *Direct evidence for neutrino flavor transformation from neutral-current interactions in the Sudbury Neutrino Observatory*, Phys. Rev. Lett. **89**, 011301 (2002), arXiv:nucl-ex/0204008.
- Q. R. Ahmad et al. (SNO Collaboration), *Measurement of day and night neutrino energy spectra at SNO and constraints on neutrino mixing parameters*, Phys. Rev. Lett. **89**, 011302 (2002), arXiv:nucl-ex/0204009.
- S. N. Ahmed et al. (SNO Collaboration), *Measurement of the total active B-8 solar neutrino flux at the Sudbury Neutrino Observatory with enhanced neutral current sensitivity*, Phys. Rev. Lett. **92**, 181301 (2004), arXiv:nucl-ex/0309004.
- K. Eguchi et al. (KamLAND Collaboration), *First results from KamLAND: Evidence for reactor anti- neutrino disappearance*, Phys. Rev. Lett. **90**, 021802 (2003), arXiv:hep-ex/0212021.
- [12] Y. Fukuda et al. (Super-Kamiokande Collaboration), *Evidence for oscillation of atmospheric neutrinos*, Phys. Rev. Lett. **81**, 1562–1567 (1998), arXiv:hep-ex/9807003.
- G. Giacomelli and A. Margiotta (MACRO Collaboration), *New MACRO results on atmospheric neutrino oscillations*, Phys. Atom. Nucl. **67**, 1139–1146 (2004), arXiv:hep-ex/0407023.
- M. C. Sanchez et al. (Soudan 2 Collaboration), *Observation of atmospheric neutrino oscillations in Soudan 2*, Phys. Rev. **D68**, 113004 (2003), arXiv:hep-ex/0307069.
- [13] W. Grimus, *Neutrino physics: Theory*, Lect. Notes Phys. **629**, 169–214 (2004), arXiv:hep-ph/0307149.
- W. Winter, *Lecture on neutrino physics at the University of Würzburg*, (2009).
- [14] C. Giunti, *Absolute neutrino masses*, Acta Phys. Polon. **B36**, 3215–3226 (2005), arXiv:hep-ph/0511131.
- [15] B. Pontecorvo, *Mesonium and Antimesonium*, Soviet Journal of Experimental and Theoretical Physics **6**, 429–+ (1958).
- Z. Maki, M. Nakagawa and S. Sakata, *Remarks on the Unified Model of Elementary Particles*, Progress of Theoretical Physics **28**(5), 870–880 (1962).
- [16] J. Schechter and J. W. F. Valle, *Neutrino Oscillation Thought Experiment*, Phys. Rev. **D23**, 1666 (1981).
- J. F. Nieves and P. B. Pal, *Rephasing-invariant CP violating parameters with Majorana neutrinos*, Phys. Rev. **D64**, 076005 (2001), arXiv:hep-ph/0105305.
- A. de Gouvea, B. Kayser and R. N. Mohapatra, *Manifest CP violation from Majorana phases*, Phys. Rev. **D67**, 053004 (2003), arXiv:hep-ph/0211394.
- [17] T. Schwetz, M. Tortola and J. W. F. Valle, *Global neutrino data and recent reactor fluxes: status of three-flavour oscillation parameters*, New J. Phys. **13**, 063004 (2011), arXiv:1103.0734.

-
- [18] J. P. Cravens et al. (Super-Kamiokande Collaboration), *Solar neutrino measurements in Super-Kamiokande-II*, Phys. Rev. **D78**, 032002 (2008), arXiv:0803.4312.
R. Wendell et al. (Kamiokande Collaboration), *Atmospheric neutrino oscillation analysis with sub-leading effects in Super-Kamiokande I, II, and III*, Phys. Rev. **D81**, 092004 (2010), arXiv:1002.3471.
K. Abe et al. (Super-Kamiokande Collaboration), *Solar neutrino results in Super-Kamiokande-III*, Phys. Rev. **D83**, 052010 (2011), arXiv:1010.0118.
- [19] A. Gando et al. (The KamLAND Collaboration), *Constraints on θ_{13} from A Three-Flavor Oscillation Analysis of Reactor Antineutrinos at KamLAND*, Phys. Rev. **D83**, 052002 (2011), arXiv:1009.4771.
- [20] H. Barth et al., *Status and perspectives of the Mainz neutrino mass experiment*, Prog. Part. Nucl. Phys. **40**, 353–376 (1998).
- [21] V. M. Lobashev et al., *Direct search for mass of neutrino and anomaly in the tritium beta-spectrum*, Phys. Lett. **B460**, 227–235 (1999).
- [22] J. Bonn et al., *The Mainz neutrino mass experiment*, Nucl. Phys. Proc. Suppl. **91**, 273–279 (2001).
C. Weinheimer, *Direct neutrino mass experiments: Present and future*, Nucl. Phys. Proc. Suppl. **118**, 279–286 (2003).
- [23] L. Bornschein (KATRIN Collaboration), *KATRIN: Direct measurement of neutrino masses in the sub- eV region*, (2003), arXiv:hep-ex/0309007.
- [24] J. Schechter and J. W. F. Valle, *Neutrinoless double-beta decay in $SU(2) \times U(1)$ theories*, Phys. Rev. **D25**, 2951 (1982).
M. Hirsch, S. Kovalenko and I. Schmidt, *Extended Black Box Theorem for Lepton Number and Flavor Violating processes*, Phys. Lett. **B642**, 106–110 (2006), arXiv:hep-ph/0608207.
- [25] H. V. Klapdor-Kleingrothaus et al., *Latest Results from the Heidelberg-Moscow Double Beta Decay Experiment*, Eur. Phys. J. **A12**, 147–154 (2001), arXiv:hep-ph/0103062.
- [26] G. Zuzel (GERDA Collaboration), *The GERDA experiment at Gran Sasso*, Acta Phys. Polon. **B41**, 1469–1476 (2010).
- [27] C. Arnaboldi et al. (CUORICINO Collaboration), *Results from a search for the $0\nu\beta\beta$ -decay of ^{130}Te* , Phys. Rev. **C78**, 035502 (2008), arXiv:0802.3439.
- [28] D. Akimov et al., *EXO: An advanced Enriched Xenon double-beta decay Observatory*, Nucl. Phys. Proc. Suppl. **138**, 224–226 (2005).
N. Ackerman (EXO Collaboration), *Status of EXO-200*, (2009), arXiv:0909.1826.
- [29] J. Lesgourgues and S. Pastor, *Massive neutrinos and cosmology*, Phys. Rept. **429**, 307–379 (2006), arXiv:astro-ph/0603494.
- [30] M. Freund, P. Huber and M. Lindner, *Extracting matter effects, masses and mixings at a neutrino factory*, Nucl. Phys. **B585**, 105–123 (2000), arXiv:hep-ph/0004085.
M. Freund, *Analytic approximations for three neutrino oscillation parameters and probabilities in matter*, Phys.Rev. **D64**, 053003 (2001), arXiv:hep-ph/0103300.

- [31] L. Wolfenstein, *Neutrino oscillations in matter*, Phys. Rev. D **17**(9), 2369–2374 (1978).
S. P. Mikheyev and A. Y. Smirnov, *Resonant neutrino oscillations in matter*, Prog. Part. Nucl. Phys. **23**, 41–136 (1989).
- [32] J. N. Abdurashitov et al. (SAGE Collaboration), *Measurement of the solar neutrino capture rate with gallium metal. III: Results for the 2002–2007 data-taking period*, Phys. Rev. **C80**, 015807 (2009), arXiv:0901.2200.
- [33] B. Aharmim et al. (SNO Collaboration), *An Independent Measurement of the Total Active 8B Solar Neutrino Flux Using an Array of 3He Proportional Counters at the Sudbury Neutrino Observatory*, Phys. Rev. Lett. **101**, 111301 (2008), arXiv:0806.0989.
B. Aharmim et al. (SNO Collaboration), *Low Energy Threshold Analysis of the Phase I and Phase II Data Sets of the Sudbury Neutrino Observatory*, Phys. Rev. **C81**, 055504 (2010), arXiv:0910.2984.
- [34] P. Adamson et al. (The MINOS Collaboration), *New constraints on muon-neutrino to electron-neutrino transitions in MINOS*, Phys. Rev. **D82**, 051102 (2010), arXiv:1006.0996.
P. Adamson et al. (The MINOS Collaboration), *Measurement of the neutrino mass splitting and flavor mixing by MINOS*, Phys. Rev. Lett. **106**, 181801 (2011), arXiv:1103.0340.
- [35] K. Abe et al. (T2K Collaboration), *Indication of Electron Neutrino Appearance from an Accelerator-produced Off-axis Muon Neutrino Beam*, (2011), arXiv:1106.2822.
- [36] S. Weinberg, *Baryon and Lepton Nonconserving Processes*, Phys. Rev. Lett. **43**, 1566–1570 (1979).
- [37] E. Ma, *Pathways to naturally small neutrino masses*, Phys. Rev. Lett. **81**, 1171–1174 (1998), arXiv:hep-ph/9805219.
- [38] J. Schechter and J. W. F. Valle, *Neutrino Masses in $SU(2) \times U(1)$ Theories*, Phys. Rev. **D22**, 2227 (1980).
T. P. Cheng and L.-F. Li, *Neutrino Masses, Mixings and Oscillations in $SU(2) \times U(1)$ Models of Electroweak Interactions*, Phys. Rev. **D22**, 2860 (1980).
- [39] R. Foot, H. Lew, X. G. He and G. C. Joshi, *Seesaw neutrino masses induced by a triplet of leptons*, Z. Phys. **C44**, 441 (1989).
- [40] P. Minkowski, *$\mu \rightarrow e$ gamma at a Rate of One Out of 1-Billion Muon Decays?*, Phys. Lett. **B67**, 421 (1977).
T. Yanagida, in KEK lectures, ed. O. Sawada and A. Sugamoto, KEK (1979).
R. N. Mohapatra and G. Senjanovic, *Neutrino mass and spontaneous parity nonconservation*, Phys. Rev. Lett. **44**, 912 (1980).
P. R. M. Gell-Mann and R. Slansky, in Supergravity, ed. P. van Nieuwenhuizen and D. Freedman (North Holland) (1979).
- [41] A. Zee, *Quantum numbers of Majorana neutrino masses*, Nucl. Phys. **B264**, 99 (1986).
- [42] K. S. Babu, *Model of 'Calculable' Majorana Neutrino Masses*, Phys. Lett. **B203**, 132 (1988).

-
- [43] R. Haag, J. T. Lopuszanski and M. Sohnius, *All Possible Generators of Supersymmetries of the s Matrix*, Nucl. Phys. **B88**, 257 (1975).
- [44] S. Coleman and J. Mandula, *All Possible Symmetries of the S Matrix*, Phys. Rev. **159**(5), 1251–1256 (Jul 1967).
- [45] J. Wess and J. Bagger, *Supersymmetry and supergravity*, Princeton, USA: Univ. Pr. (1992) 259 p.
- [46] U. Amaldi, W. de Boer and H. Furstenau, *Comparison of grand unified theories with electroweak and strong coupling constants measured at LEP*, Phys. Lett. **B260**, 447–455 (1991).
- [47] J. R. Ellis, *Supersymmetry and grand unification*, (1995), arXiv:hep-ph/9512335.
- [48] E. Witten, *Dynamical Breaking of Supersymmetry*, Nucl. Phys. **B188**, 513 (1981).
H. P. Nilles, *Supersymmetry, Supergravity and Particle Physics*, Phys. Rept. **110**, 1–162 (1984).
- [49] S. R. Coleman and E. J. Weinberg, *Radiative Corrections as the Origin of Spontaneous Symmetry Breaking*, Phys.Rev. **D7**, 1888–1910 (1973).
- [50] L. E. Ibanez and G. G. Ross, *$SU(2)$ - $L \times U(1)$ Symmetry Breaking as a Radiative Effect of Supersymmetry Breaking in Guts*, Phys.Lett. **B110**, 215–220 (1982).
J. R. Ellis, L. E. Ibanez and G. G. Ross, *Grand Unification with Large Supersymmetry Breaking*, Phys.Lett. **B113**, 283 (1982).
J. R. Ellis, L. E. Ibanez and G. G. Ross, *Supersymmetric grand unification*, Nucl.Phys. **B221**, 29–67 (1983).
- [51] G. G. Ross and R. G. Roberts, *Minimal supersymmetric unification predictions*, Nucl. Phys. **B377**, 571–592 (1992).
- [52] E. Komatsu et al. (WMAP Collaboration Collaboration), *Seven-Year Wilkinson Microwave Anisotropy Probe (WMAP) Observations: Cosmological Interpretation*, Astrophys.J.Suppl. **192**, 18 (2011), arXiv:1001.4538.
- [53] S. Borgani, A. Masiero and M. Yamaguchi, *Light gravitinos as mixed dark matter*, Phys. Lett. **B386**, 189–197 (1996), arXiv:hep-ph/9605222.
F. Takayama and M. Yamaguchi, *Gravitino dark matter without R -parity*, Phys. Lett. **B485**, 388–392 (2000), arXiv:hep-ph/0005214.
M. Hirsch, W. Porod and D. Restrepo, *Collider signals of gravitino dark matter in bilinearly broken R -parity*, JHEP **03**, 062 (2005), arXiv:hep-ph/0503059.
F. Staub, W. Porod and J. Niemeyer, *Strong dark matter constraints on GMSB models*, JHEP **1001**, 058 (2010), arXiv:0907.0530.
- [54] J. E. Kim, *Light Pseudoscalars, Particle Physics and Cosmology*, Phys. Rept. **150**, 1–177 (1987).
G. G. Raffelt, *Stars as laboratories for fundamental physics: The astrophysics of neutrinos, axions, and other weakly interacting particles*, Chicago, USA: Univ. Pr. (1996) 664 p.

- [55] E. J. Chun and H. B. Kim, *Nonthermal axino as cool dark matter in supersymmetric standard model without R-parity*, Phys. Rev. **D60**, 095006 (1999), arXiv:hep-ph/9906392.
E. J. Chun and H. B. Kim, *Axino Light Dark Matter and Neutrino Masses with R-parity Violation*, JHEP **10**, 082 (2006), arXiv:hep-ph/0607076.
- [56] J. Wess and B. Zumino, *Supergauge Transformations in Four-Dimensions*, Nucl. Phys. **B70**, 39–50 (1974).
- [57] S. J. Gates, M. T. Grisaru, M. Rocek and W. Siegel, *Superspace, or one thousand and one lessons in supersymmetry*, Front. Phys. **58**, 1–548 (1983), arXiv:hep-th/0108200.
- [58] M. Drees, R. Godbole and P. Roy, *Theory and phenomenology of sparticles: An account of four-dimensional N=1 supersymmetry in high energy physics*, Hackensack, USA: World Scientific (2004) 555 p.
- [59] I. J. R. Aitchison, *Supersymmetry and the MSSM: An elementary introduction*, (2005), arXiv:hep-ph/0505105.
- [60] M. Kuroda, *Complete Lagrangian of MSSM*, (1999), arXiv:hep-ph/9902340.
- [61] J. Rosiek, *Complete set of Feynman rules for the MSSM – ERRATUM*, (1995), arXiv:hep-ph/9511250.
- [62] M. T. Grisaru, W. Siegel and M. Rocek, *Improved Methods for Supergraphs*, Nucl. Phys. **B159**, 429 (1979).
- [63] L. O’Raifeartaigh, *Spontaneous Symmetry Breaking for Chiral Scalar Superfields*, Nucl. Phys. **B96**, 331 (1975).
- [64] P. Fayet and J. Iliopoulos, *Spontaneously Broken Supergauge Symmetries and Goldstone Spinors*, Phys. Lett. **B51**, 461–464 (1974).
- [65] P. Nath and R. L. Arnowitt, *Generalized Supergauge Symmetry as a New Framework for Unified Gauge Theories*, Phys. Lett. **B56**, 177 (1975).
R. L. Arnowitt, P. Nath and B. Zumino, *Superfield Densities and Action Principle in Curved Superspace*, Phys. Lett. **B56**, 81 (1975).
D. Z. Freedman, P. van Nieuwenhuizen and S. Ferrara, *Progress Toward a Theory of Supergravity*, Phys. Rev. **D13**, 3214–3218 (1976).
S. Deser and B. Zumino, *Consistent Supergravity*, Phys. Lett. **B62**, 335 (1976).
D. Z. Freedman and P. van Nieuwenhuizen, *Properties of Supergravity Theory*, Phys. Rev. **D14**, 912 (1976).
E. Cremmer et al., *Spontaneous Symmetry Breaking and Higgs Effect in Supergravity Without Cosmological Constant*, Nucl. Phys. **B147**, 105 (1979).
J. A. Bagger, *Coupling the Gauge Invariant Supersymmetric Nonlinear Sigma Model to Supergravity*, Nucl. Phys. **B211**, 302 (1983).
E. Cremmer, S. Ferrara, L. Girardello and A. Van Proeyen, *Yang-Mills Theories with Local Supersymmetry: Lagrangian, Transformation Laws and SuperHiggs Effect*, Nucl. Phys. **B212**, 413 (1983).

-
- [66] L. Girardello and M. T. Grisaru, *Soft Breaking of Supersymmetry*, Nucl. Phys. **B194**, 65 (1982).
- [67] S. Dimopoulos and D. W. Sutter, *The Supersymmetric flavor problem*, Nucl. Phys. **B452**, 496–512 (1995), arXiv:hep-ph/9504415.
- [68] H. P. Nilles, *Dynamically Broken Supergravity and the Hierarchy Problem*, Phys. Lett. **B115**, 193 (1982).
H. P. Nilles, *Supergravity Generates Hierarchies*, Nucl. Phys. **B217**, 366 (1983).
A. H. Chamseddine, R. Arnowitt and P. Nath, *Locally Supersymmetric Grand Unification*, Phys. Rev. Lett. **49**, 970 (1982).
R. Barbieri, S. Ferrara and C. A. Savoy, *Gauge Models with Spontaneously Broken Local Supersymmetry*, Phys. Lett. **B119**, 343 (1982).
- [69] G. F. Giudice and R. Rattazzi, *Theories with gauge-mediated supersymmetry breaking*, Phys. Rept. **322**, 419–499 (1999), arXiv:hep-ph/9801271.
- [70] L. Randall and R. Sundrum, *Out of this world supersymmetry breaking*, Nucl. Phys. **B557**, 79–118 (1999), arXiv:hep-th/9810155.
G. F. Giudice, M. A. Luty, H. Murayama and R. Rattazzi, *Gaugino mass without singlets*, JHEP **12**, 027 (1998), arXiv:hep-ph/9810442.
- [71] W. Porod, *SPheno, a program for calculating supersymmetric spectra, SUSY particle decays and SUSY particle production at e^+e^- colliders*, Comput. Phys. Commun. **153**, 275–315 (2003), arXiv:hep-ph/0301101.
- [72] R. Barbier et al., *R-parity violating supersymmetry*, Phys. Rept. **420**, 1–202 (2005), arXiv:hep-ph/0406039.
- [73] H. Dreiner, M. Kramer and B. O’Leary, *Bounds on R-parity violating supersymmetric couplings from leptonic and semi-leptonic meson decays*, Phys.Rev. **D75**, 114016 (2007), arXiv:hep-ph/0612278.
Y. Kao and T. Takeuchi, *Single-Coupling Bounds on R-parity violating Supersymmetry, an update*, (2009), arXiv:0910.4980.
H. Dreiner, M. Hanussek and S. Grab, *Bounds on R-parity Violating Couplings at the Grand Unification Scale from Neutrino Masses*, Phys.Rev. **D82**, 055027 (2010), arXiv:1005.3309.
- [74] G. R. Farrar and P. Fayet, *Phenomenology of the Production, Decay, and Detection of New Hadronic States Associated with Supersymmetry*, Phys. Lett. **B76**, 575–579 (1978).
- [75] S. Weinberg, *Supersymmetry at Ordinary Energies. 1. Masses and Conservation Laws*, Phys. Rev. **D26**, 287 (1982).
N. Sakai and T. Yanagida, *Proton Decay in a Class of Supersymmetric Grand Unified Models*, Nucl. Phys. **B197**, 533 (1982).
- [76] L. E. Ibanez and G. G. Ross, *Discrete gauge symmetries and the origin of baryon and lepton number conservation in supersymmetric versions of the standard model*, Nucl. Phys. **B368**, 3–37 (1992).

- [77] H. K. Dreiner, C. Luhn and M. Thormeier, *What is the discrete gauge symmetry of the MSSM?*, Phys. Rev. **D73**, 075007 (2006), arXiv:hep-ph/0512163.
- [78] C. Munoz, *SUSY: New perspectives and variants*, (2007), arXiv:0705.2007.
- [79] U. Ellwanger, C. Hugonie and A. M. Teixeira, *The Next-to-Minimal Supersymmetric Standard Model*, Phys. Rept. **496**, 1–77 (2010), arXiv:0910.1785.
- [80] R. D. Peccei and H. R. Quinn, *CP Conservation in the Presence of Instantons*, Phys. Rev. Lett. **38**, 1440–1443 (1977).
- [81] P. Fayet, *Supergauge Invariant Extension of the Higgs Mechanism and a Model for the electron and Its Neutrino*, Nucl.Phys. **B90**, 104–124 (1975).
P. Fayet and S. Ferrara, *Supersymmetry*, Phys.Rept. **32**, 249–334 (1977).
P. Fayet, *Spontaneously Broken Supersymmetric Theories of Weak, Electromagnetic and Strong Interactions*, Phys.Lett. **B69**, 489 (1977).
- [82] N. Sakai, *Naturalness in Supersymmetric Guts*, Z.Phys. **C11**, 153 (1981).
D. V. Nanopoulos and K. Tamvakis, *SUSY GUTS: 4 - GUTS: 3*, Phys.Lett. **B113**, 151 (1982).
- [83] J. A. Casas and C. Munoz, *A Natural solution to the mu problem*, Phys. Lett. **B306**, 288–294 (1993), arXiv:hep-ph/9302227.
- [84] J. R. Ellis et al., *Problems for (2,0) compactifications*, Phys. Lett. **B176**, 403 (1986).
B. Rai and G. Senjanovic, *Gravity and domain wall problem*, Phys. Rev. **D49**, 2729–2733 (1994), arXiv:hep-ph/9301240.
- [85] S. A. Abel, *Destabilising divergences in the NMSSM*, Nucl. Phys. **B480**, 55–72 (1996), arXiv:hep-ph/9609323.
C. Panagiotakopoulos and K. Tamvakis, *Stabilized NMSSM without domain walls*, Phys. Lett. **B446**, 224–227 (1999), arXiv:hep-ph/9809475.
- [86] S. A. Abel, S. Sarkar and P. L. White, *On the cosmological domain wall problem for the minimally extended supersymmetric standard model*, Nucl. Phys. **B454**, 663–684 (1995), arXiv:hep-ph/9506359.
- [87] V. Barger, P. Langacker and H.-S. Lee, *Properties of the lightest neutralino in MSSM extensions*, AIP Conf. Proc. **805**, 306–309 (2006), arXiv:hep-ph/0509112.
- [88] T. Asaka, K. Ishiwata and T. Moroi, *Right-handed sneutrino as cold dark matter of the universe*, Phys. Rev. **D75**, 065001 (2007), arXiv:hep-ph/0612211.
S. Gopalakrishna, A. de Gouvea and W. Porod, *Right-handed sneutrinos as nonthermal dark matter*, JCAP **0605**, 005 (2006), arXiv:hep-ph/0602027.
- [89] A. de Gouvea, S. Gopalakrishna and W. Porod, *Stop Decay into Right-handed Sneutrino LSP at Hadron Colliders*, JHEP **11**, 050 (2006), arXiv:hep-ph/0606296.

-
- [90] J. Hisano, T. Moroi, K. Tobe, M. Yamaguchi and T. Yanagida, *Lepton flavor violation in the supersymmetric standard model with seesaw induced neutrino masses*, Phys. Lett. **B357**, 579–587 (1995), arXiv:hep-ph/9501407.
- J. Hisano, T. Moroi, K. Tobe and M. Yamaguchi, *Lepton-Flavor Violation via Right-Handed Neutrino Yukawa Couplings in Supersymmetric Standard Model*, Phys. Rev. **D53**, 2442–2459 (1996), arXiv:hep-ph/9510309.
- Y. Grossman and H. E. Haber, *Sneutrino mixing phenomena*, Phys. Rev. Lett. **78**, 3438–3441 (1997), arXiv:hep-ph/9702421.
- [91] M. Hirsch, L. Reichert and W. Porod, *Supersymmetric mass spectra and the seesaw scale*, (2011), arXiv:1101.2140.
- [92] F. Borzumati and A. Masiero, *Large Muon and electron Number Violations in Supergravity Theories*, Phys. Rev. Lett. **57**, 961 (1986).
- [93] J. R. Ellis, J. S. Hagelin, D. V. Nanopoulos and K. Tamvakis, *Observable gravitationally induce baryon decay*, Phys. Lett. **B124**, 484 (1983).
- [94] M. Drees, S. Pakvasa, X. Tata and T. ter Veldhuis, *A supersymmetric resolution of solar and atmospheric neutrino puzzles*, Phys. Rev. **D57**, 5335–5339 (1998), arXiv:hep-ph/9712392.
- H. K. Dreiner, J. Soo Kim and M. Thormeier, *A Simple Baryon Triality Model for Neutrino Masses*, (2007), arXiv:0711.4315.
- H. K. Dreiner, C. Luhn, H. Murayama and M. Thormeier, *Baryon Triality and Neutrino Masses from an Anomalous Flavor $U(1)$* , Nucl. Phys. **B774**, 127–167 (2007), arXiv:hep-ph/0610026.
- [95] F. de Campos, M. Garcia-Jareno, A. S. Joshipura, J. Rosiek and J. Valle, *Novel scalar boson decays in SUSY with broken R parity*, Nucl.Phys. **B451**, 3–15 (1995), arXiv:hep-ph/9502237.
- T. Banks, Y. Grossman, E. Nardi and Y. Nir, *Supersymmetry without R-parity and without lepton number*, Phys.Rev. **D52**, 5319–5325 (1995), arXiv:hep-ph/9505248.
- A. S. Joshipura and M. Nowakowski, *'Just so' oscillations in supersymmetric standard model*, Phys.Rev. **D51**, 2421–2427 (1995), arXiv:hep-ph/9408224.
- B. de Carlos and P. White, *R-parity violation and quark flavor violation*, Phys.Rev. **D55**, 4222–4239 (1997), arXiv:hep-ph/9609443.
- H.-P. Nilles and N. Polonsky, *Supersymmetric neutrino masses, R symmetries, and the generalized μ problem*, Nucl. Phys. **B484**, 33–62 (1997), arXiv:hep-ph/9606388.
- S. Roy and B. Mukhopadhyaya, *Some implications of a supersymmetric model with R-parity breaking bilinear interactions*, Phys. Rev. **D55**, 7020–7029 (1997), arXiv:hep-ph/9612447.
- [96] R. Hempfling, *Neutrino masses and mixing angles in SUSY GUT theories with explicit R-parity breaking*, Nucl.Phys. **B478**, 3–30 (1996), arXiv:hep-ph/9511288.
- [97] M. Hirsch, M. A. Diaz, W. Porod, J. C. Romao and J. W. F. Valle, *Neutrino masses and mixings from supersymmetry with bilinear R-parity violation: A theory for solar and atmospheric neutrino oscillations*, Phys. Rev. **D62**, 113008 (2000), arXiv:hep-ph/0004115.

-
- [98] C. S. Aulakh and R. N. Mohapatra, *Neutrino as the Supersymmetric Partner of the Majoron*, Phys. Lett. **B119**, 136 (1982).
A. Masiero and J. W. F. Valle, *A model for spontaneous R parity breaking*, Phys. Lett. **B251**, 273–278 (1990).
C. Amsler and A. Masoni, *The $\eta(1405)$, $\eta(1475)$, $f_1(1420)$, and $f_1(1510)$* .
- [99] M. Hirsch and W. Porod, *R-parity violation: Hide and seek*, Phys. Rev. **D74**, 055003 (2006), arXiv:hep-ph/0606061.
- [100] M. Hirsch, A. Vicente and W. Porod, *Spontaneous R-parity violation: Lightest neutralino decays and neutrino mixing angles at future colliders*, Phys. Rev. **D77**, 075005 (2008), arXiv:arXiv:0802.2896.
- [101] M. Hirsch, A. Vicente, J. Meyer and W. Porod, *Majoron emission in muon and tau decays revisited*, Phys. Rev. **D79**, 055023 (2009), arXiv:0902.0525.
- [102] D. E. Lopez-Fogliani and C. Munoz, *Proposal for a new minimal supersymmetric standard model*, Phys. Rev. Lett. **97**, 041801 (2006), arXiv:hep-ph/0508297.
- [103] Y. Farzan and J. W. F. Valle, *R-parity violation assisted thermal leptogenesis in the seesaw mechanism*, Phys. Rev. Lett. **96**, 011601 (2006), arXiv:hep-ph/0509280.
- [104] B. Mukhopadhyaya and R. Srikanth, *Bilarge neutrino mixing in R-parity violating supersymmetry: The role of right-chiral neutrino superfields*, Phys. Rev. **D74**, 075001 (2006), arXiv:hep-ph/0605109.
- [105] R. Kitano and K. ya Oda, *Neutrino masses in the supersymmetric standard model with right-handed neutrinos and spontaneous R-parity violation*, Phys. Rev. **D61**, 113001 (2000), arXiv:hep-ph/9911327.
A. Abada and G. Moreau, *An origin for small neutrino masses in the NMSSM*, JHEP **08**, 044 (2006), arXiv:hep-ph/0604216.
- [106] D. Das and S. Roy, *One-loop contribution to the neutrino mass matrix in NMSSM with right-handed neutrinos and tri-bimaximal mixing*, Phys. Rev. **D82**, 035002 (2010), arXiv:1003.4381.
- [107] M. Chemtob and P. N. Pandita, *Nonminimal supersymmetric standard model with lepton number violation*, Phys. Rev. **D73**, 055012 (2006), arXiv:hep-ph/0601159.
- [108] P. Kant, R. V. Harlander, L. Mihaila and M. Steinhauser, *Light MSSM Higgs boson mass to three-loop accuracy*, JHEP **08**, 104 (2010), arXiv:1005.5709.
- [109] M. Hirsch, T. Kernreiter and W. Porod, *CP violation in decays of the lightest supersymmetric particle with bilinearly broken R parity*, JHEP **01**, 034 (2003), arXiv:hep-ph/0211446.
- [110] D. J. Miller, R. Nevzorov and P. M. Zerwas, *The Higgs sector of the next-to-minimal supersymmetric standard model*, Nucl. Phys. **B681**, 3–30 (2004), arXiv:hep-ph/0304049.
- [111] N. Escudero, D. E. Lopez-Fogliani, C. Munoz and R. R. de Austri, *Analysis of the parameter space and spectrum of the $\mu\nu$ SSM*, JHEP **12**, 099 (2008), arXiv:0810.1507.

-
- [112] R. Barate et al. (LEP Working Group for Higgs boson searches Collaboration), *Search for the standard model Higgs boson at LEP*, Phys. Lett. **B565**, 61–75 (2003), arXiv:hep-ex/0306033.
- G. Abbiendi et al. (OPAL Collaboration), *Search for neutral Higgs boson in CP-conserving and CP-violating MSSM scenarios*, Eur. Phys. J. **C37**, 49–78 (2004), arXiv:hep-ex/0406057.
- J. Abdallah et al. (DELPHI Collaboration), *Higgs boson searches in CP-conserving and CP-violating MSSM scenarios with the DELPHI detector*, Eur. Phys. J. **C54**, 1–35 (2008), arXiv:0801.3586.
- S. Schael et al. (ALEPH Collaboration), *Search for neutral Higgs bosons decaying into four taus at LEP2*, JHEP **05**, 049 (2010), arXiv:1003.0705.
- [113] S. Schael et al. (ALEPH Collaboration), *Search for neutral MSSM Higgs bosons at LEP*, Eur. Phys. J. **C47**, 547–587 (2006), arXiv:hep-ex/0602042.
- [114] M. Hirsch, J. C. Romao, J. W. F. Valle and A. Villanova del Moral, *Production and decays of supersymmetric Higgs bosons in spontaneously broken R-parity*, Phys. Rev. **D73**, 055007 (2006), arXiv:hep-ph/0512257.
- [115] E. Accomando et al. (ECFA/DESY LC Physics Working Group Collaboration), *Physics with $e^+ e^-$ linear colliders*, Phys. Rept. **299**, 1–78 (1998), arXiv:hep-ph/9705442.
- G. Pocsik and G. Zsigmond, *On the production of neutral Higgs boson in the Weinberg-Salam model with two Higgs doublets*, Zeit. Phys. **C10**, 367 (1981).
- [116] U. Wegner and J. Wellstein, *Bemerkungen zur Transformation von komplexen symmetrischen Matrizen*, Monatshefte für Mathematik **40**(1), 319–322 (1932).
- [117] M. Hirsch and J. W. F. Valle, *Neutrinoless double beta decay in supersymmetry with bilinear R-parity breaking*, Nucl. Phys. **B557**, 60–78 (1999), arXiv:hep-ph/9812463.
- [118] W. Porod, M. Hirsch, J. Romao and J. W. F. Valle, *Testing neutrino mixing at future collider experiments*, Phys. Rev. **D63**, 115004 (2001), arXiv:hep-ph/0011248.
- [119] D. A. Ross and J. C. Taylor, *Renormalization of a unified theory of weak and electromagnetic interactions*, Nucl. Phys. **B51**, 125–144 (1973).
- [120] J. C. Romao, M. A. Diaz, M. Hirsch, W. Porod and J. W. F. Valle, *A supersymmetric solution to the solar and atmospheric neutrino problems*, Phys. Rev. **D61**, 071703 (2000), arXiv:hep-ph/9907499.
- [121] M. A. Diaz, M. Hirsch, W. Porod, J. C. Romao and J. W. F. Valle, *Solar neutrino masses and mixing from bilinear R-parity broken supersymmetry: Analytical versus numerical results*, Phys. Rev. **D68**, 013009 (2003), arXiv:hep-ph/0302021.
- [122] A. Bartl, M. Hirsch, A. Vicente, S. Liebler and W. Porod, *LHC phenomenology of the $\mu\nu$ SSM*, JHEP **05**, 120 (2009), arXiv:0903.3596.
- P. Ghosh, P. Dey, B. Mukhopadhyaya and S. Roy, *Radiative contribution to neutrino masses and mixing in $\mu\nu$ SSM*, JHEP **05**, 087 (2010), arXiv:1002.2705.
- [123] H. Eberl, *Strahlungskorrekturen im minimalen supersymmetrischen Standardmodell*, PhD thesis, Technische Universität Wien, Wien, Austria, 1998.

- [124] K. G. Wilson, *Confinement of quarks*, Phys. Rev. **D10**, 2445–2459 (1974).
J. B. Kogut, *The lattice gauge theory approach to quantum chromodynamics*, Rev. Mod. Phys. **55**(3), 775–836 (Jul 1983).
- [125] W. Pauli and F. Villars, *On the Invariant regularization in relativistic quantum theory*, Rev. Mod. Phys. **21**, 434–444 (1949).
- [126] W. Siegel, *Supersymmetric Dimensional Regularization via Dimensional Reduction*, Phys. Lett. **B84**, 193 (1979).
- [127] D. M. Capper, D. R. T. Jones and P. van Nieuwenhuizen, *Regularization by Dimensional Reduction of Supersymmetric and Nonsupersymmetric Gauge Theories*, Nucl. Phys. **B167**, 479 (1980).
I. Antoniadis, C. Kounnas and K. Tamvakis, *Simple treatment of threshold effects*, Phys. Lett. **B119**, 377–380 (1982).
I. Jack, D. R. T. Jones, S. P. Martin, M. T. Vaughn and Y. Yamada, *Decoupling of the epsilon scalar mass in softly broken supersymmetry*, Phys. Rev. **D50**, 5481–5483 (1994), arXiv:hep-ph/9407291.
- [128] G. Passarino and M. J. G. Veltman, *One Loop Corrections for $e^+ e^-$ Annihilation Into $mu^+ mu^-$ in the Weinberg Model*, Nucl. Phys. **B160**, 151 (1979).
- [129] G. 't Hooft and M. J. G. Veltman, *Scalar One Loop Integrals*, Nucl. Phys. **B153**, 365–401 (1979).
- [130] G. J. van Oldenborgh and J. A. M. Vermaseren, *New Algorithms for One Loop Integrals*, Z. Phys. **C46**, 425–438 (1990).
- [131] T. Hahn and M. Perez-Victoria, *Automatized one-loop calculations in four and D dimensions*, Comput. Phys. Commun. **118**, 153–165 (1999), arXiv:hep-ph/9807565.
- [132] J. C. Romao, *Modern Technique for One-Loop Calculations*, (2004).
- [133] K. G. Wilson, *Nonlagrangian models of current algebra*, Phys. Rev. **179**, 1499–1512 (1969).
C. G. J. Callan and D. J. Gross, *High-energy electroproduction and the constitution of the electric current*, Phys. Rev. Lett. **22**, 156–159 (1969).
D. J. Gross and F. Wilczek, *Ultraviolet behavior of non-abelian gauge theories*, Phys. Rev. Lett. **30**, 1343–1346 (1973).
K. G. Wilson and J. Kogut, *The renormalization group and the ϵ expansion*, Phys. Rep. **12**, 75–199 (August 1974).
- [134] C. G. J. Callan, *Broken scale invariance in scalar field theory*, Phys. Rev. **D2**, 1541–1547 (1970).
K. Symanzik, *Small distance behavior in field theory and power counting*, Commun. Math. Phys. **18**, 227–246 (1970).
- [135] S. Liebler and W. Porod, *Electroweak corrections to Neutralino and Chargino decays into a W-boson in the (N)MSSM*, Nucl. Phys. **B849**, 213–249 (2010), arXiv:1011.6163.

-
- [136] S. Liebler and W. Porod, *On-shell renormalization of neutralino and chargino mass matrices in R-parity violating models - Correlation between LSP decays and neutrino mixing angles revisited*, (2011), arXiv:1106.2921.
- [137] A. Denner, *Techniques for calculation of electroweak radiative corrections at the one loop level and results for W physics at LEP-200*, Fortschr. Phys. **41**, 307–420 (1993), arXiv:arXiv:0709.1075.
- [138] P. H. Chankowski, S. Pokorski and J. Rosiek, *Complete on-shell renormalization scheme for the minimal supersymmetric Higgs sector*, Nucl. Phys. **B423**, 437–496 (1994), arXiv:hep-ph/9303309.
- [139] K. Williams, *The Higgs Sector of the Complex Minimal Supersymmetric Standard Model*, PhD thesis, Institute of Particle Physics Phenomenology, Durham University, Durham, UK, 2008.
- [140] M. Steinhauser, *Leptonic contribution to the effective electromagnetic coupling constant up to three loops*, Phys.Lett. **B429**, 158–161 (1998), arXiv:hep-ph/9803313.
- [141] K. Hagiwara, A. Martin, D. Nomura and T. Teubner, *Predictions for $g-2$ of the muon and $\alpha(QED)(M^{*2}(Z))$* , Phys.Rev. **D69**, 093003 (2004), arXiv:hep-ph/0312250.
- [142] T. Fritzsche and W. Hollik, *Complete one-loop corrections to the mass spectrum of charginos and neutralinos in the MSSM*, Eur. Phys. J. **C24**, 619–629 (2002), arXiv:hep-ph/0203159.
- [143] H. Eberl, M. Kincel, W. Majerotto and Y. Yamada, *One-loop corrections to neutral Higgs boson decays into neutralinos*, Nucl. Phys. **B625**, 372–388 (2002), arXiv:hep-ph/0111303.
- [144] N. Baro, F. Boudjema and A. Semenov, *Automatised full one-loop renormalisation of the MSSM I: The Higgs sector, the issue of $\tan(\beta)$ and gauge invariance*, Phys. Rev. **D78**, 115003 (2008), arXiv:0807.4668.
- [145] H. Eberl, M. Kincel, W. Majerotto and Y. Yamada, *One-loop corrections to the chargino and neutralino mass matrices in the on-shell scheme*, Phys. Rev. **D64**, 115013 (2001), arXiv:hep-ph/0104109.
- [146] A. Denner and T. Sack, *Renormalization of the quark mixing matrix*, Nucl. Phys. **B347**, 203–216 (1990).
- [147] P. Gambino, P. A. Grassi and F. Madricardo, *Fermion mixing renormalization and gauge invariance*, Phys. Lett. **B454**, 98–104 (1999), arXiv:hep-ph/9811470.
- [148] N. Cabibbo, *Unitary Symmetry and Leptonic Decays*, Phys. Rev. Lett. **10**, 531–533 (1963).
M. Kobayashi and T. Maskawa, *CP Violation in the Renormalizable Theory of Weak Interaction*, Prog. Theor. Phys. **49**, 652–657 (1973).
- [149] Y. Yamada, *Gauge dependence of the on-shell renormalized mixing matrices*, Phys. Rev. **D64**, 036008 (2001), arXiv:hep-ph/0103046.
- [150] D. Espriu, J. Manzano and P. Talavera, *Flavor mixing, gauge invariance and wave-function renormalisation*, Phys. Rev. **D66**, 076002 (2002), arXiv:hep-ph/0204085.

- [151] J. M. Cornwall, *Nonperturbative mass gap in continuum QCD*, UCLA/81/TEP/12.
J. M. Cornwall, *Dynamical Mass Generation in Continuum QCD*, Phys. Rev. **D26**, 1453 (1982).
J. M. Cornwall and J. Papavassiliou, *Gauge Invariant Three Gluon Vertex in QCD*, Phys. Rev. **D40**, 3474 (1989).
G. Degrossi and A. Sirlin, *Gauge invariant selfenergies and vertex parts of the Standard Model in the pinch technique framework*, Phys. Rev. **D46**, 3104–3116 (1992).
G. Degrossi, B. A. Kniehl and A. Sirlin, *Gauge invariant formulation of the S, T, and U parameters*, Phys. Rev. **D48**, 3963–3966 (1993).
J. Papavassiliou, *Gauge Invariant Proper Selfenergies and Vertices in Gauge Theories with Broken Symmetry*, Phys. Rev. **D41**, 3179 (1990).
J. Papavassiliou, *Gauge independent transverse and longitudinal self energies and vertices via the pinch technique*, Phys. Rev. **D50**, 5958–5970 (1994), arXiv:hep-ph/9406258.
J. Papavassiliou and A. Pilaftsis, *A Gauge independent approach to resonant transition amplitudes*, Phys. Rev. **D53**, 2128–2149 (1996), arXiv:hep-ph/9507246.
J. Papavassiliou and A. Pilaftsis, *Gauge-invariant resummation formalism for two point correlation functions*, Phys. Rev. **D54**, 5315–5335 (1996), arXiv:hep-ph/9605385.
- [152] A. Pilaftsis, *Gauge and scheme dependence of mixing matrix renormalization*, Phys. Rev. **D65**, 115013 (2002), arXiv:hep-ph/0203210.
- [153] A. Denner, E. Kraus and M. Roth, *Physical renormalization condition for the quark-mixing matrix*, Phys. Rev. **D70**, 033002 (2004), arXiv:hep-ph/0402130.
B. A. Kniehl and A. Sirlin, *Simple Approach to Renormalize the Cabibbo-Kobayashi-Maskawa Matrix*, Phys. Rev. Lett. **97**, 221801 (2006), arXiv:hep-ph/0608306.
B. A. Kniehl and A. Sirlin, *Simple on-shell renormalization framework for the Cabibbo-Kobayashi-Maskawa matrix*, Phys. Rev. **D74**, 116003 (2006), arXiv:hep-th/0612033.
- [154] K. P. O. Diener and B. A. Kniehl, *On-mass-shell renormalization of fermion mixing matrices*, Nucl. Phys. **B617**, 291–307 (2001), arXiv:hep-ph/0109110.
A. A. Almasy, B. A. Kniehl and A. Sirlin, *On-shell renormalization of the mixing matrices in Majorana neutrino theories*, Nucl. Phys. **B818**, 115–134 (2009), arXiv:0902.3793.
- [155] A. Freitas and D. Stockinger, *Gauge dependence and renormalization of $\tan(\beta)$ in the MSSM*, Phys. Rev. **D66**, 095014 (2002), arXiv:hep-ph/0205281.
- [156] P. Ghosh and S. Roy, *Neutrino masses and mixing, lightest neutralino decays and a solution to the μ problem in supersymmetry*, JHEP **04**, 069 (2009), arXiv:0812.0084.
- [157] S. Liebler, *CNNDecays was published in [135] and can be downloaded from: www.physik.uni-wuerzburg.de/~sliebler/CNNDecays.tar.gz*.
- [158] F. Bloch and A. Nordsieck, *Note on the Radiation Field of the electron*, Phys. Rev. **52**, 54–59 (1937).
- [159] D. R. Yennie, S. C. Frautschi and H. Suura, *The infrared divergence phenomena and high-energy processes*, Ann. Phys. **13**, 379–452 (1961).

-
- [160] T. Kinoshita, *Mass singularities of Feynman amplitudes*, J.Math.Phys. **3**, 650–677 (1962).
T. Lee and M. Nauenberg, *Degenerate Systems and Mass Singularities*, Phys.Rev. **133**, B1549–B1562 (1964).
N. Nakanishi, *A Theory of Clothed Unstable Particles*, Progress of Theoretical Physics **19**(6), 607–621 (1958).
- [161] S. Weinberg, *Infrared photons and gravitons*, Phys. Rev. **140**, B516–B524 (1965).
- [162] J. A. Aguilar-Saavedra et al., *Supersymmetry parameter analysis: SPA convention and project*, Eur. Phys. J. **C46**, 43–60 (2006), arXiv:hep-ph/0511344.
- [163] G. Aad et al. (The ATLAS Collaboration), *Expected Performance of the ATLAS Experiment - Detector, Trigger and Physics*, (2009), arXiv:0901.0512.
- [164] A. Djouadi et al., *Benchmark scenarios for the NMSSM*, JHEP **07**, 002 (2008), arXiv:0801.4321.
- [165] U. Ellwanger, C. C. Jean-Louis and A. M. Teixeira, *Phenomenology of the General NMSSM with Gauge Mediated Supersymmetry Breaking*, JHEP **05**, 044 (2008), arXiv:0803.2962.
- [166] U. Ellwanger, J. F. Gunion and C. Hugonie, *NMHDECAY: A Fortran code for the Higgs masses, couplings and decay widths in the NMSSM*, JHEP **02**, 066 (2005), arXiv:hep-ph/0406215.
U. Ellwanger and C. Hugonie, *NMHDECAY 2.0: An Updated program for sparticle masses, Higgs masses, couplings and decay widths in the NMSSM*, Comput. Phys. Commun. **175**, 290–303 (2006), arXiv:hep-ph/0508022.
U. Ellwanger and C. Hugonie, *NMSPEC: A Fortran code for the sparticle and Higgs masses in the NMSSM with GUT scale boundary conditions*, Comput. Phys. Commun. **177**, 399–407 (2007), arXiv:hep-ph/0612134.
- [167] T. Schwetz, M. A. Tortola and J. W. F. Valle, *Three-flavour neutrino oscillation update*, New J. Phys. **10**, 113011 (2008), arXiv:0808.2016.
- [168] C. Amsler et al. (Particle Data Group Collaboration), *Review of particle physics*, Phys. Lett. **B667**, 1–1340 (2008).
- [169] D. F. Carvalho, M. E. Gomez and J. C. Romao, *Charged lepton flavor violation in supersymmetry with bilinear R-parity violation*, Phys. Rev. **D65**, 093013 (2002), arXiv:hep-ph/0202054.
- [170] U. Ellwanger, J. F. Gunion and C. Hugonie, *Difficult scenarios for NMSSM Higgs discovery at the LHC*, JHEP **07**, 041 (2005), arXiv:hep-ph/0503203.
- [171] F. Franke and H. Fraas, *Mass bounds for the neutral Higgs bosons in the next-to-minimal supersymmetric standard model*, Phys. Lett. **B353**, 234–242 (1995), arXiv:hep-ph/9504279.
- [172] F. Staub, W. Porod and B. Herrmann, *The electroweak sector of the NMSSM at the one-loop level*, JHEP **10**, 040 (2010), arXiv:1007.4049.

- [173] R.-Y. Zhang, W.-G. Ma and L.-H. Wan, *Supersymmetric electroweak corrections to the chargino decay into neutralino and W boson*, J. Phys. **G28**, 169–182 (2002), arXiv:hep-ph/0111124.
- [174] B. Mukhopadhyaya, S. Roy and F. Vissani, *Correlation between neutrino oscillations and collider signals of supersymmetry in an R-parity violating model*, Phys. Lett. **B443**, 191–195 (1998), arXiv:hep-ph/9808265.
- [175] E. J. Chun, D.-W. Jung, S. K. Kang and J. D. Park, *Collider signatures of neutrino masses and mixing from R parity violation*, Phys.Rev. **D66**, 073003 (2002), arXiv:hep-ph/0206030.
- [176] M. Hirsch, W. Porod, J. C. Romao and J. W. F. Valle, *Probing neutrino properties with charged scalar lepton decays*, Phys. Rev. **D66**, 095006 (2002), arXiv:hep-ph/0207334.
- [177] M. Hirsch and W. Porod, *Neutrino properties and the decay of the lightest supersymmetric particle*, Phys. Rev. **D68**, 115007 (2003), arXiv:hep-ph/0307364.
- [178] D. Aristizabal Sierra, M. Hirsch and W. Porod, *R-parity violating sneutrino decays*, JHEP **09**, 033 (2005), arXiv:hep-ph/0409241.
- [179] D. M. Pierce, J. A. Bagger, K. T. Matchev and R. Zhang, *Precision corrections in the minimal supersymmetric standard model*, Nucl. Phys. **B491**, 3–67 (1997), arXiv:hep-ph/9606211.
- [180] F. Staub, *From Superpotential to Model Files for FeynArts and CalcHep/CompHep*, Comput. Phys. Commun. **181**, 1077–1086 (2010), arXiv:0909.2863.
- [181] S. Liebler, *MaCoR for the NMSSM can be downloaded from:*, www.physik.uni-wuerzburg.de/~sliebler/MaCoRNMSSM.tar.gz.
- [182] P. Z. Skands et al., *SUSY Les Houches Accord: Interfacing SUSY Spectrum Calculators, Decay Packages, and Event Generators*, JHEP **07**, 036 (2004), arXiv:hep-ph/0311123.
- [183] B. C. Allanach et al., *SUSY Les Houches Accord 2*, Comp. Phys. Commun. **180**, 8–25 (2009), arXiv:0801.0045.
- [184] W. R. Inc., *Mathematica Version 7*, Wolfram Research, Inc. Place of publication: Champaign, Illinois (2008).
- [185] T. Hahn, *Generating Feynman diagrams and amplitudes with FeynArts 3*, Comput. Phys. Commun. **140**, 418–431 (2001), arXiv:hep-ph/0012260.
- [186] T. Ohl, *Drawing Feynman diagrams with Latex and Metafont*, Comput.Phys.Commun. **90**, 340–354 (1995), arXiv:hep-ph/9505351.

Acknowledgments

This chapter is dedicated to all my colleagues, friends and family and can be summarized as follows: ¡Muchas gracias a todos! Merci beaucoup! Herzlichen Dank! Thank you very much!

However it is worth to write some additional words: First I want to thank Werner Porod for the possibility to work on these interesting topics under his supervision. Apart from nice discussions and good advice he is always interested to have an active and alive working group making life at the university also recreative. In addition I thank all my colleagues in Würzburg contributing to my work, namely: Björn Herrmann, Ritesh Singh, Florian Staub and Avelino Vicente. In particular Florian deserves closer attention: We shared offices for some years and discussed many physical problems, but did not forget to have a nice time. Moreover I thank him for reading this thesis, correcting some misprints and providing suggestions. Moreover I want to mention the people, with whom I discussed physical problems and had some fun abroad, namely: Alfred Bartl, Sven Heinemeyer, Martin Hirsch, and Federico von der Pahlen. I want to thank Sven for the hospitality during my two stays in Santander and Martin and Avelino for the hospitality during my stays in Valencia. Sven, Federico and Christian Schappacher gratefully pointed out some weak points in my calculations. Without Brigitte Wehner in Würzburg bureaucracy would be complicated, she allows us to focus on physical problems. Also the other professors Ansgar Denner, Thorsten Ohl, Reinhold Rückl and Walter Winter should be mentioned, since they led me to particle physics and keep it up in Würzburg. As former spokesperson of the graduate school I thank all the graduate school students for being so peaceful and gentle (In the moment of writing this sentence Matthias came in and gave me a present, what a coincidence: Thank you very much)! Some deserve my special attention: Not only at the institute but also in my leisure time I had quite some fun with Asma Chériguène, Lisa Edelhäuser, Martin Krauß, Jochen Meyer and Lukas Mitzka! In principle there are many more friends to say thank you, whom I hug symbolically! Don't be scared ;-). Last but of course not least I add my parents and my brother, who always support me!

Lieber Computer, sei bitte fromm,
dass ich zu einem Ergebnis komm!